Advances in Intelligent Systems and Computing 665

Georgi Stojanov
Andrea Kulakov *Editors*

ICT Innovations 2016

Cognitive Functions and Next Generation ICT Systems

Springer

Advances in Intelligent Systems and Computing

Volume 665

Series editor

Janusz Kacprzyk, Polish Academy of Sciences, Warsaw, Poland
e-mail: kacprzyk@ibspan.waw.pl

About this Series

The series "Advances in Intelligent Systems and Computing" contains publications on theory, applications, and design methods of Intelligent Systems and Intelligent Computing. Virtually all disciplines such as engineering, natural sciences, computer and information science, ICT, economics, business, e-commerce, environment, healthcare, life science are covered. The list of topics spans all the areas of modern intelligent systems and computing.

The publications within "Advances in Intelligent Systems and Computing" are primarily textbooks and proceedings of important conferences, symposia and congresses. They cover significant recent developments in the field, both of a foundational and applicable character. An important characteristic feature of the series is the short publication time and world-wide distribution. This permits a rapid and broad dissemination of research results.

Advisory Board

More information about this series at http://www.springer.com/series/11156

Georgi Stojanov · Andrea Kulakov
Editors

ICT Innovations 2016

Cognitive Functions and Next Generation ICT Systems

Springer

Editors
Georgi Stojanov
Paris
France

Andrea Kulakov
Skopje
Macedonia

ISSN 2194-5357 ISSN 2194-5365 (electronic)
Advances in Intelligent Systems and Computing
ISBN 978-3-319-68854-1 ISBN 978-3-319-68855-8 (eBook)
https://doi.org/10.1007/978-3-319-68855-8

Library of Congress Control Number: 2017955723

Printed on acid-free paper

This Springer imprint is published by Springer Nature
The registered company is Springer International Publishing AG
The registered company address is: Gewerbestrasse 11, 6330 Cham, Switzerland

Preface

The ICT Innovations conference is the primary scientific gathering event of the Macedonian Association of Information and Communication Technologies (ICT-ACT), whose mission is the advancement of ICT technologies. The conference provides a platform for academics, professionals, and practitioners to interact and share their research findings related to basic and applied research in ICT.

The ICT Innovations 2016 conference gathered 186 authors from 19 countries reporting their scientific work and novel solutions in ICT. Only 20 papers were selected for this edition by the International Program Committee. The committee itself consists of 111 members from 37 countries, chosen for the scientific excellence in their specific fields. Additional 19 short papers can be accessed in the Web proceedings of the conference. The first four papers in this edition are by the invited speakers at the conference.

ICT Innovations 2016 was held in Ohrid, at Metropol Hotel, in the period of September 5–7, 2016. The special conference topic was "Cognitive Functions and Next Generation ICT Systems." The conference also focused on variety of ICT fields: Ambient Intelligence, Artificial Intelligence, Assistive technologies, Big Data Analytics, Bioinformatics, Cloud Computing, Cognitive Systems, Collaborative Environments, Data Mining, Digital Signal & Image Processing, E-health, Embedded Systems, Emerging Mobile Technologies, Internet of Things, Machine Learning, Machine Translation, Machine Vision, Natural Language Processing, Pattern Recognition, Personalized Adaptive Technologies, Personalized Medicine, Robotics & Automation, Security & Cryptography, Speech Recognition & Synthesis, Visualization, Virtual Reality, Wearable Technologies, Wireless Communication & Sensor Networks, and related.

We would like to express sincere gratitude to the invited speakers for their inspirational talks, to the authors for submitting their works to this conference, and to the reviewers for sharing their experience during the selection process. Special thanks go to Bojana Koteska, Monika Simjanoska, Eftim Zdravevski, and Petre Lameski for their technical support during the conference and for their assistance in the preparation of the conference proceedings.

September 2016

Georgi Stojanov
Andrea Kulakov

Organization

ICT Innovations 2016 was organized by the Macedonian Society of Information and Communication Technologies (ICT-ACT), co-organized together with the Faculty of Computer Science and Engineering, University Ss. Cyril and Methodius, Macedonia.

Conference and Program Chairs

Georgi Stojanov	The American University of Paris, France
Andrea Kulakov	University Ss. Cyril and Methodius, Macedonia

Program Committee

Achkoski Jugoslav	Military Academy "General Mihailo Apostolski," Macedonia
Ackovska Nevena	University Ss. Cyril and Methodius, Macedonia
Ahmed Gaber Suliman Mohamed	Universiti Tunku Abdul Rahman, Malaysia
Alti Adel	University of Setif, Algeria
Alzaid Hani	King Abdulaziz City for Science and Technology, Saudi Arabia
Antovski Ljupcho	University Ss. Cyril and Methodius, Macedonia
Armenski Goce	University Ss. Cyril and Methodius, Macedonia
Astsatryan Hrachya	National Academy of Sciences of Armenia, Armenia
Baicheva Tsonka	Institute of Mathematics and Informatics, Bulgaria
Bakeva Verica	University Ss. Cyril and Methodius, Macedonia
Bao Vo Nguyen Quoc	Posts and Telecommunications Institute of Technology, Vietnam

Basnarkov Lasko	University Ss. Cyril and Methodius, Macedonia
Bela Genge	Petru Maior University of Tg Mures, Romania
Beus-Dukic Ljerka	University of Westminster, UK
Boggia Gennaro	DEI - Politecnico di Bari, Italy
Borštnar Kljajić Mirjana	University of Maribor, Slovenia
Bosnacki Dragan	Eindhoven University of Technology, the Netherlands
Burrull Francesc	Universidad Politecnica de Cartagena, Spain
Chatvichienchai Somchai	University of Nagasaki, Japan
Chen Qiu	Kogakuin University, Japan
Chorbev Ivan	University Ss. Cyril and Methodius, Macedonia
Chung Ping-Tsai	Long Island University, USA
Cico Betim	South East European University, Macedonia
Dahiya Deepak	Ansal University Gurgaon, India
Davcev Danco	University Ss. Cyril and Methodius, Macedonia
De Nicola Antonio	ENEA, Italy
Devedzic Goran	University of Kragujevac, Serbia
Dimitrova Vesna	University Ss. Cyril and Methodius, Macedonia
Dimitrovski Ivica	University Ss. Cyril and Methodius, Macedonia
Drlik Martin	Constantine the Philosopher University in Nitra, Slovakia
Filiposka Sonja	University Ss. Cyril and Methodius, Macedonia
Frasheri Neki	Polytechnic University of Tirana, Albania
Fujinami Kaori	Tokyo University of Agriculture and Technology, Japan
Gavrilov Andrey	Novosibirsk State Technical University, Russia
Gievska-Krilu Sonja	University Ss. Cyril and Methodius, Macedonia
Gjorgjevik Dejan	University Ss. Cyril and Methodius, Macedonia
Gligoroski Danilo	Norwegian University of Science and Technology, Norway
Gusev Marjan	University Ss. Cyril and Methodius, Macedonia
Hadzi-Velkov Zoran	University Ss. Cyril and Methodius, Macedonia
Hao Tianyong	Guangdong University of Foreign Studies, China
Hsieh Fu-Shiung	Chaoyang University of Technology, Taiwan
Huraj Ladislav	University of Ss. Cyril and Methodius in Trnava, Czechia
Ilarri Sergio	University of Zaragoza, Spain
Jakimovski Boro	University Ss. Cyril and Methodius, Macedonia
Janev Valentina	Institute Mihajlo Pupin, Serbia
Jecheva Veselina	Burgas Free University, Bulgaria
Kalajdziski Slobodan	University Ss. Cyril and Methodius, Macedonia
Kaloyanova Kalinka	University of Sofia, Bulgaria
Koceski Saso	University Goce Delcev, Macedonia
Kon-Popovska Margita	University Ss. Cyril and Methodius, Macedonia
Kraljevski Ivan	Voice INTER Connect, Germany

Kulkarni Siddhivinayak	Federation University Australia, Australia
Kumar Singh Brajesh	RBS College, India
Kurti Arianit	Linnaeus University, Sweden
Lazarova-Molnar Sanja	University of Southern Denmark, Denmark
Lim Hwee-San	Universiti Sains Malaysia, Malaysia
Loshkovska Suzana	University Ss. Cyril and Methodius, Macedonia
Madevska Bogdanova Ana	University Ss. Cyril and Methodius, Macedonia
Madzarov Gjorgji	University Ss. Cyril and Methodius, Macedonia
Marina Ninoslav	University St Paul the Apostle, Macedonia
Markovski Smile	University Ss. Cyril and Methodius, Macedonia
Matovski Darko	University of Southampton, UK
Michalak Marcin	Silesian University of Technology, Poland
Mihova Marija	University Ss. Cyril and Methodius, Macedonia
Mileva Aleksandra	University Goce Delcev, Macedonia
Mishev Anastas	University Ss. Cyril and Methodius, Macedonia
Mishkovski Igor	University Ss. Cyril and Methodius, Macedonia
Mitreski Kosta	University Ss. Cyril and Methodius, Macedonia
Mitrevski Pece	University St. Clement of Ohrid, Macedonia
Mohammed Ammar	Cairo University, Egypt
Nancovska Serbec Irena	University of Ljubljana, Slovenia
Nicolau Viorel	Dunarea de Jos University of Galati, Romania
Nicolin Alexandru	National Institute of Physics and Nuclear Engineering, Romania
Pantano Eleonora	Middlesex University, UK
Patel Shushma	South Bank University, UK
Peachey Paul	University of South Wales, UK
Petkovic Predrag	University of Niš, Serbia
Pirlo Giuseppe	Bari University, Italy
Pop Florin	University Politehnica of Bucharest, Romania
Radevski Vladimir	South East European University, Macedonia
Senthil Kumar A.V.	Hindusthan College of Arts and Science, India
Serova Elena G.	St. Petersburg State Economic University, Russia
Siládi Vladimír	Matej Bel University, Slovakia
Silva Manuel	Instituto Superior de Engenharia do Porto, Portugal
Sokolova Ana	University of Salzburg, Austria
Spasov Dejan	University Ss. Cyril and Methodius, Macedonia
Stojanovic Igor	University Goce Delcev, Macedonia
Stoyanov Stanimir	University of Plovdiv "Paisii Hilendarski," Bulgaria
Subramaniam Chandrasekaran	Kumaraguru College of Technology, India
Sun Chang-Ai	University of Science and Technology Beijing, China
Thepade Sudeep	Pune University, India

Trajanov Dimitar	University Ss. Cyril and Methodius, Macedonia
Trajkovic Ljiljana	Simon Fraser University, Canada
Trajkovik Vladimir	University Ss. Cyril and Methodius, Macedonia
Treesatayapun Chidentree	Cinvestav-Saltillo, Mexico
Trung Huynh Hieu	Industrial University of Ho Chi Minh City, Vietnam
Velinov Goran	University Ss. Cyril and Methodius, Macedonia
Vrdoljak Boris	University of Zagreb, Croatia
Wibowo Santoso	CQUniversity, Australia
Xu Shuxiang	University of Tasmania, Australia
Yang Chao-Tung	Tunghai University, Taiwan
Yue Wuyi	Konan University, Japan
Zdravev Zoran	University Goce Delcev, Macedonia
Zdravkova Katerina	University Ss. Cyril and Methodius, Macedonia
Zeng Xiangyan	Fort Valley State University, USA

Organizing Committee

Cveta Martinovska	University Goce Delcev, Macedonia
Gjorgji Madzarov	University Ss. Cyril and Methodius, Macedonia
Elena Vlahu-Georgievska	University St. Clement of Ohrid, Macedonia
Azir Aliu	South East European University, Macedonia
Ustijana Reckoska Shikoska	University St Paul the Apostole, Macedonia

Technical Committee

Bojana Koteska	University Ss. Cyril and Methodius, Macedonia
Monika Simjanoska	University Ss. Cyril and Methodius, Macedonia
Eftim Zdravevski	University Ss. Cyril and Methodius, Macedonia
Petre Lameski	University Ss. Cyril and Methodius, Macedonia

Contents

Invited Keynote Papers

Towards Multimodal Affective Stimulation: Interaction Between Visual, Auditory and Haptic Modalities

Bipin Indurkhya(✉)

Jagiellonian University, Cracow, Poland
bipin.indurkhya@uj.edu

1 Affective Computing

Affective computing is concerned with designing and implementing emotionally intelligent machines. Three major subareas of research in this field are: (1) sensing the emotional state of the user, (2) expressing or displaying emotional states in a robot or an avatar, and (3) manipulating the users emotional state. For example, Picard [1] has designed a system to infer emotional state of the user based on their facial expressions. This system is designed to help people with autism to assess emotional state of the person with whom they are communicating. Once the emotional state of the user is detected, it can also be use as an interface to affect the state of the system. For example, Lee et al. [2] have designed an emotionally reactive TV, which uses a soft ball as an emotion-based interface. The user can squeeze the ball or throw it, and the TV responds accordingly.

The architecture of an affective system is based on extracting the emotional state of the user based on their facial expressions, prosody of their speech, gestures, postures, biometric signals such as galvanic skin response, and then responding to the user in an appropriate manner. For example, a social robot, on detecting that the user is feeling sad, might try to cheer them up. An emotionally intelligent tutor would detect stress in the student, and will present another example to illustrate the concept being learnt.

2 Affect Generation

Techniques for manipulating the users emotional state are studied under affect generation, where the focus is on synthesizing stimuli to induce an emotional state in the user. This is a new and emerging research area under affective computing. Affect generation can be used for entertainment, but also to design systems to support human decision-making. For example, a study by Dazinger et al. [3] has shown that the judges decisions are affected by when they had their last meal. This suggests a simple non-technical affect generation system of providing refreshments at regular intervals.

G. Stojanov and A. Kulakov (eds.), *ICT Innovations 2016*,
Advances in Intelligent Systems and Computing 665,
https://doi.org/10.1007/978-3-319-68855-8_1

There are many techniques for affect generation. We could use images, sounds including music, or haptic stimulation, which consist of applying vibrations to some part of the body. Though the use of images and auditory stimuli for affect generation has been extensively studies, there is little research on how haptic stimulations affect emotional state of the user.

Some applications have been developed for communicating information through haptic stimulations. For example, Jayant et al. [4] implemented a VBraille system for a mobile phone, where the braille pattern is communicated to a blind user through vibrations. Tomohiro and Sugiyama [5] have developed a haptic feedback system to help navigate a blind person to their destination. More recently, such technologies have been deployed in systems for surgical training (haptic feedback provides the feeling of human tissue) and 3-d computer-aided design systems (provide the tactile feeling for the object being designed).

Some of these techniques have also been applied for affect generation by haptic stimulation. For instance, Tsetserukou et al. [6] implemented a system that applies tactile stimulation in the chest area to facilitate affective communication in Second Life.

Given that visual, auditory, and haptic stimuli can carry affective information, a research question is how these modalities interact together, and if we can use multimodal stimuli to implement affect generation more effectively than either modality alone.

3 Multisensory Integration of Percepts

Several studies have explored how humans integrate sensory information from multiple modalities. Most of these studies use the conflict paradigm, where conflicting inputs are provided in two different modalities. For example, the McGurk affect demonstrates that syllable people hear depends on the mouth movement they see (McGurk and McDonald [7]). Similarly, the ventriloquist effect illustrates that when the visual and auditory stimuli provide conflicting information about the direction of sound, visual stimulus usually dominates (Alais and Burr [8]). In another study, Shams et al. have found that when a flash appears on the screen only once but accompanied by two beeps, people usually report seeing two flashes, thereby demonstrating the dominance of auditory mode over visual. Indeed, Yokosawa and Kanaya [9] have pointed out that the interaction between visual and auditory modality is rather complex and depends on the congruency between the two modalities.

Similarly, the complexity of interaction between the visual and the tactile stimuli is demonstrated by the rubber-hand effect. The participant watches a rubber hand being stroked, while having her or his own hand being stroked simultaneously (but out of sight). It takes only a few seconds for the participant to attribute body ownership and awareness to the rubber hand to such an extent that when the rubber hand is hit or stabbed, they feel as if their own hand was hit or stabbed (Botvinick and Cohen [10]).

Interaction between the audio and tactile stimuli is demonstrated by the parchment skin illusion (Jousmki and Hari [11]). Participants rub their hands

together and this sound is recorded. Then they rub their hands together again, while listening to the playback of the previously recorded sound in which the high frequency component is amplified. Most of the participants then report feeling as if their hands are dry like parchment paper.

Based on various such studies, it has been suggested that multisensory integration is a complex mechanism involving top-down and bottom-up processes, and incorporating statistical optimization of the available information (Ernst and Banks [12]; Tsakiris and Haggard [13]).

Multimodal integration has also been studied for affective effects. Fagel [14] found that when facial expressions and speech prosody provide conflicting emotions, sometimes emotion manifested in one of the channels dominates, but sometimes a new emotion emerges from the interaction. For example, sad video and happy audio might be interpreted as angry, and happy video and sad audio might be interpreted as depressed. (See also Li et al. [15])

4 Integration of Visual-Haptic Stimuli

In our past research (Akshita et al. [16]), we did a study on the interaction of emotional cues presented in visual and haptic modalities. Our goal was to use the insights from this study to create multimodal affective interfaces that are more effective than the usual monomodal interface. For example, when you are viewing an image or a video, your emotional experience could be enhanced by adding accompanying haptic stimulation via the vibrations from a phone, a smartwatch, or some other such device.

Our study was carried out in four steps: (1) create an affective visual dataset; (2) create an affective haptic dataset; (3) understand affective visual-haptic interaction; and (4) explore this interaction in terms of haptic features. We used the cicumplex model of emotion, which represents emotional response in a two-dimensional space of valence and arousal (Larsen and Diener [17]). Arousal represents the intensity of emotional response, and valence represents its pleasantness. So, for example, bordeom has low arousal and negative valence; serenity has low arousal and positive valence; happiness has high arousal and positive valance; and anger has high arousal and negative valence.

In the first step, we used the International Affective Picture System dataset called IAPS (Lang et al. [18]), which is a well-cited dataset in emotion research containing 1192 images with different valence and arousal ratings. We verified the validity of the IAPS for Indian participants by taking a representative sample of 120 images, and measuring their valence and arousal ratings with eight Indian participants. We found no statistical difference between our measured ratings and those in the IAPS dataset, which meant that we can assume that the IAPS ratings apply to Indian participants as well.

In the second step, we constructed a haptic dataset along the four dimensions of intensity, frequency, waveform and rhythm. First we sampled each dimension based on the limits of human perception and the haptic device, which was the ViviTouchTM actuator with a frequency range of 0 to 200 Hz. This generated a

set of 390 stimuli. Next, we pruned the dataset by performing a discrimination test to ensure that the participants can distinguish between pairs of neighbouring stimuli. This gave us (10 rhythm patterns) × (3 waveforms: sinusoidal, sawtooth, pulse) × (3 frequencies: 55 Hz, 110 Hz, 165 Hz) × (2 intensity levels: 20 dB, 35 dB) = 180 stimuli. We presented these stimuli to 16 participants in two sessions, and asked them to assign each stimulus to one of the nine emotional groupings based on its valence and arousal. This gave us our haptic dataset of 180 stimuli, each with its valence and arounsal ratings.

In the third step, we studied how visual and haptic modalities interact together. For this, we created four sets of supporting stimuli, where visual and hapic stimuli cohere with each other: so low valance low valance, low arousal low arousal, high valence high valence, and high arousal high arousal. Similarly, we also created four sets of conflicting stimuli: low valence high valence, high valence low valence, low arousal high arousal, high arousal low arousal. In each set, there were five stimuli. Nineteen participants took part in this study.

In analyzing the results, we compared the affective response of each combined visual-haptic stimulus with the responses of the visual-only and haptic-only situation. For the case of valence-supporting set, we found no significant difference among visual only, haptic only and visual-haptic combined situations. For valence-conflicting set, we found that visual-haptic ratings were similar to visual-only ratings. For the arousal, we found that for both support and conflict situations, the visual-haptic arousal was significantly higher than the visual-only arousal. This shows that adding haptic stimulation enhances the arousal of a visual stimulus.

In the fourth step, we explored in more detail which features of the haptic stimuli have the most influence on the arousal value. We experimented with 24 participants in two groups. We found that waveform and rhythm do not have any significant effect on the increase of the arousal value, but intensity and frequency do affect the arousal value significantly. This suggests that to enhance the arousal value of a visual stimulus, we need to focus on the frequency and intensity of the accompanying haptic stimulation.

5 Integration of Audio-Haptic Stimuli

In a related work, we conducted experiments to study the interaction between auditory and haptic modalities. For this study, we used the International Affective Digitized Sounds (IADS) system (Bradley and Lang 2007), which is a dataset containing 167 different environmental sounds with associated valence and arousal ratings. Nineteen participants took part in this experiment. Similar to the visual-haptic case, we created four sets of supporting stimuli, and four sets of conflicting stimuli and measured the affective response for each stimulus.

Then we compared the affective response of each combined audio-haptic stimulus with the responses of the auditory-only and haptic-only situation. We found that in the conflicting case, the auditory-haptic valence is similar to auditory-only valence. In the supporting case, there is a more complex interaction:

combining high-valence audio and high-valence haptic stimuli results in an auditory-haptic stimulus that has a lower valence, which seems counterintuitive and needs further investigation. For arousal, in most cases, the presence of haptic stimuli increases the arousal of the auditory stimuli. However, in case of conflicting arousal, when the auditory arousal is high, there is no significant difference between auditory-haptic and auditory-only arousal.

6 Conclusion and Future Work

Our preliminary research shows that adding haptic stimulation increases the arousal response of the accompanying visual or auditory stimulus. However, this needs to be investigated further by using other haptic devices, and other parts of the body like the wrist (for smartwatches). Haptics is a relatively unexplored modality for commuincating information and emotions. But several researchers are now studying characteristics of haptic processing, and experimenting with novel devices and interfaces. We can expect many innovations in this area in the near future.

Another interesting research direction is to explore if the affective value of a visual or auditory stimulus can be predicted from its low-level features. For example, if we look at an image from the IAPS dataset, is it possible to predict its affective value by processing the image and extracting various low-level (and high-level as well) features from it. If such techniques can be developed and validated, then we will have a way to quickly assign an affective value to an image, and generate an appropriate accompanying haptic stimulation.

It would also be useful to explore techniques that dampen the arousal response, for they may be used to lessen the effect of viewing disturbing and traumatic images.

As we were not able to find any way to influence the valance response of a visual or auditory stimulus, further studies are needed to explore other ways to manipulate valence.

Our brain naturally integrates inputs from different modalities to construct an object representation that we consider as real. Studying these integration mechanisms and incorporating them into virtual reality and mixed reality systems remains a challenge for the future technology.

References

1. Picard, R.W.: Future affective technology for autism and emotion communication. Philos. Trans. Roy. Soc. B. Biol. Sci. **364**(1535), 3575–3584 (2009)
2. Lee, C.H.J., Chang, C., Chung, H., Dickie, C., Selker, T.: Emotionally reactive television. In: Proceedings of the 12th International Conference on Intelligent User Interfaces, pp. 329–332. ACM (2007)
3. Danziger, S., Levav, J., Avnaim-Pesso, L.: Extraneous factors in judicial decisions. Proc. Nat. Acad. Sci. **108**(17), 6889–6892 (2011)

4. Jayant, C., Acuario, C., Johnson, W., Hollier, J., Ladner, R.: V-braille: haptic braille perception using a touch-screen and vibration on mobile phones. In: Proceedings of the 12th international ACM SIGACCESS conference on Computers and accessibility, pp. 295–296. ACM (2010)
5. Amemiya, T., Sugiyama, H.: Design of a haptic direction indicator for visually impaired people in emergency situations. Comput. Helping People Spec. Needs pp. 1141–1144 (2008)
6. Tsetserukou, D., Neviarouskaya, A., Prendinger, H., Ishizuka, M., Tachi, S.: iFeel_IM: innovative real-time communication system with rich emotional and haptic channels. In: CHI 2010 Extended Abstracts on Human Factors in Computing Systems, pp. 3031–3036. ACM (2010)
7. McGurk, H., MacDonald, J.: Hearing lips and seeing voices (1976)
8. Alais, D., Burr, D.: The ventriloquist effect results from near-optimal bimodal integration. Curr. Biol. **14**(3), 257–262 (2004)
9. Yokosawa, K., Kanaya, S.: Ventriloquism and audio-visual integration of voice and face. Brain and Nerve= Shinkei Kenkyu no Shinpo **64**(7), 771–777 (2012)
10. Botvinick, M., Cohen, J.: Rubber hands' feel'touch that eyes see. Nature **391**(6669), 756 (1998)
11. Jousmäki, V., Hari, R.: Parchment-skin illusion: sound-biased touch. Curr. Biol. **8**(6), R190–R191 (1998)
12. Ernst, M.O., Banks, M.S.: Humans integrate visual and haptic information in a statistically optimal fashion. Nature **415**(6870), 429–433 (2002)
13. Tsakiris, M., Haggard, P.: The rubber hand illusion revisited: visuotactile integration and self-attribution. J. Exp. Psychol. Hum. Percept. Perform. **31**(1), 80 (2005)
14. Fagel, S.: Emotional McGurk effect. In: Proceedings of the International Conference on Speech Prosody, Dresden, vol. 1. Citeseer (2006)
15. Li, A., Dang, J.: A cross-cultural investigation on emotion expression under vocal and facial conflict-also an observation on emotional McGurk effect. In: International Symposium on Biomechanical and Physiological Modeling and Speech Science, Kanazawa, I, pp. 37–50 (2009)
16. Alagarai Sampath, H., Indurkhya, B., Lee, E., Bae, Y., et al.: Towards multimodal affective feedback: interaction between visual and haptic modalities. In: Proceedings of the 33rd Annual ACM Conference on Human Factors in Computing Systems, pp. 2043–2052. ACM (2015)
17. Larsen, R.J., Diener, E.: Promises and problems with the circumplex model of emotion (1992)
18. Lang, P.J., Bradley, M.M., Cuthbert, B.N.: International affective picture system (IAPS): technical manual and affective ratings. NIMH Center for the Study of Emotion and Attention, pp. 39–58 (1997)

Cognitive and Emotive Robotics: Artificial Brain Computing Cognitive Actions and Emotive Evaluations, Since 1981

Stevo Bozinovski[1,2(✉)]

[1] Mathematics and Computer Science Department,
South Carolina State University, Orangeburg, USA
sbozinovski@scsu.edu
[2] Faculty of Computer Science and Engineering,
Sts Cyril and Methodius University, Skopje, Macedonia

Abstract. This plenary keynote paper marks 35-th anniversary of description of the first artificial brain, a neural network which in addition of computing cognitive actions, computes emotive evaluations of the consequence of those actions. It was designed in 1981, as part of an effort within the Adaptive Networks Group of the COINS Department of University of Massachusetts in Amherst to solve the problems of (1) designing a delayed reinforcement learning mechanism for artificial neural networks and (2) designing a self learning system which will learn without external reinforcement of any kind. This paper describes steps which led toward solution of those problems. The proposed artificial brain, named Crossbar Adaptive Array, can be viewed as a model of cognition-emotion interaction in biological brains, and can be used in building brains for cognitive and emotive robotics.

Keywords: Emotional robots · Computer simulation of the brain · Cognition-emotion interaction · Secondary reinforcement · Emotion backpropagation · Adaptive Networks Group · Crossbar Adaptive Array · Artificial brain

1 Introduction

Contemporary robotics devotes a significant attention to emotional expressions produced by robots. There are already robots on the market such as Nao, Pepper, and Romeo [1], which are able to engage in emotion colored conversation with humans. It is important step forward in Artificial Intelligence (AI), which started by neglecting importance of emotion and focusing mostly on cognition. There is also an effort of simulation of brain functioning [2], including real connections between brain neurons [3]. Those efforts need a model of the brain functioning which includes emotions among other activities of the brain.

The first AI paper which mentioned interaction with cognition, emotion, and motivation was written in 1967 by Simon [4]. The first paper that proposes a working model, both in mathematics and simulation, including emotions and cognition was written in 1981 [5–7]. The paper introduced a neural network named Crossbar Adaptive Array (CAA), which can compute in crossbar fashion, in the same memory structure,

G. Stojanov and A. Kulakov (eds.), *ICT Innovations 2016*,
Advances in Intelligent Systems and Computing 665,
https://doi.org/10.1007/978-3-319-68855-8_2

both cognitive decisions about actions and behaviors, and feelings from consequences of those actions. CAA was the first artificial brain.

Now, on the 35-th anniversary, this paper describes and comments on that work, the context which led to the work, as well as consequences, follow ups of that work. After this introduction, the paper starts with the pioneering events of development of Artificial Intelligence in Macedonia and knowledge on abstract automata graphs as well as self-organizing systems, which provided ground for designing the CAA. The third chapter describes people and events, who influenced the work described here to be carried out within the Adaptive Networks Group (ANW) of the University of Massachusetts at Amherst. The fourth chapter describes the 1980/81 ANW group. The fifth chapter describes the research challenges posed in front of ANW group in 1981. The sixth chapter describes the two approaches and the two architectures developed inside ANW group to solve the challenges. The seventh chapter points out the 1981 results. The eight chapter comments on follow-up works related to the CAA architecture, carried out by members of the 1981 ANW group.

2 Abstract Automata, Chess Playing Programs, Neural Networks

In 1968, the first paper written in Macedonian language [8], started development of Computer Sciences, including Artificial Intelligence in Macedonia [9]. The paper was presented as a lecture at the Seminar on Cybernetics organized by professor Gorgi Cupona. It was based on the third chapter of the book of Glushkov [10, 11].

The concept of automaton is related to artificial neural networks from the early works on automata theory (e.g. [12]). The attached concept of *state* and automaton graph (e.g. [13]) makes it basis for Computer Sciences, including Artificial Intelligence. The concept of state apace is one of the bases for disembodied intelligence while the concept of agent (automaton interacting with its environment) is crucial for embodied AI. Using automata to model Turing Machines, agents, and neural networks is described for example in [9].

In 1981, development of CAA architecture was based on introducing emotionally colored states [5–7] in the representation of the problem, solution of which was the proposed CAA architecture. Example of emotionally colored graph of an automaton is given in Fig. 1.

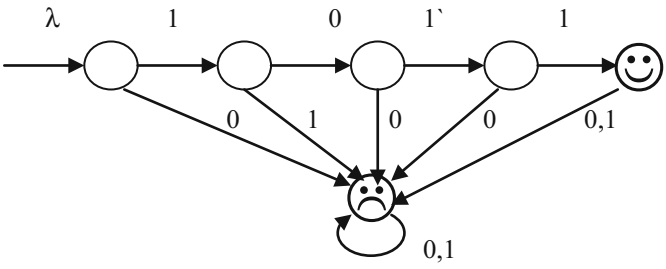

Fig. 1. Emotional graph of an automaton.

This automaton recognizes the language {1011}, a problem stated in the lectures on theory of compotation given by Moll and Arbib in 1980 and 1981 at the COINS department at UMass/Amherst. The author of this text attended the lectures and learned from lecture notes which later become a book [14]. In the lectures and the book the goal (accepting) state was denoted by a double circle which is usual in the theory of automata and formal languages. In Fig. 1 the accepting (goal) state is emotionally colored with emoticon ☺, while the "no-hope" (trap) state which in [14] has no special denotation, here is represented by emoticon ☹. Now the author of this book is teaching theory of computation at South Carolina State University, and emotionally colored graphs are a tool in teaching formal language acceptors and other problems related to automata and search spaces.

In mentioning the pioneering steps in development of AI in Macedonia, let us mention that the first AI computer program by a Macedonian author was written by the author of this text and it was a chess endgame with two kings and a rock. It was written in Fortran for IBM 1130 computer, in 1969. It had a main program named SAH which was doing interaction with a human player over the console typewriter. On demand by the human (call DATSW), it was drawing the current position on the system plotter. There were three subroutines: POTEZ subroutine evaluated the move of the human player for correctness, KODER encoded the move written in standard chess notation (e.g. KE6) into internal representation and vice-versa, and POZIC analyzed the position and decided the program move. There was one function, MATIR, which decided whether the position is a checkmate.

The first neural network program by a Macedonian author was written 1970 [15] and was simulating a perceptron according to the book [11]. The first paper published in a journal was about a neural network simulating Pavlov's classical conditioning. [16]. The first paper presenting a realization of a perceptron using digital circuits appeared in 1976 [17] showing realization of a perceptron by digital circuits, by an array or counters. By 1978, a perceptron was simulated which was able to learn to recognize 26 letter of Latin alphabet.

3 Minsky, Klopf, Arbib

Here we will mention three people relevant for the 1981 event described in this paper.

In 1969 Marvin Minsky and Seymour Papert wrote a book about perceptrons [18]. They mentioned some issues related to ability of perceptrons to recognize patterns. Minsky was very influential, partly because he was a MIT professor, partly due to his book on computation [19], where the treated abstract automata as neural elements, and partly because of his influential papers. The book was interpreted by some people that it says basically that the neural networks approach toward artificial intelligence is not a promising one. The result was that NSF stopped funding artificial neural networks (ANN) research, and in USA at the end of 1979 there were no groups working on ANN financed by NSF.

Klopf worked with Avionics Laboratory, Wright Patterson Air Force Base (WPAFB) in Dayton, Ohio [20]. He proposed that Air Force should finance a research on goal seeking systems from goal seeking components. In 1977 a group was formed at

the Computer and Information Science (COINS) Department at the University of Massachusetts at Amherst, which will work on the topic.

Arbib wrote a book named "Brain, Machine, and Mathematics" [21], which was published also in Russian language in 1968 [22]. In 1969 he published a book on abstract automata [23]. The author of this text became familiar with the books of Arbib's [22] and Minsky's [18] as a student of Electrical Engineering Department in Zagreb, being regular visitor of the Foreign Language Bookstore (popular name "Russian Bookstore"). In 1978 the author of this text met Arbib at the symposium Informatica 1978 in Bled. After that, obtaining a Fulbright scholarship, the author of this text went to University of Massachusetts in Amherst. It is interesting that in the time when in USA research on artificial neural networks did not receive federal funding, a researcher from Macedonia joined a group funded by US military. It was result of the momentum gained in 1968 when the author of this text for the first time has seen the chapter about self-organizing system in the Glushkov's book [11].

4 Adaptive Networks Group (ANW), 1980–1981

The members of Adaptive Networks Group in 1980–1981 were Klopf (WPAFB Project Officer), Nico Spinelli (Principal Investigator), Arbib (advisor) Barto (postdoc), and the graduate students Sutton, Anderson, Jack Porterfield, Ted Selker, and Bozinovski. The group worked on neural networks with focus on reinforcement learning [24, 25]. By 1981 two very important papers were published. One [26] was about establishing relation between Rescorla-Wagner theory of classical conditioning [27] and Widrow-Hoff optimization procedure [28]. The other [29] was a great demonstration of possibility offered by reinforcement learning, a solution of a landmark learning task.

5 ANW Challenges, 1981

In 1981 Sutton pointed out a challenge of delayed reinforcement learning which was never solved with a neural network. The problem was how to build a neural network agent which will be able to learn in cases when reinforcement does not appear after every action of the agent, but rather occasionally, for example at the goal state. There are many examples of such problem, one of them being the game of chess where a player performs a move M but it will not receive evaluation (positive or negative reinforcement) until many moves later; when by backpropagation reasoning it might be possible to say that the move M was good or bad. Sutton stated an instance of such a problem, a maze learning instance, where a path should be learned in a maze, but reinforcement (e.g. food) is only available at the goal state of the maze. The other instance was pointed out by Anderson, and it was the well known pole balancing task. The task can be described as: given dynamics of a cart-pole system, and using input force, balance the pole such that it remains in vertical position. So the challenge was to build a neural network which will be able to learn in cases of delayed reinforcement.

In 1981 Bozinovski pointed *the challenge of self-learning*, learning without any external reinforcement, neither advice giving teacher nor a scalar (punish/reward) type of reinforcement. He also took a challenge to build such a system.

6 Two Approaches Toward the Challenges

There were two approaches and two architectures developed to solve the delayed reinforcement learning problem. The first one was Actor/Critic (A/C) architecture by Barto and Sutton, experiments for which were carried out by Sutton; the approach was based on external reinforcement. The second one was Crossbar Adaptive Array (CAA) architecture by Bozinovski who also carried out the experimental work; the approach was self learning, learning without any external reinforcement. For both approaches, the dynamics of cart-pole system was carried out by Anderson, following the description given in [30]. Figure 2 show both approach architectures.

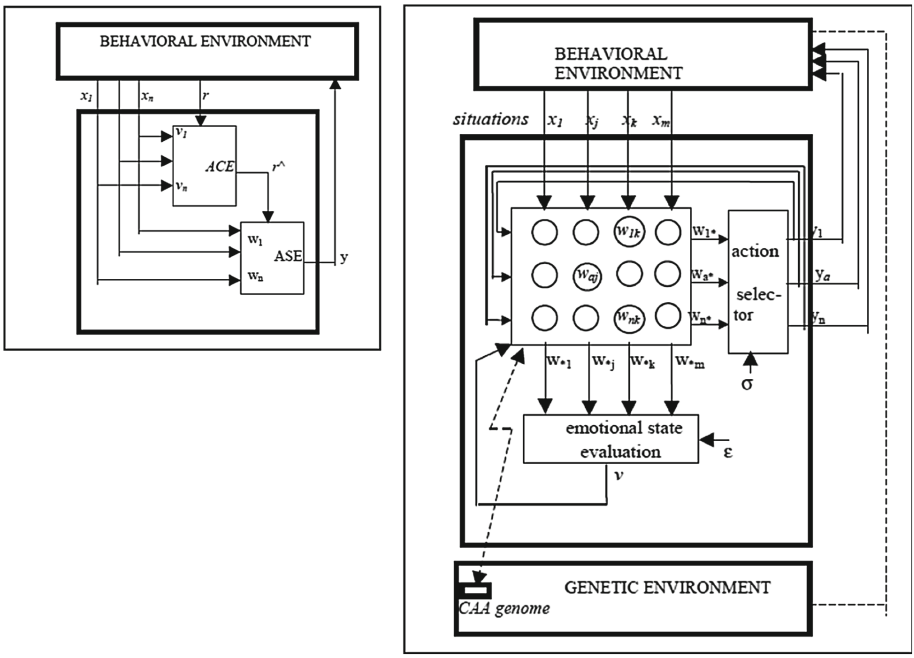

a. A/C architecture **b.** CAA architecture

Fig. 2. The architectures used to solve the delayed reinforcement learning problem.

The challenged graphs on which the A/C and CAA architectures were tested are shown in Fig. 3. Example of a challenge maze for the A/C architecture is shown in Fig. 3a. Sutton has chosen as challenge mazes from animal learning, theory, with one positively reinforcing state, the goal state. Here the goal state is represented as double

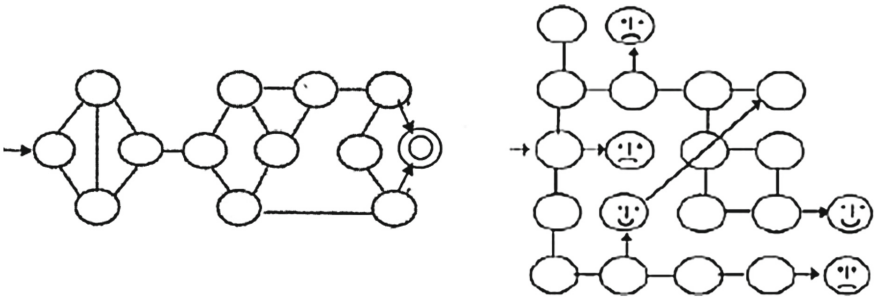

a. A/C challenge **b.** CAA challenge

Fig. 3. Challenging environments for delayed reinforcement learning architectures

circled, as in automata theory. Figure 3b shows a maze which was challenge for the CAA architecture. Bozinovski has chosen to model the mazes from the 1980 VAX/VMS computer game "Dungeons and dragons". Figure 3b shows such a maze which is simplification of the dungeon named Telengard. It had one goal state but also three states that should be learned to avoid, and one teleportation state going through which CAA also felt positive reinforcement although it is not a goal state. The non-neutral states were emotionally colored. From the very beginning, emotionally colored states were part of the CAA design.

6.1 Crucial Concept of Actor/Critic Architecture: Prediction

The basic idea of the A/C architecture was the concept of *prediction of reinforcement*. A predictor module, named adaptive critic element (ACE) will be built, which will be able to receive a primary reinforcement r from the environment, either occasionally or only once, and will be able to supply an internal reinforcement $r^{\wedge}$ to the element ASE (associative search element) after every action performed by ASE. Basically ASE was a standard reinforcement learning module which receives reinforcement after each action, where reinforcement is produced by a system other than environment, in this case the system ACE. The search is achieved by introducing *Gaussian noise*. Learning rules are high order second order and even higher with introduced eligibility traces. The two memory structures are of same dimension. Inputs x to both ACE and ASE elements have eligibility traces. The equations are rather complex and of higher than the first order. The detailed description is given in [31].

6.2 Crucial Concept of Crossbar Adaptive Array Architecture: Emotion

As Fig. 2b shows, the CAA architecture has a system of *state evaluation*. That concept introduced 1981 [7] was a new concept in reinforcement learning research. At that time it was not known to the ANW Group that such a concept was already used in Dynamic Programming [32]. Eight years later, in 1989, Dynamic Programming will be explicitly

related to reinforcement learning by Watkins [33]. However by introducing state evaluation concept the 1981 CAA implicitly related reinforcement learning to Dynamic Programming.

The 1981 CAA also related the state evaluation to feeling and emotion. Evaluation of an internal consequence state was *felt* by the CAA agent. Introducing a single memory structure which computes both the learned actions and the feelings due to the consequence of those actions, made the CAA architecture the first artificial brain. It modeled the cortex (cognitive) part as well as limbic system (emotive) part of the brain. As opposite the A/C architecture contained only the cognitive part of the brain (computing learned action as well as prediction of that action).

The search process is defined by a variable named searching strategy σ. It can be a random walk, in which case is modeled as a uniform (rather than Gaussian) distribution. It models curiosity of the system.

There is only one memory structure of the same size as one of the A/C memory structures. It computes in a crossbar fashion both actions (behaviors) and emotional evaluations. The learning process is described with a single, first order equation.

$$w_{aj} = w_{aj} + v_k \tag{1.1}$$

which, written as difference equation is

$$w_{aj}(t) = w_{aj}(t-1) + x_j(t-1)y_a(t-1)v(t) \tag{1.2}$$

Here w_{aj} is memory value associated with performing action a in situation j, and v_k is emotion evaluation obtained from the consequence situation k.

The *CAA crossbar learning procedure is given by a pseudocode* describing a step of the procedure

(1) state *j:* compute action *a* biasing on $w_{*}j$, sent it to the environment
i: the environment gives back the state *k*
(2) state *k:* compute emotion *vk* using $w_{*}k$. then compute overall emotion *v*
(3) state *j:* increment w_{aj} using *v* (backpropagate emotion and learn)
(4) change state: *j* = *k;* goto 1

The pseudocode way of description given in CAA later become a became a standard way of describing a learning procedure in a reinforcement learning research.

6.3 CAA Secondary Reinforcement Learning (Emotion Backpropagation)

The emotion backpropagation process used in CAA follows the concept of secondary reinforcement, known in psychology (e.g. [34]): A primary external reinforcement *r* creates an internal state *s* in a brain, after which the state *s* becomes reinforcement itself (secondary reinforcer). A brain then tends to achieve state *s* expecting from there to reach reinforcement *r*. It is actually an emotion backpropagation mechanism.

As Fig. 4 shows, a state, j, performs an action, *a.* It will transition the system to the emotionally colored state k, and that emotion will be backpropagated to the action *a*. The

action will be updated in value such that the chance of being chosen next time is increased. Now the action a is motivationally colored. It contains motivation (or intention) to be chosen, because it will bring the agent to a positive emotion. This backpropagation chain of emotionally colored states and motivation colored actions is the basis of the CAA secondary reinforcement learning an emotion backpropagation. Let us note that CAA offered a first model which mathematically connects all the three general functions of the brain: the cognitive (knowing and understanding), the conative (intentions, dispositions), and the emotive (emotions) e.g. [35].

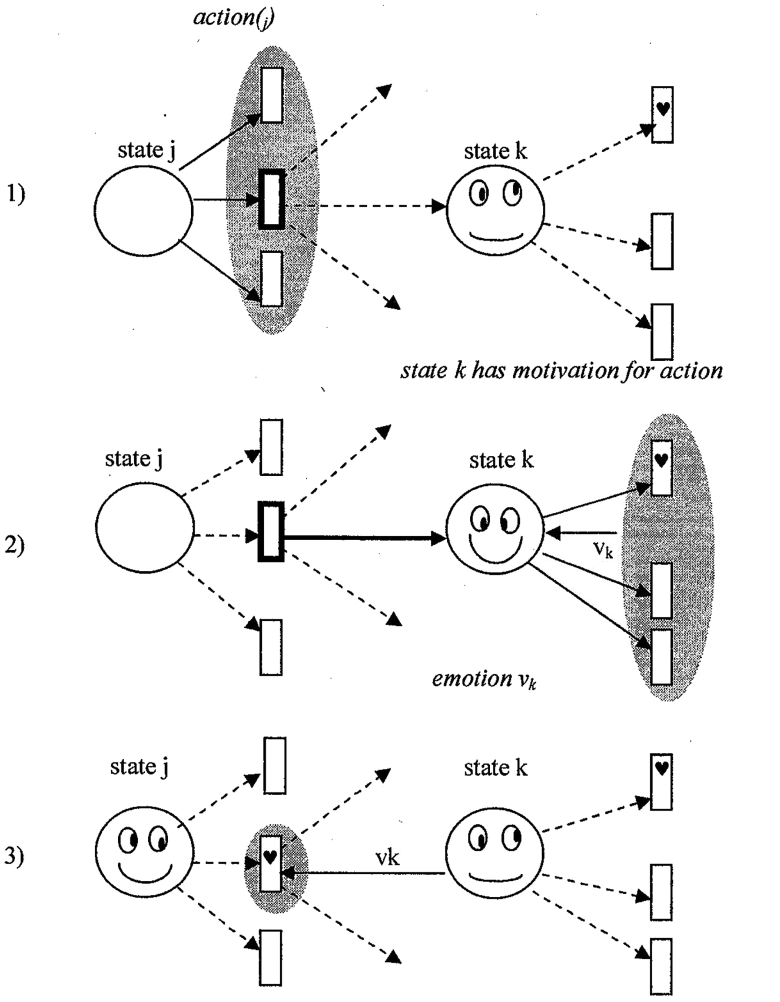

Fig. 4. The CAA secondary reinforcement (emotion backpropagation) mechanism.

6.4 CAA Self-Learning Solution

The other ANW challenge, proof of possibility of a self learning system was also solved by the CAA approach. The solution was in introducing a genetic environment in addition to behavioral environment, where from the CAA architecture inherits, by way of genetic strings (chromosomes), the initial, intrinsic emotions. That was something new in neural network research. Example of such intrinsic emotion is "if you feel cold, that is dangerous situation, try to avoid it". The concept of "cold" is related to "danger" by genetics, it is not learned, because it is basic survival need. Once initial emotions are defined by genetics, then using the emotion backpropagation mechanism, an agent is able to learn a behavioral policy in an environment. The CAA also is able to exporting the memory after learning, as a chromosome, following the principle of Lamarckian evolution.

7 1981 Results

In 1981 the only architecture that solved the delayed reinforcement learning challenge was the CAA architecture. It also solved the self learning challenge. The solution was presented in front of ANW group [5] and as overhead presentation for the COINS department under title "Adaptive Arrays". Separate presentation was given on pole balancing problem [36] in which it was also reported on parallel programming with inter-process communication by which the problem was solved: two processes CAA (written by Bozinovski) and ENVIRONMENT which contained the cart-pole dynamics (written by Anderson) were running on separate terminals and interchanging information via VAX/VMS system mailboxes, The system software routine for inter-process communication was written by Bob Heller. That was a pioneering work on application of parallel programming in Artificial Intelligence.

The CAA architecture also solved the problem of self-learning, i.e. learning without external reinforcement. For that, it introduced genetic environment and intrinsic emotions that are genetically given, as well as genetic strings, chromosomes, which are inherited from genetic environment to be primary reinforcers.

8 After 1981: Relevant Works

The CAA architecture was described in 1982 in an abstract [6] and as a paper [7]. The A/C approach showed the solution of pole balancing problem in 1983 [31]; it is interesting that in that paper the terms "delayed reinforcement learning" and "secondary reinforcement learning" were not used, although those were key terms of the challenge of the ANW group in 1981.

In 1986 a book appeared [37] after which it was clear that the neural network research should become part of the mainstream Machine Learning and Artificial Intelligence. However in 1987 there was a European meeting on Machine Learning where there was still a view that neural nets are not part of mainstream Machine Leaning. Some works of the participants were published, and some were presented as

position papers with no publication. Bozinovski presented a position paper of CAA research, in front of the audience in which was Watkins, who had a presentation on search and cross-validation and his paper was published [38].

Two years later in 1989 Watkins presented method of learning from delayed rewards named Q-learning method [33]. The work showed solution of maze learning instance of the delayed reinforcement learning, under name "learning with delayed rewards". In 1990 the work was shown together with Suttoin and Barto [39]. The eight years earlier CAA memory was reintroduced, and named Q-table, where Q-elements Q (a,s) and exactly the same and with the same meaning in a crossbar CAA memory. The learning rule, named Q-learning was first order, confirming the CAA solution, as difference from higher order learning rules used in A/C architecture. Relation between Q learning and CAA crossbar learning is evaluated in two ways. One is that CAA learning is a fore-runner of Q learning [40]. We argue that Q learning is an eight years later extension of CAA crossbar learning with addition of a forgetting parameter.

Later the CAA approach was developed into a Consequence Driven Systems theory, which models, among other concepts, personality, motivation, emotion, curiosity, and learning (e.g. [41]).

The self learning approach by CAA in 1981 was reintroduced in 2004 [42], where the concept of intrinsic motivation was used rather than the concept of emotion. The "classical RL system" [43] was redrawn to represent a self-learning system with no external reinforcement, as shown 22 years earlier [7].

9 Conclusion

In the time of increased interest of robotics industry toward emotion-showing robots, we point out that robotics has still a challenge in dealing with emotion-cognition interaction which is a phenomenon in a human brains. This paper points toward the first operational, mathematical and programming model of emotion-cognition interaction, which was proposed in 1981 as part of research carried out by ANW group of University of Massachusetts at Amherst. The paper also points toward some follow ups of the efforts invested by the ANW group in 1981.

Acknowledgement. The author was able to study the Glushkov's book due to 1968 ideas of Gorgi Cupona for development of computer sciences in Macedonia. The author would like to thank Michael Arbib and Nico Spinelli who enabled working with the 1980/81 ANW group. The author would also like to thank Andrew Barto for allowing the author to join the Adaptive Networks Group again in 1995/96.

References

1. Softbank Robotics: Robots. http://www.ald.softbankrobotics.com
2. Furber, S.: To build a brain. IEEE Spectr. **49**(8), 45–49 (2012)
3. Strickland, E.: A wiring of the brain. IEEE Spectr. **50**(5), 12–14 (2013)
4. Simon, H.: Motivational and emotional controls of cognition. Psychol. Rev. **74**, 29–39 (1967)

5. Bozinovski, S.: Crossbar Adaptive Array. ANW Group, Computer and Information Science Department, University of Massachusetts at Amherst, 25 November 1981
6. Bozinovski, S.: A self-learning system using secondary reinforcement. In: Abstracts of the Sixth European Meeting on Cybernetics and Systems Research - 1982, Abstract 87. Austrian Society of Cybernetic Studies, Vienna (1982)
7. Bozinovski, S.: A self-learning system using secondary reinforcement. In: Trappl, R. (ed.) Cybernetics and Systems Research, pp. 397–402. North-Holland, New York (1982)
8. Bozinovski, S.: Abstract Automata. In: Cupona, G. (ed.) First Seminar on Cybernetics, Mathematical Institute with Numeric Center, Skopje (1968) (in Macedonian)
9. Bozinovski, S.: Professor Cupona and the first lecture on abstract automata in Macedonia. Math. Maced. **8**, 79–94 (2010)
10. Glushkov, V.: Introduction to Cybernetics. Academy of Sciences of Ukrainian SSR, Kiev (1964). (in Russian)
11. Glushkov, V.: Introduction to Cybernetics. Belgrade University, Belgrade (1967). (Translated to Serbian)
12. Kleene, S.: Representation of events in neural nets and abstract automata. In: Shannon, C., McCarthy, J. (eds.) Automata Studies, pp. 3–42. Princeton University Press, Princeton (1956)
13. Moore, E.: Gedanken-experiments on sequential machines. In: Shannon, C., McCarthy, J. (eds.) Automata Studies, pp. 129–156. Princeton University Press, Princeton (1956)
14. Arbib, M.A., Kfoury, A.J., Moll, R.N.: A Basis of Theoretical Computer Science. Springer, New York (1981)
15. Bozinovski, S.: Perceptron problematics: teaching in pattern recognition. Paper for the First-of-May student research competition. University of Zagreb (1970). (in Croatian)
16. Bozinovski, S.: Introduction to psychocybernetics. Rev. Psychol. **5**, 115–128 (1975). Zagreb. (in Croatian)
17. Bozinovski, S., Fulgosi, A.: The influence of similarity and the transfer of training on the perceptron training. In: Proceedings of Symposium Informatica, 3-12-1-5, Bled (1976). (in Croatian)
18. Minsky, M., Papert, S.: Perceptrons: an Introduction to Computational Geometry. MIT Press, Cambridge (1969)
19. Minsky, M.: Computation: Finite and Infinite Machines. Prentice-Hall, Upper Saddle River (1967)
20. Klopf, H.: Brain functioning and adaptive systems. Air Force Technical Report, AFCRL 72-0164 (1972)
21. Arbib, M.: Brains, Machines, and Mathematics. McGraw-Hill, New York (1965)
22. Arbib, M.: Brain, Machine, and Mathematics. Nauka, Moskow (1968). (in Russian)
23. Arbib, M.: Theories of Abstract Automata. Prentice-Hall, Upper Saddle River (1969)
24. Mendel, J., McLaren, R.: Reinforcement learning control and pattern recognition systems. In: Mendel, J., Fu, K.-S. (eds.) Learning and Pattern Recognition Systems, pp. 287–318. Academic Press, Gurugram (1970)
25. Widrow, B., Gupta, N., Maitra, S.: Punish/Reward: learning with a critic in adaptive threshold systems. IEEE Trans. Syst. Man Cybern. **3**(5), 455–465 (1973)
26. Sutton, R., Barto, A.: Toward a modern theory of adaptive networks: expectation and prediction. Psychol. Rev. **88**, 135–170 (1981)
27. Rescorla, R.A., Wagner, A.R.: A theory of Pavlovian conditioning: variations of the effectiveness of reinforcement and non-reinforcement. In: Blake, A., Procasy, C. (eds.) Classical Conditioning II: Current Research and Theory. Appleton-Century-Crofts, New York (1972)

28. Widrow, B., Hoff, G.: Adaptive switching circuits. IRE WESCON Conv. Rec. pp. 96–104 (1960)
29. Barto, A.G., Sutton, R.S., Brouwer, P.S.: Associative search network: a reinforcement learning associative memory. Biol. Cybern. **40**, 201–211 (1981)
30. Cannon, R.: Dynamics of Physical Systems. McGraw Hill, New York (1967)
31. Barto, A., Sutton, R., Anderson, C.: Neuronlike elements that can solve difficult learning control problems. IEEE Trans. Syst. Man Cybern. **13**, 834–846 (1983)
32. Bellman, R.: Dynamic Programming. Princeton University Press, Princeton (1957)
33. Watkins, C.: Learning from delayed rewards. Ph.D. thesis, Kings College, Cambridge, England (1989)
34. Keller, F., Shoenfeld, W.: Principles of Psychology. Appleton-Century-Crofts, New York (1950)
35. Bozinovski, S.: Robotics and Intelligent Manufacturing System. Gocmar Press, New York (1997). (in Macedonian)
36. Bozinovski, S.: Inverted pendulum learning control. ANW Memo, Computer Science Department, University of Massachusetts, Amherst, 10 December 1981
37. Rumelhart, D., McClelland, J., The PDP Group: Parallel Distributed Processing: Explorations in the Microstructure of Cognition. MIT Press (1986)
38. Watkins, C.: Combining cross-validation and search. In: Bratko, I., Lavrac, N. (eds.) Progress in Machine Learning, Proceedings of the 2nd European Working Session on Learning, pp. 79–87, Sigma (1987)
39. Barto, A., Sutton, R., Watkins, C.: Learning and sequential decision making. In: Gabriel, M., Moore, J. (eds.) Learning and Computational Neuroscience: Foundations of Adaptive Networks, pp. 539–602. MIT Press, Cambridge (1990)
40. Barto, A.: Reinforcement learning. In: Omidvar, O., Elliot, D. (eds.) Neural Systems for Control, pp. 7–30. Academic Press, Gurugram (1997)
41. Bozinovski, S.: Motivation and emotion in anticipatory behavior of consequence driven systems. In: Butz, M., Sigaud, O., Gerard, P. (eds.) Proceedings of the Workshop on Adaptive Behavior in Anticipatory Learning Systems, Edinburg, pp. 100–119 (2002)
42. Barto, A., Singh, S., Chentanez, N.: Intrinsically motivated learning of hierarchical collections of skills. In: Proceedings of the 3rd International Conference on Developmental Learning (ICDL 2004), LaJolla, CA (2004)
43. Sutton, R., Barto, A.: Reinforcement Learning. MIT Press, Cambridge (1998)

Metaphors of Creativity

Tony Veale(✉)

University College Dublin, Dublin, Ireland
tony.veale@ucd.ie

1 Introduction

What is creativity? This question is far more likely to elicit an anecdote, an aphorism or a metaphor than it is a literal definition. Creativity is an elusive phenomenon to study, made all the more vexing by our fundamental inability to pin it down in formal terms. As a category of human behaviour, creativity appears to resist all attempts at classical categorization via necessary and sufficient features. Indeed, it may well the case be that there exists no single creativity mechanism, and that all instances of creative behaviour are best corralled into a meaningful synthesis only by a system of family-resemblances. For example, recognizing that different solutions might be considered creative in different ways, Newell and Simon [17] suggest four different criteria for identifying a creative answer or solution:

1. The answer has novelty and usefulness (either for the individual or society)
2. The answer demands that we reject ideas we had previously accepted
3. The answer results from intense motivation and persistence
4. The answer comes from clarifying a problem that was originally vague.

A given solution may be considered highly creative yet satisfy just one or more of these criteria. Nonetheless, no criterion seems to hit the mark. For instance, consider (1) in the context of linguistic creativity. In the course of an average day, most speakers of a language will utter some statements that are so specific to their ephemeral contexts that they will never have been uttered before (or likely to be ever again); since these utterances serve some communicative function, they are thus both novel and useful, yet they can hardly be considered creative (except in the unconventional, generative-linguistics sense of Chomsky [1], which describes to the ability of language users to generate an infinitude of different sentences). It appears then that the meaning of novelty in (1) already presupposes a notion of creativity. Likewise, the rejection of Habeas Corpus as a legal concept in time of war (or terrorist threat) is not as creative as (2) would suggest, for true creativity in such a context would find a way of preserving a treasured belief in troubling situations. Meanwhile, the intense motivation and persistence of (3) is as much a characteristic of tenacious plodders as it is of creative individuals, while for some problems, pedants are every bit as capable as insightful thinkers of providing the clarity called for in (4).

G. Stojanov and A. Kulakov (eds.), *ICT Innovations 2016*,
Advances in Intelligent Systems and Computing 665,
https://doi.org/10.1007/978-3-319-68855-8_3

While these criteria are flawed, note how each criterion simply recapitulates the meaning of a conventional metaphor of creativity. For instance, (1) is consonant with the view that creative solutions are fresh and innovative, perhaps even ground breaking; (2) suggests that one must think outside the box and reject conventional categories and labels; (3) suggests that to be creative, one must expend copious amounts of mental energy in tenaciously exploring a particular avenue or wide-ranging conceptual space; and (4) espouses the common belief that creativity requires illumination and insight. These metaphors allude to a wealth of intuitions that cannot be summarized in the neat bullet points of (1) thru (4), and one cannot but feel that Newell, Shaw and Simons attempt at a literal exposition of the facts seriously short-changes these metaphors. A more considered exploration of the underlying metaphors, to perhaps achieve a synthesis at both the source and target levels of description, may yield a tighter and less fragmentary perspective on creativity.

Languages like English have very few non-metaphoric terms for creativity, which suggests that it is a concept largely understood in metaphoric terms. This metaphoric basis may well explain why creativity is so difficult to define formally, since formal definitions typically require literal precision. However, the lack of a literal substrate should not obviate our search for formal insight, since it has become a firmly established tenet of research in Cognitive Linguistics that metaphor constitutes much more than ripples on the surface of natural language, but a conceptual phenomenon that reveals the deep currents and undertows of thought itself (e.g., see Lakoff and Johnson [2]; Johnson [3]; Martin [4]; Veale and Keane [5]; Barnden [6], Gibbs [7]; Veale [8]; Veale et al. [9]). The study of our most widely used metaphors thus opens a window onto the conceptual processes that underpin not just language but other aspects of cognition, illuminating the mechanisms we use for reasoning about time, space, culture and society. The success of the metaphor programme in Cognitive Linguistics suggests that the metaphors we use to talk about a particular concept of cognitive interest can sometimes be as revealing as any formal theory. This is especially so when the concept in question is culturally entrenched and possesses a rich but polymorphic basis in folk wisdom. Creativity appears to be one such concept, for it makes its presence known in many contexts (e.g., linguistic, artistic, scientific, humour) and many guises (e.g., jokes, theories, products, solutions and pranks) that it easily defies a reductionist or essentialist account of its workings.

If the latter is indeed the case, we have good reason to believe that a diverse, non-essentialist account of creativity can be constructed by surveying the folk beliefs of creative agents themselves, as revealed through the metaphors they employ to describe this much-valued ability. This belief is supported by the fact that models of creative behaviour have traditionally been informed by specific metaphors of mind and intelligence, though some theoretically-motivated (and theory-motivating) metaphors may appear less conventional than others. For instance, Koestler [10] roots his theory of creativity in the notion of bisociation, which he defines as an operation over incongruous "mental matrices". While the notion of a mental matrix lacks formal structure in Koestler's writing, he exploits

this vagueness to offer a visual, geometric metaphor for bisociative combination. From this metaphoric perspective, Koestler's matrices become planar surfaces, so that bisociation can be said to occur at the unexpected juncture of orthogonal planes. In more contemporary terms, bisociation can be seen as an influential precursor to Fauconnier and Turner's [11,12] theory of Conceptual Integration or Blended Spaces, which, as the name suggests, is similarly grounded in a spatial metaphor of conceptual organization.

Linguistic metaphors for creative behaviour have a diverse presence in English, though as we shall argue, the most common metaphors can most naturally be clustered into four families: metaphors of space; metaphors of vision; metaphors of force; and metaphors of boundary realignment. In the sections that follow, we consider each of these families of metaphor in turn, and consider the extent to which each family offers real insight into a cognitive model of creativity. Our goal is to identify a metaphor schema that can be genuinely informative on the topic of creativity, providing theoretical useful insights into the nature of both the processes and representations needed to model creative thought.

2 Spatial Metaphors

This family of metaphors views creative behaviour as a process of exploration in a conceptual space, through which a variety of alternate pathways may be pursued. These metaphors are extensions of conventional spatial metaphors for rational, problem-solving behaviour. For instance, it is commonplace in English to think of problem solving as involving some or all of the following: "finding a solution", "hitting a dead-end", "backtracking", "pursuing a particular avenue" and "reaching a goal". Since problem-solving is a purposeful cognitive activity, this spatial perspective can thus be seen as an extension of the conventional metaphor Purposeful Action Is A Journey.

The resulting metaphor of Problem-Solving Is Search has been more influential than any other in shaping the agenda for research in problem solving and creativity (e.g., see Heaton [13]), not least because it allows one to extend the underlying spatial metaphor in a way that best exploits the processing capabilities of computers (see Veale and O'Donoghue [14]). In Newell et al. [15] employed the specific extension Solutions Are Points In A Search Space to give formal structure to the intuition behind the conventional spatial metaphors. A solution space is a collection of connected points, each of which represent a candidate solution to a problem, though most points will represent solutions that are either incomplete, impracticable or far from ideal. From this perspective, problem-solving is a process of mental path-finding from a start state a point in solution space that represents just the information that one can glean from the original problem specification to a desired goal state through a series of intermediate points or stages. The intrinsic connectivity of a solution space means that one can navigate the space much as one would navigate a real landscape, by using cues from the immediate neighbourhood (such as the metaphoric equivalent of gradient) as well as educated guesses to establish a path from the start

state to the goal state. Problem-solving behaviour can be considered rational only if it leads one to navigate the solution space of a problem in a systematic manner. For instance, strategies that cause one to visit the same points twice, or which lead one to wander aimlessly in circles can hardly be called intelligent or creative. Ultimately, however, the intelligence implied by a particular solution is very much a function of the path constructed (e.g., how short? how obvious? How much conceptual distance does it cover?), and as such, the Problem-Solving Is Search metaphor can be seen as extending the Source-Path-Goal image schema described by Johnson [3].

Johnsons Source-Path-Goal schema has additional implications for a spatial perspective on creativity. For example, a natural by-product of this schema is the Problem-Solving Is Locomotion metaphor, in which the imagination is viewed as a space that can be traversed by different locomotive means of varying reliability and speed. Conventional wisdom thus conceives of creative individuals as "quick-witted" fliers who undertake wide-ranging "flights of the imagination". When not flying, creative agents make speedy progress through solution space by "mental leaps", while less creative individuals take "baby steps". Creative leaps are subsequently explained to these plodders in the form of a guided walk through.

It is the "mental agility" of creative individuals that allows them to reach parts of the solution space that previously went unexplored by other, more conventional means. It is thus commonplace to describe creative thinkers as "explorers" and "pioneers" who open up "new fields" of inquiry. Creative endeavour is often idealized as a search for an elusive goal, a quest for true knowledge to find the holy-grail of a particular field. "Nimble-minded" searchers reach virgin areas of a conceptual space by "leaps of the imagination" that bypass intermediate points in the space and allow thinkers to seemingly pursue multiple alternate paths at once. Since these virgin areas lack maps, they represent the "perilous and uncharted waters" of creative discovery.

3 Visual Metaphors

Mental leaps allow some individuals to travel considerable distances within a solution space, and this distance is one conventional barometer of creative ability. This spatial quantity has a visual correlate in another family of metaphors which view creativity as an ability to "see" across large distances. Thus, creative thinkers possess "foresight" and are sufficiently "far-seeing" to perceive the "far-ranging" consequences of their actions. Such "visionaries" typically "see" solutions fully formed, without having to plod through the intermediate points in solution space from start to goal states. Like locomotive speed and agility, visual metaphors of creativity imply that creative behaviour is a natural endowment or gift, an ability that one exercises without necessarily understanding. Thinkers with "mental acuity" can "see the value" of unorthodox solutions, while people who refuse to see the products of a creative process are derided as "blinkered", "blind", "lacking in imagination" or as suffering from "tunnel-vision".

Visual metaphors of creativity can be thought of as extensions of the more general metaphor schema Creativity Is Perception. Thus, it is commonly said that creative individuals perceive patterns and connections between objects that are not visible to lesser thinkers. For instance, chess grandmasters achieve victory not by scouring the chess search space faster than their opponents - as a computers might play chess - but by perceiving the relevant patterns that exist between pieces on the board. It is often said that creative thinkers "feel" their way to a solution using intuition rather than reasoning, and such thinkers are called "highly perceptive".

Nonetheless, the visual perspective on creativity has become lexically entrenched in English through the words "insight" and "imagination", while the suddenness of creative thought, the essential quickness that is spatially captured by "mental leap", is captured by the image-based expression "flashes of insight".

4 Force Metaphors

While insight may occur in "flashes", it is also commonly said that "inspiration strikes". The latter typifies a family of metaphors that view creativity as a natural force. Broadly speaking, force metaphors can be sub-categorized into four types: natural forces, supernatural forces, mechanical forces and biological forces.

Metaphors based on natural forces tend to view creativity as powerful and unpredictable as the most intense forms of weather. Creativity can be seen as lightning that, in the case of inspiration, can "strike" without warning. This unpredictability is tempered somewhat in one particular variation that describes a reliable source of creativity, such as an individual or research team with a compelling track record, as "bottled lightning". Those groups that cannot harness creative lightning in this way can nonetheless attempt to recreate the weather conditions that give to it, through the popular group activity of "brainstorming". The goal of most think-tanks and research-groups is to facilitate those work processes that allow creativity to be harnessed as a form of energy. It is common then in these contexts to talk of "creative energy" that forms a "creative flow" that can be "tapped into".

If brainstorming seems like a corporate take on the rain-dance, perhaps it is because supernatural metaphors express a compatible view of creativity as a "divine force" that can be invoked with the appropriate rituals, or one that inhabits only certain individuals as the result of a "divine gift". Given the great power that is associated with creative ability, those thinkers that can harness it effectively are commonly described as "wizards" or "magicians", while creativity itself becomes a kind of "magic". Perhaps this latter view also excuses our traditional inability to formally define creativity, since magic and science are mutually incompatible pursuits.

Complementing this magical view of creativity is a sub-family of force metaphors that view creativity as a mechanical phenomenon that can be harnessed for

engineering purposes. Thus, one commonly reads of the "engines of innovation" and "creative dynamos" that drive technological progress. In this view, creativity is a driving mechanism forever pushing forward, one that can be "fuelled" or, to use a popular steam engine metaphor, "stoked". Such engines need the right operating conditions to produce the necessary output, so anything that staunches the creative flow - like some forms of intellectual property law - are said to "put the brakes on creativity".

Tempering the hard edge of these mechanical metaphors is another subfamily that instead emphasises the biological life-force of creativity. From this perspective, creativity is a fuel that flows in the blood, hence the common phrase "to get the creative juices flowing". A creative imagination is often called a "fertile imagination", while those who generate many new ideas possess a form of intellectual "fecundity". Fertility is also implicit in the idioms "germ of an idea", "planting the seeds" and "giving birth to a theory", while ideas whose creativity is not borne out on closer analysis are allowed to "wither on the vine". This view that Ideas-Are-Fruits (of a fertile imagination) is in turn a specialization of the schema Ideas-are-Food, for just as foods are a source of physical energy, ideas are a source of mental energy, where the most innovative and creative ideas are deemed fresh and the most substantial and intellectually nourishing are described as meaty.

5 Boundary Metaphors

The spatial perspective on creativity suggests that creative individuals are capable of far-ranging exploration of a conceptual space, while more mundane thinkers are fundamentally limited in the scope of their inquiries. This notion of limit or boundary is consonant with the view of mundane thinkers as "blinkered", "blind" and "narrow-minded". Indeed, creativity is popularly conceived as a process of "pushing boundaries", "pushing the envelope" or "broadening horizons", while a creative product, if sufficiently innovative, is often considered "ground-breaking", "a breakthrough" or a "break-out success". It seems then that, in addition to the Source-Path-Goal schema, descriptions of creativity also show evidence of being deeply influenced by the Container schema of Johnson [3]. This schema structures our knowledge of containers, real and abstract, by positing a boundaries that separate the inside of a container and its contents from the outside world. By shifting, blurring, transcending or re-orienting these boundaries, a creative individual can dramatically alter the representation of a given domain or problem space, to reveal solutions that could not previously be perceived.

Since containers are multiply bounded objects, container metaphors express a particular view of creativity as a process that transcends specific categories, paradigms or frames of reasoning. Categorization is, after all, a process of boundary imposition, wherein a given object is granted category membership only if it lies within the established boundaries of the category. Creative processes like metaphor are effective at moving these boundaries to accommodate new and

strikingly different members. Since categorization is often performed on the basis of visual cues, some key boundary metaphors are also visual metaphors. A blurring of boundary lines allows one to "see the big picture". In contrast, an ability to see boundaries that are not obviously present is also useful to the creative individual, who is able to "see the wood for the trees". As seen through the Container schema, conventional frames of reference become convenient boxes that constrain habitual thought processes and allow us to make quick, if mundane, inferences. These boxes also carry labels that describe their contents, but an open-minded individual can look past conventional labels and is able to "think outside the box". Two-dimensional variations of container metaphors are also common currency when talking about creativity. Thus, inspiration is often said to arrive "from left field", while unconventional creative thinkers are given licence to "colour outside the lines". A radical shift in the positioning of these lines has come to be called a "paradigm shift" (see Kuhn [16]).

A paradigm-shift not only transcends conventional boundaries, but re-orients them, frequently resulting in a radical re-orientation of attitudes and beliefs within a given field of research. In recent times, a creative product that causes an "upheaval" of an entire field or market has come to be called a "breakout" technology that in turn establishes new directions in research. If sufficiently radical, a creative disruption is deemed a "revolution" which, following the literal sense of the word, "over-turns" prevailing wisdom by turning a widely-head belief or theory "on its head". In an extension of the problem-solving view of creativity, it is popularly conceived that creativity allows quick-witted agents to prevail against difficult odds. A creative agent can prevail in an adversarial setting by "turning the tables" on a more-literal minded opponent, in effect turning the opponents weapons, traps or strategies (whether physical or verbal) against himself, causing them to backfire.

6 Analysis

Of the metaphor families surveyed here, spatial metaphors undoubtedly exercise the strongest influence on theories of intelligence and creative behaviour, succeeding more than any other family of metaphor in framing the creativity debate amongst theorists. Of course, such metaphors as "to find a solution" have long been entrenched in Western languages like English, but their theoretical value was most potently harnessed in the 1950s by the work of Newell and Simon (see Newell et al. [15]; Newell and Simon [17,18]), whose concept of a Solution Space was to establish the dominant vocabulary for AI and Creativity research until the present day. More recently, this particular metaphor of a solution space or search space, and the view of intelligence as rational search that it engenders, has given birth to a variety of more elaborate variations, such as Boden's [19,20] Conceptual Space perspective. Not all creative activities are equally innovative or ground-breaking, so Boden identifies two modalities of creative activity, exploratory and transformational. Exploratory creativity is the more mundane of the two modalities, and involves a process of navigation in a

Conceptual Space to locate solutions that exhibit both novelty and utility relative to some value system. Transformational creativity, a much rarer and intense form of creative endeavour, actually transforms the Conceptual Space itself, by modifying the rules or axioms that define the space. Perkins [21] is not so interested in transforming the Conceptual Space as identifying topographic aspects of the space that are more or less conducive to creativity activity. Among the colourful topographical region types that Perkins identifies are Klondike spaces, Oasis zones and clueless plateaux.

In cognitive linguistic terms, the utility of spatial metaphors in creativity research arises from the temporal perspective they offer, since they essentially provide a serial scan of the creative process (see Langacker [22]). That is, one can tease out from these metaphors a sequence of actions and states that are implicated in creative patterns of thought. In contrast, visual metaphors appear to offer just a summary scan of the creative process as an irreducible mental function, one perceived as a natural ability (sight) whose particular mechanics such as image projection onto the retina, transmission via the optic nerve, etc. are irrelevant to the workings of the metaphor. Nonetheless, visual metaphors can be seen as corollaries of a spatial perspective on creativity. To effectively traverse a conceptual space, one needs visual acuity to recognize relevant landmarks, perceive and avoid obstacles and to look ahead to a goal that may be too distant to see for less creative individuals. In turn, this level of visual acuity implies that a conceptual space is sufficiently illuminated for these landmarks and obstacles to be perceived against their conceptual backdrop.

This illumination is often provided by a metaphorical source that offers the most romantic perspective on creativity of any of the families we have considered. Lightning is sudden, unpredictable and very powerful, precisely the kind of illumination that romanticists associate with the creative mind-set. This basis in romanticism notwithstanding, the Creativity as A Force schema is not entirely devoid of computational resonance, and is tangentially related to some notable attempts to frame an algorithmic perspective on creativity. For instance, the fluid analogy work of Hofstadter [23] employs a metaphorical notion of temperature to reflect the amount of creative energy in a dynamical system. A hot system is one in creative ferment, where greater slippage is allowed between disconnected states that are not, strictly speaking, linked by a deductive chain of reasoning. A hot system is thus more likely to make potentially unsound, if ultimately valuable, mental leaps across a conceptual space. In contrast, a cold system is one that permits only sound, rule-based exploration of the conceptual space. Since a consistently hot system is too unsound to be useful, and a consistently cold system is too rigid to be innovative, temperature (and thus creative energy) must be rationed judiciously. It is best if the temperature starts high, to allow early exploratory steps to have more divergent consequences. Temperature should then gradually drop over time, to lock these early, creative gambits into a progressively sounder and more convergent chain of processing. This notion of temperature a physical metaphor widely used in computer science in a problem-solving technique called simulated annealing essentially controls the amount of

freedom exhibited by a creative system. It is a particularly useful notion to adopt when transition between states in a conceptual space is probabilistically defined, so that temperature becomes an important parameter of the probability distribution function. In such cases, a high temperature can enable a transition that is deemed to have an otherwise low probability of being useful, or one that appears to momentarily take the exploration process in a direction away from its goal. In non-probabilistic systems, however, it is harder to find a concrete role for temperature.

These three families of Space, Vision and Force do not so much offer different, even contradictory, descriptions of creativity, but actually describe complementary aspects of a complex phenomenon that together offer a more coherent view of creativity than either can do in isolation. Consider spatial metaphors of creativity: while conveying a valuable and informative process-level view of creativity as a form of conceptual exploration, this spatial perspective is hardly more informative than the spatial view of intelligence that underlies symbolic Artificial Intelligence. However, the important difference between both spatial perspectives is precisely that which is conveyed by metaphors of force and vision: creative exploration is often swift enough to suggest extraordinary powers of mental locomotion, and perceptive enough in its identification of novel and unconventional pathways to suggest an almost divine form of inspiration (where solutions appear, like lightning, to arrive out of the blue). Metaphors of force and vision are thus necessary adjuncts to a spatial conception of creativity. Unfortunately, necessity does not imply informativeness, for these adjuncts merely reflect how the end product of creativity is perceived by an observer (sudden, swift and electric), and lack any genuine representational or algorithmic insight.

We need to look elsewhere then for such insights. Fortunately, boundary metaphors make strong representational commitments to source elements such as boxes, boundaries, lines, fields and tables that can be given specific conceptual interpretations that are, in turn, suggestive of specific cognitive processes. For instance, boxes are frames of reference, categories or labels; lines and boundaries are rules and constraints; fields and paradigms are domains, or more specifically, mental spaces; and tables are strategies. Boundary metaphors thus suggest representational and algorithmic aspects of a computational theory of creativity, and may provide the missing ingredient that is lacking in a synthesis of space, force and vision metaphors. Nonetheless, boundary metaphors must be made to work for us in a theoretical sense, to provide true hypothesis-forming and explanatory power rather than simply adding another layer of poetic rhetoric to an already over-romanticized field of inquiry.

Toward this end, the Trajector-Landmark schema of Langacker [22,24] provides a basic theoretical ground against which boundary metaphors of creativity can more formally be analysed, within a cognitive-linguistic framework. In this schema, a trajector concept is conceived to hold a spatial, possibly locomotive, relationship with a landmark concept. Interpreted relative to a spatial model of creative exploration, the creative process (the explorer) itself becomes the trajector, moving through a space shaped by conceptual boundaries. This space

will be punctuated by landmarks, conceptual structures which include not just boundaries, but significant gradients, way-points and signposts (e.g., recall the oasis zones and clueless plateaux of Perkins [21]). For a conventional AI system, boundaries define the limits of exploration and serve as obstacles that are to be avoided (by look-ahead or by backtracking). In contrast, boundary metaphors of creativity imply that a creative system may be capable of dismantling or moving a troublesome landmark, to reconceptualize it in a less troublesome form or place. However, we must be wary here to avoid the phenomenological trap of the vision and force metaphors earlier: it is all very well to say that creative individuals can transcend boundaries, to think outside the box, but we need to understand this transcendence in genuine representational and processing terms.

We can begin to reach such an understanding by noting that to dismantle a landmark concept, one must shift ones attention from the whole to its parts, effectively reversing or undoing the individuation process that first brought the landmark into focus relative to the conceptual background. Likewise, we note that the reconstruction of a landmark, in a more conducive form or in a different area of the conceptual space, requires a subsequent shift back and a re-individuation of the landmark, from its parts (perhaps newly construed or aligned) to form a new whole. Each of the boundary metaphors we have considered implies such a dramatic shift of focus, either from the inside to the outside of a container, from the right-side to the left-side of a boundary or from the up-side to the down-side of an axis or division. We might ask then, what specific cognitive mechanisms or well-understood phenomena exhibit such a radical shift of attention, and whether such a mechanism or phenomenon might play an explanatory role in a theory of creativity?. One phenomenon that appears to fit this description rather snugly is figure-ground reversal. Perhaps it is this relatively well-understood cognitive phenomenon that boundary metaphors allude to? If so, the implications for conceptual representation and processing are direct and computationally informative.

7 Figure-Ground Reversal

Figure-ground reversal (henceforth FGR) is a phenomenon most commonly associated with visual perception, and indeed, few readers will be unfamiliar with the gestalt switches required to process such trick images as the Necker cube (see Fineman [25]). Nonetheless, FGR is not a phenomenon that is necessarily restricted to image processing, and may apply to any representation in which a figure-ground distinction is present, as in the cognitive representation of conceptual structure (e.g., see Langacker [22,24]). Ultimately, not all conceptual features are created equal, and in a given conceptual representation some will conventionally be considered more core or prototype-defining than others (see Lakoff [26]). Sowa [27] refers to this perspective as the egg-yolk theory of meaning, where those features deemed core will occupy the yolk of the concept, while those that play a more peripheral role occupy the egg white. In general then, FGR is a possibility in any conceptual structure in which salience can be redistributed from primary to secondary features of the representation, that is, from

those conceptual elements that are marked, privileged, prototype-defining or otherwise highlighted (the egg yolk), to those that are not (the egg white). For instance, the primary features of a Chair concern its role as a seat or resting place, while its secondary features concern its physical structure (e.g., wooden, rigid, legged, etc.). For most examples of a category or theory what we might call the unexceptional cases the primary and secondary features are in harmony, to the extent that the latter can serve as reliable proxies for the former (Gendler [28]). This correlation should not be surprising, since for example, it is the rigid and legged structure of a chair that allows it to serve its primary role as a seat. However, in exceptional cases the secondary features diverge from the primary features and this otherwise reliable correlation breaks down, e.g., in the case of beanbag chairs. To the extent that exceptional cases are useful cases (e.g., insofar as beanbags are useful chairs), their novelty marks them as creative examples of a theory or category.

7.1 Thought Experiments

Gendler [28,29], whose topic of interest is thought experimentation (see also Mach [30]; Kuhn [16]), claims that all thought experiments (or Gedanken experiments) essentially involve the construction of exceptional cases, since it is exceptional cases that best expose the limits of existing categories and theories. For instance, the Aristotelian theory of falling objects which claims that all objects fall at a speed proportional to their weight is seen as illogical once we ponder the Galilean case of a composite object comprising two stones, one large and one small, connected by a rope. The primary feature here is weight, while the secondary (apparently dependent) feature is speed. Galileos exceptional case exposes a break between weight and speed, since the composite object should fall both faster than the heavier stone alone (because the composite is heavier still), and slower (because the light stone would act as a drag on the heavy stone). Following Gendler, the creativity needed for a successful thought experiment is precisely the creativity needed to formulate an appropriate exceptional case.

Not every exceptional case will be creative, just as that not every novel artefact is useful or every divergence from the norm is profitable. In thought experiments, one explicitly aims to create, via an exceptional case, a perspicuous representation in which backgrounded instinctive knowledge about a domain of experience is dredged from the level of unarticulated intuition onto the plane of ideas (Mach [30]). Heaton [13] defines a perspicuous representation (in the sense of Wittgenstein) as one that brings about a Gestalt switch by highlighting a new aspect of our use of words. Perspicuity at a representational level seems to be what visual metaphors of creativity describe as illumination and what Newell and Simon [17] label as clarity. Insights about exceptionality and thought experiments (from Mach and Gendler) seem broadly applicable then to creative reasoning in general, for what is creativity but the generation of exceptional objects? After all, jokes are exceptional narratives, metaphors are exceptional comparisons, works of art are exceptional artifacts, and so on. It may seem that we have traded one vague term, creativity, for another, exceptional,

but Gendlers distinction between primary and secondary features offers a means of grounding a definition of exceptionality in terms of a specific representation of features (i.e., Lakoffs radial categories, or Sowas egg-yolk theories of meaning), and a specific process for manipulating the salience of these features (i.e., FGR). In this view, exceptional examples, either of a theory or a category, should emphasise secondary features at the expense of primary features, severing the fragile dependency between both levels of representation to introduce a greater degree of creative freedom in how the category or theory is used.

7.2 Trickery

Figure-ground reversal appears to play a central role in a diverse range of exceptional social constructions, from pranks, swindles, jokes and magical illusions to trickery of an intellectual variety, in scientific discovery and formal reasoning. Consider pranks, swindles and magic tricks first. In each of these activities, ones attention is deceptively drawn to a highlighted sequence of ultimately meaningless gestures, while actions of real significance are executed in the background. Magic illusions, jokes and pranks are, after all, humorous tricks in which an audience willingly participates, while swindles are tricks (often magical in appearance) where the goal is to not the entertainment of the audience but the enrichment of the performer. The arsenal of sleight-of-hand skills (such as misdirection, palming and card forcing) employed by professional tricksters, whether magicians or swindlers, are instances of figure-ground reversal that keep the key actions of a trick hidden in the background, while those actions that are either peripheral, unnecessary or unduly attention-grabbing (such as the financial carrot dangled by confidence tricksters) are foregrounded as eye-catching flourishes. In the case of stage magic, the initial FGR must be followed by a second act of reversal that dramatically foregrounds and makes visible the unseen effects of the sleight of hand, as when a rabbit is pulled from what was, apparently, an empty hat. In the case of a criminal swindle of the bait and switch variety, the unfortunate dupe is left to perform this second FGR for himself at a later time, e.g., upon discovering that a briefcase apparently filled with $100 dollar bills is in fact filled with old newspapers. This discovery, incongruous at first, is resolved only when the dupe recognizes the swindle for what it is, in much the same way that many theorists consider humour to be the result of a process of incongruity resolution (e.g., see Attardo et al. [31], Veale [32]; and see Ritchie [33] for an excellent survey). Figure-ground-reversal is not a specific tool of the trickster, like palming, forcing or misdirection, but a general mode of operation, and it is vital that we not confuse the strategy for the tactic.

7.3 Jokes

Figure ground reversal manifests itself in humour in a variety of guises, from the explicitly obvious to the sublimely implicit. Instances of the first kind include jokes in which participants explicitly manipulate the physical ground of a scenario rather than the figure itself (e.g., twisting an entire room just to screw

in a lightbulb). Jokes that employ FGR as an explicit physical device in this way will all invariably seem alike, as if instantiating the same narrative template or Ur-skeleton (see Hofstadter and Gabora [34]). Instances of the second kind do not fit into standard templates, and are, unsurprisingly, harder to diagnose, producing humour that is much less formulaic.

Consider the joke Tim hasnt played water polo since that tragic day when his horse drowned. There are two crucial points to note about this joke. First, there is nothing in the text that forces a humorous interpretation, for the most charitable interpretation simply concerns a sportsman with multiple interests who gives up all sports on the death of a beloved horse. Second, though the joke can be said to hinge on the semantic conflicts inherent in the juxtaposition of Water(-Sports) and Polo to create the blended concept Water-Polo (e.g., land/water, wet/dry, animate(horse)/inanimate(canoe), etc.), these conflicts in themselves do not provide the humour nor do they necessitate a humorous resolution, for otherwise, the blend Water-Polo would itself be humorous. Like thought experiments, jokes exploit unarticulated knowledge to imagine exceptional circumstances that bring this knowledge into the foreground. It is the way this knowledge is framed and exploited, rather than the knowledge itself (which already exists; see Mach [30]), that leads to insight in the case of Gedanken experiments and humour in the case of jokes.

Blends like Water-Polo obey a variety of optimality principles (see Fauconnier and Turner [12]) two of which, unpacking and web, are of direct relevance to this joke. These principles effectively enable elements of the input space Polo, such as Horse, to remain accessible (with some cognitive effort) after the blend, even though these elements are not projected into the blend space itself. In furnishing a link between Water-Polo and Horse, the blend thus enables the listener to bind the backgrounded Horse of Water-Polo to the foregrounded horse of the narrative. Listeners willingly jump then to the improbable construal that the horse drowns while playing polo in a swimming pool, even though more probable construals exist, simply because they can, for listeners opportunistically seek out humorous interpretations of a text whenever they are licensed by context (see Veale [32] for an elaboration of this opportunistic view of humour). Overall then, the joke employs an FGR to re-emphasise the concept of a Polo Horse in the context of Water-Sports, while simultaneously backgrounding the concept Canoe, allowing one to imagine water-polo played with horses instead of canoes. This in turn yields a coherent explanation for the drowning of the horse and the protagonists subsequent disavowal of his sport.

We note that while the General Theory of Verbal Humour (or GTVH) as described in Attardo et al. [31], provides an explicit logical mechanism for resolving jokes that employ figure-ground reversal, this mechanism precludes the extremely subtle form of FGR described above, and addresses instead the Ur-jokes in which rooms are rotated to twist in a light-bulb and so on. The significant and deep role that FGR has to play in humour is still largely unacknowledged in the GTVH.

7.4 Formal Reasoning

Creativity of an intellectual variety, as found in science, mathematics and philosophy, is also frequently categorized as a benign form of trickery, in which a theorist is said to employ a particular trick, twist or reversal. Philosophers in particular are known to set traps for their readers, to catch them in the contradictions that lurk beneath lazy or habitual thought processes. Consider formal reasoning, which concerns the truth-values of conjectures within a logical system and how they may be ascertained by a sound process of proof. This process either converts conjectures into theorems, or rejects them as falsehoods, via a proof that is ultimately grounded in a system of axioms and postulated truths. In figure-ground terms, conjectures serve as the highlighted figures in the proof process, since these are the objects of inquiry on which our attention is primarily focussed. In contrast, axioms and postulates serve as the background elements relative to which the truth of falsity of conjectures is explored. As befitting their postulated, axiomatic status, the truth of these background beliefs is never questioned, at least in conventional logic systems.

Now, FGR can occur in a formal setting in two different ways. In the first case, an axiom is foregrounded with the revisable status of a conjecture, so that its truth can be openly questioned. In the second, a conjecture is given axiomatic status and moved back into the postulated ground. As an example of the first case, consider fuzzy logic, a creative variation on classical propositional logic in which the axiomatic law of excluded middle is denied. This rejection allows fuzzy propositions to be quantifiably true and false at the same time. In a similar fashion, new geometries can be constructed by denying axiomatic status to a postulate of Euclidean geometry. For instance, by rejecting the parallel postulate, one can construct new geometries in which parallel lines are allowed to intersect, as is the case in Riemannian geometry. The second case of FGR effectively describes a reasoning process called proof by contradiction or reductio ad absurdum. Here, the negated form of a given conjecture is added as an axiom to the formal system in which its truth is to be ascertained. It is assumed that the formal system is logically sound prior to this addition, and so does not contain any contradictions. Any contradiction that can thus be generated in the new system must thus be caused by the addition of this new axiom. Since negation of the conjecture leads to a contradiction, the original conjecture must be true. One of the oldest and most elegant uses of this procedure is Euclid's demonstration of the infinitude of prime numbers. By assuming as axiomatic the existence of a highest prime number, Euclid's proof then demonstrates how one can construct an even higher prime number. This contradiction is then resolved by negating the original conjecture and concluding that no finite number can be the highest prime, ergo, the set of primes must be infinite.

7.5 Levels of Reversal

Figure-ground reversal is an equally valuable strategy in more empirical scientific endeavours, such as scientific discovery and, in particular, pharmaceutical development. Perhaps the most famous example of the latter concerns the

development of Viagra, a drug originally formulated by Pfizer to treat high blood-pressure. Early clinical trials proved unsatisfactory and were cancelled, yet when participants in the trials were asked to return their unused pills, few complied. Further investigation revealed the drug to have interesting side-effects that proved to be much more marketable than the drugs intended primary effect.

Products like Viagra provide clear examples of the role of FGR in serendipitous scientific discovery. While every drug has a range of effects on the human body, the primary effect (the figure) is that which is marketed by the pharmaceutical company. In contrast, any secondary effects are relegated to the background for marketing purposes, to literally appear as small-print on the back of the packaging. However, these secondary effects may sometimes be seen as primary, as with Aspirin, which is now aggressively marketed as a clot-busting blood thinner rather than as a pain-killer. In the case of Viagra the figure-ground reversal is more symmetrical: the primary effect becomes an unfortunate side-effect (users are warned of sudden dangerous drops in blood pressure), while an unintended but serendipitous sexual side-effect has become the primary selling point of the drug.

This kind of serendipity in the pharmaceutical industry suggests that the secondary characteristics of an object - those which do not satisfy the a priori goals of an agent - may have more value than its primary characteristics. Of course, it is important that "value" is construed as broadly as possible. For instance, if value is construed as "efficacy as a blood pressure treatment", then Viagra has low value, However, if the broader construal of value "usefulness in meeting a widespread demand" is employed, Viagra has considerably more value to Pfizer and its customers.

Serendipitous discovery thus involves two levels of FGR, tactical and strategic. In the case of Viagra, the tactical level describes the primary and secondary effects of the drug itself. In contrast, the strategic level describes the primary and secondary goals of the scientists: the scientific goal of "find an efficacious treatment for high blood pressure" serves as figure to the business-oriented ground goal of "find an effective treatment that will generate substantial revenue for the company". Both levels occur in lock-step when creative agents conclude that a figure-ground reversal at the tactical level can be supportive of a figure-ground reversal at the strategic level.

8 Synthesis

Metaphors of boundary transcendence, and thus our intuitions about FGR and exceptional cases, are clearly coherent with a metaphoric view of creativity as agile exploration in a bounded conceptual space. But it is equally important, however, that the computational interpretations of these metaphors are also mutually coherent within a single computational framework. To see why this is indeed the case, we need to return to Newell, Simon and Shaws spatial metaphors of Problem-Solving Is Search and Solutions Are Points In A Search Space.

Recall that a search space can be envisioned as an interconnected system of states - descriptions of that subset of the world relevant to the problem at

hand - where those states that differ by the application of a single problem-solving operation are directly connected. Problem-solving becomes a process of exploratory path-finding in this space, to identify a pathway of successive problem-solving operations (a meta-connection of sorts) that connects the given start state to a satisfactory goal state. For deterministic problems, there exists a definitive rule-based procedure for choosing the appropriate operation to apply at each state in the search space. For instance, the behaviour of the dealer in Blackjack is entirely determined by the rules of the game, thereby precluding any creative or unpredictable behaviour by the dealer. In contrast, the behaviour of poker players is not similarly determined. It follows that creativity can only occur when solving problems that are effectively non-deterministic, involving large search spaces for which there exists no practical, non-speculative procedure for identifying satisfactory pathways. In creative exploration, many of the states in a search space may yield useful and novel candidate solutions, and thus, we expect FGR to be a non-deterministic process that can divergently generate a potentially large number of valid reconfigurations of a conceptual structure (see Guilford [35] for a discussion of divergent problem solving, and Finke et al. [36] for a discussion of fecund generation within an exploratory model of creativity).

The application of FGR to a conceptual representation of primary and secondary features is not a deterministic process, but a process that occurs within a large search space in which many different states might be considered valid goals. Imagine, for the sake of simplicity, that the default representation of a concept C is given by an ordered tuple of features of the form

$$<F1, F2, F3, Fn, fn+1, fn+2, fn+3, fm>$$

where Fi denotes a primary or foregrounded feature and fj denotes a secondary or background feature. By features we mean more than atomic symbols; Fi and fj may denote modifiable parameters with a range of possible values, or even conceptual sub-structures in their own right that recursively contain their own sub-features. The tuple perspective is thus rich enough to represent blended concepts like Water-Polo or the conceptual structures representing an interpretation of a given joke text.

There are two basic operations that can be applied to the elements of a tuple to effect an FGR:

$$Fi \rightarrow fi \quad \text{(feature backgrounding)}$$

$$fi \rightarrow Fi \quad \text{(feature foregrounding)}$$

For a concept representation with m features, if we assume that each feature can hold one of n different values, then every variation of values in this representation will correspond to one of n^m different tuples. Furthermore, since any combination of features in a tuple can either be foregrounded or backgrounded, there are 2^m different figure-ground configurations of a given tuple. The corresponding search space defined by these tuples will thus comprise $n^m 2^m$ unique

states. Recall that FGR, as realized through the operations of feature backgrounding and feature foregrounding described above, is just one of potentially many transition mechanisms through which a conceptual explorer can move from state to state and traverse this search space. FGR should thus be seen as a mechanism that applies selectively within the context of a larger exploration process, to transcend boundaries, to sidestep obstacles or to find short-cuts when conventional transition mechanisms appear futile. In other words, only part of the exploration of a conceptual space need be exceptional? for the whole exploration to be judged as creative and to produce exceptional outputs.

We can also imagine a series of conventional, non-FGR operations of the form:

$$Fi \rightarrow \#value \quad \text{(assignment to a foregrounded feature)}$$

The specific range of allowable values will of course depend on the type of the feature. However, by not providing a transition type of the form $fi \rightarrow \#value$, we make the assumption that only foregrounded features can be modified. Without FGR, any feature that is initially backgrounded will thus remain constant throughout the exploration process.

A sequence of FGR operations of the form $fi \rightarrow Fi$ might therefore enable a subsequent sequence of non-FGR operations of the form $Fi \rightarrow \#value$ that would not otherwise be possible, and these assignments might then be locked in via another sequence of operations of the form $Fi \rightarrow fi$. The state visited in this way might require a much longer sequence of non-FGR operations to reach, or might not even be reachable at all without FGR. While this application of FGR might not appear to be transformative in the strong sense of Boden [19,20] it is state transforming rather than space transforming the effect may be equally dramatic, allowing an exploratory process to perform a mental leap between distant points of the conceptual space. Nonetheless, let us suppose that some elements of a tuple, fi and fj say, are so conventionally de-emphasised that they are effectively viewed as constants. In such a case, fi and fj serve no useful role within the tuple, so much so that one conventionally imagines the tuple without them. To such a thinker, the search space is dramatically reduced; it now contains a more manageable $n^{m-2}2^{m-2}$ states rather than $n^m 2^m$ (a reduction by a factor of $4n^2$), but one of the $n^m 2^m - n^{m-2}2^{m-2}$ lost states may be a truly creative solution, or may comprise a necessary intermediate state on the path leading to a creative solution. However, now imagine a creative individual who foregrounds these effectively hidden elements fi and fj in order to modify their contents. Such an act of FGR may well appear to observers as the addition of two new elements to the tuple, which in turn will appear to transform the conceptual space defined by possible configurations of this tuple. In this way, FGR, if applied to elements of a representation made moribund by convention and habitual thought processes, can appear as the radical transformation of a space which Boden [19] ascribes to the most original and creative of individuals.

In this synthesis, which combines exploration within a conceptual space with FGR as a possible transition mechanism between distant states, the following metaphoric perspectives on creativity become computationally realizable:

1. Creativity involves mental leaps. A mental leap is an FGR-based transition between states in a conceptual space that would otherwise require a substantial sequence of non-FGR transitions to achieve. Alternately, the conceptual distance (as measured by relative position in a taxonomy) between two states that can be connected by the application of FGR may be large enough to be called a leap.
2. Creativity requires mental acuity. The selective foregrounding or backgrounding of features implies a perceptiveness that is not typically associated with conventional deductive processes. It allows a thinker to construct a perspicuous representation that makes clear any tacit knowledge underlying a domain. Mental acuity is especially relevant to the manipulation of backgrounded features, since their lack of emphasis should make them harder to perceive.
3. Creativity requires mental agility. Figure-ground reversal may allow a transition out of a state that might otherwise be considered a dead-end and from which an otherwise deductive process might be forced to backtrack. In this way, FGR allows an exploratory process to transcend boundaries and sidestep obstacles.
4. Creativity is the result of a sudden mental force. An FGR-based mental leap so shortens the pathway between starting state and goal state that the search is deemed swift and the result sudden. The swiftness of the process is attributed to greater locomotive force in the traversal of the search space.

To summarize, then, this synthesis views creativity as arising from the exploration of a conceptual space, but one that involves some degree of discontinuity in traversal, ranging from a clever twist to a mental leap or the radical transformation of the space itself, all facilitated by the use of figure-ground reversal.

9 Conclusions

In trying to corral different folk intuitions about the meaning of creativity into a single, coherent framework, one is reminded of Wittgensteins remark: One is often bewitched by a word. For example, by the word know (Wittgenstein [37]). Understanding how and when to use a given word, whether knowledge or creativity, does not imply a genuine understanding of the cognitive mechanism to which such a word may allude, any more than one can base a theory of knowledge or creativity on the dictionary definition of such a word. Following Wittgenstein, one must question whether the seductive, often shamming power of words actually creates the illusion that creativity is a genuine mental phenomenon or that people can be genuinely creative, any more than people can ever truly know a subject and possess genuine knowledge. Wittgensteins therapeutic view of philosophy might thus lead us to reject the very idea of creativity as a special kind of intellectual function, and instead recognize this idea as simply a delusion of

language. As he claims in the Philosophical Investigations: Philosophy is a battle against the bewitchment of our intelligence by means of language (Wittgenstein [38]). Here Wittgenstein appears to suggest that language is both the source of the bewitchment as well as its remedy (see Heaton [13]). Thus, if the notion of creative processing is cognitively real, then language, and the linguistic intuitions that underpin the use of words like creativity, may offer the truest insights into its function; in other words, let the use of words teach you their meaning (Wittgenstein, ibid).

We began this paper with a consideration of five different, and apparently antithetical, families of creativity metaphor. Rather like the clich of the blind men who each examine a different part of an elephant only to arrive at radically different conclusions, these metaphors appear to suggest radically different views on the workings of creativity, yet they ultimately describe the same underlying mechanism. Through an analysis of the source-domain implications of these metaphors, and a subsequent computational synthesis of their target-domain correspondences, we have shown that these families are complementary, and can be unified into a coherent, theory-shaping whole.

References

1. Lees, R.B., Chomsky, N.: Syntactic structures. Language **33**(3 Part 1), 375–408 (1957)
2. Lakoff, G., Johnson, M.: Metaphors We Live By. Chicago University Press, Chicago (1980)
3. Johnson, M.: The Body in the Mind: The Bodily Basis of Imagination, Reason, and Meaning. Chicago University Press, Chicago (1987)
4. Martin, J.H.: A Computational Model of Metaphor Interpretation. Academic Press Professional Inc., Cambridge (1990)
5. Veale, T., Keane, M.T.: Conceptual scaffolding: a spatially founded meaning representation for metaphor comprehension. Comput. Intell. **8**(3), 494–519 (1992)
6. Barnden, J.A.: Belief in metaphor: taking commonsense psychology seriously1. Comput. Intell. **8**(3), 520–552 (1992)
7. Gibbs, R.W.: The Poetics of Mind: Figurative Thought, Language, and Understanding. Cambridge University Press, Cambridge (1994)
8. Veale, T.: Exploding the Creativity Myth: The Computational Foundations of Linguistic Creativity. Bloomsbury Academic, London (2012)
9. Veale, T., Shutova, E., Klebanov, B.B.: Metaphor: a computational perspective. Synth. Lect. Hum. Lang. Technol. **9**(1), 1–160 (2016)
10. Koestler, A.: The Act of Creation. Macmillan, New York (1964)
11. Fauconnier, G., Turner, M.: Conceptual integration networks. Cogn. Sci. **22**(2), 133–187 (1998)
12. Fauconnier, G., Turner, M.: The Way We Think: Conceptual Blending and the Mind's Hidden Complexities. Basic Books, New York (2002)
13. Heaton, J.M.: Wittgenstein and Psychoanalysis. Totem Books, Flint (2000)
14. Veale, T., O'Donoghue, D., Keane, M.T.: Computation and blending. Cogn. Linguist. **11**(3/4), 253–282 (2000)
15. Newell, A., Shaw, J., Simon, H.A.: Preliminary description of general problem solving program-I (GPS-I). WP7, Carnegie Institute of Technology, Pittsburgh, PA (1957)

16. Kuhn, T.S., Hawkins, D.: The structure of scientific revolutions. Am. J. Phys. **31**(7), 554–555 (1963)
17. Newell, A., Simon, H.A.: GPS, a program that simulates human thought. In: Feigenbaum, E.A., Feldman, J. (eds.) Computers and Thought, pp. 279–293. R. Oldenbourg KG (1963)
18. Newell, A., Simon, H.A., et al.: Human Problem Solving, vol. 104. Prentice-Hall, Englewood Cliffs (1972)
19. Boden, M.A.: The Creative Mind: Myths and Mechanisms. Weidenfeld and Nicholson, London (2004)
20. Boden, M.A.: Computer Models of Creativity, pp. 351–372. Cambridge University Press, Cambridge (1998)
21. Perkins, D.N.: Archimedes' Bathtub: The Art and Logic of Breakthrough Thinking. WW Norton & Company, New York (2000)
22. Langacker, R.: Concept, Image, and Symbol: The Cognitive Basis of Grammar. Mouton de Gruyter, Berlin, New York (1991)
23. Hofstadter, D.R.: Fluid Concepts and Creative Analogies: Computer Models of the Fundamental Mechanisms of Thought. Basic Books, New York (1995)
24. Langacker, R.W.: Foundations of Cognitive Grammar: Theoretical Prerequisites, vol. 1. Stanford University Press, Palo Alto (1987)
25. Fineman, M., Fineman, M.B.: The Nature of Visual Illusion. Courier Corporation, North Chelmsford (1996)
26. Lakoff, G.: Women, Fire and Dangerous Things: What Concepts Reveal about the Mind. Chicago University Press, Chicago (1987)
27. Sowa, J.F., et al.: Knowledge Representation: Logical, Philosophical, and Computational Foundations, vol. 13. MIT Press, Cambridge (2000)
28. Gendler, T.S.: Thought Experiment: On the Powers and Limits of Imaginary Cases. Garland Publishing, London (2000)
29. Gendler, T.S.: Galileo and the indispensability of scientific thought experiment. Br. J. Philos. Sci. **49**(3), 397–424 (1998)
30. Mach, E.: The science of mechanics, trans. TJ McCormack, new introduction by K. Menger, 6th edn. Open Court, La Salle (1960)
31. Attardo, S., Hempelmann, C.F., Di Maio, S.: Script oppositions and logical mechanisms: modeling incongruities and their resolutions. Humor: Int. J. Humor Res. **15**(1), 3–46 (2002)
32. Veale, T.: Incongruity in humor: root cause or epiphenomenon? Humor: Int. J. Humor Res. **17**(4), 419–428 (2004)
33. Ritchie, G.: Developing the incongruity-resolution theory. Technical report, Edinburgh Research Archive, Scotland (1999)
34. Hofstadter, D., Gabora, L.: Synopsis of the workshop on humor and cognition. Humor: Int. J. Humor Res. **2–4**, 417–440 (1989)
35. Guilford, J.P.: The Nature of Human Intelligence. McGraw-Hill, New York (1967)
36. Finke, R.A., Ward, T.B., Smith, S.M.: Creative Cognition: Theory, Research, and Applications. MIT Press, Cambridge (1992)
37. von Wright, G.H.: Wittgenstein on certainty. In: Problems in the Theory of Knowledge/Problèmes de la Théorie de la Connaissance, pp. 47–60. Springer (1972)
38. Malcolm, N.: Wittgenstein's philosophical investigations. Philos. Rev. **63**(4), 530–559 (1954)

Socially Intelligent Robots, the Next Generation of Consumer Robots and the Challenges

Amit Kumar Pandey[1,2(✉)]

[1] SoftBank Robotics, Paris, France
[2] euRobotics Topic Group on Socially Intelligent Robots and Societal Applications (SIRo-SA), Paris, France
akpandey@softbankrobotics.com
https://www.ald.softbankrobotics.com/en, http://www.amitkpandey.com

1 New Wave of Social Robots and the Need of Social Intelligence

We are evolving, so as our society, lifestyle and the needs. AI and ICT have been with us for decades, and now penetrating more in our day-to-day life, so as the robots. But, where are all these converging together? Towards creating a smarter eco-system of living, where robots will coexist with us in harmony, for a smarter, healthier, safer and happier life. Such robots have enormous potential to play essential roles in our everyday life, such as in scenarios like companionship, child-care, educational, special educational, edutainment, healthcare, and co-worker. The question is how? The answer will be the Social Intelligence (SI) of the robots. SI of such consumer Robots will be the key technology and the next big R&D challenge at the cross-section of robotics, AI and cognition. SI will enable such robots to behave in socially expected and accepted manners. However, there are still various technological and scientific constraints that end-users, robot providers and other involved stakeholders face, which prevent social robots from entering the market with full potential. There is a great need to create common ground and shared understanding about social robots, its potentials and applications, and the barriers. For the long term success of such robots, there is a need for these robots to behave in socially accepted and expected ways. In this regard, connectivity, learning and collective intelligence are some of the key building blocks (Fig. 1).

2 Social Intelligence and Robot Learning from Human

Social robots have a new range of applications. Such robots are supposed to be working in the human environment, which is different from the natural or industrial setups, as shown in the figure below (Fig. 2).

The fact that there are humans in the environment creates a new set of R&D challenges to be solved, for such robots to serve, assist, accompany people and behave in the manner accepted and appreciated by people and does not create

G. Stojanov and A. Kulakov (eds.), *ICT Innovations 2016*,
Advances in Intelligent Systems and Computing 665,
https://doi.org/10.1007/978-3-319-68855-8_4

Fig. 1. Social robots.

Fig. 2. High-level spectrum of operation environment for robots. Human-awareness and social awareness are the key factors for social robots.

any negative feeling of surprise or anger. These robots should explicitly consider the presence of human in all their planning and decision making strategies, whether it is for motion, manipulation, interaction or learning. This prompts new research challenges and the need of a coherent theories, models and architectures. Development of the key cognitive abilities and basic socially intelligent behaviors of the robots, raise new challenges, which cannot be handled appropriately by simple adaptation of state of the art robotics planning, control and decision making techniques of the robots designed to work in non-human environment.

Human-awareness and social awareness are the key factors. Among other factors, a Socially Intelligent Robot should be able to "behaves by taking into account the socio-cultural norms and expectations, and be able to reason about the exchange of the favours and the supports the interacting agents (the humans and the robot) as well as the environment can provide".

In [1], a layered approach for embodiment of social intelligence of robots have been proposed. It identifies some of the socio-cognitive abilities and building blocks leading to more complex behaviors. Perspective taking [2,3], i.e. reasoning from other perspective and affordances analysis [4], i.e. what can be done with particular object, are some of such basic abilities towards achieving social intelligence of the robot. Social learning is another mechanism to acquire knowledge through day-to-day integration and a powerful tool towards building complex social intelligence [5–9].

Another questions to look into, in the context of social robots at home and at public places, are the ethical, social and legal aspects. In [10], a system is presented capable of learning to maintain privacy, but on the other side also illustrates the cases of potential dilemma of Privacy vs. Ethics for a Socially Intelligent Robot (related video [11]).

3 SoftBank Robotics, Developing Robots for Well Being of Society and Smarter Living

We at SoftBank Robotics believe that robots will play a key role in everyday life, and that robots will co-exist with us, leading to a smarter, healthier and happier life. Robots of all shapes and sizes are now entering into our day to day life, whether at the shopping mall, hospital, museum, railway station, elderly care facility, school or even within the home. These robots are increasingly being deployed to learn and assist humans in many different ways. The social intelligence of the robots, along with the ability to connect and communicate with the rest of the ecosystem, will be the paramount, and only possible as new and relevant applications are created for these social and humanoid robots. As a leader in the burgeoning robotics space, SoftBank Robotics is committed to developing the best robotic experiences for the consumer. By reinforcing the potential for humanoid robots, the experience of interacting with an intelligent, connected form factor becomes second nature for society and more quickly accepted into everyday life. In this regard, there is also a great need to bridge the two communities: Robotics and ICT.

For example, the Pepper robot is currently deployed in thousands of homes and public places; Romeo, a research prototype, aims to be daily life companion for people needing physical and cognitive assistance; NAO is supporting both research and youth education as a teaching tool for STEM programs and supporting special education programs for children with ASD (Fig. 3).

Fig. 3. Romeo, Pepper and NAO.

4 Some Key European Union Projects and Activities, Breaking the Scientific and Technological Barriers

SoftBank Robotics is currently leading the way for social robots in the society through its active involvement and contribution in many European Union projects. For example, the MuMMER [12] project, putting Pepper robot in mall. The project aims to improve the social interaction and engagement capabilities of the robot and incorporate some social navigation skills. The L2ToR [13] projects aiming to explore the role of social robot to teach second language to children, whereas the DREAM [14] project aims to explore the role of a social robot in robot-assisted therapy for children with Autism Spectrum Disorder (ASD). The recently started CARESSES [15] project, aims to make the robot culturally-intelligent to assist and accompany elderly people in more connecting

and trustworthy manner. Romeo2 [16] projects explores the role of humanoid robot for everyday companion for elderly people and to provide physical and cognitive support.

There is also a huge ongoing effort in Europe through partnership of euRobotics AISBL [17] (an international non-profit association for all stakeholders in European robotics) and European Commission, which aims to shape the future of robotics in Europe through SPARC [18] (one of the largest civilian-funded robotics innovation programme in the world) for Horizon 2020 (H2020). Within this mechanism, there are various topic groups [19,20], which provides input for the Multi-Annual Roadmap (MAR) and Strategic Research Agenda (SAR). Some of these topic groups are also working on the aspects of social robots, e.g. the topic groups on Socially Intelligent Robots and Societal Applications (SIRo-SA) (coordinated by Amit Kumar Pandey), Natural Interaction with Social Robots (coordinated by Vanessa Evers, M. Chetouani, Kerstin Dautenhahn), AI and Cognition in Robotics (coordinated by Alessandro Saffiotti, Markus Vincze), etc.

5 Conclusion

A very exciting, smarter and fun future of Human-Robot coexistence awaits. Intelligent Service Robots in Smart ICT and IoT world are the Next Big things. For this, we need to move towards a new kind of Intelligence: Social Intelligence, which needs expertise from diverse domains. The key is to equip the robots with the capabilities to reason about Humans and Human-Centered Environment. All these also requires a new paradigm of Evaluation and Benchmarking for Social Intelligence of robots.

Being so divers, there is a place to play the role by different people, and a multi-disciplinary effort will be needed. We are at the beginning of Personal Service Robots, a long way to go and many questions have to be addressed by larger communities, e.g. social, legal, privacy, ethics related aspects of socially intelligent robots.

References

1. Pandey, A.K., et al.: Towards socially intelligent robots in human centered environment. PhD thesis, Toulouse, INSA (2012)
2. Pandey, A.K., Alami, R.: Mightability maps: a perceptual level decisional framework for co-operative and competitive human-robot interaction. In: 2010 IEEE/RSJ International Conference on Intelligent Robots and Systems (IROS), pp. 5842–5848. IEEE (2010)
3. Pandey, A.K., Alami, R.: Taskability graph: towards analyzing effort based agent-agent affordances. In: 2012 IEEE RO-MAN, pp. 791–796. IEEE (2012)
4. Pandey, A.K., Alami, R.: Affordance graph: a framework to encode perspective taking and effort based affordances for day-to-day human-robot interaction. In: 2013 IEEE/RSJ International Conference on Intelligent Robots and Systems (IROS), pp. 2180–2187. IEEE (2013)

5. Pandey, A.K., Gelin, R.: Human robot interaction can boost robot's affordance learning: a proof of concept. In: 2015 International Conference on Advanced Robotics (ICAR), pp. 642–648. IEEE (2015)
6. Pandey, A.K., Ali, M., Alami, R.: Towards a task-aware proactive sociable robot based on multi-state perspective-taking. Int. J. Soc. Robot. **5**(2), 215–236 (2013)
7. Pandey, A.K.: Learning to be proactive. https://youtu.be/lw0tem5hStE
8. Pandey, A.K.: Learning task semantics. https://youtu.be/O7ZSNEYDuWQ
9. Pandey, A.K.: Learning affordances and activities. https://youtu.be/Vnofhx4b6Us
10. Pandey, A.K., Gelin, R., Ruocco, M., Monforte, M., Siciliano, B.: When a social robot might learn to support potentially immoral behaviors on the name of privacy: the dilemma of privacy vs. ethics for a socially intelligent robot. In: Privacy-Sensitive Robotics 2017. HRI (2017)
11. Pandey, A.K.: Learning privacy vs. ethics for a socially intelligent robot. https://youtu.be/Udwf-9iwmvY
12. MUMMER. http://mummer-project.eu
13. L2TOR. http://www.l2tor.eu
14. DREAM. http://www.dream2020.eu
15. CARESSESROBOT. http://www.caressesrobot.org
16. ROMEO. http://projetromeo.com/en
17. EU-Robotics. https://www.eu-robotics.net
18. SPARC-Robotics. http://www.sparc-robotics.net/
19. EU-Robotics. https://www.eu-robotics.net/eurobotics/topic-groups-/index.html
20. EU-Robotics. https://www.eu-robotics.net/cms/upload/topic_groups/list-Topic-groups-2017-01.pdf

Proceeding Papers

Hand Gesture Recognition Using Deep Convolutional Neural Networks

Gjorgji Strezoski(✉), Dario Stojanovski, Ivica Dimitrovski, and Gjorgji Madjarov

Faculty of Computer Science and Engineering, Ss. Cyril and Methodius University, Rugjer Boshkovikj 16, 1000 Skopje, Macedonia
{gjorgji.strezoski,dario.stojanovski,ivica.dimitrovski, gjorgji.madjarov}@finki.ukim.mk

Abstract. Hand gesture recognition is the process of recognizing meaningful expressions of form and motion by a human involving only the hands. There are plenty of applications where hand gesture recognition can be applied for improving control, accessibility, communication and learning. In the work presented in this paper we conducted experiments with different types of convolutional neural networks, including our own proprietary model. The performance of each model was evaluated on the Marcel dataset providing relevant insight as to how different architectures influence performance. Best results were obtained using the GoogLeNet approach featuring the Inception architecture, followed by our proprietary model and the VGG model.

Keywords: Gesture recognition · Computer vision · Convolutional neural networks · Deep learning · Inception architecture · GoogLeNet

1 Introduction

Hand gestures provide a separate complementary modality to speech for expressing ones ideas. Information associated with hand gestures in a conversation is degree, discourse structure, spatial and temporal structure. The approaches present can be mainly divided into Data-Glove based and Vision based approaches [1]. These two approaches are fundamentally different due to the different nature of the sensory data collected. The Data-Glove based approach collects data from sensors attached to a glove mounted on the hand of the user. Using this methodology only necessary information is gathered, which minimizes the need of data preprocessing and reduces the amount of junk data. Nevertheless, using a Data-Glove in real life scenarios is often infeasible and can present different issues like connectivity, sensor sensitivity and many other hardware related problems [2].

Vision based approaches on the other hand offer the convenience of hardware simplicity - they only require a camera or some sort fo scanner. This type

G. Stojanov and A. Kulakov (eds.), *ICT Innovations 2016*,
Advances in Intelligent Systems and Computing 665,
https://doi.org/10.1007/978-3-319-68855-8_5

of approach complements biological human vision by artificially describing the visual field. While this type of approach is way cheaper than its Data-Glove counterpart, it produces a large body fo data that need to be carefully processed in order to get only the necessary information. Having in mind that to tackle this problem the recognition system needs to be insensitive to lighting conditions, background invariant and also subject and camera independent [3]. Also a challenging part of the hand gesture recognition problem is the fact that these systems need to provide real-time interaction. While this does not affect the model training directly it implies that later classification needs to be conducted in a manner of milliseconds.

Given the constraints presented by the nature of hand gesture recognition, a generally invariant approach is required which will retain consistent performance in various conditions. In recent years deep learning has stepped up the game when it comes to computer vision problems. Deep learning approaches have shown to be superior in various computer vision challenges on multiple topics. This spike in the performance of these models is partially due to the recent advances in GPU design and architectures. GPUs are parallel in nature and are especially well adjusted for training these types of models. While there is a vast variety of deep architectures, research has shown that Convolution Neural Networks (CNNs) are most applicable to computer vision problems. This compatibility rests on the biological similarity of convolutional neural networks with the vision part of the human brain [4]. Having said that, humans have the most sophisticated vision system, which similarly to convolutional neural networks consists of hierarchically distributed layers of neurons which act as processing units. Parameter sharing between neurons from different levels in the structure yield different connection patterns with different connection weights, which in turn concludes the process with classification.

Since these types of architectures have gained popularity during the past few years, the industry leaders like Google, Nvidia, Microsoft, Deep Mind, IBM, Clarifai and others have developed their own architectures designed to tackle diverse problems. Most of these architectures are available for personal and academic purposes under open licenses ergo researchers and professionals alike can modify the code, adjust the model and fine-tune the existing parameters. There is also a vast academic community which continuously pushes performance limits of deep models. Berkeley developed Caffe which is one of the best performing deep learning framework and Oxfords Visual Geometry Group introduced state of the art performance with a weakly supervised deep detection architecture. Similarly to these advances Microsoft released its deep learning flagship CNTK, Google released TensorFlow and Nvidia released the cuDNN framework which optimizes GPU operations for maximum performance.

Having given a brief introduction into the field, our research contributions to this area are three fold:

- We evaluate several plain and pre-trained convolutional neural networks on different datasets and compare their performance.

- We train a robust deep model for hand gesture recognition with high accuracy rate.
- We report good performance in a temporal manner with just 2 ms classification time on the fully trained model, making it a real-time functional model.

The rest of the paper is organized as follows. Section 2 outlines current approaches on hand gesture recognition, with emphasis deep learning methods and state of the art performance. Section 3 presents the details of the experimental scheme and an overview of the pre-trained and plain models used in our work. We present and elaborate on the performance achieved using every approach and provide insight on the findings of our research in Sect. 4. Finally, we conclude our work and discuss future development in Sect. 5.

2 Related Work

Hand gestures are a fundamental part in human-human communication [2]. The efficiency of information transfer using this technique of communication is remarkable, therefore it has sparked ideas for utilization in the area of human-computer interaction. For this to be possible the computer needs to recognize the gesture shown to it by the person controlling it. That is the sole process of hand gesture recognition. In a classical manner, the most common approach to solving these types of problems is applying feature extraction techniques. A particular technique is matching the image of the hand a predefined template [5]. Template matching has shown to be ineffective due to the high variety of environments, hand forms and variations of different gestures. Other classical approaches featuring different feature extractors have the flaw of not being flexible enough to changing datasets and alternating conditions. In these cases the robustness and invariance of the approaches with deep convolutional neural networks makes them ideal candidates for these types of problems.

As we mentioned before, deep learning methods have been used to solve a diverse field of computer vision problems in recent years. When it comes to problems that are representable via images, the parallel nature of convolutional neural networks allows them to elegantly apply to the matrix representation of the data. Additionally, multi-column deep CNNs that employ multiple parallel networks have been shown to improve recognition rates of single networks by 30–80% for various image classification tasks [6]. Neverova et al. [7] successfully combined RGBD data from the hand region with upper-body skeletal motion data using convolutional neural networks (CNNs) for recognizing 20 Italian sign language gestures. However, their technique was intended for gestures performed indoors only. Barros et al. [8] designed a Multichannel Convolutional Neural Network (MCNN) which allows hand gesture recognition with implicit feature extraction in the architecture itself. They report state of the art results on two dataset containing images of static hand gestures. The first dataset was generated using a robot in laboratory conditions, mimicking real world scenarios with four types of hand gestures. As a secondary dataset, they evaluated their system on data containing ten different hand gestures made in real, uncontrolled environments.

Ohn-Bar and Trivedi evaluated various handcrafted spatio-temporal features and classifiers for in-car hand-gesture recognition with RGBD data [3]. They reported the best performance with a combination of histogram of gradient (HOG) features and an SVM classifier. Molchanov et al. fused information of hand gestures from depth, color and radar sensors and jointly trained a convolutional neural network with it. They demonstrated successful classification results for varying lighting conditions and environments [6]. In turn, the before mentioned efforts provided the necessary background for conducting our experiments and motivated our work.

3 Experimental Design

Recent advances in the design of models with deep architectures, especially convolutional networks have paved the way for a vast number of different CNN architectures designed to handle all sorts of data. Following the work in [6–11] we decided to test the best performing models in some of the most challenging visual classification tasks like the ImageNet Large Scale Visual Recognition Challenge (ILSVRC), on hand gesture recognition. Furthermore, we propose our own CNN designed with robustness and efficiency in mind.

3.1 Dataset

For the purpose of training and testing our model we used the Marcel dataset which consists of 6 hand signs (A, B, C, FIVE, POINT, V) performed by 24 persons on three different types backgrounds. Different people and backgrounds were used in order to increase diversity and information contained within the dataset. In terms of background, the images in the Marcel dataset were recorded in front of an uniform light background, uniform dark background and a complex background [12]. Because of the different people included in the creation of this dataset there are also variabilities in hand shape and sizes. This dataset results in a total of 4937 train images and 675 test images. For the testing and validation of the different models performance we used five fold cross-validation. The distribution of images in each of the classes in both the training and testing set are shown in Table 1.

3.2 Data Augmentation

Because the deep architectures that we trained in our experiments require a large mass of data to train properly, we used data augmentation on the images in the dataset. This was done in order to gain quantity while still introducing some novelty in terms of information to our dataset. Our augmentation consists of horizontal mirroring of every image in the training set, effectively doubling the size of the dataset [13]. Horizontal mirroring data augmentation is labeled label-safe in this type of images. Additionally we trained our models using a gray-scale representation, thus removing the color factor. Samples of this dataset on a light plain background are illustrated in Fig. 1

Table 1. Number of images in each class

	Train	Test	Total
A	1331	99	1430
B	489	104	593
C	573	116	689
FIVE	655	138	793
POINT	1396	121	1517
V	436	97	533

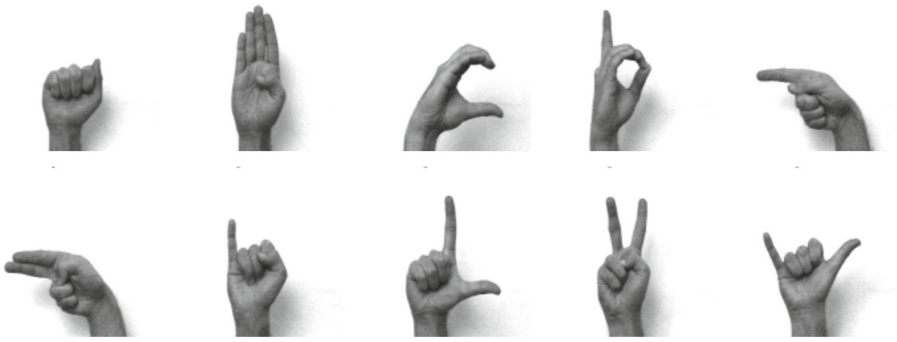

Fig. 1. Samples of the Marcel dataset on plain background

3.3 GoogLeNet

GoogLeNet is a deep convolutional neural network designed by Google featuring their popular Inception architecture. This architecture not only allows for approximation of a optimal local sparse structure by readily available dense components but also reduces data dimensionality [9] wherever the computational requirements would increase rapidly. GoogLeNet is the particular incarnation of the Inception architecture that had the lowest error rate in the ILSVRC 2014 challenge.

We trained this model on the Marcel training dataset for 30 epochs with a batch size of 16 images and a 20% step degradation function. The initial learning rate was setup to 0.001 and because of the mixed presence of different backgrounds (complex, plain light, plain dark). Also we subtracted the total RGB mean of the complete dataset before data iteration. Additionally all of the images were maximized to a size of 256×256px to fit the receptive field of the CNN. Whenever the original proportions of the input image could not be maintained, cropping was introduced to the central region of the image. The total training time of this model was 2 h on a NVidia GTX 980 Ti.

3.4 AlexNet

Following its success on the ILSVRC-2010 challenge and relatively simple structure with just 5 convolutional layers and 3 fully connected layers, AlexNet provides the simplicity and efficiency of a shallow model combined with the predictive performance of a deep model [10].

We trained this model for 20 epochs using an initial learning rate of 0.001 and a batch size of 16 images. In order to encourage faster learning we applied an exponential learning rate degradation function with a gamma factor od 0.02. In this case we also subtracted the mean file from the input images in both the training and testing phase. The total training time of this model was 1 h on a NVidia GTX 980 Ti.

3.5 LeNet

The LeNet model is specifically designed for handwritten and machine printed character recognition. Having in mind the similarity of the characters with hand gesture contours, whether printed or written, given the suitable preprocessing this model should perform well. This model features 7 layers (not counting the input layer) and a receptive field of 28×28px. This receptive field yields the need of a region-of-interest (ROI) selector or a smart cropping mechanism, in order to fit the images into the input space of the model. After cropping the images to their central section where the gesture is usually contained using PIL in Python, a resize function scaled the images to 28×28 pixels.

For this experiment we trained the LeNet model for 35 epochs with a initial learning rate od 0.01 and a step degradataion function of 25% step frequency.

3.6 VGG Net

The Visual Geometry Group model is described as a very deep convolutional neural network [11] that has a fixed input size of 224×224px RGB image. As a preprocessing step in the training process of this network we subtracted the mean RGB value, computed on the training set, from the input images. This model features a small receptive field and convolutional filters with 3×3px dimensions. The stack of convolutional layers also contain spatial pooling layers with a 2×2px window, that passes the data with stride 2 [11]. After the convolutional stack there is a series of three fully connected layers. The last fully connected layer performs the classification over the 6 classes.

We trained this model for 35 epochs with a batch size set to 128. Because this network is deeper than most other architectures it takes less epoch to converge, so during training we noticed convergence around the 17 epoch. Learning started with a base learning rate of 0.001, which degraded with a step degradation function 33%, 3 times on a regular interval.

3.7 Custom Model

Our custom model was originally designed for pixel based segmentation of images. Since the process of segmentation essentially rests on pure classification, small corrections to the kernel and filter sizes of the architecture allowed for this architecture to achieve relatively good performance in this task. This model has 13 layers that contain 5 convolutional and 5 pooling layers [13]. Before the softmax classifier there is a fully connected layer aggregating the convolved features generated to this point. Finally the input layer creates a 194×194px receptive field.

Generally, the advantage of this model is the smaller kernels and higher number of neurons per layer. This approach provided a better compromise between training times and level of details. The smaller kernels are the culprit when it comes to longer training times but the also capture smaller details than larger ones would. Because training is slow the overfitting stadium of the training period comes at a later stage.

Table 2. Layer configuration in custom model

	Type	Units	Kernel
0	Input	194×194	N/A
1	Convolutional	192×192	4×4
2	Max pooling	96×96	2×2
3	Convolutional	92×92	4×4
4	Max pooling	46×46	2×2
5	Convolutional	42×42	5×5
6	Max pooling	21×21	2×2
7	Convolutional	18×18	4×4
8	Max pooling	9×9	2×2
9	Convolutional	6×6	5×5
10	Max pooling	3×3	2×2
11	Fully connected	600	1
12	Softmax	6	1

This model was implemented in Berkeley's Caffe framework using the Python wrapper. Each of the neurons contained in this network relies on the Rectified Linear Unit activation firs introduced in [10]. In the custom model classification is performed using a Softmax classifier with 6 output neurons (one for each class). Table 2 shows the models configuration layer by layer with unit numbers and kernel sizes. We performed experiments with adding various dropout layer throughout the architecture for gaining sparseness and speeding up the training process. These modifications to the architecture yielded worse performance in

terms of accuracy so dropout was excluded from the final design. A conclusion that can be drawn from this is that the increased number of neurons per layer is in fact helping with performance (due to smaller kernels) and holds no redundant information.

As with the previous models, this model was trained no more than 25 epochs in its best run. For increased performance (and reduced speed) we started training this model with an initial learning rate of 0.002 and degraded this rate using a 20% step degradation function.

4 Results and Discussion

In this particular research, it was important to evaluate performance in both accuracy and operation timing due to the potential of applying this types of models in a real-time control scenario. In terms of accuracy, the GoogLeNet model performed best with a Top-1 classification accuracy of 78.22% and Top-3 classification accuracy of 90.41%. While it is the best model in term of accuracy, because of its depth and complexity, classification and training times are the longest with 4 min per epoch in a training setting and 2.8 ms propagation time of a test image from the input layer to the end of the network.

Table 3. Accuracy scores for each models best run

	Top-1	Top-3
GoogLeNet	78.22%	90.41%
AlexNet	42.18%	60.9%
Custom model	64.17%	84.32%
LeNet	28%	47.19%
VGG model	64.19%	83.33%

Table 4. Average classification and training epoch duration on a GPU

	Training epoch (min)	Classification per image (ms)
GoogLeNet	4	2.8
AlexNet	2	1
Custom model	2.5	0.5
LeNet	0.4	0.6
VGG model	5	2

The VGG model and our custom model have similar accuracies in both the Top-1 and Top-3 categories, with 64.19% and 83.33% for the VGG model and

64.17% and 84.32% for our custom model respectfully. The AlexNet and LeNet models performed significantly worse than the previous three models as shown in Tables 3 and 4.

When it comes to classification and training duration, as expected the most simple and shallow architectures provide the best timings in both areas. The LeNet model performed best in terms of timing with 0.4 min per epoch in the training setting and 0.6 milliseconds for predicting the class of a single image. Nevertheless, its good performance on the timing evaluation, the bad classification accuracy makes this model unsuitable for any kind of real time control. High error rate in classification would make the system unreliable. On the other hand the GoogLeNet model was the slowest of all tested models with 4 min per training epoch and almost three milliseconds per classification of a single image. Our custom model and the VGG model had the best ratio of classification accuracy and timing making them most suitable for real time use. The GoogLeNet model would also perform well in this type of setting but it would require more expensive hardware (GPU) and plenty of optimizations to gain in responsiveness. Responsiveness is a major concern in systems control and human-robot interaction.

5 Conclusion and Future Work

Regarding future work in this direction, we are exploring methodologies for improving our own model and its predictive power. Additionally, because of the short classification process duration, application of this model in a real-time setting is part of our future work as well. This is possible with XBox Kinect sensor technology, providing stable and consistent data feed to the model. Using the XBox Kinect sensor we would also be able to generate our own datasets for retraining and improving classification rates.

An interesting future approach would be the development of a continuous training of the model so that with each correct classification we would adjust the weights and activations of network it self. Basically that would enable the model to get progressively better with time, without the need of a separate training phase.

Acknowledgments. We would like to acknowledge the support of the European Commission through the project MAESTRA Learning from Massive, Incompletely annotated, and Structured Data (Grant number ICT-2013-612944).

References

1. Shastry, K.R., Ravindran, M., Srikanth, M., Lakshmikhanth, N., et al.: Survey on various gesture recognition techniques for interfacing machines based on ambient intelligence. arXiv preprint arXiv:1012.0084 (2010)
2. Singer, M.A., Goldin-Meadow, S.: Children learn when their teacher's gestures and speech differ. Psychol. Sci. **16**(2), 85–89 (2005)

3. Ohn-Bar, E., Trivedi, M.M.: Hand gesture recognition in real time for automotive interfaces: a multimodal vision-based approach and evaluations. IEEE Trans. Intell. Transp. Syst. **15**(6), 2368–2377 (2014)
4. Strezoski, G., Stojanovski, D., Dimitrovski, I., Madjarov, G.: Content based image retrieval for large medical image corpus. In: Hybrid Artificial Intelligent Systems, pp. 714–725. Springer, Heidelberg (2015)
5. Bilal, S., Akmeliawati, R., El Salami, M.J., Shafie, A.A.: Vision-based hand posture detection and recognition for sign languagea study. In: 2011 4th International Conference on Mechatronics (ICOM), pp. 1–6. IEEE (2011)
6. Molchanov, P., Gupta, S., Kim, K., Kautz, J.: Hand gesture recognition with 3d convolutional neural networks. In: Proceedings of the IEEE Conference on Computer Vision and Pattern Recognition Workshops, pp. 1–7 (2015)
7. Neverova, N., Wolf, C., Taylor, G.W., Nebout, F.: Multi-scale deep learning for gesture detection and localization. In: Computer Vision-ECCV 2014 Workshops, pp. 474–490. Springer, Heidelberg (2014)
8. Barros, P., Magg, S., Weber, C., Wermter, S.: A multichannel convolutional neural network for hand posture recognition. In: Artificial Neural Networks and Machine Learning–ICANN 2014, pp. 403–410. Springer, Heidelberg (2014)
9. Szegedy, C., Liu, W., Jia, Y., Sermanet, P., Reed, S., Anguelov, D., Erhan, D., Vanhoucke, V., Rabinovich, A.: Going deeper with convolutions. In: Proceedings of the IEEE Conference on Computer Vision and Pattern Recognition, pp. 1–9 (2015)
10. Krizhevsky, A., Sutskever, I., Hinton, G.E.: Imagenet classification with deep convolutional neural networks. In: Advances in neural information processing systems, pp. 1097–1105 (2012)
11. Simonyan, K., Zisserman, A.: Very deep convolutional networks for large-scale image recognition. arXiv preprint arXiv:1409.1556 (2014)
12. Marcel, S., Bernier, O., Viallet, J.E., Collobert, D.: Hand gesture recognition using input-output hidden Markov models. In: FG, p. 456. IEEE (2000)
13. Strezoski, G., Stojanovski, D., Dimitrovski, I., Madjarov, G.: Deep learning and support vector machine for effective plant identification. In: Proceedings of ICT Innovations 2015 Conference Web Proceedings, pp. 221–233 (2015)

Computer-Based Statistical Description of Phonetical Balance for Romanian Utterances

A. Cocioceanu[1], T. Ivănoaica[1,2], A.I. Nicolin[1,2(✉)], and M.C. Raportaru[1]

[1] Department of Computational Physics and Information Technologies, Horia Hulubei National Institute for Physics and Nuclear Engineering, Reactorului 30, Magurele, Romania
alexandru.nicolin@nipne.ro
[2] University POLITEHNICA of Bucharest, Splaiul Independentei 313, Bucharest, Romania

Abstract. Motivated by the advent of security solutions which rely on voice biometrics, we revisit by means of extensive computer-based investigations the concept of phonetical balance for Romanian utterances. We show that the standard distribution of phonems offers only a partial description of the phonetics of the language and that more detailed statistical indicators are needed. To this end, we introduce a simple indicator that measures vowel-consonant (or consonant-vowel) sequences and analyze the distribution of consonant clusters for Romanian words. Our results show that the distribution of consonant clusters is scale-free-like (akin to the distribution of words and phrases in large texts) and that large clusters of vowels or consonants are infrequent. This, in turn, indicates that utterances consisting of words which are statistically unrepresentative with respect to the previous indicators are good candidates for benchmarking the efficency of voice biometrics solutions.

1 Introduction

One of the important changes imposed by the Digital Era concerns the way in which we secure and have access to our assets. Traditionally understood as a physical object that belongs to the owner, the key that grants access to one's assets has gradually shifted towards something the owner knows and, more recently, towards who the owner is. In fact, the etymology of the word shows the key as a metal piece for opening locks (via Middle English *keie* cognate with the Middle Low German *keie*, which means lance or spear), emphasizing the physical nature of the object. The Digital Era, however, has transformed the key into a piece of information, something that (only) the owner knows, usually in the form of an alphanumeric sequence that the owner provides before accessing some digital resources, such as financial data in e-banking systems, medical files on e-health platforms, personal data on cloud storage provides, etc. [1]. In a way, the plethora of digital security solutions, in particular the software ones, such as the hashing methods used to conceal the digital keys, the mechanisms and algorithms used to tunnel and wrap them, the certification systems used to secure

G. Stojanov and A. Kulakov (eds.), *ICT Innovations 2016*,
Advances in Intelligent Systems and Computing 665,
https://doi.org/10.1007/978-3-319-68855-8_6

the data transfers, etc., mask the central position that the alphanumeric digital keys currently have in the information ecosystem. Moreover, although numerous hybrid authentication methods exist, e.g., the two-factor authentication, where the addition of a new recognition method is improving the authenticity of the owner's identity [2], we observe that one component of this scheme remains invariant: the (tried and tested) alphanumeric key.

Naturally, the assets themselves have shifted towards the digital realm as well, as have many of our activities. In fact, digital technologies have substantially changed the way we socialize and entertain ourselves, the way we work and learn, and so on, and we now have a new discipline, namely digital sociology, solely dedicated to the way these technologies are impacting our everyday life [3].

Finally, the past decades have placed more emphasis on (implicitly automated) biometrics security solutions, which allow the owner of some assets to access them not by using something that he possesses or something that he knows, as done in the past, but rather by identifying himself as the owner [4]. The term biometrics itself is defined as "automated recognition of individuals based on their behavioral and biological characteristics" (see ISO/IEC JTC1 SC37), the most common biometric traits used for authentication of users being the fingerprint, the face, the iris, the palm-print, the retina, and the voice. In fact, any human physiological and/or behavioral characteristic can be used as a biometric characteristic, as long as it satisfies a series of requirements such universality, i.e., every person using the system should possess the trait, uniqueness, i.e., the trait should be sufficiently different for individuals in the relevant population such that they can be distinguished from one another, etc., but at the moment the voice is one of the most used traits [4].

As part of building a voice-biometrics identification system which is largely text-independent (i.e., no pass phrase) and shows little sensitivity to ambiental noise [5], we revisit by means of extensive computer-based investigations the concept of phonetical balance for Romanian utterances. The goal of our investigation is to have statistical descriptors of the phonology of the Romanian language that will be helpful in the development stages of the aforementioned voice-biometrics identification system. To this end, we go beyond the standard distribution of phonems and analyze the distribution of consonant clusters for Romanian words to identify the most important ones. Moreover, we propose a simple indicator that measures vowel-consonant sequences to show that large clusters of vowels or consonants are infrequent.

2 Distribution of Phonems

While the mathematics behind the distribution of phonems in a given text is relatively simple, the main technical challenge comes from finding a set of texts, usually very large, that are representative for the language under scrutiny. In the case of Romanian language [6] the text was acquired using the Web-as-resource or Web-as-corpus approach (considering as sources mainly online Romanian newspapers and transcripts of the discussions in the European parliament) [7], which

produced more than 9 million phrases, the largest Romanian plain text corpus to date [7]. The results of this analysis clearly show that the 34 phonems identified are qualitatively different, some of them being very common, while others somewhat infrequent. In fact, the first six phonems correspond to more than 50% of the entire phonem usage, while the last six phonems have an occurrence frequency in between 0.27% and 0.03%.

The aforementioned distribution of phonems (complemented with related results in Ref. [8]) gives an accurate *global* description of the Romanian language which can be now compared with languages (such as English and French) for which such statistical descriptions have a long history. We note, however, that in the case of smaller texts this statistical description is insufficient, as two small texts of similar if not identical distribution of phonems may be, in fact, substantially different from a phonetic point of view. As an elementary example we note here two simple Romanian sentences, namely S1: "Oaia e proastă" (in English: The sheep is dumb) and S2: "Ia ta e poroasă" (in English: Your blouse is porous), which consist of the same phonems but differ considerably. The first sentence, for instance, has a series of four subsequent vowels (namely "oaia e") and a consonant cluster of two letters (namely "st"), while the second has no consonant cluster and the longest series of vowels is of length two (namely "ae" and "oa").

In the language of statistical physics, if the statistical ensemble is very large, than the distribution of phonems becomes the key descriptor of the text under scrutiny, as all other features (say, vowel and consonant clusters, distribution of words, and so on) average out. For short texts, however, the distribution of phonems should be complemented with additional information about the vowel-consonant sequences and the types of consonant clusters.

3 Distribution of Consonant Clusters

Motivated by the previous example we embarked on a detailed statistical study of the Romanian vocabulary using the database of Dexonline [9], which is an open source collection of the main dictionaries of the Romanian language. For our analysis we used a set of more than 90.000 words, which roughly correspond to the lexicon in Ref. [10], which is the main dictionary of the Romanian language.

Through a thorough statistical analysis we identified all two-consonant clusters, independent of their position in a word, and ranked them according their occurrence race. To simplify the analysis, the results for the letter *s* include also the letter *ș*, while those for the letter *t* also include the letter *ț*. The bubble-plot in Fig. 1 shows the main consonant clusters, indicating their occurrence through the size of the bubble. The main message of the plot is that there are a few frequent consonant clusters (such as "st", "nt", "tr", "pr", etc.) which appear in 5% to 10% of all words in the Romanian vocabulary and numerous other infrequent clusters (such as "lb", "sf", etc.). A rapid inspection of the plot shows the tendency to have consonant clusters using the letters in the second half of the consonant series. Moreover, there is a clear assymetry with respect to the

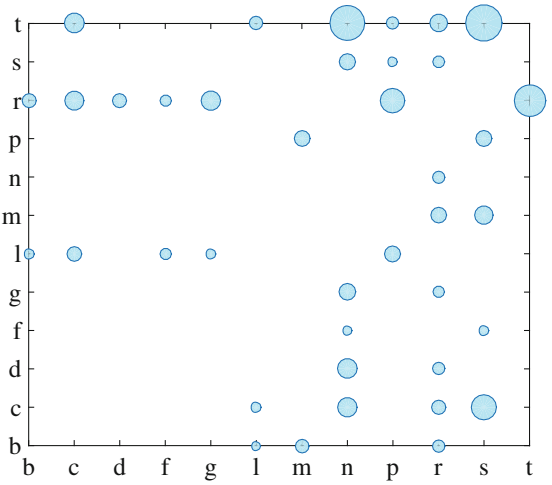

Fig. 1. Bubble plot of the main two-letters consonant clusters observed in Romanian words. The size of the bubble is proportional to the number of words in which the cluster appears.

first diagonal, meaning that the frequency rates of a given cluster and its inverse are substantially different. To understand this property let us look at the "tr" cluster which is more frequent than the "rt" cluster, or, more clearly at the "st" and "ts" ones. The first order of the consonants, "st", corresponds to one of the most important Romanian cluster, while "ts" is inexistent.

What is more interesting is that the distribution of the consonant clusters follows a free-scale-like distribution. Taking $P(k)$ as the probability that a given cluster appears in k words, we observed (see Fig. 2, the upper panel) that $P(k) \approx k^{-\gamma}$ where $\gamma \approx 3.2$. This statistical behavior shows a striking resemblance to the so-called Zipf law which states that the frequency of a given word is inversely proportional to its rank in the frequency table [11]. A classical textual econometrics study on the Brown Corpus of American English showed "the" as the most frequent word in the vocabulary (with an occurrence rate of almost 7%), "of" as the second most frequent word with an occurrence rate of roughly 3.5%, etc. Similarly, it has been shown that the distribution of word sequences (the so-called n-gramas) follows the same pattern, provided the reference texts are large enough [12]. The key feature of the Zipf law is that on a log-log plot the distribution is linear with a negative slope, which is similar to what we noticed in Fig. 2 (the upper panel). In our case "st" was the most frequent consonant cluster with a frequency rate of 9.4%, "nt" was the second most frequent cluster (8.5% frequency rate), "tr" was the third one (7% frequency rate), etc. This distribution is typical to many systems, ranging from social networks (such as the collaboration of movie actors in films and the co-authorship of papers), the internet, the protein-protein interactio, etc. [13]. While Zipf's law has been verified in numerous contexts the mechanisms behind it remain largely elusive, despite numerous models which capture some of its features. Zipf, for example,

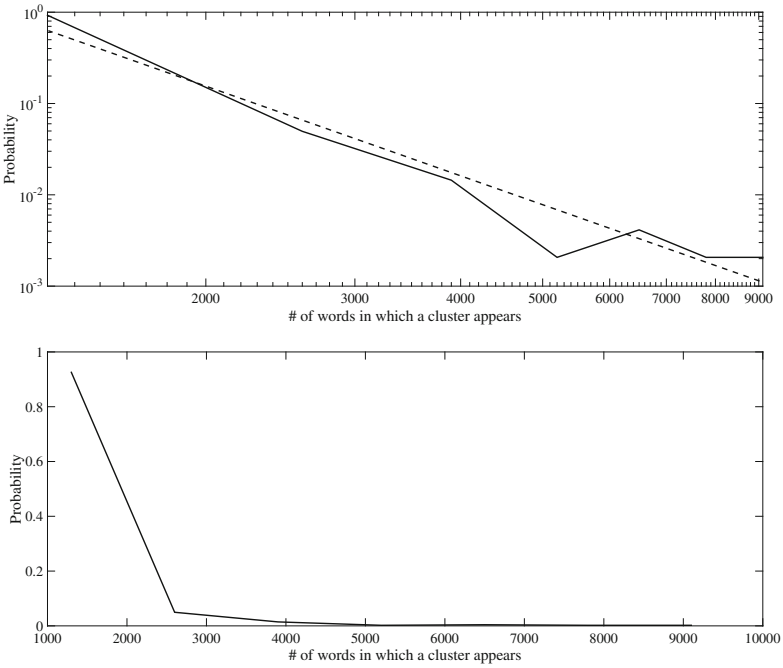

Fig. 2. (Upper panel) Distribution of the probability that a given cluster appears in a given number of Romanian words. Please note that the plot is log-log. The dashed line shows the linear fit (in log-log axes) of the function and corresponds to a slope of −3.2. (Lower panel) The same distribution as in the upper panel on a graph without log-log axes. Please notice the rapid decay of the distribution for a number of words larger than 2000.

understood the law through the principle of least effort, which has been often revisited by means of advanced mathematical models [14], while others consider the *preferential attachment* mechanism which basically says that the speakers tend to use some words more often than others [15].

It is tempting to see the correlation between the frequency rates of the consonant clusters and their etymology, but such an analysis is of little insight, as the Romanian dictionaries only record the language from which a given words entered into the Romanian vocabulary, and not the language of origin [16]. Finally, we note that the distribution of three- and four-letters consonant clusters brings only a small correction to the aforementioned statistics and that a detailed study will be reported elsewhere.

4 Phonetical Balance

The previous discussion on consonant clusters brings some clarification to the phonology of Romanian language, but an instrument is needed to quantify the vowel-consonant sequences. To this end, we introduce for each word in the vocabulary the function

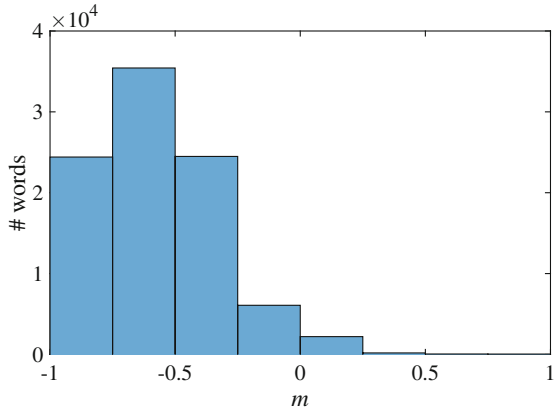

Fig. 3. Distribution of the number of Romanian words as function of the parameter m introduced in Eq. (1). Please note that because of the low number of bins in the histogram it appears, quite erroneously (see Fig. 4), to have a continuous transition from one set of m-values to another. The plot is, however, extremely useful because it allows an easy assessment of the average value of m, which is around -0.5.

$$m = \frac{1}{n-1} \sum_{j}^{n-1} l(j)l(j+1), \tag{1}$$

where n is the number of letters of the word and l is a boolean function equals to 1 if the j-th letter is a vowel and -1 if the j-th letter is a consonant. Please note that a normalization factor equal to $1/(n-1)$ has been introduced in the definition of m such that from the values of m one can directly compare words of different lengths. For words consisting of perfect sequences of vowels and consonants such as "calamitate" (in English: calamity), "repetare" (in English: repetition), "sare" (in English: salt), etc., the m-function is numerically equal to -1, while for the (admittedly fewer) words consisting almost entirely of vowels or consonants, such as "oaie" (in English: sheep) and "ouă" (in English: egs) on the vowel side and "strâmb" (in English: crooked) and "prompt" (in English: prompt) on the consonant side, the m-function is always larger than 0. In fact for "oaie" and "ouă" the m-function is equal to exactly $+1$ but this is valid for a very short list of words.

In Figs. 3 and 4 we show the distribution of the number of Romanian words as function of the parameter m, using a histogram plot with different number of bins, to show that the majority of words corresponds to negative values of m ($\overline{m}$, the average value of m being, in fact, very close to -0.5), thereby indicating that most Romanian words are structured as (slightly) imperfect vowel-consonant sequences. Figure 4, in particular, shows extremely clearly that there is a large set of words, around 18.5% of the investigated vocabulary, which corresponds to $m = -1$.

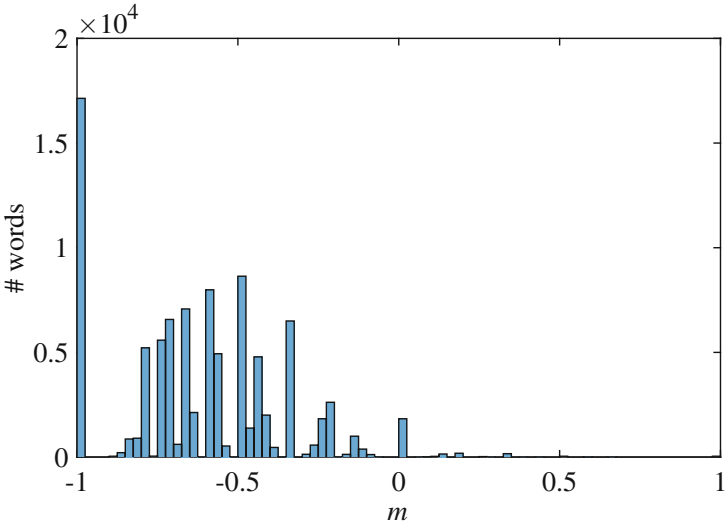

Fig. 4. Detailed distribution of the number of Romanian words as function of the parameter m introduced in Eq. (1). Please note the isolated cluster close to $m = -1$ and the bunch in between $m = -0.8$ and $m = 0$. From the graph one can easily assess that there are around 17.500 words with an m-value very close to $m = -1$.

This shows, incidentally, that the first sentence discussed in Sect. 2 consists of words from the tail of the distribution of m (though the consonant cluster is one of the very frequent ones), while the second sentence consists of words from the bulk part of the distribution. Let us also note that approximately 26% of the Romanian words correspond to $m < -0.75$. Finally, let us mention that it is very tempting to compute the global m value considering the reported frequencies of Romanian words [17], but the computations were done before the advent of the computer and the validity of some of the reported frequencies has been questioned [16]. We can, however, use Eq. (1) for entire sentences, just like for words, and obtain $m_{S1} = 3/11$ for the first sentence and $m_{S2} = -5/11$, for the second one, which indicates that the first sentence is *less representative* in a statistical sense with respect to the vowel-consonant (or consonant-vowel) sequences than the second one.

5 Conclusions

In this paper we have analyzed by computational means the phonetical balance of Romanian words and introduced two indicators that go beyond the standard distribution of phonems. We have shown that the distribution of consonant clusters in Romanian words obeys a scale-free-like distribution and that large clusters of vowels or consonants are infrequent. The distribution of consonant clusters is similar to the well-known Zipf law that gives the distribution of words

and short sentences in that it shows that there are a few very frequent consonant clusters and numerous others which are considerably less frequent. Our results suggest that a reliable voice-based biometrics solution should be particularly benchmarked against utterances which consist of words with infrequent consonant clusters and words with positive m-values, as their statistical unrepresentativeness makes them good candidates for identifying the flaws of a given biometrics solution.

As a natural extension of this work we intend to refine the current results by taking into account the position of a consonant cluster with respect to the syllables of a word. Moreover, future research should be focused on a global indicator (such as the Shannon entropy) which considers not only the relations between the nearest neighbours letters, but also long-range in-word correlations between letters and clusters.

Acknowledgement. The work was supported by the Horizon 2020 SpeechXRays project. This project has received funding from the European Union's Horizon 2020 research and innovation programme under grant agreement No. 653586. The authors thank Dan Caragea and Mihai Bărbulescu for insightful discussions.

References

1. Bonneau, J., Herley, C., van Oorschot, P.C., Stajano, F.: Passwords and the evolution of imperfect authentication. Commun. ACM **58**, 78–87 (2015)
2. See, for example, Apple's Touch ID, the biometric fingerprint plus PIN code, the Google 2-Step Verification, and the user telephone number plus user password
3. Lupton, D.: Digital Sociology. Routledge, Abingdon (2014)
4. Jain, A.K., Flynn, P., Ross, A.A. (eds.): Hanbook of Biometrics. Springer, New York (2008)
5. See, in particular, the SpeechXRays project (http://www.speechxrays.com) which "will develop and test in real-life environments a user recognition platform based on voice acoustics analysis and audio-visual identity verification" which uses "text-independent speaker identification (no pass phrase)" and "low sensitivity to surrounding noise" (as retrived June 2016). The testing will be done in Greek and Romanian (2016)
6. See a detailed description of the Romanian language on its Wikipedia entry at https://en.wikipedia.org/wiki/Romanian_language
7. Stanescu, M., Cucu, H., Buzo, A., Burileanu, C.: ASR for low-resourced languages: building a phonetically balanced Romanian speech corpus. In: 20th European Signal Processing Conference (EUSIPCO 2012) (2012). ISSN 2076-1465
8. Stanescu, M., Buzo, A., Cucu, H., Burileanu, C.: Statistical phonetic analysis of the Romanian language for speech recognition and synthesis tasks. In: 54th International Symposium ELMAR (2012)
9. The Dexonline dictionary is publicly available at https://dexonline.ro and consists of more than fifty distinct dictionaries (see the complete list at https://dexonline.ro/surse) which have a very broad coverage. The dictionaries go from general-use prescriptive dictionaries and thesauruses to topical and orthographic dictionaries
10. Explanatory Dictionary of the Romanian Language (in Romanian), Romanian Academy, "Iorgu Iordan" Liguistic Institute, Editura Univers Enciclopedic, 2nd Edn. (1996)

11. Zipf, G.K.: Human Behavior and the Principle of Least Effort. An Introduction to Human Ecology. Addison-Wesley Press, Boston (1949)
12. Ha, L.Q., Sicilia-Garcia, E.I., Ming, J., Smith, F.J.: Extension of Zipf's law to words and phrases. In: Proceedings of 19th International Conference on Computational Linguistics - COLING (2012)
13. Barabasi, A.-L., Reka, A.: Emergence of scaling in random networks. Science **286**, 509–512 (1999)
14. i Cancho, R.F., Sole, R.V.: Least effort and the origins of scaling in human language. Proc. Nat. Acad. Sci. **100**, 1788–1791 (2003)
15. Lin, R., Ma, Q.D.Y., Bian, C.: Scaling laws in human speech, decreasing emergence of new words and a generalized model (2015). arXiv:1412.4846v2
16. Dinu, M.: Personalitatea Limbii Române, Cartea Românească (1996). (in Romanian)
17. Juilland, A., Edwards, P., Juilland, I.: Frequency Dictionary of Romanian Words. Mouton & Comp., Clearwater (1965)

Distributed Private Key Generator for ID-Based Public Key Infrastructure

Pance Ribarski(✉) and Ljupcho Antovski

Faculty of Computer Sciences and Engineering, Ss. Cyril and Methodius University, Skopje, Macedonia
{pance.ribarski,ljupcho.antovski}@finki.ukim.mk

Abstract. We recognize the need of certificateless PKI to reduce the step of obtaining the public key. This leads to ID-Based cryptography where we have PKI with full power to generate private keys for any identity. We solve this problem by implementing distributed key generation to form a group of players which will act as private key generator for ID-Based PKI. The implementation is done on the Android platform, showing the possibilities of running PKI on cheap and widely available hardware.

Keywords: Distributed key generation · ID-based cryptography · PKI · Implementation · Android

1 Introduction

Ever since 1984 when Shamir [15] introduced the notion of identity-based public key encryption (IBE), this new scheme was fully adopted and researched through the years. Shamir's paper was only the introduction and left open questions for future research on the topic. His work only covered ID-Based signatures, not full ID-Based cryptography. Papers followed immediately in 1987 [6,16], in 1989 [17] and in 1991 [12]. However, all these schemes were unsatisfactory. The first fully functional IBE scheme was proposed by Boneh and Franklin [3] in 2001[1].

Shortly, in IBE scheme the public key is a well-known string that is tied to the identity of the client. This string can be the client's email, telephone number, website, or some other string that is well-known in the protocol where IBE is used. This leads to the notion of certificateless public key crypto (certificateless PKC). Obviously, the positive thing here is removing the need for obtaining certificates from public key infrastructure (PKI). But, the downside is the extreme power given to the private key generator (PKG) of the ID-Based PKI. In this paper we introduce a solution to this problem by implementing real-world distributed key generation scheme (DKG scheme) on the Android platform. We are showing that everyday mobile devices can be used as distributed PKG in certificateless PKI. Afterwards, the given solution can be plugged in any protocol that employs ID-Based PKC in the mobile world.

[1] Please refer to [10] for more extensive overview on IBE schemes and papers.

G. Stojanov and A. Kulakov (eds.), *ICT Innovations 2016*,
Advances in Intelligent Systems and Computing 665,
https://doi.org/10.1007/978-3-319-68855-8_7

Related Eork. There has been a lot of work towards distributed key generation. One of the earliest works on distributed key generation is Pedersen's verified secret sharing in 1992 [13]. His work shows how to compute on shared secrets, thus opening the way for distributed key generation. Following his work, Gennaro published papers in 1997 and 1998 on the topics of VSS and distributed key generation for discrete-log cryptosystems [8,9]. After them, there are papers starting to investigate asynchronous secret sharing and DKG systemts [4]. These papers are followed by papers with real implementation of DKG systems for the internet [11]. Afterwards, some authors started using bivariate functions in VSS schemes for more efficient distributed key generation schemes [1,18]. Our work is based on the research of Pedersen on verifiable secret sharing and Gennaro's papers for discrete-log distributed key generation schemes. Our aim is to implement a real-world distributed key generation algorithm in ID-Based PKC scenario, having in mind mobile devices.

Organization of this Paper. The Sect. 2 introduces secret sharing theory, the notion of secure secret sharing and secret sharing without honest dealer. This section also covers the introduction of ID-Based cryptography and the open problem we are trying to solve. The Sect. 3 gives solution to the open problem with ID-Based single center of power PKG. It outlines the protocol, the PKG initialization and the key extraction protocol. Finally, the Sect. 4 gives final words on the topic.

2 Basics

2.1 Secret Sharing

The notion of secret sharing means dividing a secret information into pieces and giving those pieces to players in the secret sharing protocol. After the sharing process, every player has a piece of the secret information without having any knowledge about the secret. When enough players gather together, the secret information can be reconstructed. If less than enough players gather, the secret information can not be reconstructed. This neccessary number of players is called a threshold value.

The roles in the secret sharing protocol are a Dealer and Players. The Dealer has the secret information, divides it into pieces and shares the pieces to the Players. During the process of dividing the secret, the Dealer decides on the threshold value and the number of Players. Because the Dealer has the secret in the beginning, it is considered that he/she is honest, and further more, forgets the secret immediatelly after the dealing. When the number of gathered players is greater or equal than the threshold value, then the secret information is reconstructed by combining their pieces.

Definition 1. A secret scharing scheme (t, n) is the process of sharing a secret S into pieces $S_1, S_2, \ldots, S_n$ in a way that:

– Any t gathered pieces can reconstruct S;
– Any $t-1$ or less pieces can not give away any information about S.

The secret sharing scheme consists of two phases:

– Sharing phase: the Dealer divides the secret S and shares piece S_i to Player P_i, $i = 1, \ldots, n$;
– Reconstruction phase: all players gather their pieces, at least the threshold number of pieces will reconstruct S.

This is called a secret sharing scheme with n players and threshold value t.

The secret sharing was invented in 1979 by Shamir [14] and by Blakley [2] independantly from each other. The concept is used where sensitive data is used and they should not be visible all the time. This refers to, for example, cryptographic keys, secret documents, PIN numbers and other similar types of data. Using the secret sharing scheme (see Defintion 1), we can split this sensitive data across more data centers (or databases). In this way, not one (or any number lower than the threshold value) data center can access the data. Only when enough centers gather (the threshold value), the sensitive data can be reconstructed and used.

Adi Shamir's Secret Sharing. The secret sharing scheme from Shamir [14] gives a way to share a secret with threshold value t. The scheme is using the fact that exactly t points are enough to define a polynom of degree $t-1$. Knowing this, we can define the Shamir's scheme for secret sharing.

Let n be the number of players in the secret sharing protocol. Let s be the secret that needs to be shared with the players in the execution of the protocol. Let t be the threshold value, i.e. the lowest number of players needed for reconstruction of the secret. This is called a (n, t) secret sharing scheme. The Dealer of the secret defines the polynom $f(x)$ as follows:

$$f(x) = s + a_1 x + a_2 x^2 + a_3 x^3 + \ldots + a_{t-1} x^{t-1} \tag{1}$$

The coefficients $a_1, a_2, a_3, \ldots, a_{t-1}$ are random integers, and the zero coefficient is the secret s that needs to be shared. The Dealer calculates pieces of the secret for each Player P_i, $i = 1, \ldots, n$ as $(i, f(i))$, $i = 1, \ldots, n$. The Dealer sends the pair $(i, f(i))$ to the player P_i. The data transfer must be secure, nobody must gain access to the data for the Player P_i except P_i.

Since exactly t points are enough for defining a polynom of degree $t-1$, we need at least t points (t pairs given to the Players) to reconstruct $f(x)$. We do this by using Lagrange interpolation of polynomials. The interpolated polynom over the given points is the linear combination:

$$L(x) = \sum_{j=1}^{t} f(i_j) l_j(x) \tag{2}$$

where $l_j(x)$ is the Lagrange base polynom:

$$l_j(x) = \prod_{1 \le m \le t,\, m \ne j} \frac{x - i_m}{i_j - i_m}\ ,\ j = 1, 2, \ldots, t \tag{3}$$

By solving $L(x)$ we actually get interpolated $f(x)$. But, the interest in the interpolation should be diverted only to the zero coefficient - the secret s. There is no need to calculate the other coefficients in $f(x)$, those are random integers that are not connected to the secret. To calculate only the zero coefficient we have the following:

$$l_j(0) = (-1)^{t-1} \prod_{1 \le m \le t,\ m \ne j} \frac{i_m}{i_j - i_m},\ j = 1, 2, \ldots, t \tag{4}$$

Verified Secret Sharing (VSS). The secret sharing scheme allows sharing a secret to players in the protocol. In this simple case (as the Shamir's scheme), the players are supposed to be honest and play along correctly in the protocol. In scenarios where we have a malicious dealer which does not want the secret to be reconstructed, the dealer can make deliberate mistakes in the sharing phase. In these scenarios we want to the use the so-called verified secret sharing. It was first introduced in 1985 by Chor et al. [5].

To implement a VSS we need an extension in the sharing phase. In this phase, the players can make more rounds of communication to verify the received pieces of the secret information. If the dealer is malicious and gives wrong pieces of the secret information, this phase can detect that and stop the execution of the protocol. If all the shared pieces pass this verification test, then we can calculate the secret if enough players give their pieces.

Feldman VSS. The Feldman verified secret sharing scheme [7] is an upgrade over the Shamir secret sharing scheme [14]. Feldman used the homomorphic property to get a verified secret sharing scheme. Just like in the Shamir's scheme, we define n, s and t to be the number of players in the protocol, the secret which has to be shared and the threshold value of the number of players. Then, the Dealer defines the polynomial $f(x)$ as in Eq. 1 where the coefficients $a_1, a_2, a_3, \ldots, a_{t-1}$ are random integers and the zero coefficient s is the secret. Then, the Dealer calculates the pieces for the players as pairs $(i, f(i)),\ i = 1, \ldots, n$. Additionally, the Dealer calculates the commitments to the coefficients of $f(x)$ and the evaluation in i: $c_0 = g^s, c_1 = g^{a_1}, \ldots, c_{t-1} = g^{a_{t-1}}$ and $d_i = g^{f(i)}$.

After this, the Dealer sends the point $(i, f(i))$, the commitments c_i and d to the Player P_i. The Player P_i is now in position to verify that $f(i)$ is really the evaluation of $f(x)$ in i by calculating:

$$c_0 c_1^i \ldots c_{t-1}^{i^{t-1}} =$$
$$g^s (g^{a_1})^i \ldots (g^{a_{t-1}})^{i^{t-1}} =$$

$$g^s g^{a_1 i} \dots g^{a_{t-1} i^{t-1}} =$$
$$g^{s+a_1 i+\dots+a_{t-1} i^{t-1}} =$$
$$g^{f(i)} = d_i$$

By using the homomorphic property of the exponents in the group G it is possible to get a verification scheme. The difference between the Pedersen's scheme and the Shamir's scheme is that here the Dealer sends additional t elements from the group G, the Dealer makes additional t exponentiations and the Player P_i computes additional t exponentiations and t multiplications of the elements from G.

Sharing Without an Honest Dealer. Shamir's and Feldman's schemes require an honest Dealer. Some protocols require secret sharing scheme where the Dealer does not have to be honest. These schemes are usualy employed in DKG protocols. Pedersen first presented this kind of scheme in 1992 [13]. The additional property over the previous secret sharing scheme allows use of this scheme in protocols where you can not trust any entity to know the secret in the phase of sharing. In this scheme nobody knows the secret S until the reconstruction phase. In Pedersen's secret sharing scheme [13] there is actually execution of n parallel secret sharing schemes without an honest dealer. Every Player P_i shares their secret S_i to the other players. Every Player gets $n-1$ other pieces of shared secrets. The shared secret S across the group of Players is some arithmetic operation over all the S_i pieces (for example, sum of all S_i). If the Players have to do some operation with S (for example extract a key in ID-Based cryptography), each P_i does operation over their own S_i to contribute to the final result.

2.2 ID-Based Cryptography

In public crypto every player owns private and public key. The private key should be secured and the public key is shared with everybody. When Player A wants to send message to Player B, he/she encrypts it with the public key of the Player B. When Player B wants to decrypt the message, he/she uses the private key of Player B. If the Player A wants to prove the authenticity of the message, he/she signs it with the private key of the Player A, and when Player B wants to check whether the message is from Player A, they use the public key of Player A.

In the above scenarios we see that both players have to obtain the public keys from each other in some way. If the players communicate often, then the price of obtaining keys is negligible. But, if the protocols assume short communication between players that interchange all the time, then the price of obtaining the public keys becomes substantial.

In scenarios where the players are all part from some organization, then this organization creates an entity which helps managing the keys. This entity is called Public Key Infrastructure (further in the text PKI). Having a PKI, players are enabled players to obtain public keys from other players easily and

in a secure way. In the PKI infrastructure there is a Certificate Authority that signs the public key of the members of the PKI. The signatures and the public key that are tightly coupled to specified player are called a certificate. If there is a breach in the private key for some member, then the PKI will issue a new certificate with the new public key for the member, i.e. revoke the old key. The cryptography that is based on PKI is called a certificate-based cryptography.

The ID-Based cryptography is tackling the problems of certificates. By introducing an identification as public key, the ID-Based cryptography eliminates the need for certificates. Therefore, it is also called certificateless cryptography. The elimination of certificates is a big advantage for ID-Based cryptography. But, the design of the PKI infrastructure for ID-Based cryptography opens another problem. The Private Key Generator (further in the text as PKG), is the entity that generates private keys for given identities. This means that the PKG has the power to generate private key for any identity. The PKG has substantially more power than the Certificate Authority in regular PKI. Solution to this problem is given in [3] and states that the master private key of the PKG should be divided amongst more entities in such way that generating a private key for given identity would require all of them or certain threshold value of them. This paper offers implemented solution to divide the center of power in the DKG by using secret sharing without honest dealer for sharing the master key of the DKG.

3 Implementation

We implemented DKG for ID-Based PKG, effectively rendering a secure certificateless API. First we define the following:

Definition 2. Secure PKI for ID-Based cryptography represents a system for Private Key Generator with the following characteristics:

- The system consists of n players with t threshold value,
- There is no player that has the power to generate private key for any given identity,
- Only t or more players can generate private key for a given identity.

1 Generate $f_i(x)$:
- Choose at random $a_{i,j}, j = 0, ..., t-1$ the coefficients of $f_i(x)$ where the zero coefficient is the s ecret of the DKG Player P_i

2 Calculate the commitments:
- Calculate the commitments of the coefficients of $f_i(x)$: $c_{i,j} = g\_public^{s_i}, j = 0, ..., t-1$

3 Evaluate the polynomial:
- Evaluate the polynomial for the other players $eval_i = f_i(j), j = 1, ..., n, j \neq i$

Scheme 3.1. Initialization step for DKG Player P_i

1 Share the commitments:
- DKG Player P_i prepares commitments $c_{i,j}, j = 0, ..., t-1$ for DKG Player $P_j, j = 1, ..., n, j \neq i$

2 Share the evaluations:
- DKG Player P_i prepares the evaluation of the polynom $f_i(j)$ for DKG Player P_j, $j = 1, ..., n$

3 Send the message:
- DKG Player P_i sends the message *commandReceivePieces* to every DKG Player $P_j, j = 1, ..., n, j \neq i$

Scheme 3.2. DKG Player P_i is sharing the commitments and evaluations

The proposed system uses elliptic curves and pairings over elliptic curves. We use the pairing-friendly Barreto-Naehrig family of curves. In the following subsections we define the protocol, the setup of the system and the extraction of keys.

Protocol. The proposed protocol assumes synchronious communication where the channels between the players are secure and untappable. The roles in the protocol are DKG Player and Client. The DKG Players are the PKG body of the PKI, and the Clients are users of the PKI which need to get private key from the PKG.

Setup. In the beginning all the DKG Players establish communication channels with each other. The setup is initiated from a random DKG Player, called a Leader. The first task of the Leader is to setup the elliptic curve and its properties, the pairing type, the three pairing groups G_1, G_2 and G_3, the number n of DKG Players and the threshold value t of the PKG. Then, the Leader sends message *commandInit* to all the other DKG Players and all the players execute the initialization step (scheme 3.1). After the initialization step finishes, all the DKG Players send back the message *commandInitFinished* to the Leader.

After receiving $n-1$ messages *commandInitFinished*, the Leader starts the second phase of the setup protocol. In this phase, the Leader sends the message *commandSharePieces* to all DKG Players. Every DKG Player upon receiving this message starts sharing the commitments and evaluations of their polynom (scheme 3.2).

After the DKG Player P_i receives a message *commandReceivePieces* saves the commitments and evaluation from $P_j, j = 1, \ldots, n, j \neq i$. After saving, the DKG Player P_i sends the message *commandSharePiecesFinished* to the Leader. After receiving $n-1$ messages *commandSharePiecesFinished*, the Leader starts the third phase - verification by sending the message *commandVerifyCommitmentsAndEvals* to all DKG Players. After the DKG Player P_i receives this message, they start the procedure for verification (scheme 3.3).

1 Calculate the commitment to the group secret:
- DKG Player P_i calculates $g\_pow\_s\_public = \prod_{j=1}^{n} c_{j,0}$

2 Verification of commitments and the evaluation of $f(x)$ from DKG Player $P_j, j = 1, ..., n, j \neq i$:
- DKG Player P_i checks if the following holds
  $c_{j,0}c_{j,1}...c_{j,t-1} \stackrel{?}{=} g^{f_j(i)}, j = 1, ..., n, j \neq i$

3 Sending success message:
- If all the verifications are in order, DKG Player P_i send the message *commandVerifyCommitmentsAndEvalsFinished* to the Leader

Scheme 3.3. DKG Player P_i verifies received commitments and evaluations

1 Leader sends $(n-1)$ messages to the other playeres:
- byte: 1
- Integer: 2
- G1: 1

2 Other $(n-1)$ players send one message to the Leader:
- byte: 1

Scheme 3.4. Messages sent in the first phase: initialization of DKG Players. Here we see the content of each sent message in terms of type of the variables.

After the Leader receives $n-1$ messages *commandVerifyCommitmentsAndEvalsFinished*, finishes the setup protocol. This means that the DKG Players successfully created a PKG group and can start issuing private keys.

The price represented in bandwidth and calculations in the first phase of the setup are given in the following schemes.

Key Extraction. When the setup protocol is executed, the DKG Players successfully create a group which can act as PKG. The key extraction phase begins with the Client asking any DKG Player for the public parameters of the PKG.

1 All players calculate:
- scalar doubling: $2n + 1$
- G1 scalar multiplication: $2n(k-1) + k + 1$
- scalar addition: $n(k-1)$

2 Leader calculates
- G1 serialization: 1

3 Other $(n-1)$ players calculate
- G1 deserialization: 1

Scheme 3.5. Arithmetic operations in the first phase: initialization of DKG Players. Here we see the arithmetic operations each player performs.

1 The Leader sends $(n-1)$ **messages to the other players:**
- byte: 1

2 All players send one message to all other players (totalling $n(n-1)$ **messages):**
- byte: 1
- G1: $k+1$
- Scalar: 1

3 All players send one message to the Leader (totalling $n-1$ **messages):**
- byte: 1

Scheme 3.6. Messages sent in the second phase: sharing of pieces. Here we see the content of each sent message in terms of type of the variables.

1 All players calculate:
- G1 serizalization: $k+1$
- Scalar serialization: k

Scheme 3.7. Arithmetic operations in the second phase: sharing of pieces. Here we see the arithmetic operations each player performs.

1 The Leader sends $(n-1)$ **messages to the other players:**
- byte: 1

2 All players send one message to the Leader (totalling $n-1$ **messages):**
- byte: 1

Scheme 3.8. Messages sent in the third phase: verification. Here we see the content of each sent message in terms of type of the variables.

1 All players calculate:
- G1 exponentiation: 1
- Scalar doubling: 1
- G1 doubling: 1
- Scalar exponentiation: k
- G1 scalar multiplication: $n+k$
- G1 multiplication: k
- Scalar addition: k
- G1 equality: 1

Scheme 3.9. Arithmetic operations in the third phase: verification. Here we see the arithmetic operations each player performs.

1 Asking public information about the PKI:
- The User send a message *commandSendPlayersList* to DKG Player
- DKG Player receives *commandSendPlayersList* and sends *commandReceivePlayersList* together with the public parameters about the PKI

2 Asking for private key pieces
- The User sends a message *commandClientGetSumOfEvals* to all DKG Players together with their identificator id
- Every DKG Player P_i calculates and sends $priv_i = id^{s_{i,0}}$ and $g\_public^{s_{i,0}}$ with the message *commandClientReceiveSumOfEvals*

3 Verify the received key pieces:
- When the Client receives *commandClientReceiveSumOfEvals* they verify $priv_i = id^{s_{i,0}}$ by calculating $e_1 = Pairing(g\_public, priv_i)$ and $e_2 = Pairing(g\_public^{s_{i,0}}, id)$ and checking whether $e_1 \stackrel{?}{=} e_2$. If the verification is successful, the piece $priv_i$ from DKG PLayer P_i is accepted

4 Verification and private key creation:
- When the User verifies n pieces, they calculate the private key $d_{id} = \prod_{i=1}^{n} priv_i$
- The calculated private key is verified by calculating $e_1 = Pairing(g\_public, d_{id})$ and $e_2 = Pairing(g\_pow\_s\_public, id)$ and verifiying $e_1 \stackrel{?}{=} e_2$. If the verification is successful, the private key d_{id} is accepted for the identity id issued by the PKI

Scheme 3.10. Key extraction algorithm

1 The Client sends n messages to all DKG Players:
- byte: 1
- String: 1

2 All DKG Players send one message to the Client(totalling n messages):
- byte: 1
- G2: 1

Scheme 3.11. Messages sent while executing key extraction protocol. Here we see the content of each sent message in terms of type of the variables.

These parameters can be access on some kind of a bulletin board too. After getting the public parameters, the Client establishes communication channels with the DKG Players. Then the Client and the DKG Players follow the key extraction algorithm (scheme 3.10).

The price of the key extraction algorithm is represented by the schemes depicting bandwidth (scheme 3.11) and arithmetic operations (scheme 3.12).

1 All DKG Players calculate:
- SHA1 hash $h_1(byte[]) -> G2$: 1
- G2 scalar multiplication: 1
- G2 serialization: 1

2 The Client calculates:
- G2 deserialization: 1
- pairing: $2(n+1)$
- G3 equality: $n+1$
- G2 multiplication: n

Scheme 3.12. Arithmetic operations while executing key extraction protocol. Here we see the the arithmetic operations each player performs.

4 Conclusion

This paper tackles the open problem of central power in the PKG in ID-Based PKC. By using distributed key generation techniques, we successfully removed this central power from only one entity, and divided the power to generate secret keys to a group of entitites. If there is a malicious entity in the group, he/she will not be able to generate private keys for arbitrary identities. Further more, by implementing this protocol on the Android platform, we gave a real-world example that low-cost hardware can be used for PKI infrastructures. This solution can be easily plugged in any ID-Based PKC protocol which requires distributed PKG. We give detailed information about all the bandwidth and computation need for running the protocol. Implementors can easily decide if this solution fits in their protocols, or in their production solutions.

This work was partially financed by the Faculty of Computer Science and Engineering at the "Ss. Cyril and Methodius University" within the project SEG.

References

1. Backes, M., Kate, A., Patra, A.: Computational verifiable secret sharing revisited. In: Proceedings of 17th International Conference on The Theory and Application of Cryptology and Information Security, ASIACRYPT 2011, pp. 590–609. Springer, Berlin (2011). http://dx.doi.org/10.1007/978-3-642-25385-0_32
2. Blakley, G.: Safeguarding cryptographic keys. In: Proceedings of 1979 AFIPS National Computer Conference, pp. 313–317. AFIPS Press, Monval (1979)
3. Boneh, D., Franklin, M.K.: Identity-based encryption from the weil pairing. In: Proceedings of 21st Annual International Cryptology Conference on Advances in Cryptology, CRYPTO 2001, pp. 213–229. Springer, London (2001). http://dl.acm.org/citation.cfm?id=646766.704155
4. Cachin, C., Kursawe, K., Lysyanskaya, A., Strobl, R.: Asynchronous verifiable secret sharing and proactive cryptosystems. In: Proceedings of 9th ACM Conference on Computer and Communications Security, CCS 2002, pp. 88–97. ACM, New York (2002). http://doi.acm.org/10.1145/586110.586124

5. Chor, B., Goldwasser, S., Micali, S., Awerbuch, B.: Verifiable secret sharing and achieving simultaneity in the presence of faults. In: Proceedings of 26th Annual Symposium on Foundations of Computer Science, SFCS 1985, pp. 383–395. IEEE Computer Society, Washington, DC (1985). http://dx.doi.org/10.1109/SFCS.1985.64
6. Desmedt, Y., Quisquater, J.J.: Public-key systems based on the difficulty of tampering (is there a difference between DES and RSA?). In: Proceedings on Advances in cryptology—CRYPTO 1986, pp. 111–117. Springer, London (1987). http://dl.acm.org/citation.cfm?id=36664.36673
7. Feldman, P.: A practical scheme for non-interactive verifiable secret sharing. In: Proceedings of 28th Annual Symposium on Foundations of Computer Science, SFCS 1987, pp. 427–438. IEEE Computer Society, Washington, DC (1987). http://dx.doi.org/10.1109/SFCS.1987.4
8. Gennaro, R., Jarecki, S., Krawczyk, H., Rabin, T.: Secure distributed key generation for discrete-log based cryptosystems. J. Cryptol. **20**(1), 51–83 (2007). http://dx.doi.org/10.1007/s00145-006-0347-3
9. Gennaro, R., Rabin, M.O., Rabin, T.: Simplified VSS and fast-track multiparty computations with applications to threshold cryptography. In: Proceedings of 17th Annual ACM Symposium on Principles of Distributed Computing, PODC 1998, pp. 101–111. ACM, New York (1998). http://doi.acm.org/10.1145/277697.277716
10. Joye, M., Neven, G.: Identity-Based Cryptography. Cryptology and Information Security Series, vol. 2. IOS Press, Amsterdam (2008)
11. Kate, A., Goldberg, I.: Distributed key generation for the internet. In: 29th IEEE International Conference on Distributed Computing Systems, ICDCS 2009, pp. 119–128, June 2009
12. Maurer, U.M., Yacobi, Y.: Non-interactive public-key cryptography. In: Proceedings of 10th Annual International Conference on Theory and Application of Cryptographic Techniques, EUROCRYPT 1991, pp. 498–507. Springer, Berlin (1991). http://dl.acm.org/citation.cfm?id=1754868.1754924
13. Pedersen, T.: Non-interactive and information-theoretic secure verifiable secret sharing. In: Feigenbaum, J. (ed.) Advances in Cryptology CRYPTO 1991. Lecture Notes in Computer Science, vol. 576, pp. 129–140. Springer, Berlin (1992). http://dx.doi.org/10.1007/3-540-46766-1_9
14. Shamir, A.: How to share a secret. Commun. ACM **22**(11), 612–613 (1979). http://doi.acm.org/10.1145/359168.359176
15. Shamir, A.: Identity-based cryptosystems and signature schemes. In: Proceedings of CRYPTO 1984 on Advances in Cryptology, pp. 47–53. Springer-Verlag New York, Inc., New York (1985). http://dl.acm.org/citation.cfm?id=19478.19483
16. Tanaka, H.: A realization scheme for the identity-based cryptosystem. In: A Conference on the Theory and Applications of Cryptographic Techniques on Advances in Cryptology, CRYPTO 1987, pp. 340–349. Springer, London (1988). http://dl.acm.org/citation.cfm?id=646752.704736
17. Tsujii, S., Itoh, T.: An ID-based cryptosystem based on the discrete logarithm problem. IEEE J. Sel. Areas Commun. **7**(4), 467–473 (1989). http://dx.doi.org/10.1109/49.17709
18. Wu, Q., Chen, H., Li, Z., Jia, C.: On a practical distributed key generation scheme based on bivariate polynomials. In: 2011 7th International Conference on Wireless Communications, Networking and Mobile Computing (WiCOM), pp. 1–4, September 2011

Relation Between Statistical Tests for Pseudo-Random Number Generators and Diaphony as a Measure of Uniform Distribution of Sequences

Sashe Gjorgjievski, Verica Bakeva(✉), and Vesna Dimitrievska Ristovska

Faculty of Computer Science and Engineering, University "Ss Cyril and Methodius", P.O. Box 393, Skopje, Republic of Macedonia
sasepp007@yahoo.com, {verica.bakeva, vesna.dimitrievska.ristovska}@finki.ukim.mk

Abstract. In this paper we investigate the relation between statistical tests for pseudo-random number generators and the diaphony as a measure of uniform distribution of sequences. In order to find some relations many experiments are done. For these experiments we use generators and tests from Diehard battery. For all generated sequences, the diaphony is calculated and the tests from Diehard battery are done. Also, we made experiments using two deterministic sequences: the sequence of Van der Corput and the sequence of equidistant points.

Keywords: Uniformity · Randomness · Statistical tests · Diaphony · Diehard battery

1 Introduction

Pseudo-random number generator (PRNG) is a device producing a sequence of numbers $s_1, s_2, \ldots$ with a given distribution which is supposed to be uniform, where $s_1, s_2, \ldots$ are elements of a given set of numbers. A sequence of random numbers s_1,s_2,… must have two important properties: uniformity (i.e. they are equally probable everywhere) and independence (i.e. the current value of a random variable has no relation with the previous values). In fact, in practice, we cannot design a perfect PRNG, since the way we are building the device is not a random one, which affects the uniformity and independency of the produced sequences. That is why the word "pseudo" is used and we have to measure the randomness of the obtained sequences.

There are a lot of tests for such measurements and all of them are measuring the difference between the generated pseudo-random sequences and the theoretically supposed ideal random sequence. We say that a PRNG is passing a test if the random sequences produced by that PRNG are passing the test with a probability near to 1. We can classify PRNGs depending of the tests they have passed. So, for obtaining a better classification we should have many different tests.

G. Stojanov and A. Kulakov (eds.), *ICT Innovations 2016*, Advances in Intelligent Systems and Computing 665,
https://doi.org/10.1007/978-3-319-68855-8_8

On the other side, a diaphony is a measure for uniform distribution of a given sequence. The ideal uniformly distributed sequence has the diaphony equal to 0. Since the formula for computing of diaphony includes limit, practically, it is not possible to compute the exact value of the diaphony, but we can approximate it with a desired accuracy.

Our idea is to find a relation between statistical tests for goodness of PRNG and diaphony of the obtained sequences. The main question is: "Is it possible to replace statistical tests for randomness with the diaphony, if its value is in an interval $[0,\varepsilon)$, for previous given small number ε?" In order to answer this question we made many experiments using generators and statistical tests from Diehard battery [1].

This paper is organized as follows. In Sect. 2 we give a short explanation for two number generators used in Diehard battery: "Mother of all generators" and "31-bit generator". In Sect. 3 we present statistical tests from Diehard battery. The definition of diaphony is given in Sect. 4. In the same section we present Van der Corput sequence as approximately ideal uniform sequence. In Sect. 5, the experimental results are given. At the end, we give some conclusions.

2 Generators of Pseudo Random Numbers

In our experiments, we used 16 pseudo random generators introduces by George Marsaglia, but in this paper we present the results of two chosen generators: "Mother of all generators" and "31-bit generator". We chose these two generators since the first one is "good" generator (almost all sequences passed all statistical tests) and the second one is "not so good" (there are sequences which do not pass all tests). Further on, we will give a brief description of these two generators.

- **Mother of all Generators**

This generator creates a binary file with 11 megabytes of 32-bit integers. This is achieved by using the following "multiply with carry" generator [1]:

$$x_n = 2111111111 \cdot x_{n-4} + 1492 \cdot x_{n-3} + 1776 \cdot x_{n-2} + 5115 \cdot x_{n-1} + carry \, mod \, 2^{32}.$$

The advantage of this generator is that it has very large period which is 2^{160}. The *carry* part in the next step of the iteration process is the numerator when the module is $b = 2^{32}$. For example, if the linear combination with the current 4 x-values x_1, x_2, x_3, x_4 and the *carry* gives the result: $73 \cdot b + 2245$, then the new x will be 2245, while the new *carry* will be 73.

The biggest advantage of this special "multiply with carry" generator is that it allows use of modules 2^{16} and 2^{32} in that way that avoids the trailing bits disadvantages common for congruential sequences for such modules.

When concretely executing this program, we will be prompt to enter 4 initial values (seeds) of integer numbers for x_1, x_2, x_3, x_4 and the *carry*. Then as described above, the new values of x and c are being produced, and so on. Thus, a binary file of integers is being created, which further will be used to check whether the generated sequence passes the Diehard statistical tests.

- **31-bit Generator**

The 31-bit generator creates a binary file with 11 megabytes of 31-bit integers. In the literature, this generator is also known by the name "RAN2" generator. This generator is a combination of two linear congruential generators. The generated random numbers, are then additionally randomized with shuffling [4].

After that the generated 31-bit random numbers are being shifted to the left for 1 bit, which means that the leading beats are fulfilled [1]. From the other side this means that the last bit of all integer numbers generated with this PRNG will be equal to 0. By saying that, we should expect that all Diehard statistical tests which use 32-bits from left to right will show spectacular failures.

This generator is very simple for use, since we should enter only 1 initial seed (integer number). After that the rest of 31-bit integers are being produced and written in a binary file. This file is used for further analysis to check whether the produced sequence passes the statistical tests in Diehard battery.

3 Diehard Tests

Diehard tests are a battery of statistical tests for measuring the quality of a random number generator. It contains 16 statistical tests. This battery was developed by George Marsaglia over several years and first published in 1995. It is a complete, thorough and comprehensive set of statistical tests for PRNG [2]. This set of statistical tests serves as some kind of litmus for checking and eventual certification of PRNG. If a PRNG passes Diehard statistical tests, then it can be used in more serious scientific researches.

Further on, we give an overview of these tests [1, 3].

- **Birthday Spacings Test**

For this test we choose m birthdays in a year of n days. The spacing between the birthdays needs to be listed. If the number of values that occurred more than once in the list is the variable J, than it has asymptotical Poisson distribution with mean $m^3/(4n)$.

By doing a lot of experiments it is received that the values of n have to be very large so the results could be compared with the expected Poisson distribution with mean $m^3/(4n)$. The default setup uses $n = 2^{24}$ and $m = 2^9$, so that enables us to take the Poisson with $\lambda = \frac{2^{27}}{2^{26}} = 2$ as the concrete distribution for J. For a sample of 500 J's a chi-square test is performed to provide a p value. The first test uses the first bits from 1–24 counting from left to right from the integers in the specified file and the file is closed and reopened. The same is done with the bits from 2–25 to provide birthdays, and the file is closed and reopened again. And so on until the last sequence of bits from 9–32. Each set of bits provides a p-value, so we have nine p-values. At the end a Kolmogorov – Smirnov ($K - S$) test is taken for the acquired 9 p-values.

- **Overlapping 5-Permutation Test (OPERM-5)**

The overlapping 5 permutation test gets its name since it takes 5! possible orderings of five consecutive integers. These tests are overlapping m-tuple tests for which elements of the overlapping 5-tuples are not independent, or even successive states of a Markov

chain. Let $s_1, s_2, \ldots$ be uniform variates produced by a RNG. Each of the overlapping 5-tuples $(s_1, s_2, s_3, s_4, s_5)$, $(s_2, s_3, s_4, s_5, s_6)$, $(s_3, s_4, s_5, s_6, s_7)$, is in one of 120 possible states:

$$S_1 : x_1 < x_2 < x_3 < x_4 < x_5; \quad S_2 : x_1 < x_2 < x_3 < x_5 < x_4; \quad S_3 : x_1 < x_2 < x_4 < x_3 < x_5; \ldots,$$
$$S_{120} : x_5 < x_4 < x_3 < x_2 < x_1.$$

This test actually uses 1 000 000 sets of 5 integers. It is obvious that these sets overlap between each other (some integers belong to more than 2 sets). Because each numbers provide a state it comes that thousands of different states are being observed, resulting with counting of the number of occurrences of each state. Than the quadratic form in the weak inverse 120×120 covariance matrix is being made, equivalent to the likelihood ratio test which expects that the counts will have normal distribution.

In our experiments, the test is performed twice.

- **Binary Rank Tests**

Binary rank tests use some of the characteristics of the matrixes and their ranks. *N*-dimensional cube is taken using the columns of a matrix as axes. If the rank of the matrix is the same as the size of the matrix, then we can get to whatever point in the *N*-dimensional cube. The actual values of the ranks are being compared with the ranks previously calculated. This is made by performing a chi-squared test to compare how well the sample fits the expected distribution.

- **31×31 Binary Matrix**

A 31×31 binary matrix is generated formed of 31 integers in each row. 31 bits are being used (only the last bit is not taken) of those 31 integers. If the rank of the matrix is r then $0 \leq r \leq 31$. But in practice, ranks are rarely less than 28, so if that is the case those kinds of ranks are being combined with those for rank 28. After that a sample of 40 000 matrixes is taken and then a chi-squared test is performed to calculate the actual value of the ranks which can be 31, 30, 29 and ≤ 28. If 40 000 matrixes are taken as a sample it is clear that $40\,000 \cdot 31 = 1\,240\,000$ integers are used in this test.

- **32×32 Binary Matrix**

A 32×32 binary matrix is random generated formed of 32 integers in each row. If the rank of the matrix is r then $0 \leq r \leq 32$. But in practice ranks are rarely less than 29, so if that is the case those kinds of ranks are being combined with those for rank 29. After that a sample of 40 000 matrixes is taken and then a chi-squared test is performed to calculate the actual value of the ranks which can be 32, 31, 30 and ≤ 29. If 40 000 matrixes are taken as a sample it is clear that $40\,000 \cdot 32 = 1\,280\,000$ integers are used in this test.

- **6×8 Binary Matrix**

A 6×8 binary matrix is generated from 6 random integers and 8 bits from those integers. If the rank of the matrix is r then $0 \leq r \leq 6$. But in practice ranks are rarely less than 4, so if that is the case those kinds of ranks are being combined with those for

rank 4. After that a sample of 100 000 matrixes is taken and then a chi-squared test is performed to calculate the actual value of the ranks which can be 6, 5 and ≤ 4. If 100 000 matrixes are taken as a sample it is clear that 100 000 · 8 = 800 000 integers are used in this test.

In our experiments, the test is performed 25 times. At the end a Kolmogorov-Smirnov (K-S) test for 25 obtained *p*-values is performed to check whether they all together are uniformly distributed at [0,1).

- **Bitstream Test**

The file that is tested is considered as a stream of bits. So called 20 letter words are taken, overlapping between each other. The first word is from the 1^{st} to 20^{th} bit, then the second from 2^{nd} to 21^{st} bit etc. Then the number of the missing 20 letter words is counted in a string of 2^{21} overlapping words. Their number is expected to be normally distributed with mean 144 909 and sigma 428. It leads to a uniform [0, 1] *p*-value.

In our experiments, the test is repeated 20 times and we perform a Kolmogorov – Smirnov test on the obtained 20 *p*-values.

- **The Tests OPSO, OQSO and DNA**
- **OPSO Overlapping Pairs Sparse Occupancy Test**

In this test a 2-letter words from an alphabet of 1024 letters are being considered. Each of the 2 letters are determined by a specified 10 bits from a 32 bit integers in the sequence to be tested. With OPSO, 2^{21} overlapping words are being generated and then the number of the missing words (i.e. 2-letter words which do not appear in the entire sequence) is counted. This number is almost normally distributed with mean 141909 and a standard deviation sigma 290. It leads to a uniform [0, 1] *p*-value. The test is executed 23 times, first using the bits from 1 to 10, then 2–11, 3–12, …, 23–32 bits of the $2^{21} + 1$ "keystrokes".

- **OQSO Overlapping Quadruples Sparse Occupancy Test**

Similar as in OPSO, in this test a 4-letter words from an alphabet of 32 letters are being considered. Each of the 4 letters are determined by a specified 5 bits from a 32 bit integers. With OQSO 2^{21} overlapping words are being generated and then the number of the missing words is counted. This number is almost normally distributed with mean 141 909 and a standard deviation sigma 295 determined by simulation. Again, *p*-value is uniformly distributed on [0,1]. The test is executed 28 times, first using the bits from 1 to 5, then 2–6, 3–7, …, 28–32 bits of the $2^{21} + 3$ "keystrokes".

- **DNA**

Like the previous 2 tests, in this test a 10-letter words from an alphabet of 4 letters {C, G, A, T} are being considered. Each of the 10 letters are determined by a specified 2 bits from a 32 bit integers. With DNA 2^{21} overlapping words are being generated and then the number of the missing words in the whole sequence is counted. This number is almost normally distributed with mean 141 909 and a standard deviation sigma 339 determined by simulation. As previous, *p*-value is uniformly distributed on [0,1]. The test is executed 31 times, first using the bits from 1 to 2, then 2–3, 3–4, …, 31–32 bits of the $2^{21} + 9$ "keystrokes".

- **Count the 1's Test on a Stream of Bytes**

In this test as its name suggests the number of 1's in a stream of bytes is counted. Each byte can contain from 0 to 8 1's with different probabilities: $\frac{1}{256}, \frac{8}{256}, \frac{28}{256}, \frac{56}{256}, \frac{70}{256}, \frac{56}{256}, \frac{28}{256}, \frac{8}{256}, \frac{1}{256}$. The stream of bytes provides a string of overlapping 5-letter words. Each letter takes value A, B, C, D, E. The letters are determined by the number of 1's, in that byte: 0, 1, or 2 $\rightarrow A$, 3 $\rightarrow B$, 4 $\rightarrow C$, 5 $\rightarrow D$, and 6, 7 or 8 $\rightarrow E$. So, which letter will be taken depends from the number of 1's in the stream. The number of 5 letters overlapping words is 5^5. From a string of 256 000 five letter words, frequencies for each word are being counted. The quadratic form in the weak inverse of the covariance matrix of the cell counts provides a chi-square test (the ordinary Pearson sums of (OBS-EXP)^2/EXP on counts for 5- and 4-letter cell counts). The test returns 2 p-values for both 5- and 4-letter cell counts.

- **Count the 1's Test for Specific Bytes**

In this test as its name suggests the number of 1's in specific bytes from each 32 integer are being counted. From each integer, a specific byte is chosen, say the left-most: bits 1 to 8. Each byte can contain from 0 to 8 1's with different probabilities: $\frac{1}{256}, \frac{8}{256}, \frac{28}{256}, \frac{56}{256}, \frac{70}{256}, \frac{56}{256}, \frac{28}{256}, \frac{8}{256}, \frac{1}{256}$. The letters are determined by the number of 1's, in that byte: 0, 1, or 2 $\rightarrow A$, 3 $\rightarrow B$, 4 $\rightarrow C$, 5 $\rightarrow D$, and 6, 7 or 8 $\rightarrow E$. So, which letter will be taken depends from the number of 1's in that byte. So the words of 5 letters are being formed from the specified bytes from successive integers. The number of 5 letters overlapping words (each "letter" taking values A, B, C, D, E) is 5^5. From a string of 256 000 five letter words frequencies for each word are being counted. The quadratic form in the weak inverse of the covariance matrix of the cell counts provides a chi-square test (the ordinary Pearson sums of (OBS-EXP)^2/EXP on counts for 5- and 4-letter cell counts). The test is executed 25 times, first using first byte (bits from 1 to 8), then second byte (bits 2-9), …, 25$^{\text{th}}$ byte (bits 25-32) and the corresponding p-values of Pearson chi-square tests are found.

- **Parking Test**

In this test we park a car (it is a circle with radius 1) in a square of side 100 (so the square is with 100 $\times$ 100 size). Then we do the same with the second, third car and so on. If a crash occurs when we try to park a car, the process for that particular car is repeated from the beginning choosing different random location for parking. The number of successfully parked cars is being counted after 12 000 attempts. This number has approximately normal distribution with the average of 3 523 with sigma 21.9. At the end a Kolmogorov-Smirnov (K-S) test for 10 obtained p-values is performed to check whether they all together are uniformly distributed at [0,1).

- **Minimum Distance Test**

Again we take a square but now with a side of 10 000 choosing 8 000 random points in it. If we denote the minimum distance between $\frac{n(n-1)}{2}$ pairs of random points with d, and if the points are independent and uniformly distributed, then d^2 should be exponentially distributed with mean 0.995. Then $1 - \exp(-d^2/0.995)$ should also be uniform on

[0,1) and a Kolmogorov-Smirnov test on the resulting uniform values serves as a test of uniformity for random points in the square. The Kolmogorov-Smirnov test is based on the full set of 100 random choices of 8000 points in the 10 000 × 10 000 square.

- **3D Spheres Test**

Here we take a cube with side 10 000 and choose 4 000 random points in it. At each point, center a sphere large enough to reach the next closest point. Then the distribution of the volume of the smallest such a sphere is found and it is approximately exponentially distributed with mean $\frac{120\pi}{3}$. Then the cube of radius r^3 is also exponential with mean 30 (obtained by extensive simulation). With this test, we generated 20 times by 4 000 such spheres. Next, using the transformation $1 - \exp(-r^3/30)$, each minimum cube of radius r^3 lead to a uniform distributed variable on [0, 1). Then a K-S test is done on the 20 p-values.

- **Squeeze Test**

In this test random integers are floated to get uniform distributions on [0, 1). Starting with $k = 2^{32}$, the test finds J, the number of iterations necessary to reduce k to 0 using the reduction $k = \lfloor kU \rfloor$, where U is a random uniform. A sample of 100 000 J's is used for χ^2-test of the cell frequencies.

- **Overlapping Sums Test**

Let $m \geq 100$ be a fixed integer. Take a sequence of independent and identically distributed $U(0, 1)$ random variables $U_1, U_2, \ldots$ and form the overlapping sums $S_1 = U_1 + U_2 + \ldots + U_m$, $S_2 = U_2 + U_3 + \ldots + U_{m+1}$, and so on. The random variables $S_i, i = 1, 2, \ldots, m$ are virtually normal with a covariance matrix which is easy to calculate. Clearly, $E(S_i) = m/2$, and $D(S_i) = m/12$, $i = 1, 2, \ldots, m$. Furthermore, if $1 \leq i < j \leq m$, then S_i and S_j have a sum S of $m - j + i$ uniform values in common with $X = S_i - S, S$, and $Y = S_k - S$ being mutually independent. Therefore, $cov(S_i, S_j) = (m - j + i)/12$.

Thus, if C denotes the $m \times m$ covariance matrix of the S_i's, the matrix $12C$ is Toeplitz with diagonals m, $m - 1$, …, 1. A cholesky factorization yields $C = VV^{\mathrm{T}}$, where V is lower triangular. Since V^{-1}, the inverse of a lower triangular matrix is easily computed, we can convert the vector $\boldsymbol{S}$ of S_i's to independent normal variables via the linear transformation $\boldsymbol{X} = V^{-1}\boldsymbol{S}$ which can be tested for normality or uniformity after converting to uniforms via the normal cumulative distribution function. After 10 times applying of K-S test, another K-S test is performed on the obtained 10 p-values. The combination of the two Kolmogorov – Smirnov (K-S) tests expands the size of the detected circuits.

- **Runs Test**

The RUNS test counts the number of runs up and run downs in a sequence of 10 000 uniform variables [0,1) acquired by floating the 32-bit integers from the specified file. Because the covariance matrix for the runs up and runs down is known, a chi-square test may be carried out for quadratic forms in a weak inverse of the matrix in order to get a p-value. Performing this 10 times the p-values are obtained, and then for these 10 p-values a K-S test is executed. After that the whole test is performed again.

- **Craps Test**

This test is somehow connected with the Craps game. The test plays $n \geq 200\ 000$ games of craps and counts the number of wins and the number of throws necessary to end each game. The number of wins should be very close to normal with mean np and variance $np(1 - p)$ where $p = 244/495$. Throws necessary to complete the game can vary from 1 to ∞, but all throws ≥ 21 are lumped together. A χ^2-test is made on the number-of-throws cell counts. Each 32-bit integer from the test file provides the value for the throw of a die, by floating to [0,1), multiplying by 6 and taking 1 plus the integer part of the result.

Note that the most of the tests in DIEHARD return a p-value, which should be uniform on [0,1) if the input file contains truly independent random bits. Those p-values are obtained by $p = F(X)$, where F is the assumed cumulative distribution function of the sample (random variable X) – often normal. But that assumed F is just an asymptotic approximation, for which the fit will be worst in the tails. Therefore $p < 0.025$ or $p > 0.975$ means that the RNG has "failed the test at the 0.05 level".

4 Diaphony and Van der Corput Sequence

Let $s \geq 1$ be a fixed integer and $\xi = (\vec{x}_i)_{i \geq 0}$ be an arbitrary sequence of points in $[0,1)^s$. For each integer $N \geq 1$ and an arbitrary subinterval J of $[0,1)^s$ with a volume $\mu(J)$, we denote by $A(\xi, J, N)$ the number of the points $\vec{x}_n$ of the sequence ξ whose indices n satisfy the inequalities $0 \leq n \leq N - 1$ and belong to the interval J. The sequence ξ is called **uniformly distributed** in $[0,1)^s$ if the equality:

$$\lim_{N \to \infty} \frac{A(\xi, J, N)}{N} = \mu(J) \tag{1}$$

holds for every subinterval J of $[0,1)^s$.

The **diaphony** is a quantitative measure for uniform distribution of sequences in $[0,1)^s$. Zinterhof [5] uses the trigonometric functional system τ to introduce the "classical" diaphony

$$\tau = \{e_{\vec{m}}(\vec{x}) = \exp(2\pi i < \vec{m}, \vec{x} >) : \vec{m} = (m_1, m_2, \ldots, m_s)\} \in \mathbb{Z}_s, \tag{2}$$

$\vec{x} = (x_1, x_2, \ldots, x_s)\} \in [0,1)^s$, where $< \vec{m}, \vec{x} >$ is the inner product between the vectors $\vec{m}$ and $\vec{x}$. The classical diaphony is defined as follows.

Definition 1 [5]. For each integer $N \geq 1$ the **classical diaphony** $F_N(\tau, \xi)$ of the first N elements of the sequence $\xi = (\vec{x}_i)_{i \geq 0}$ of points in $[0,1)^s$ is defined as:

$$F_N(\tau, \xi) = \sqrt{\sum_{\vec{h} \in Z^s, \vec{h} \neq \vec{0}} R^{-2}(\vec{h}) \left| \frac{1}{N} \sum_{n=0}^{N-1} \exp(2\pi i < \vec{h}, \vec{x}_n >) \right|^2}, \tag{3}$$

where for a vector $\vec{h} = (h_1, \ldots, h_s) \varepsilon Z^s$, the coefficient $R(\vec{h})$ is defined by $R(\vec{h}) = \prod_{j=1}^{s} \max(1, |h_j|)$.

In this paper we take one-dimensional version of the diaphony.

The following theorem gives necessary and sufficient condition for uniformity of a sequence $\xi = (\vec{x}_i)_{i \geq 0}$.

Theorem 1 [5]. The sequence $\xi = (\vec{x}_i)_{i \geq 0}$ of points in $[0,1)^s$ is uniformly distributed if and only if the limit equality is fulfilled.

$$\lim_{N \to \infty} F_N(\tau, \xi) = 0 \tag{4}$$

At the end, we give the definition of the sequence of Van der Corput since this sequence is a typical example of "very good" uniformly distributed sequence and as such it is used in our investigation.

Definition 2 [6]. Let $b \geq 2$ is an integer number and let $\Sigma = (\sigma_i)_{i \geq 0}$ is a sequence of permutations on the set $\{0,1, \ldots, b-1\}$. If an arbitrary integer number $i \geq 0$ has its representation in a number system with a base b:

$$i = \sum_{j=0}^{s} a_j(i) b^j \tag{5}$$

where $j \geq 0$, $a_j(i) \in \{0,1, \ldots, b-1\}$, then the generalized sequence of Van der Corput is defined as:

$$S_b^{\Sigma}(i) = \sum_{j=0}^{s} \sigma_j\big(a_j(i)\big) b^{-j-1} \tag{6}$$

Actually the so called sequence of Halton (which first was defined in the 1960 by the American scientist Halton) is practically used in this paper so we will also give its definition. Now if we set $\Sigma = I$ in the previous definition where I stands for the sequence of identities, we will get the sequence of Halton.

Definition 3 [7]. Let $b \geq 2$ is an integer number. If an arbitrary integer number $i \geq 0$ has its representation in a number system with a base b given by (5) then the sequence of Halton is defined as:

$$S_b^{I}(i) = \sum_{j=0}^{s} a_j(i) b^{-j-1}. \tag{7}$$

5 Experiments

We made many experiments using the generators from the Diehard battery. There are 16 generators integrated in this packet and we generated 25 random sequences by a generator. Here, we present only the results for 5 sequences for the following two generators: "Mother of all generators" (Table 1) and "31-bit-generator" (the so called RAN2 generator) (Table 2). In the tables, we give p-values for Birthday Spacing test, OPERM-5 test, 31 × 31 Binary matrix, 32 × 32 Binary matrix, 6 × 8 Binary matrix test, Count the 1's Test for stream of bytes, Parking, Minimum Distance, 3DSphere, Squeeze, Overlapping Sums, Run and Craps test. The bolded values of p's mean that the test fails. For the other tests (which are performed more than once), we give the number of passed tests over the total number of tests. These tests are: Bitstream, OPSO, OQSO, DNA and Count the 1's for specific bytes.

In the third column, we present the p-value for the standard Pearson test for the uniform distribution. Note that, here p-value has the normal meaning. If $p > 0.05$, we conclude that the test passes at the 0.05 level of significance.

And, in the second column we give the corresponding value of diaphony (see the formula (3)). In order to apply this formula we have to divide all elements in the sequences with the maximum element to obtain sequences with elements in [0,1).

Analyzing the results in Table 1, we can conclude that the diaphony for all five sequences is very close to 0 and all of them pass the Pearson χ^2-test. This confirm that the sequences generated using "Mother of all generators" are uniformly distributed. Also, these sequences pass almost all other tests. This means that the sequences are random ones.

On the other side, from results in Table 2, the conclusions for diaphony and Pearson χ^2-test are similar as in the previous case. Namely, the diaphony for all five sequences is very close to 0 and all of them pass the Pearson χ^2-test. But, many of test for randomness fail. All five sequences did not pass Birthday test, 32 × 32 Binary matrix test, Count the 1's Test on a stream of bytes, all 20 Bitstream tests. Also, 3 (from 5) sequences fail for 6 × 8 Binary matrix test, one sequence fails one Run test and other sequence fails one Overlapping 5-Permutation Test.

From the results in these two tables we can conclude that there is a relation between the diaphony and Pearson χ^2-test. This is expected since the both of them measure the uniformity of a sequence. But, we cannot find any relation between the diaphony and other tests for randomness.

In order to confirm this, we made experiments performing the Diehard battery tests for the sequence of Van der Corput and the sequence of equidistant points. Both of them are not random sequences. They are strongly deterministic. The concrete value of diaphony for Van der Corput sequence (with 2 867 190 elements) is 1.75×10^{-6} and for the sequence of equidistant points (with 2 867 190 elements) is 5.94×10^{-15}. Also, p-values of Pearson χ^2-test for the both sequences are 1 which means that the both sequences are uniformly distributed. But, the both sequences did not pass any other tests for Diehard battery. The Squeeze, Overlapping Sums, Run and Craps test did not give any results. Note that for applying of the tests in Diehard battery, all elements from

Table 1. Results for "Mather of all generators"

Mother of all generator	Diaphony	Pearson χ^2	Birth-Test	OPERM-5	Binary-31	Binary-32	Binary6x8	Bitstream	OPSO	OQSO	DNA	Count Bytes	Count Stream	Parking	Minim.D	3DSpheres	Sqeeze	O-SUM	Runs Test	Craps Test
		p-value	*p*-value	*p*-value	*p*-value	*p*-value	*p*-value	No. of passed tests / total no. of tests					*p*-value	*p*-value	*p*-value	*p*-value	*p*-value	*p*-value	*p*-value	*p*-value
Seq. 1	0.001 647	0.834	0.737	0.550 0.237	0.779	0.325	0.075	19/20	20/23	27/2 8	31/31	22/25	0.680 0.076	0.648	0.256	0.173	0.710	0.063	0.101 0.538 **0.002** 0.530 0.101	0.092
Seq. 2	0.000 804	0.962	0.390	0.047 **0.000**	0.540	0.499	0.687	18/20	19/23	26/2 8	30/31	23/25	0.239 0.167	0.374	0.913	0.211	0.711	0.576	0.492 0.783 0.361 0.431	0.34 9 0.72 1
Seq. 3	0.001 098	0.799	0.335	0.886 0.098	0.903	0.722	0.269	20/20	23/23	27/2 8	28/31	23/25	0.516 0.301	0.302	0.533	0.431	0.887	0.799	0.799 0.083 0.477 0.924	0.09 7 0.55 1
Seq. 4	0.001 228	0.121	0.680	0.367 0.653	0.334	0.476	0.087	18/20	23/23	28/2 8	28/31	20/25	0.928 0.319	0.747	0.718	0.662	0.752	0.634	0.480 0.065 0.774 0.537	0.02 8 0.48 8
Seq. 5	0.001 094	0.471	0.698	0.313 0.067	0.570	0.596	0.246	20/20	19/23	25/2 8	30/31	22/25	0.505 0.398	0.855	0.733	0.643	0.973	0.599	0.481 0.405 0.610 0.409	0.83 2 0.24 5

Table 2. Results for "31-bit-generator"

31 bit generator	Diaphony	Pearson χ^2	Birth-Test	OPERM-5	Binary-31	Binary-32	Binary6x8	Bitstream	OPSO	OQSO	DNA	Count Bytes	Count-Stream	Parking	Minim.D	3DSpheres	Sqeeze	O-SUM	Runs Test	Craps Test
		p-value	*p*-value	*p*-value	*p*-value	*p*-value	*p*-value	No. of passed tests / total no. of tests					*p*-value	*p*-value	*p*-value	*p*-value	*p*-value	*p*-value	*p*-value	*p*-value
Seq.1	0.000739	0.673	**0.997**	0.330 **0.990**	0.538	**1.000**	**0.975**	**0/20**	22/23	26/28	27/31	22/25	**1.000** **1.000**	0.871	0.136	0.538	0.491	0.569	0.475 0.572 0.466 0.335	0.256 0.120
Seq. 2	0.001195	0.176	**0.998**	0.861 0.766	0.538	**1.000**	**0.992**	**0/20**	20/23	27/28	28/31	23/25	**1.000** **1.000**	0.382	0.645	0.371	0.790	0.801	0.045 0.267 **0.980** 0.073	0.674 0.294
Seq. 3	0.000856	0.833	**0.996**	0.973 0.315	0.862	**1.000**	0.917	**0/20**	20/23	27/28	28/31	21/25	**1.000** **1.000**	0.232	0.379	0.682	0.110	0.918	0.619 0.727 0.571 0.059	0.079 0.890
Seq. 4	0.001037	0.527	**0.999**	0.569 0.103	0.925	**1.000**	0.960	**0/20**	21/23	26/28	29/31	20/25	**1.000** **1.000**	0.710	0.630	0.387	0.301	0.857	0.771 0.311 0.375 0.324	0.815 0.525
Seq. 5	0.000667	0.575	**0.997**	0.665 0.399	0.847	**1.000**	**0.992**	**0/20**	21/23	26/28	26/31	22/25	**1.000** **1.000**	0.417	0.722	0.599	0.047	0.943	0.911 0.911 0.174 0.215	0.154 0.410

these sequences (which are in [0,1)) are multiplied with the maximum element, to obtain sequences of integers ready for use as input in program for Diehard tests.

6 Conclusions

In this paper we investigate the relation between statistical tests for pseudo-random number generators and the diaphony as a measure of uniform distribution of sequences. Although, we expected that we will find some relation between the both categories, it is not the case. This kind of diaphony is only a measure of uniformity and cannot be used for measuring the randomness of sequences. We found relation only between the diaphony and Pearson χ^2-test which is expected. So, statistical tests are tools for checking sequence randomness (uniformity and independence), and the diaphony is a measure only for uniformity of sequences. These two measures are not equivalent.

Acknowledgements. This work was partially financed by the Faculty of Computer Science and Engineering at the "Ss. Cyril and Methodius" University in Skopje.

References

1. http://stat.fsu.edu/pub/diehard/
2. Marsaglia, G., Tsang, W.W.: Some difficult-to-pass tests of randomness. J. Stat. Softw. **7**(3), 1–9 (2002)
3. Narasimhan, B.: JDiehard: an implementation of Diehard in Java. In: Hornik, K., Leisch, F. (eds.) DSC 2001, Proceedings of the 2nd International Workshop on Distributed Statistical Computing, Vienna, Austria, pp. 1–9 (2001)
4. Zeeb, C.N., Burns, P.J.: Random number generator recommendation. Colorado State University, Department of Mechanical Engineering, Fort Collins, CO
5. Zinterhof, P.: Uber einige Abschatzungen bei der approximation von Funktionen mit Gleichverteilungsmethoden. S. B. Akad. Wiss. Math.-Naturw. Klase Abt.II **185**, 121–132 (1976)
6. Faure, H.: Discrépances de suites associées a un systéme de numeration (an dimension un). Bull. Soc. Math. Fr. **109**, 143–182 (1981)
7. Halton, J.H.: On the efficiency of certain quasi – random sequences of points in evaluating multi – dimensional integrals. Numer. Math. **2**, 84–90 (1960)

Pattern Recognition of a Digital ECG

Marjan Gusev[1(✉)], Aleksandar Ristovski[2], and Ana Guseva[2]

[1] FCSE, Ss. Cyril and Methodious University, Skopje, Macedonia
marjan.gushev@finki.ukim.mk
[2] Innovation Dooel, Skopje, Macedonia
{aleksandar.ristovski,ana.gusheva}@innovation.com.mk

Abstract. The process of assisted ECG diagnosing mimics the way a medic would act upon. Such a process inevitably comprises the feature extraction step, when the standard ECG signal components: the QRS complex, the P wave and T wave are detected. Using a pattern recognition algorithm for the purpose is one of the available options. In this article, the pattern recognition approach for the feature extraction routine is explained by analysis of consecutive steps and its effectiveness is discussed in comparison to other means of QRS complex detection.

Keywords: Pattern recognition · QRS detection · Performance engineering

1 Introduction

Although the digitalization of the ECG signal is not a new concept to the technological advancement, its benefits are recently taking into practice. Thus, the digitalized recordings are much more feasible to archiving data relative to hard copied recordings, which is why contemporary instruments are more often featuring a digital output, at the very least, supplementary to the standard output.

Regardless the cause, the process of data interpretation by a virtual AI agent corresponds to the process used by cardiologists. An ECG recording consists of a QRS complex, preceded by a P wave and followed by a T wave [4]. The depiction of these components is inevitably the first step of the analysis, irrelevant to whether a medic or an AI agent is conducting the evaluation. The form of a QRS complex in Lead I, along with the other morphological components, are shown in Fig. 1.

The process of detecting the components can vary. Each approach has its own pros and cons, but, what is of greatest importance is the effectiveness in successfully matching the actual component constellation. When evaluating effectiveness, a certain degree of disparity is tolerable. However, the degree of disparity depends firmly on the properties of the statistical population that is chosen. The superiority of the approach is related to having high effectiveness when processing a problem set that consists of statistical samples that are untypical if

G. Stojanov and A. Kulakov (eds.), *ICT Innovations 2016*,
Advances in Intelligent Systems and Computing 665,
https://doi.org/10.1007/978-3-319-68855-8_9

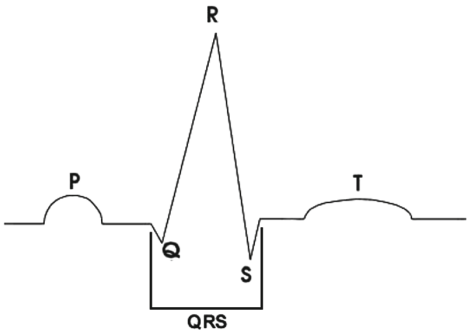

Fig. 1. A QRS complex preceded by a P wave and followed by a T wave

compared to ECG recordings of a statistical population with normatively normal ECG recordings, i.e. a population with low rate of divergent properties.

Considering that an approach is evidently effective, it needs to be able to detect a wide range of cardiac irregularities. By using pattern recognition, not only a considerable rate of component detection is achieved, but the number of irregularities that can be detected is prominent.

2 Background

There are twelve standard leads of ECG. Each of them features a unique representation of the signal components and it is not always that a component is present in the lead recording. This is so not due to the individual properties of the subject recorded, but rather has to do with the general physiology of the human body [3]. In addition, each signal component takes different form depending on which lead it has been registered [6]. That is why the normative criterion correspondent to a certain lead is analyzed when devising a pattern.

The pattern recognition used in the discussed approach so far has been solely applied for detection of QRS complexes in lead I of the ECG signal. In this case, after the positioning of the QRS complexes has been established, the P waves and T waves can be located much more easily by conducting a search in the interval between two neighboring QRS complexes. However, the pattern recognition can be done for other leads as well, by using a pattern built suitably for a specific lead and the signal component that needs be detected.

There are normative clauses that define a QRS signal in lead I. These include the normative duration: between 0.06 s and 0.10 s - standard value for adults and same for all leads, and the normative amplitude: 500 to 2000 μV for lead I [3]. It is relevant to say that the amplitudes' values are devised as relative difference between the R peaks' amplitude and the Q and S peaks' amplitudes, and not as relative difference between the R peaks amplitudes and zero.

While the duration of the QRS complex is an acknowledged standard, the amplitude is affected by a greater number of factors. These include the size

of the ventricular chambers - the larger the chamber, the larger the voltage, and the proximity of precordial (chest) electrodes to the ventricular chambers - the closer, the larger the relative Q-R and R-S voltage differences. Additionally, there are other factors that need be taken into account: certain cardiac conditions can cause the R peak not to be centrally in-between the Q and S peaks. Such predicaments strongly indicate that it is of high interest to construct a pattern which is individual to a patient.

The form of the pattern has a "V" shape - although the QRS complex has an inverted "V" shape, it needs be turned upside down due to the inversion that occurs during the pattern check. Pragmatically, a pattern cannot be defined as a single one dimensional line when used on one dimensional ECG data, and it must have a surface area, i.e. be planar. That is achieved by having a pair of one dimensional border lines: linear lower boundary and linear upper boundary. This two linear components never intersect to form a closed planar geometric form, meaning that there is a gap between them so that the linear ECG signal can enter and exit the pattern, as presented in Fig. 2.

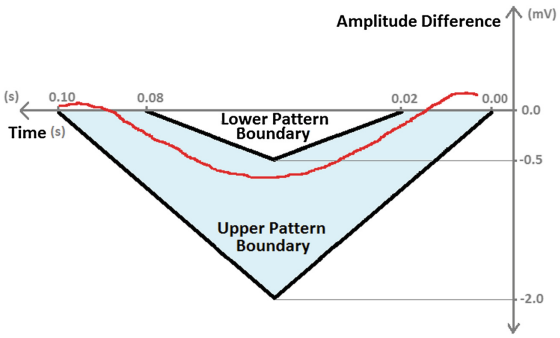

Fig. 2. A QRS component (red) entering the pattern surface area (blue)

The linear ECG signal spans across two axes: the horizontal axis with time as its dimension, and the vertical axis with the amplitude value as its dimension. The digitalized ECG signal consists of an array of samples: the index of the element represents the instance of time while the value of the array element represents the amplitude value at the corresponding time.

3 Building a Pattern

In respect to the temporal normative clause, the upper boundary has a length equal to the maximum duration of the QRS complex, whereas the lower boundary equals the minimum duration of the QRS complex. Just as the ECG signal takes form of an array of amplitudes, both the upper and lower pattern boundary need to have the exact same digital form representation. The parameter sampling time/sampling frequency has a key role in devising the size of the pattern

Algorithm 1. Construct QRS Pattern

```
1: procedure CALCULATE PATTERN LENGTH
2:     if usingSampleTime then
3:         numberOfElements ←maxLength / sampTime
4:     else
5:         if usingSamplingFrequency then
6:             numberOfElements ←maxLength * sampFreq
7:     if usingSamplingFrequency%2 = 0 then
8:         numberOfElements ←numberOfElements - 1
```

in time, that is, the number of elements in the array that the boundaries are represented by (numberOfElements). To calculate the number of elements of the array which represents the upper boundary, the maximum length of the QRS complex in time (maxLength) is divided by the sample time (sampTime), i.e. multiplied by the sampling frequency (sampFreq). Because the pattern needs to have a central element for the R peak, if the array length is not an odd number, the length is trimmed by one (Algorithm 1).

Although the length of the lower boundary corresponds to the minimum length of the QRS complex duration, it is feasible to use a lower pattern boundary with the same length as the higher pattern boundary length so that the implementation of the algorithm that does the pattern check is made simpler. That is why in order to keep the pattern functionality, the elements in range [0, (maximum length −minimum length)/2] and [maximum length/2 + minimum length/2, maximum length] have a practically unattainable value. This modification is shown on Fig. 3.

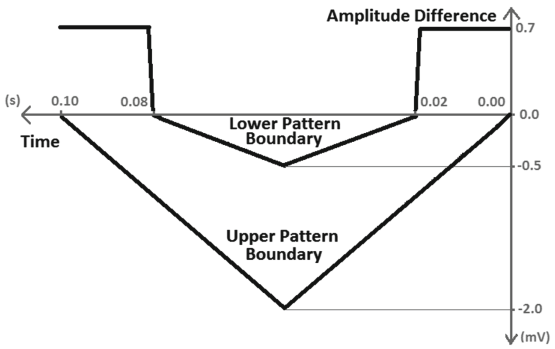

Fig. 3. A pattern with the unattainable values of the lower and upper boundaries

Both the amplitudes of the first elements and last elements of the pattern arrays have a value of zero. The amplitude value of the middle element representing the R peak of the upper boundary is the value of the maximum R peak amplitude $-2000\,\mu V$, while the amplitude value of the middle element

representing the R peak of the lower boundary is the value of the minimum R peak amplitude $-500\,\mu V$. The inclination from the first element towards the peak and the inclination from the peak towards the last element is linear, meaning that the absolute difference between neighboring elements in the array is constant. This incremental (ampincrement), i.e. decremental value (ampDecrement) is calculated for the upper boundary of the pattern, proportionally to the maximum amplitude value and the number of elements in the interval [0, maximum length/2 − flatPeakRadius] (1). The variable flatPeakRadius depicts the length of the optionally flattened peak of the pattern, since having a flattened peak at times proved to increase the effectiveness of the QRS detection. The variable middleIndex represents half the length of the pattern, with pattern elements' indexing starting from 0. For the lower pattern boundary, the incremental/decremental values are proportional to the minimum amplitude value and the number of elements in the interval [(maximum length − minimum length)/2, maximum length/2], whilst the optional flattened peak radius is unnecessary.

$$ampl_{Increment} = -ampl_{Decrement} = \frac{-maxAmplitude}{middleIndex - flatPeakRadius} \quad (1)$$

For the construction of personalized patterns, besides changing the maximum and minimum amplitudes, along with the maximum and minimum lengths of the QRS complex, several other changes can greatly increase the pattern effectiveness: applying an amplitude offset to both the upper and lower boundary, and applying a flat peak to the R segment of the pattern. What the former modification does is it adds or subtracts a constant value to each of the array element values, shifting the pattern along the amplitude axis. The latter modification gives a series of elements within a certain radius from the middle array element a unified amplitude value - the maximum and minimum amplitude values for the upper and lower boundaries accordingly. This modification causes change in the incremental/decremental value of the neighbor elements.

4 Using a Prebuilt Pattern for ECG Analysis

The algorithm input data consists of the digital ECG signal and the sampling time/sampling rate, while the algorithm output consists of a set of detected signal components. According to the needs, the output data is an array containing either the components' locations in the signal (timestamps, i.e. the indices of the signal array elements) along with the amplitude values, or either only the components' locations. Regardless the lead that is being processed or the signal component targeted for detection, the entire algorithm implementation stays the same.

What makes the approach interesting is the fact that the voltage relative to zero is irrelevant. What is taken into account is the relative amplitude difference between the amplitude of an array element and the amplitudes of the elements in the range [t-pattern length, t), where t is the time stamp of an element, belonging to the interval [(pattern length)/2, ECG signal length].

Algorithm 2. Find QRS Complexes

```
1: procedure CHECK FOR PATTERN MATCH
2:     for i = patternLength; i < ecgLength; i++ do
3:         QRSComplex ← True
4:         j ← patternLength − 1
5:         while j > 0 AND QRSComplex do
6:             Diff ← ecgSignal[i] − ecgSignal[i − j]
7:             QRSComplex ← (Diff > lowPattern[patternLength − j − 1])
   AND (Diff > highPattern[patternLength − j − 1])
8:             j ← j − 1
```

For each of the elements of the array representing the digital ECG signal in the interval [(pattern length)/2, ECG signal length] a pattern check is done (the variable ecgLength depicts the number of elements of the array representing the signal). That is achieved by calculating the relative difference with each of the previous elements of the array, whilst the number of the previous elements corresponds with the number of elements in the pattern (patternLength). For each relative distance calculated, the difference needs to be lower then a corresponding element value of the upper boundary of a pattern and greater then a corresponding element value of the lower boundary of a pattern. The boolean variable QRSComplex gets the value of an individual check and serves as an indicator for the check of a single QRS complex. As soon as the check fails, the search continues by looking for a next QRS complex. (Algorithm 2).

Because of how the difference of values is calculated and the order in which the check is done, the original signal is being inverted both in terms of the amplitude and in temporal terms. The double inversion is shown in Fig. 4.

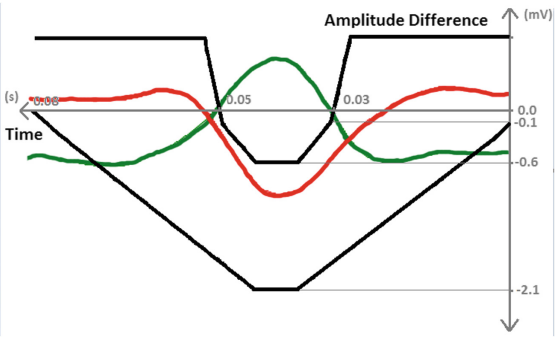

Fig. 4. A personalized pattern with the original (green) and inverted signal (red)

The proposed approach can detect an R pattern that fully lies somewhere in the ECG recording. In order to utilize the volume of data processed, i.e. to enable detection of components that are partially part of the recording (signal

components that are partially present at the begging and the end of the ECG recording), a partial pattern check is in favor. However, in order for the partial pattern recognition to work, it is necessary for the local maximum of the partial signal component be present in the ECG recording. Taken that the element currently processed lies within the interval [(pattern length)/2, pattern length] (at the beginning of the recording) a pattern check is done for the elements down to the first element in the recording. At the end of the recording the same check is done with some slight modifications in the algorithm.

5 Evaluation and Discussion

Before the QRS detection phase is to occur, the records are submitted to metadata format unification, signal filtration and normalization, as suggested in previous related work of the authors [11]. The filtering phase deals with the removal of baseline wander, caused mostly by perspiration, respiration and body movement by using high-pass filtering, while the high frequency noise such as power-line interference, electromyography (EMG) noise, and instrumentation noise is dealt with by using low-pass filtering [2,13]. A bandpass filter with low-pass frequency of 40 Hz and high-pass frequency of 0.5 Hz can be implemented by a variety of filters, such as FIR filter (realized by the ARMA filtering method. An IIR filter (realized as Butterworth filter) achieves superior performance, but still lacks the precision when compared to DWT or similar techniques [9].

Although the duration of the ECG signal components tends to stay within corespondent marginal values in case of non-pathological cardiac conditions and a number of pathological ones, the amplitude variations are substantial. The pattern recognition approach used has taken care of the relative vertical amplitude shift, the differences in vertical scaling cause certain issues during the QRS detection phase, such as inadequate effectiveness rate, or considerable rate of false positives, due to P or T waves taken for QRS complexes. Therefore, simple linear scaling transforms sufficiently scale up the signals' amplitudes.

To maximize the effectiveness of the QRS complex detection and to minimize the false positive rate, for each of the databases tested a batch analysis was performed, to derive an optimal pattern for a particular database. However, since a single pattern has been used per database, the efficiency is not comparable to the efficiency of approaches that deal with arrhythmia classification. Consequently, the efficiency is significantly higher for databases that do not contain morphologically abnormal QRS complexes.

Three databases published by Physionet [5] were chosen as a subject to the conducted analyses: the MIT-BIH Arrhythmia Database [10], the MIT-BIH Normal Sinus Rhythm Database and the ECG-ID Database [7]. For each database, several parameters such as number of True Positives (TP), the number of False Negative (FN) and False Positives (FP) constitute the effectivity outliners: Sensitivity (2), Specificity (3) and Accuracy (4).

$$Sensitivity = \frac{TP}{TP + FN} \tag{2}$$

$$Specificity = \frac{TP}{TP + FP} \tag{3}$$

$$Accuracy = \frac{TP}{TP + FP + FN} \tag{4}$$

The MIT-BIH Arrhythmia Database is commonly used for arrhythmia classification benchmarking, set to include a variety of rare but clinically important phenomena that would not be well-represented by a small random sample of Holter recordings. Although the goal of the work does not include achieving high efficiency in the QRS detection for such databases, it is important to demonstrate how the findings match up to advanced detection and classification algorithms. This database consists of 48 records, belonging to 47 subjects, studied by the BIH Arrhythmia Laboratory between 1975 and 1979. Each record last little over 30 min, all of which have been accompanied with annotations (temporally annotated QRS complexes).

Out of these 48 recordings, 39 recordings were included in the batch analysis. The records that were omitted are the following: records 102, 104, 107, 717 due to the use of Pacemaker, which distorts the QRS complex morphology in a way that it cannot pass the pattern check; the patients that correspond with the records 108, 114, 200 and 207 have been under the therapy of Digoxin, which is known for causing potent ventricular ectopies; record 214 due to inadequate signal normalization (in the beginning of the signal, a few strong ventricular ectopies are present that consequently interfere with the normalization range).

The 39 recordings that were part of the batch analysis account 92,633 annotations. The optimal pattern reached true positive rate, i.e. sensitivity rate of 95.94%, or 88,875/92,633 correctly annotated beats. The number of false positives is 3,300, delivering specificity rate of 96.41%. The accuracy rate is 92.64%.

The Normal Sinus Rhythm Database, as the name implies, consists of records of people with no significant arrhythmic behavior. The database counts 18 records. However, five of the records feature generic ECG pattern that is presumably artificially generated, most likely, a malfunction in the Physionet system. The records of this database account more then 2 days continuous recording. Therefore, only the first 30 min are taken into account for the batch analysis.

The 13 recordings that were part of the batch analysis account 31,740 annotations. The optimal pattern reached true positive rate, i.e. sensitivity rate of 99.89%, or 31,690/31,740 correctly annotated beats. The number of false positives is 47, delivering specificity rate of 99.85%. The accuracy rate is 99.87%.

Finally, the ECG-ID Database contains 310 records obtained from 90 people, collected periodically for over 6 months. The database was consolidated in order to conduct research in the field of biometric recognition via typical ECG characteristics. This database features a statistical population representing typical samples, i.e. rate of arrhythmia very close to the average rate of arrhythmia occurrence. Unfortunately, only the first 10 beats of each recording have been annotated.

The 310 recordings that were part of the batch analysis account 3,102 annotations. The optimal pattern reached true positive rate, i.e. sensitivity rate of 95.23%, or 2,954/3,102 correctly annotated beats. The number of false positives is 175, delivering specificity rate of 94.40%. The accuracy rate is 90.14%.

It was anticipated that the pattern recognition approach would excell at effectivity when subjected on normal sinus rhythm signal. On the other hand, the conducted analyses from the MIT-BIH Database and the ECG-ID Database might as well seem satisfactory given the fact that the single pattern - pattern recognition approach is not meant to suite specific scenarios where substantial aberration in the signal morphology is present. However, such effectiveness indicators do not stand reliable given the important and crucial impact they could have when a patients' well being is of concern.

Related work in the field of ECG QRS detection is notably focused on the detection of abnormal hearth behavior, which is to be expected. Hence, most of the work published deals with classification of QRS complexes according to their morphological, and closely related, physiological distinctions. Most of the QRS detection methods involve wavelet transforms [8] and neural networks for the QRS complex classification [14]. However, there are also other, rather atypical approaches to the matter, such as mathematical morphologies [12] and derivatives [1].

Regarding the effectiveness in the QRS detection methods, Martinez et al. [8] made a summarization of the QRS detection results of a set of algorithms that are appraised as state of the art algorithms in the field. The asseblage features QRS sensitivity in the range of 98.30%–99.89%, for the MIT-BIH Database. These algorithms rely on wavelet transforms since the variety of filtering techniques gives an increase to the sensitivity.

6 Conclusion

Although the pattern recognition method might appeal unconventional in comparison to the other QRS detection methods, the onset results are promising. It has exceled at sensitivity and specificity in the detection of QRS complexes of a normal sinus rhythm, which was confirmed by the results of the Physionet NSR Database analysis.

What is of great importance to the effectiveness of an algorithm which deals with any type of QRS detection method, are the supplementary signal filters. However, it is very important to stay low on complexity and demand for system resources.

Although this version of the pattern recognition detection is not implemented as a real-time streaming algorithm, conventional to be used by mobile devices, the algorithm design would allow such an implementation with an ease, hence, expanding the algorithm applicability. However, the eventual goal of any feature work would be the increase of effectivity. Hence, the algorithm design would easily allow is the simultaneous recognition of multiple patterns, which will introduce the functionally of heart beat classification and will engage a potential for machine learning and fuzzy logic.

References

1. Arzeno, N.M., Deng, Z.D., Poon, C.S.: Analysis of first-derivative based QRS detection algorithms. IEEE Trans. Biomed. Eng. **55**(2), 478–484 (2008)
2. Blanco-Velasco, M., Weng, B., Barner, K.E.: ECG signal denoising and baseline wander correction based on the empirical mode decomposition. Comput. Biol. Med. **38**(1), 1–13 (2008)
3. Burns, N.: Cardiovascular physiology. Retrieved from School of Medicine, Trinity College, Dublin (2013)
4. Garcia, T.B., et al.: 12-Lead ECG: The Art of Interpretation. Jones & Bartlett Publishers, Burlington (2013)
5. Goldberger, A.L., Amaral, L.A., Glass, L., Hausdorff, J.M., Ivanov, P.C., Mark, R.G., Mietus, J.E., Moody, G.B., Peng, C.K., Stanley, H.E.: Physiobank, physiotoolkit, and physionet components of a new research resource for complex physiologic signals. Circulation **101**(23), e215–e220 (2000)
6. Katz, L.N., Pick, A.: Clinical Electrocardiography. Lea & Febiger, Philadelphia (1956)
7. Lugovaya, T.: Biometric human identification based on electrocardiogram. Master's thesis, Faculty of Computing Technologies and Informatics, Electrotechnical University LETI, Saint-Petersburg, Russian Federation (2005)
8. Martínez, J.P., Almeida, R., Olmos, S., Rocha, A.P., Laguna, P.: A wavelet-based ECG delineator: evaluation on standard databases. IEEE Trans. Biomed. Eng. **51**(4), 570–581 (2004)
9. Milchevski, A., Gusev, M.: Performance evaluation of FIR and IIR filtering of ECG signals. In: ICT Innovations 2016. Advances in Intelligent Systems and Computing, AISC, Springer series (2016, in press)
10. Moody, G.B., Mark, R.G.: The impact of the MIT-BIH arrhythmia database. IEEE Eng. Med. Biol. Mag. **20**(3), 45–50 (2001)
11. Ristovski, A., Guseva, A., Gusev, M., Ristov, S.: Visualization in the ECG QRS detection algorithms. In: MIPRO, Proceedings of 39th International Convention on ICT, IEEE Conference Proceedings, pp. 218–223 (2016)
12. Trahanias, P.: An approach to QRS complex detection using mathematical morphology. IEEE Trans. Biomed. Eng. **40**(2), 201–205 (1993)
13. Van Alste, J., Schilder, T.: Removal of base-line wander and power-line interference from the ECG by an efficient FIR filter with a reduced number of taps. IEEE Trans. Biomed. Eng. **12**, 1052–1060 (1985)
14. Xue, Q., Hu, Y.H., Tompkins, W.J.: Neural-network-based adaptive matched filtering for QRS detection. IEEE Trans. Biomed. Eng. **39**(4), 317–329 (1992)

Performance Evaluation of FIR and IIR Filtering of ECG Signals

Aleksandar Milchevski(✉) and Marjan Gusev

FCSE, Ss. Cyril and Methodious University,
Rugjer Boshkovikj 16, 1000 Skopje, Macedonia
milchevski@gmail.com, marjan.gushev@finki.ukim.mk

Abstract. When a wearable ECG sensor transmits signals to a mobile device, the mobile applications needs to be very efficient and save the limited mobile phone resources. This motivates us to find an algorithm implementation that is not computationally intensive, but still very efficient in denoising the ECG signal. The use of a window-based design Finite Impulse Response (FIR) and Infinite Impulse Response (IIR) filters are analysed in this paper. Several filters have been designed and the computational efficiency have been analysed both theoretically and experimentally. The results show that the designed IIR outperforms the FIR filter achieving a better computational efficiency with a minimal distortion of the ECG signal.

Keywords: DSP · Performance · Speedup

1 Introduction

The electrocardiogram (ECG) has been one of the most used biomedical signals since the beginning of the twentieth century. The information obtained from the ECG can be used as an indication in the diagnoses of several medical conditions, such us myocardial infarction [10,11], pulmonary embolism [3], epileptic seizures [14], arrhythmia [8], etc. An important precondition in all of these procedures is the successful acquisition and denoising of the ECG.

A method for removal of the baseline wander and power-line interference from the ECG can use a Finite Impulse Response (FIR) filter with a reduced number of taps in order to increase the efficiency. For example, a highpass filter with a cut-off frequency of 0.7 Hz was used for the baseline wander removal [13]. A notch Infinite Impulse Response (IIR) filter can also filter out the power line interference in the recording of the ECG [9]. Another approach for ECG denoising is with the use of the Discrete Wavelet Transform (DWT). One such method uses DWT for simultaneous denoising and feature extraction [2]. Other techniques used for the ECG denoising include: Principal Component Analysis (PCA) [7], Independent Component Analysis (ICA) [1], Empirical Mode Decomposition (EMD) [12].

G. Stojanov and A. Kulakov (eds.), *ICT Innovations 2016*,
Advances in Intelligent Systems and Computing 665,
https://doi.org/10.1007/978-3-319-68855-8_10

A lot of issues challenged the programming of wearable ECG sensors and their implementation in combination of smart mobile devices and cloud computing [4]. To realize an efficient implementation of ECG denoising by devices with a small computational complexity, we analyse the use of a window-based design FIR filter and a Butterworth IIR filter. Several filters have been designed and the execution time has been analysed both theoretically and experimentally. Filtering design issues are explained in Sect. 2 and the complexity is analyzed in Sect. 3. Section 4 presents the testing methodology and evaluation of results. Finally, the conclusions are presented in Sect. 5.

2 Filter Design for FIR and IIR Denoising of the ECG

The goal of this research is to compare FIR and IIR filters for denoising the ECG signal. The initial assumption is to design filters that have almost equal performance characteristics and then to analyze the computational complexity of the both approaches.

The windowing design method is a simple method to design a FIR filter. The procedure begins by modelling the ideal frequency response of the filter and then by computing the impulse response. However, the computed impulse response is not finite, hence, there is a need for windowing operation in order to obtain a finite impulse response. The choice of the window is a trade-off between the size of the main lobe influencing the transition width and the peaks of the side lobes influencing the ripples in the non-transition bands.

The Butterworth IIR filter is one of the vastly used IIR filters. The magnitude response of the filter is maximally flat i.e. it is a monotonic function. Compared to the other well known IIR filters (such us the Chebyshev and elliptic filters) requires a higher order to obtain the same design specifications. However, it has a more linear phase characteristic. Although originally designed as an analog filter it can be digitized using a bilinear transform (1), setting a relation between the analogue and digital frequencies, marked by ω_a and ω_d correspondingly, where T is the sampling period.

$$\omega_a = \frac{2}{T} tan \frac{\omega_d T}{2} \tag{1}$$

The design approaches to realize similar performance characteristics of the designed FIR and IIR filters is not an easy task, since it is hard to set the order of the filters so they are equally good, because both filters have positive properties which the other filter does not. For example, the designed FIR filter has a linear phase characteristic and the designed Butterworth filter has maximally flat magnitude response.

Therefore, we have set a goal to design filters that will have an equal width of the transition band, the passband ripple, and the stopband attenuation. The design process should determine the filter order M and the filter kernel coefficients.

The transition width W of a FIR filter depends on the filter order M_{FIR} and the type of window used. For the Hamming window, the transition width

expressed in Hz is approximated with the Eq. (2), where Fs is the sampling frequency.

$$W = \frac{3.3}{M_{FIR}} Fs \tag{2}$$

Considering that the transition width is distributed equally from the critical frequency F_c (set to 40 Hz in this case) the normalized passband and stopband frequencies, correspondingly marked by θ_p and θ_s, can be calculated by (3) and (4) correspondingly.

$$\theta_p = (40 - W/2)(2/Fs) \tag{3}$$

$$\theta_s = (40 + W/2)(2/Fs) \tag{4}$$

After determination of the stopband and passband frequencies, the order of the digital Butterworth filter can be found with the Eq. (5), where R_s is the stopband attenuation and R_p the passband ripple.

$$M_{IIR} = \left\lceil \frac{log_{10}[(10^{-0.1R_s} - 1)(10^{-0.1R_p} - 1)]}{2log_{10}\frac{tg(\frac{\pi}{2}\theta_s)}{tg(\frac{\pi}{2}\theta_p)}} \right\rceil \tag{5}$$

To eliminate the high-frequency noise in the ECG signal, we designed a low-pass FIR filter using the Hamming window with length of 101 element, using $M = 100$ and calculating the convolution coefficients $w[i]$ for $i = 0, \ldots, M$ by $w[i] = 0.54 - 0.46cos(2\pi i/M)$.

The cut-off frequency is set to 40 Hz. The minimum stopband attenuation for the Hamming window is -53 dB, and the transition width $(3.3/M)500$ Hz, determining the transition band for the designed filter $(31.75, 48.25)$ Hz, as presented in Fig. 1.

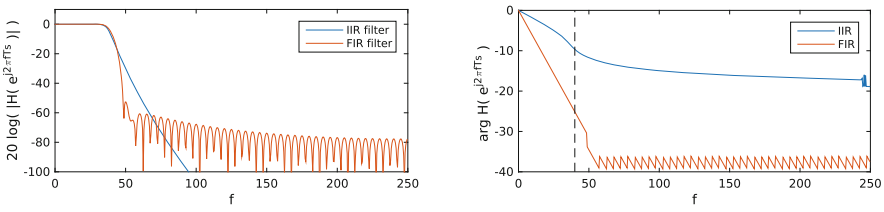

Fig. 1. Amplitude and phase response of the designed lowpass filters

A low-pass Butterworth IIR filter is also designed to eliminate the high-frequency noise with design parameters presented in Table 1.

Figure 2 shows the output of the low-pass FIR filter. The blue line is the input in the filter (original ECG signal) and the red line in the figure is the output from the filter. It can be seen that the noise initiated by a power supply has been successfully removed. The Butterworth IIR filter shows the same results of removing the high-frequency noise in the ECG signal.

Table 1. Design parameters of the lowpass Butterworth filter

Passband corner frequency	$f_p = 30\,\text{Hz}$
Stopband corner frequency	$f_s = 50\,\text{Hz}$
Passband ripple	$Rp = 0.1\,\text{dB}$
Stopband attenuations	$Rs = 30\,\text{dB}$

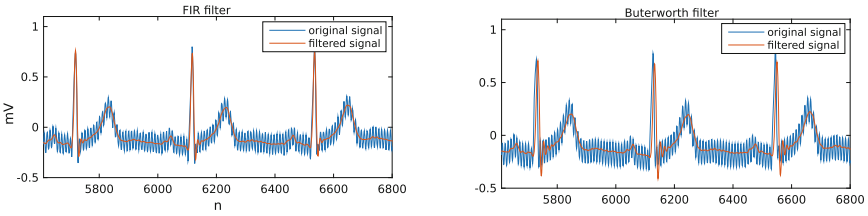

Fig. 2. Results by applying a low-pass filter

A high pass filter can be used to eliminate the low-frequency noise initiated by a physical movement or breathing, represented by low frequencies. Similarly to the previous section we design two filters for this task: a FIR filter using Hamming window and a digital Butterworth IIR filter. The filters are evaluated on an ECG that contains baseline drift artifacts.

A high pass filter with a narrow transition band is required in order to preserve the details and characteristic features from the ECG as much as possible. In order to achieve this, the filter order must be increased significantly compared to the previous section. For this case, we design a FIR filter with an order of 1000 and a cutoff frequency of 0.5 Hz. The design parameters for the fourth order Butterworth IIR filter are shown in Table 2.

Table 2. Design parameters of the highpass Butterworth filter

Passband corner frequency	$f_p = 0.2\,\text{Hz}$
Stopband corner frequency	$f_s = 0.8\,\text{Hz}$
Passband ripple	$Rp = 0.1\,\text{dB}$
Stopband attenuations	$Rs = 30\,\text{dB}$

Figure 3 shows the results obtained when an ECG signal is processed by a high-pass filter. The analysis shows that the baseline drift is removed successfully with both designed filters.

However, a distortion of the results is present when applying the IIR Butterworth filter due to non-linear phase, as presented by the yellow line in Fig. 4 when an ECG signal (blue line) is processed.

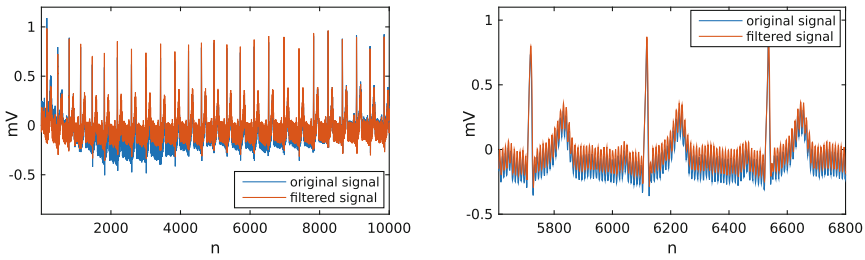

Fig. 3. Results by applying a high-pass filter

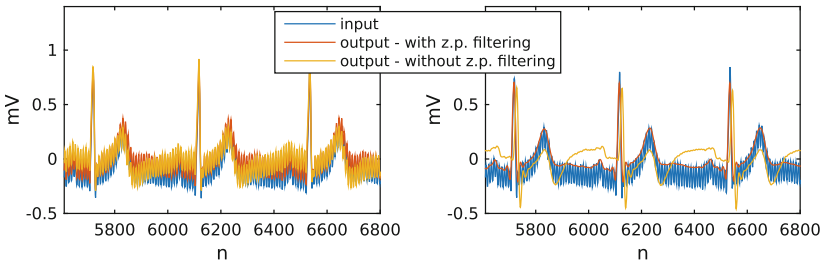

Fig. 4. A distortion by the non-linear phase and its elimination on a high-pass and band-pass Butterworth filter, respectively

The solution for this problem in the case of the high-pass IIR filter is the use of the zero-phase digital filtering. The technique consists of two steps: in the forward step the input signal is filtered with the designed filter and in the backward step the obtained result is flipped in time prior to the filtering with the same filter [5]. This procedure squares the amplitude response of the filter and zeros the phase response, which cancels out the distortions due to the non-linear phase of the designed filter, as presented by the red line in Fig. 4. The negative side is that the number of operations using this technique is doubled and additional requirements are set, such as to buffer the whole input and output streams.

The bandpass filter combines the properties of the two previously designed filters i.e. it should remove both low-frequency and high-frequency noise. Again, two filters are designed: a FIR filter using Hamming window and a digital Butterworth IIR filter. The order of the combined FIR filter is equal to the higher value of 1000, and the two critical frequencies are 0.5 Hz and 40 Hz. The design parameters for the Butterworth filter are combined from Tables 1 and 2. The order of the designed Butterworth filter is 10. It should be noted that an attempt was made to design a Butterworth filter with a narrower transition band and smaller ripples, however, the obtained filter was unstable.

Figure 5 presents the results of processing an ECG signal with the designed bandpass FIR filters. The results show that the baseline drift and the high-frequency noise are removed successfully.

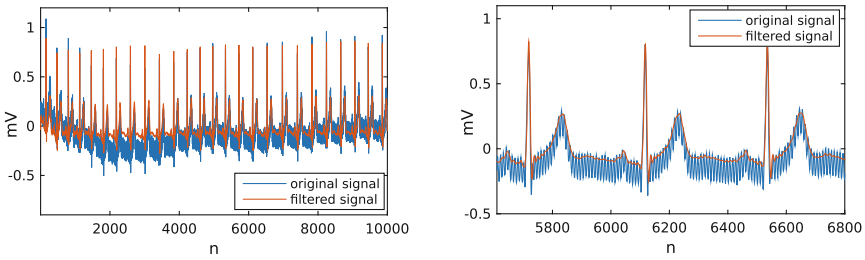

Fig. 5. Results by applying a bandpass filter to an ECG signal

3 Programming Issues and Complexity Analysis

One sample of the output of an M-th order FIR filter defined by a transfer function in (6) is calculated and can be programmed by (7).

$$H(z) = b_0 + b_1 z^{-1} + b_2 z^{-2} + \ldots + b_M z^- M \tag{6}$$

$$y[n] = b_0 x[n] + b_1 x[n-1] + \ldots + b_M x[n-M] \tag{7}$$

The number of arithmetic operations is easy to obtain i.e. the number of multiplications is $M+1$ and the number of additions is M, with a total of $2M+1$ operations. The number of memory accesses per sample is $2M+1$ to access the filter kernel coefficients and a corresponding segment of the input stream, plus the access to the processed output.

A programming solution P1 that aims at keeping low memory buffers uses buffers of only last M input stream samples and M filter coefficients. Although this solution requires smaller memory requirements, still it generates additional M rotation operations per sample, to keep the buffer elements of the input stream aligned to the last processed sample. Another solution (P2) will be to buffer the whole input data stream, requiring a high memory capacity, but without memory rotation operations. A solution that uses a circular buffer was reported in the case of a wavelet filter [6] can also be used in this case leading to a programming solution P3 without extended memory capacity requirements and additional memory rotation operations.

The number of arithmetic operations for the IIR filter can be obtained by a transfer function (8) and calculated by (9).

$$H(z) = \frac{b_0 + b_1 z^{-1} + b_2 z^{-2} + \ldots + b_M z^- M}{1 + a_1 z^{-1} + a_2 z^{-2} + \ldots + a_M z^- M} \tag{8}$$

$$\begin{aligned} y[n] = \; & b_0 x[n] + b_1 x[n-1] + \ldots + b_M x[n-M] \\ & -a_1 x[n-1] + \ldots + a_M x[n-M] \end{aligned} \tag{9}$$

Therefore, the number of multiplications is equal to $M+(M+1) = 2M+1$, the number of additions and subtractions is M, thus, the total number of arithmetic

operations equals to $4M+1$. Additionally, a total of $4M+2$ memory accesses are required to access the filter kernel coefficients and the corresponding segments of the input stream samples and previous outputs.

To eliminate the distortion introduced by the high-pass filtering, the number of operations is doubled due to the use of the zero phase filtering technique, ending with a total of $2(4M+1) = 8M+2$ arithmetic operations. In addition, the sequence has to be inverted prior to the second operation, and then once again at the end, which asks for two more runs of the whole procedure to scan the input stream. If expressed as a number of operations per sample, this will need 2 more memory rotation operations per sample. Thus, the total number of memory accesses per sample is equal to $8M+6$.

The zero phase technique makes an additional requirement, such as the necessity to store the whole input and output streams. Similar to the previous analysis of programming approaches, one can use the P1 approach to saving the memory buffers and use only 4 buffers with a length of M for the input and output streams and to keep the filter kernel coefficients. This solution can be realized to process the input stream and write data to the output file, then to invert the file and process once again and finally to invert the result file. In this case, the solution requires rotation of $2M$ buffer elements to keep the updated input and output data elements aligned to the last processed sample.

The second programming solution P2 requires big memory buffers to store the input and output streams. However, it does not need to rotate the buffer elements and does not need to write the file and invert the file. The third solution P3 uses a circular buffer and does not need memory rotation operations, but still needs to keep the output stream elements in the memory to enable the zero phase elimination with the reverse calculation.

4 Performance Evaluation

The memory accesses, storage requirements, and cache behaviour complicate the overall analysis and an experimental analysis was used for further clarification.

The performance of the designed filters has been tested with a real implementation with an input signal with a length of 10000 up to 500000 samples, where the sampling frequency is 500 Hz. The designed FIR filter has order of $M = 1000$ elements and the Butterworth IIR filter $M = 10$. The experiments were performed on a computer with 4 core processor with 1.2 GHz and 4 GB RAM. The execution code was compiled for one core without compiler optimization to extract the essential behavior of the algorithm.

The experiments were conducted for the following programming solutions:

- *P1* - small buffer requirements with corresponding memory rotation operations,
- *P2* - high buffer requirements without memory rotation operations, and
- *P3* - using a circular memory buffers.

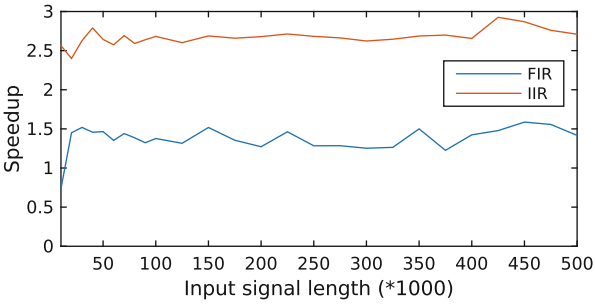

Fig. 6. Speedup of the P2/P3 solutions over the P1 solution for IIR and FIR filters

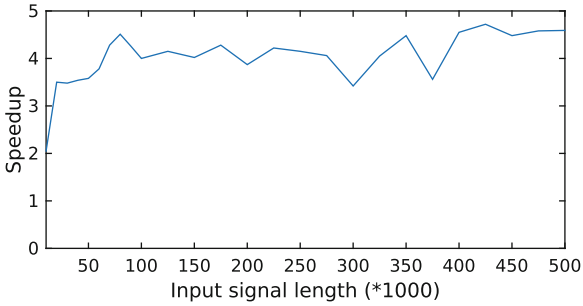

Fig. 7. Speedup of the designed IIR over FIR filter

We have provided at least five test runs for each input signal and calculated the corresponding average response time.

The speedup comparing two different solutions is calculated as a ratio of the corresponding default response time and the new analyzed solution. We will present speedup comparison of different solutions for the same filter and also a speedup of the IIR filter over the FIR filter.

Note that the time response of the programming approach P3 is almost the same as the P2, with difference that can be neglected. Since the P3 requires smaller memory buffers, we will only compare the P3 solution over the P1.

Figure 6 presents the time performance speedup of obtained programming solutions P3 (or P2) over the P1. The average speedup of the P3 solution over the P1 solution is 1.373 for the IIR filter and 2.672 for the FIR filter. A higher speedup is obtained in the case of FIR filter since the filter length is bigger and more memory rotate operations are required. The solution that uses a circular buffer outperforms the conventional solution, not just in reduced memory requirements, but also in response time performance.

The speedup of the IIR filter over the FIR filter for the same transition band, passband ripple and stopband attenuation is presented in Fig. 7. An average speedup value is 4 and slightly rises as the filter length is higher.

The presented analysis shows that the designed Butterworth filter is computationally more efficient compared to the designed FIR filter. Another positive side of the Butterworth filter is that it has maximally flat magnitude response which the window based designed FIR does not. Although the zero phase elimination required double the number of computations, still it was more efficient.

5 Conclusion and Future Work

The analyzed FIR and Butterworth filters are computationally efficient, but they lack a precision when compared to DWT or similar techniques. For example, the denoising techniques based on DWT are better suited for non-stationary signals, such as the ECG, and also provide a better starting point for further feature extraction.

However, the simplicity and efficient algorithm realization with small memory requirements and processing power are the main features motivating us to use them in the development of a mobile cloud application.

The theoretical analysis and experiments prove that the Butterworth IIR filter outperforms the FIR filter in obtaining a flat amplitude characteristic and also the programming solution obtains smaller response times compared to the FIR filter. In addition, a software solution that uses a circular buffer outperforms the conventional approach of using classical memory buffers.

The provided analysis is useful to be applied to mobile devices in the IoT world for healthcare, where the essential approach is toward saving the battery life, constrained by limited memory capacity and processing power.

References

1. Barros, A.K., Mansour, A., Ohnishi, N.: Removing artifacts from electrocardiographic signals using independent components analysis. Neurocomputing **22**(1), 173–186 (1998)
2. Faezipour, M., Tiwari, T.M., Saeed, A., Nourani, M., Tamil, L.S.: Wavelet-based denoising and beat detection of ECG signal. In: IEEE/NIH Life Science Systems and Applications Workshop, LiSSA 2009, pp. 100–103. IEEE (2009)
3. Geibel, A., Zehender, M., Kasper, W., Olschewski, M., Klima, C., Konstantinides, S.: Prognostic value of the ECG on admission in patients with acute major pulmonary embolism. Eur. Respir. J. **25**(5), 843–848 (2005)
4. Gusev, M., Stojmenski, A., Chorbev, I.: Challenges for development of a mobile application for ECG detection and feature extraction. J. Emerg. Res. Solut. ICT **1**(2) (2016, in Press)
5. Gustafsson, F.: Determining the initial states in forward-backward filtering. IEEE Trans. Signal Process. **44**(4), 988–992 (1996)
6. Milchevski, A., Gusev, M.: Improved pipelined wavelet implementation for filtering ECG signals. Technical report 7/2016, University Sts Cyril and Methodius, FCSE, LiiT (2016)
7. Moody, G.B., Mark, R.G.: QRS morphology representation and noise estimation using the Karhunen-Loeve transform. In: Proceedings of the Computers in Cardiology 1989, pp. 269–272. IEEE (1989)

8. Owis, M.I., Abou-Zied, A.H., Youssef, A.B.M., Kadah, Y.M.: Study of features based on nonlinear dynamical modeling in ECG arrhythmia detection and classification. IEEE Trans. Biomed. Eng. **49**(7), 733–736 (2002)
9. Pei, S.C., Tseng, C.C.: IIR multiple notch filter design based on allpass filter. IEEE Trans. Circuits Syst. II: Analog Digit. Signal Process. **44**(2), 133–136 (1997)
10. Schröder, R.: Prognostic impact of early ST-segment resolution in acute ST-elevation myocardial infarction. Circulation **110**(21), e506–e510 (2004)
11. Schroder, R., Wegscheider, K., Schroder, K., Dissmann, R., Meyer-Sabellek, W., Group, I.T., et al.: Extent of early ST segment elevation resolution: a strong predictor of outcome in patients with acute myocardial infarction and a sensitive measure to compare thrombolytic regimens. A substudy of the international joint efficacy comparison of thrombolytics (INJECT) trial. J. Am. Coll. Cardiol. **26**(7), 1657–1664 (1995)
12. Taigang, H., Clifford, G., Tarassanko, L.: Application of ICA in removing artefacts from the ECG. Neural Process. Lett. **10**(1), 1–5 (2004)
13. Van Alste, J., Schilder, T.: Removal of base-line wander and power-line interference from the ECG by an efficient FIR filter with a reduced number of taps. IEEE Trans. Biomed. Eng. **BME–32**(12), 1052–1060 (1985)
14. Zijlmans, M., Flanagan, D., Gotman, J.: Heart rate changes and ECG abnormalities during epileptic seizures: prevalence and definition of an objective clinical sign. Epilepsia **43**(8), 847–854 (2002)

Influence of Fuzzy Tolerance Metrics on Classification and Regression Tasks for Fuzzy-Rough Nearest Neighbour Algorithms

Andreja Naumoski(✉), Georgina Mirceva, and Petre Lameski

Faculty of Computers Science and Engineering,
Ss. Cyril and Methodius University in Skopje, Skopje, Macedonia
{andreja.naumoski, georgina.mirceva,
petre.lameski}@finki.ukim.mk

Abstract. In this paper, we investigate the influence of the fuzzy tolerance relationship (fuzzy similarity metrics) on two fuzzy and two fuzzy-rough nearest neighbour algorithms for both classification and regression tasks. The fuzzy similarity metric plays a major role in construction of the lower and upper approximations of decision classes, and therefore has high influence on the accuracy of the algorithm. The experimental results evaluated on the four approaches show the difficulty to estimate a single metric that will be good in all cases. Moreover, the choice of similarity metric on some datasets has not influence at all. This require further investigation, not only with similarity metrics, but also for evaluating the algorithms with different T-norms and implicators.

Keywords: Fuzzy tolerance relationship · Fuzzy rough sets · *k*-nearest neighbour · Classification · Regression

1 Introduction

From the set of well-used machine learning algorithms, the *k*-nearest neighbour (*k*-NN) is among the simplest algorithms. It is a non-parametric, instance-based learning, or lazy learning algorithm, that can be used for both classification and regression tasks. If *k*-NN is used for classification, the output is a class membership derived by a majority voting of its neighbours. In classification task, the class membership is assigned to the class that is most common among the *k* nearest neighbours, while in regression the output is average values of the *k* neighbours. An extension of the *k*-NN algorithm to fuzzy set theory (*k*-FNN) was introduced in [1]. This extension allows partial membership of an object to different classes and the algorithm is aware of the relative closeness of the test instance. Nonetheless, this improved extension is not without problems, as the author argued in [2], the *k*-FNN is not able to deal with the insufficient knowledge that is part of each real-time problem. The problem lies in need of satisfying the rule that all predicted membership degrees of various classes need to sum up to 1. Consequently, the algorithm makes clear-cut predictions, by removing every training pattern from the test object, and therefore no suitable neighbour is found. The authors

G. Stojanov and A. Kulakov (eds.), *ICT Innovations 2016*,
Advances in Intelligent Systems and Computing 665,
https://doi.org/10.1007/978-3-319-68855-8_11

in [2] tried to solve this problem by introducing fuzzy-rough ownership function (this algorithm is referred as *k*-FRNNOn throughout this paper), which does not refer to the main ingredients of the rough set theory: lower and upper approximations. Therefore, in [3] the authors proposed alternative algorithms to cope with this problem. These approaches, named FRNN and VQNN in this paper, uses test objects, that are nearest neighbours, to construct the lower and upper approximation of each decision class [3]. Later it computes the membership of the test object to these approximations [3].

The two algorithms in [3] are very flexible, and can be defined with different fuzzy-rough approximations, including implicator/T-norm combination [4] and vaguely quantified rough set (VQRS) model [3, 5]. That's why the aim of this paper is to investigate the influence of four fuzzy similarity metrics on the AUC-ROC metric (for classification task) and Relative Root Mean Square Error (RRMSE) metric (for regression task) using various datasets with four *k*-FNN algorithms. Furthermore, the overall results between the fuzzy *k*-NN and fuzzy-rough *k*-NN are compared.

The rest of the paper is organised as follows. Section 2 provides necessary details for fuzzy rough set theory, while Sect. 3 is concerned with the definition of the fuzzy and fuzzy-rough *k*-NN algorithms. Section 4 outlines the experimental approach and presents experimentation results on a series of classification and regression problems. The paper is concluded in Sect. 5.

2 Definition of Fuzzy Rough Sets

The definition of the fuzzy rough set theory is closely related to the properties of both fuzzy and rough set theory. First, the rough set theory [6] provides understating how the knowledge can be extracted from a particular domain, so it's able to retain the information content while reducing the amount of knowledge involved [3]. The fuzzy-rough set theory provides advantages for both rough and fuzzy sets. In order to join the advantages of indiscernibility and the fuzzy uncertainty, in this section define some key elements that are necessary for rough sets.

In order to solve classification or regression problems, let's consider simple information system (U, A), where U is a non-empty set of finite objects (the universe of discourse) and A is a non-empty finite set of attributes. Furthermore, for machine learning task, the set A is union between C (the set of conditional attributes) and d (the decision or class attribute). The relationship between the elements of the information system (U, A) is defined as $U \rightarrow Va$ for every $a \in A$, where Va is the set of values that attribute a may take. According the rough set theory, with any $B \subseteq A$ there is an associated equivalence relation R_B:

$$R_B = \{(x, y) \in U^2 | \forall a \in B, a(x) = a(y)\}. \tag{1}$$

If $(x, y) \in R_B$, then x and y are indiscernible by attributes from B. "The equivalence classes of the B-indiscernibility relation are denoted $[x]_B$. If $A \subseteq U$, then A can be approximated using the information contained within B by constructing the B-lower and B-upper approximations of A" [3]:

$$\overline{R_{B,A}} = \{x \in U | [x]_B \subseteq A\} \tag{2}$$

$$\underline{R_{B,A}} = \{x \in U | [x]_B \cap A \neq 0\}. \tag{3}$$

The tuple $(\overline{R_{B,A}}, \underline{R_{B,A}})$ is called a rough set. However, using this definition above, the methods can only operate when dataset contains only discretised values. Therefore, it is necessary to perform a discretization step before analysing the dataset. In this step, applying fuzzy theory is intuitive and logical step of events, and also flexible. By applying fuzzy theory, we apply the means of fuzzy relations R in U, so $U \rightarrow [0, 1]$, so the algorithm assigns to each couple of objects a degree of similarity. In order this to work, it is assumed that R is at least fuzzy tolerance relations satisfying two conditions: $R(x, x) = 1$ and $R(x, y) = R(y, x)$ for x and y in U. Given y in U, its forest Ry is defined by $Ry(x) = R(x, y)$ for every x in U [3]. So now, we can define the fuzzy lower and upper approximations of A by R. There are several ways to construct the fuzzy upper and the lower approximations, but one general definition [5, 7] is following:

$$\overline{R_A}(x) = \inf_{y \in U} I(R(x, y), A(y)) \tag{4}$$

$$\underline{R_A}(x) = \sup_{y \in U} T(R(x, y), A(y)). \tag{5}$$

In Eqs. 4 and 5, I is an implicator and T is a T-norm. In order to get the traditional lower and upper approximations, we need to set A as a crisp set and R is an equivalence relation in U. An implicator I is a $[0, 1]^2 \rightarrow [0, 1]$ mapping that is decreasing in its first and increasing in its second argument, satisfying $I(0, 0) = I(0, 1) = I(1, 1) = 1$ and $I(1, 0) = 0$. On the other hand, T-norm T is an increasing, commutative, associative $[0, 1]^2 \rightarrow [0, 1]$ mapping that satisfies $T(x, 1) = x$ for x in $[0, 1]$.

Defined in this way, the fuzzy rough set approximations are very sensitive to noise values, which means a small change in a single object can result in changes of approximations. This is due to the use of *sup* and *inf*, which generalize the existential and universal quantifier [3]. In context of classification and regression tasks, this will have effect on the accuracy of the predictive model. Therefore, another algorithm proposed in [3], the concept of quantified rough sets (VQRS) is introduced in [3]. This algorithm uses linguistic quantifiers, as opposed to the traditional T-norms and implicators, to decide to what extend an object belongs to the lower and upper approximation. In this algorithm the couple (*Q1, Q2*) represents the fuzzy quantifiers that model of linguistic quantifiers, then the lower and upper approximation of A by R are defined as follows:

$$\underline{R_{Q1}}(y) = Q_1\left(\frac{|R_y \cap A|}{R_y}\right) = Q_1\left(\frac{\sum_{x \in X} \min(R(x, y), A(y))}{\sum_{x \in X} R(x, y)}\right) \tag{6}$$

$$\overline{R_{Q2}}(y) = Q_2\left(\frac{|R_y \cap A|}{R_y}\right) = Q_2\left(\frac{\sum_{x \in X} \min(R(x,y), A(y))}{\sum_{x \in X} R(x,y)}\right), \tag{7}$$

where the fuzzy set intersection is defined by the min T-norm and the fuzzy set cardinality by the sigma-count operation [3]. If we make comparison between the fuzzy lower and upper approximations, the VQRS approximations do not extend the classical rough set and they can be still fuzzy.

3 The Algorithms

3.1 *k*-Fuzzy Nearest Neighbour Classification (*k*-FNN and *k*-FRNNOn)

The first fuzzy *k*-NN (*k*-FNN) algorithm based on fuzzy theory proposed in [1], have purpose to classify test objects based on their similarity for a given number of neighbours together with the training objects in combination with the neighbours' membership degrees whatever they are crisp or fuzzy relative to the class labels. In order this to work, extension of the function needed to classify object y that belongs to class C is computed as:

$$C'(y) = \sum_{x \in N} R(x,y)C(x). \tag{8}$$

In this formula N is a set of the K nearest neighbours of y, and $R(x, y)$ is a similarity between x and y that has values in the interval [0,1]. There is great difference on how $R(x, y)$ is calculated in crisp, fuzzy and fuzzy-rough sets. If we consider a classical or crisp *k*-NN, the function $R(x, y)$ is defined as:

$$R(x,y) = \frac{\|y-x\|^{-2/(m-1)}}{\sum_{j \in N} \left\|y-j\right\|^{-2/(m-1)}}, \tag{9}$$

where $\| y - x \|$ denotes the Euclidean norm, and m is a parameter that controls the overall weighting of the similarity. If we take a closer look on the relationship between the variables in this formula, it is easy to note that the degree of closeness of neighbours will influence the impact that their class membership has on the process of obtaining the membership of the test object. The first attempt to merge this algorithm with the concepts from the fuzzy rough set theory was presented in [4, 7]. The authors from these papers, constructed fuzzy-rough ownership function in order to handle both "fuzzy uncertainty" and the "rough uncertainty". The fuzzy-rough ownership function for object y and class C is defined as:

$$\tau_C(y) = \frac{\sum_{x \in U} R(x,y)C(x)}{|U|}, \tag{10}$$

while the fuzzy relationship R is given as:

$$R(x,y) = \exp\left(\sum_{a\in C} \underbrace{\left(\frac{U}{2\sum\limits_{x\in U}\|a(y)-a(x)\|^{2/(m-1)}}\right)}_{Band} (a(y)-a(x))^{2/(m-1)}\right), \quad (11)$$

where m controls the weighting of the similarity (as in k-FNN) and *Band* is a parameter that decides the bandwidth of the membership. In terms of applying this in k-NN classification problem, Eq. 11 will consider the confidence that y will be classified in C. This algorithm will be referred as k-FRNNOn in this paper.

Compared with the k-FNN algorithm, k-FRNNOn algorithm takes into account all training objects, and not limiting his search space only on the set of neighbours. By doing this, the algorithm does not require the number of neighbours to be considered. It is obvious that the very distant training objects will not influence the outcome, which is very different from the case of k-FNN. It is important to note that this algorithm doesn't uses lower and upper approximations to determinate the class membership [2].

3.2 *k*-Fuzzy-Rough Nearest Neighbour (FRNN and VQNN) Algorithms

The authors in [3] proposed two algorithms that combines the fuzzy-rough approximations with the ideas of the k-FNN approach, i.e. the FRNN and k-FNN algorithm with VQRS approximations (VQNN). According [3], the algorithm uses lower and upper approximations of the decision class that is calculated by means of the nearest neighbour of a test object y. This give to the algorithm a good clue to predict the membership of the test object to that class. For further details, the reader can read paper [3]. In order these two algorithms to perform a crisp classification, the algorithms output the decision class with the resulting best fuzzy lower and upper approximation memberships. In this way both algorithms utilize the information for the fuzzy lower and upper membership approximations to determinate the class membership [3]. Because these algorithms depend from the choice of the fuzzy tolerance relationship as any k-FNN algorithm, a general way of constructing R given by [3] is defined as follows:

$$R(x,y) = \min_{a\in C} R_a(x,y), \quad (12)$$

which $R_a(x, y)$ is the degree to which objects x and y are similar for attribute a. In this paper, we investigate the influence of four possible $R_a(x, y)$ (fuzzy tolerance relationship) definitions:

$$R_a(x,y) = 1 - \frac{|a(x)-a(y)|}{a_{\max}-a_{\min}} \quad (13)$$

$$R_a(x,y) = \exp(-\frac{(a(x)-a(y))^2}{2\sigma_a^2}) \tag{14}$$

$$R_a(x,y) = \max(\min(\frac{(a(y)-(a(x)-\sigma_a))}{(a(x)-(a(x)-\sigma_a))}, \frac{((a(x)+\sigma_a)-a(y))}{((a(x)+\sigma_a)-a(x))}), 0) \tag{15}$$

$$R_a(x,y) = \max(0, \min(1, \frac{\beta - \alpha * a(x) - a(y)}{\sigma_a})), \alpha = 0.5, \beta = 1.0, \tag{16}$$

where σ_a^2 is the variance of attribute a, and $a_{\max}$ and $a_{\min}$ are the maximal and minimal occurring value of that attribute. The four similarity fuzzy metrics will be further tested and we will examine their influence on the four algorithms. Each fuzzy tolerance relationship will be referred with the equation number, i.e. similarity 14 will be referred as Eq. 14.

4 Experimentation

4.1 Experimental Setup

This section presents the experimental setup of the fuzzy and fuzzy-rough classification algorithms *k*-FNN, *k*-FRNNOn, FRNN and VQNN evaluation, over sixteen benchmark datasets from [8, 9]. Datasets WatersClass (C4–C8) are used to experimentally evaluate the influence of the methods on classification tasks, while the Datasets Waterreg (R1–R8) have been derived from [10], in order to show the influence of the similarity metric in regression tasks. Detail description for each dataset can be found in Table 1. All datasets contain real value attributes.

Table 1. Characteristics of the datasets used for experimental evaluation

Dataset for classification	Classification		Datasets for regression	Regression	
	Objects	Attributes		Objects	Attributes
Glass (C1)	214	10	Waterreg1 (R1)	218	17
Ionosphere (C2)	351	35	Waterreg2 (R2)	218	17
Vote (C3)	435	17	Waterreg3 (R3)	218	17
Waveform (C4)	5000	41	Waterreg4 (R4)	218	17
Waterclass1 (C5)	218	22	Waterreg5 (R5)	218	17
Waterclass2 (C6)	218	112	Waterreg6 (R6)	218	17
Waterclass3 (C7)	57	22	Waterreg7 (R7)	218	17
Waterclass4 (C8)	57	96	Waterreg8 (R8)	218	17

Since, we don't study the effect of the number of k nearest neighbours, but the effect of the similarity metrics, we leave the default values for each algorithm as they are proposed in their original papers. For the *k*-FNN and *k*-FRNNO, we also leave the

default value of m to 2. As we mentioned, for FRNN approach we used the Algebraic T-norm (T $(x, y) = x * y$) and the KD implicator ($I(x, y) = \max(1 - x, y)$), while the VQNN approach as defined in [3] is used with the following settings: $Q_1 = Q(0.1; 0.6)$ and $Q_2 = Q(0.2; 1.0)$, according Eq. 17.

$$Q_{(\alpha,\beta)}(x) = \begin{cases} 0, & x \leq \alpha \\ \frac{2(x-\alpha)^2}{(\beta-\alpha)^2}, & \alpha \leq x \leq \frac{\alpha+\beta}{2} \\ 1 - \frac{2(x-\alpha)^2}{(\beta-\alpha)^2}, & \frac{\alpha+\beta}{2} \leq x \leq \beta \\ 1, & \beta \leq x \end{cases}. \tag{17}$$

Because k-FNN algorithm has no option for similarity metric, that's why we give results only for one experiment. The presentation of the experiments is divided in two separate tables for both classification and regression tasks.

4.2 Experimental Results

In this section, the results from the classification experiments are presented. In the tables, all results are given for each algorithm in the following form: Method$^{\text{Similarity Metric}}$. The evaluation metric used to analyse the results is the AUC-ROC metric for classification task, and Relative Root Means Square Error (RRMSE) for regression task.

In Table 2, the experimental results depict the influence of each similarity metric for each algorithm. If we compare the results obtained by each of the algorithms, it is noticeable that FRNN and VQNN algorithms achieved best AUC-ROC accuracy. Looking in the results achieved between fuzzy k-NN and fuzzy-rough k-NN algorithms, the results are tie. A more detail investigation shows that between k-FRNNOn

Table 2. Results for AUC-ROC for classification task using the train dataset for testing. Bolded results show the best result for each method, while underlined results show the best result per dataset.

Classical	C1	C2	C3	C4	C5	C6	C7	C8
k-FNN	1	1	0.950	1	0.887	0.887	0.966	0.966
k-FRNNOn[14]	0.429	0.487	0	0.203	**0.443**	0.493	**0.384**	0.412
k-FRNNOn[15]	**0.434**	**0.587**	0	0.199	0.413	**0.538**	0.352	0.399
k-FRNNOn[16]	0.358	0.513	0	**0.222**	0.440	0.483	0.357	**0.500**
k-FRNNOn[17]	0.429	0.487	0	0.203	**0.443**	0.493	0.384	0.421
FRNN[14]	0.949	**1**	**0.941**	0.999	0.743	0.849	0.812	0.963
FRNN[15]	0.955	**1**	**0.941**	**1**	0.753	0.884	0.814	0.979
FRNN[16]	**0.998**	**1**	**0.941**	**1**	**0.854**	**0.935**	**0.952**	**0.991**
FRNN[17]	0.949	**1**	**0.941**	0.999	0.783	0.849	0.812	0.963
VQNN[14]	0.954	**0.992**	**0.993**	0.980	0.764	0.839	0.741	0.856
VQNN[15]	0.944	0.991	**0.993**	0.979	0.741	0.870	0.703	0.902
VQNN[16]	**0.971**	0.987	**0.993**	**0.990**	**0.800**	**0.909**	**0.757**	**0.951**
VQNN[17]	0.954	**0.992**	**0.993**	0.980	0.764	0.839	0.741	0.856

algorithm and the rest of the algorithms there is not a huge difference in the accuracy, except for C2 and C8 datasets. In most cases, various similarity metrics achieved highest train accuracy. Therefore, it is difficult to tell what is the best similarity metric for this algorithm. However, similarity metric 16 obtained best results compared with the rest of the metrics for the FRNN algorithm and in some cases for the VQNN algorithm.

Regarding the overall test AUC-ROC results, the situation is different here, where the fuzzy-rough algorithms outperformed the fuzzy *k*-NN approach in all datasets. Comparing the influence of the similarity metric for each of the fuzzy-rough approaches, it is obvious that Similarity 16 metric is oppressed by the Similarity metrics 14 and 17. However, this is a general rule, but not an absolute rule, where we can see in some cases that other similarity metric achieves relatively good results. It is interesting to note, on both training and test experiments, some datasets are immune to the influence of the similarity metric. In our case the dataset C3 exhibits this behaviour.

Regarding the regression task, we analysed 8 datasets, and the experimental results for RRMSE by using the train and test dataset for testing are presented in Tables 4 and 5, respectively.

The overall comparison of the results given in Table 4 shows slightly better results for the fuzzy-rough algorithms compared to the fuzzy algorithms. Comparing each similarity metric, the results reveal that the metric 14 and 17 achieve better results using the FRNN algorithm, while metric 15 using the VQNN algorithm.

Same as in Table 3, the algorithms using fuzzy-rough theory obtained better results than the fuzzy algorithms. Comparing the similarity metric, FRNN algorithm achieve better results using metric 14 and 17, while no pattern was noticed using VQNN algorithm. In both cases *k*-FNNOn algorithm obtained same results in both training and test experiments, and the similarity metric does not have influence.

Table 3. Results for AUC-ROC for classification task using the test dataset for testing. Bolded results show the best result for each method, while underlined results show the best result per dataset.

Classical	C1	C2	C3	C4	C5	C6	C7	C8
k-FNN	0.777	0.794	0.843	0.858	0.497	0.492	0.547	0.561
k-FRNNOn^{14}	0.417	0.484	0	0.203	**0.443**	0.530	**0.462**	**0.473**
k-FRNNOn^{15}	**0.430**	**0.584**	0	0.200	0.441	**0.559**	0.437	0.457
k-FRNNOn^{16}	0.360	0.505	0	**0.222**	0.431	0.512	0.448	0.530
k-FRNNOn^{17}	0.417	0.484	0	0.203	**0.443**	0.520	**0.462**	**0.473**
FRNN^{14}	0.886	**0.952**	**0.888**	**0.904**	0.551	**0.535**	**0.569**	**0.642**
FRNN^{15}	0.873	0.946	**0.888**	0.894	**0.577**	0.521	0.567	0.606
FRNN^{16}	**0.892**	0.946	**0.888**	0.846	0.567	0.510	0.559	0.566
FRNN^{17}	0.886	**0.952**	**0.888**	**0.904**	0.551	**0.535**	**0.569**	**0.642**
VQNN^{14}	0.889	**0.938**	**0.981**	**0.950**	**0.555**	**0.555**	0.516	0.615
VQNN^{15}	0.887	**0.938**	**0.981**	0.948	**0.555**	0.523	0.514	0.565
VQNN^{16}	**0.906**	0.925	**0.981**	0.930	0.542	0.513	**0.525**	**0.618**
VQNN^{17}	0.886	**0.938**	**0.981**	**0.950**	**0.555**	**0.555**	0.516	0.615

Table 4. Results for RRMSE for regression task using the train dataset for testing. Bolded results show the best result for each method, while underlined results show the best result per dataset.

Classical	C1	C2	C3	C4	C5	C6	C7	C8
k-FNN	0.721	0.692	0.845	0.856	0.981	0.979	0.886	0.891
k-FRNNOn[14]	0.390	0.542	0.846	0.595	0.913	0.340	0.422	0.992
k-FRNNOn[15]	0.390	0.542	0.846	0.595	0.913	0.340	0.422	0.992
k-FRNNOn[16]	0.390	0.542	0.846	0.595	0.913	0.340	0.422	0.992
k-FRNNOn[17]	0.390	0.542	0.846	0.595	0.913	0.340	0.422	0.992
FRNN[14]	**0.662**	**0.622**	**0.834**	**0.855**	0.280	0.346	0.898	**0.873**
FRNN[15]	0.610	0.575	0.776	0.796	0.945	**0.946**	0.852	0.855
FRNN[16]	0.491	0.461	0.643	0.669	**0.973**	**0.946**	**0.921**	0.869
FRNN[17]	**0.662**	**0.622**	**0.834**	**0.855**	0.279	0.346	0.898	**0.873**
VQNN[14]	0.708	0.692	**0.849**	0.873	0.886	0.877	**0.872**	0.905
VQNN[15]	**0.719**	**0.695**	0.846	**0.882**	**0.915**	**0.898**	0.801	**0.908**
VQNN[16]	0.623	0.619	0.764	0.845	0.423	0.133	0.503	0.462
VQNN[17]	0.708	0.692	**0.849**	0.873	0.886	0.877	**0.872**	0.905

Table 5. Results for RRMSE for regression task using the test dataset for testing. Bolded results show the best result for each method, while underlined results show the best result per dataset.

Classical	C1	C2	C3	C4	C5	C6	C7	C8
k-FNN	0.789	0.761	0.945	0.960	0.017	0.021	0.932	0.934
k-FRNNOn[14]	0.384	0.535	0.843	0.592	0.902	0.140	0.396	0.958
k-FRNNOn[15]	0.384	0.535	0.843	0.592	0.902	0.140	0.396	0.958
k-FRNNOn[16]	0.384	0.535	0.843	0.592	0.902	0.140	0.396	0.958
k-FRNNOn[17]	0.384	0.535	0.843	0.592	0.902	0.140	0.396	0.958
FRNN[14]	**0.770**	**0.736**	**0.937**	0.955	0.118	0.160	**0.989**	**0.954**
FRNN[15]	0.759	0.722	0.933	**0.958**	**0.977**	0.125	0.976	0.935
FRNN[16]	0.759	0.726	0.934	0.953	0.489	**0.533**	0.278	0.121
FRNN[17]	**0.770**	0.735	**0.937**	0.955	0.118	0.160	**0.989**	**0.954**
VQNN[14]	0.785	0.761	0.930	0.945	**0.976**	0.963	**0.927**	**0.941**
VQNN[15]	**0.811**	0.778	0.939	0.969	0.975	**0.964**	0.842	0.893
VQNN[16]	**0.811**	**0.791**	**0.940**	**0.987**	0.642	0.369	0.569	0.478
VQNN[17]	0.785	0.761	0.930	0.945	**0.976**	0.963	**0.927**	**0.941**

5 Conclusion

In this paper, we investigated the influence of the fuzzy similarity metric (fuzzy tolerance relationship) on four approaches; two of them are based on fuzzy techniques (*k*-FNN and *k*-FNNOn), and the other two techniques are based on fuzzy-rough approach (FRNN and VQNN). Both classification and regression experimental results show that in some cases it is hard to determinate the right fuzzy similarity metric, and

on some datasets the change of the metric has no effect. There is no major difference between the results for classification and regression task, but compared globally, the results from the test set are better using fuzzy-rough approach than the fuzzy approach alone.

Finally, as a future work we plan to investigate the impact of averaging the lower and/or upper approximations, and to investigate the influence of T-norm and T-conorm in the process of task at hand.

Acknowledgement. This work was partially financed by the Faculty of Computer Science and Engineering at the Ss. Cyril and Methodius University in Skopje.

References

1. Keller, J.M., Gray, M.R., Givens, J.A.: A fuzzy K-nearest neighbour algorithm. IEEE Trans. Syst. Man Cybernet. **15**(4), 580–585 (1985)
2. Wang, X., Yang, J., Teng, X., Peng, N.: Fuzzy-rough set based nearest neighbour clustering classification algorithm. In: Wang, L., Jin, Y. (eds.) FSKD 2005. LNCS (LNAI), vol. 3613, pp. 370–373. Springer, Heidelberg (2005)
3. Jensen, R., Cornelis, C.: A new approach to fuzzy-rough nearest neighbour classification. In: Rough Sets and Current Trends in Computing, 310–319. Springer, Heidelberg (2008)
4. Sarkar, M.: Fuzzy-rough nearest neighbour's algorithm. Fuzzy Sets Syst. **158**, 2123–2152 (2007)
5. Cornelis, C., De Cock, M., Radzikowska, A.M.: Vaguely quantified rough sets. In: An, A., Stefanowski, J., Ramanna, S., Butz, C.J., Pedrycz, W., Wang, G. (eds.) RSFDGrC 2007. LNCS (LNAI), vol. 4482, pp. 87–94. Springer, Heidelberg (2007)
6. Radzikowska, A.M., Kerre, E.E.: A comparative study of fuzzy rough sets. Fuzzy Sets Syst. **126**(2), 137–155 (2002)
7. Wang, X., Yang, J., Teng, X., Peng N.: Fuzzy-rough set based nearest neighbour clustering classification algorithm. In: Lecture Notes in Computer Science, vol. 3613, pp. 370–373 (2005)
8. Blake, C.L., Merz, C.J.: UCI Repository of machine learning databases. University of California, Irvine (1998). http://archive.ics.uci.edu/ml/
9. Naumoski, A., Mircev, M.: Novel fuzzy measure of similarity for fuzzy-rough feature selection. In: Loskoska, S. Koceski, S. (eds.) ICT Innovations 2015, pp. 11–21 (2015). ISSN 1857-7288
10. Naumoski, A.: Multi-target modelling of diatoms diversity indices in Lake Prespa. Appl. Ecol. Environ. Res. **10**(4), 521–529 (2012)

On the Kalman Filter Approach for Localization of Mobile Robots

Kristijan Petrovski(✉), Stole Jovanovski, Miroslav Mirchev, and Lasko Basnarkov

Faculty of Computer Science and Engineering, Ss. Cyril and Methodius University, Rudjer Boshkovikj 16, P.O. 393, 1000 Skopje, Republic of Macedonia
{petrovski.kristijan.1,jovanovski.stole}@students.finki.ukim.mk, {miroslav.mirchev,lasko.basnarkov}@finki.ukim.mk
http://finki.ukim.mk/

Abstract. In this work we analyze robot motion given from the UTIAS Multi-Robot Dataset. The dataset contains recordings of robots wandering in a confined environment with randomly spaced static landmarks. After some preprocessing of the data, an algorithm based on the Extended Kalman Filter is developed to determine the positions of robots at every instant of time using the positions of the landmarks. The algorithm takes into account the asynchronous time steps and the sparse measurement data to develop its estimates. These estimates are then compared with the groundtruth data provided in the same dataset. Furthermore several methods of noise estimation are tested, which improve the error of the estimate for some robots.

Keywords: Robot localization · Extended Kalman Filter · Noise estimation · Real-world data

1 Introduction

In many research areas there are similar types of problems requiring some kind of localization in space, such as in robotics [1,2], wireless sensor networks [3,4], vehicle [5] and wildlife tracking [6] etc. Plenty of different approaches have been developed for solving these problems among which the Extended Kalman Filter (EKF) described in [7] has been one of the most employed, particularly in robot localization [1]. A good introduction to the Extended Kalman Filter is given in [8]. The EKF has been obtained by extending the applicability of the classical Kalman filter [9] to problems with a nonlinear model or measurement function. All varieties of the Kalman filter belong to the group of Bayesian approaches for localization, such as particle filters and multi-hypothesis tracking, surveyed in [10]. Although localization problems have been widely addressed there are still many aspects, particularly those which are application specific, that can be further analyzed.

G. Stojanov and A. Kulakov (eds.), *ICT Innovations 2016*,
Advances in Intelligent Systems and Computing 665,
https://doi.org/10.1007/978-3-319-68855-8_12

An implementation of EKF applied on a real dataset of several robots measuring distances to several reference points is presented in [11]. There the authors develop a general method that utilizes a decentralized robot network, where robots communicate state estimates of objects in the environment for purposes of localization. They obtain the same results as with a centralized network with the added benefit that the robots can use the Markov property to reduce memory, without taking into account the knowledge of other robots.

In this paper we provide a case study of the problem of localization using the Extended Kalman Filter applied on the same dataset as above, focusing on single robot localization. Due to the nature of data provided, several aspects of the problem are studied such as tackling asynchronous measurements at arbitrary timestamps and running the EKF in steps of varying duration. Methods that estimate the measurement and process noise are characterized, while the inherent bias of the measurement data is examined in detail and then corrected, as in [11]. These findings could be helpful in a more appropriate application of the EKF for localization problems and its further refinements.

The organization of the paper is the following. First, in Sect. 2 a presentation is given of the dataset used in the experimentation. Section 3 contains a description of the application of the localization method (EKF), while Sect. 4 shows techniques of determining the characteristics of noise from the data in order to incorporate them in the EKF. Section 5 presents an explanation of how the data is preprocessed and offers some numerical results for localization based on several parameters. Finally, in Sect. 6 we give some conclusions and discuss possible directions for future work.

2 Data Description

This paper uses the UTIAS Multi-Robot Cooperative Localization and Mapping Dataset [12]. The dataset is created by 9 runs of separate experiments. In each experiment 5 robots move randomly in a confined environment for a certain amount of time. They can perceive each other and 10 stationary landmarks for the purpose of localization. While moving, each robot collects groundtruth, control and measurement data:

- the groundtruth data records the robot's position and orientation (x, y, θ), and the landmark's positions (x, y) in the laboratory reference system. This data is obtained with a 10-camera Vicon motion system that collects data every 0.01 s on average with an accuracy of 10^{-3} m.
- the control data is composed of records of the robot's forward and angular speed (v, ω). For each robot they are issued roughly every 0.015 s.
- the measurement data consists of estimates of distances from the landmarks and other robots and the angle at which they are perceived ($\mathbf{z} = (d, \theta)$), as seen from the reference system located at the robot where the measurements are taken. These readings are sparser occurring every 0.2 s on average.

Each of the 9 experiments has a different running time and different landmark positions. In some of them a certain number of obstacles are placed in the environment.

3 EKF Algorithm

The Kalman filter is a sequential Bayesian inference method generally applied in systems evolving in time, where the state estimate at the next moment is obtained in two steps. In the first step, referred as prediction, a state estimation is based on some model of the dynamics of the system. The second step is correction, because the estimate is improved using some measurements. The literature on the Kalman filter is abundant and the authors refer the novice reader to [8].

This section simply applies the Kalman filtering procedure given in the same work, by skipping the derivation and only focusing on the points that are typical for this work. This analysis uses the Extended Discrete Kalman Filter since the measurements are non-linear functions of the state variables. To create a model that produces trajectories comparable with the groundtruth, linear approximation can be applied, and then the following model of motion can be used

$$\begin{aligned} x_{k+1}^{-} &= x_k + v_k \cos\theta_n \Delta t_k, \\ y_{k+1}^{-} &= y_k + v_k \sin\theta_n \Delta t_k, \\ \theta_{k+1}^{-} &= \theta_k + \omega_k \Delta t_k, \end{aligned} \tag{1}$$

where the minus in the superscript means that the value is predicted, subscripts denote the number of iteration, while Δt_k is the time interval between two consecutive measurements, which as was said before is not constant. To shorten the notation one can put the state variables in a column vector $\mathbf{x} = (x, y, \theta)^T$ and thus obtain a simple version of the evolution model $\mathbf{x}_{k+1} = \mathbf{f}(\mathbf{x}_k)$. The error of the estimate is the difference between the state vector and the corresponding vector obtained from the groundtruth data $\mathbf{x}_g = (x_g, y_g, \theta_g)^T$

$$\mathbf{e} = \mathbf{x} - \mathbf{x}_g. \tag{2}$$

Then, the prediction error covariance matrix of the Kalman filter-$\mathbf{P}$, which is the expectation of the product $\mathbf{e}\mathbf{e}^T$ evolves according to

$$\mathbf{P}_{k+1}^{-} = \mathbf{A}\mathbf{P}_k\mathbf{A}^T + \mathbf{Q}_k, \tag{3}$$

where $\mathbf{Q}_k$ is the model error covariance matrix and $\mathbf{A}$ is the system dynamics matrix

$$\mathbf{A} = \begin{bmatrix} 1 & 0 & -v_k \sin\theta_k \Delta t_k \\ 0 & 1 & v_n \cos\theta_k \Delta t_k \\ 0 & 0 & 1 \end{bmatrix}. \tag{4}$$

When the measurements arrive, the predicted state can be improved, which according to the second step in Kalman filtering is a linear combination of the predicted state and the difference between the measurements and their estimates

$$\mathbf{x}_{k+1} = \mathbf{x}_{k+1}^{-} + \mathbf{K}_k \left(\mathbf{z}_{k+1} - \mathbf{H}_k \mathbf{x}_{k+1}^{-} \right). \tag{5}$$

In the last equation the measurements at moment $k+1$ are packed in the vector $\mathbf{z}_{k+1}$, their estimates are the product $\mathbf{H}_k \mathbf{x}_{k+1}^{-}$, while $\mathbf{K}_k$ is the Kalman gain matrix that optimizes the correction. The matrix elements of $\mathbf{H}_k$ relate the measurement z_i with the state variables x_j with $H_{i,j} = \frac{\partial z_i}{\partial x_j}$. As given above, the measurements for a certain robot are distances from it to some landmark or other robot and the angle at which the other robot or landmark is estimated to be seen. Focusing on a robot denoted with index r, the distance to the landmark l is

$$d_{r,l} = \sqrt{(x_r - x_l)^2 + (y_r - y_l)^2}, \tag{6}$$

while in robot's coordinate system the landmark is estimated to be seen at angle

$$\theta_{r,l} = \arctan\left(\frac{y_l - y_r}{x_l - x_r} \right) - \theta_r, \tag{7}$$

where the last expression can be obtained with simple analytic geometry. The landmarks are assumed to have known positions (x_l, y_l). Then, the matrix elements $H_{r,l}$ for all robots r and for all measurements to the landmarks l can be obtained with straightforward calculus. The only non-zero elements are the following

$$\begin{aligned}
\frac{\partial d_{r,l}}{\partial x_r} &= \frac{x_r - x_l}{d_{r,l}}, \\
\frac{\partial d_{r,l}}{\partial y_r} &= \frac{y_r - y_l}{d_{r,l}}, \\
\frac{\partial \theta_l}{\partial x_r} &= \frac{y_l - y_r}{(x_l - x_r)^2} \cdot \frac{1}{1 + \left(\frac{y_l - y_r}{x_l - x_r} \right)^2}, \\
\frac{\partial \theta_l}{\partial y_r} &= -\frac{1}{x_l - x_r} \cdot \frac{1}{1 + \left(\frac{y_l - y_r}{x_l - x_r} \right)^2}, \\
\frac{\partial \theta_l}{\partial \theta_r} &= -1.
\end{aligned} \tag{8}$$

According to the Kalman filter theory the optimal Kalman gain at iteration k is

$$\mathbf{K}_k = \mathbf{P}_{k+1}^{-} \mathbf{H}_k^T \left(\mathbf{H}_k \mathbf{P}_{k+1}^{-} \mathbf{H}_k^T + \mathbf{R}_{k+1} \right)^{-1}, \tag{9}$$

where $\mathbf{R}_{k+1}$ is the measurement error covariance matrix.

The Extended Kalman Filter expects discrete concurrent control and measurement data, where each control reading is used to obtain *a priori* state estimate (Eq. (1)) and the concurrent measurement reading is used to obtain *a posteriori* state estimate (Eq. (5)). For the purpose of this dataset a constant time

step could not be used as the data readings occur asynchronously. Furthermore, as the robots do not receive a measurement simultaneously with each control datum, the robot's position can not be updated until it receives a measurement reading. This means that the robot's *a priori* state estimate is updated asynchronously as new control data come in, and when it obtains a measurement datum, that is used that to get *a posteriori* state estimate. As the control data arrives much more frequently, one can assume that for a measurement datum that updates the *a priori* state, there was a previous control datum shortly before it i.e. the control and measurement readings occurred at roughly the same time.

4 Noise Estimation Procedures

As is given, the Kalman Filter has unspecified values for the process and measurement noise in Eqs. (3) and (9), respectively. These are unique to the environment and the robot's hardware, but as they are not available for the dataset a method needs to be developed that estimates them.

4.1 Estimating the Measurement Noise

The measurement noise quantifies the uncertainty of the robot's abilities to discern targets using various sensors. For this problem it can be calculated as the covariance matrix of the difference $\mathbf{e}_z = \mathbf{z} - \hat{\mathbf{z}}$ between the measurement estimate of a relative target's state $\hat{\mathbf{z}}$ obtained from the dataset, and the actual relative target's state $\mathbf{z}$, shown in [8].

Using relative range and bearing (d, θ) from the measurement data and the robot's actual groundtruth state (x, y, θ), estimated absolute target states can be calculated. The difference between these estimates and the actual absolute target states can be used for measurement noise computation (i.e. the difference between the positions the robot perceives the targets and the positions at which they are actually located). The covariance matrix of these differences can be used in Eq. (9).

However, one can expect that the distance noise level depends on the angle at which the robot located the target (for example if a robot located the target at an obtuse angle it might cause a bigger distance error, than if the target was centred in its field of view). This hypothesis is confirmed in Fig. 1, that shows the distance measurement error depending on the measurement angle. The scattered points correspond to all measurements for all robots for the first 8 experiments.[1] As expected the results show that the distribution of the distance measurement error is correlated with the measurement angle, with smaller distance errors occurring for measurements near the centre axis of the robot, and bigger distance errors occurring at the edges of the robot's field of view, resembling a parabolic curve.

For this reason a method is proposed, which takes care to change the distance measurement noise estimate depending on the measurement angle. First

[1] The 9-th experiment is excluded, as it has different environment conditions.

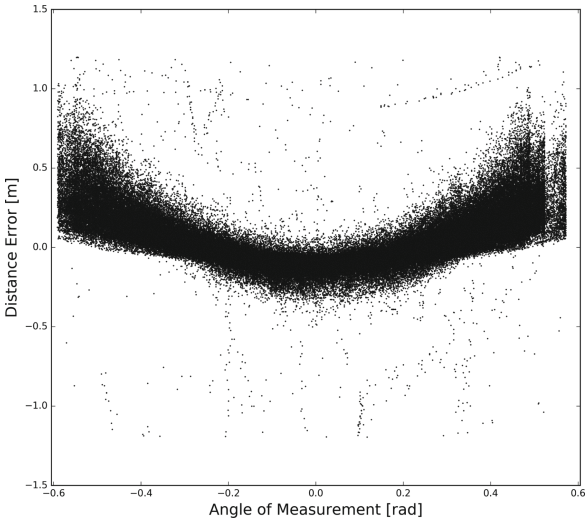

Fig. 1. Distance error versus the measurement angle. Every robot roughly has a field of view spanning in the range of −0.6 to 0.6 radians. For the purposes of this plot one percent of extreme values were removed.

the measurement data is segmented into 150 equal width bins, based on the measurement angle, then for each bin the average and variation of the errors is calculated. To further smooth the data a second degree polynomial line[2] is fitted over these values, and then finally these smoothed values are used for the estimation. The obtained results are shown in Fig. 2. As a result, for each measurement that belongs to a particular bin the EKF can use separate values. The variation per each bin is used as the covariance noise estimate in Eq. (9). Furthermore, the Kalman filter expects the noise to have a mean of 0, while in Fig. 1 the measurement distance error is shown to be positively biased. For this reason Eq. (5) is amended, with the addition of the bin average of the measurement distance error, which causes the measurement distances to be centred around zero. The results obtained from applying this method are shown in Sect. 5.

4.2 Estimating the Process Noise

The process noise represents the difference between the system evolution according to the model and its real counterpart. In Kalman filter theory it is quantified with the covariance matrix of the error $\mathbf{e} = \mathbf{x}_k - \hat{\mathbf{x}}_k$ between the actual state of the robot $\mathbf{x}_k$ and its version obtained by evolving the previous actual state for one step by the model $\hat{\mathbf{x}}_k = \mathbf{f}(\mathbf{x}_{k-1})$.

To estimate the process noise one can run the whole experiment and calculate the average error between the robot's estimated state (1) obtained using the

[2] We use a regression ridge model for smoothing.

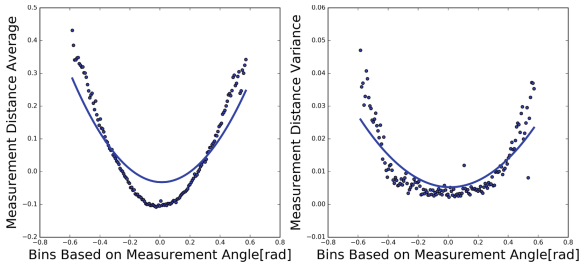

Fig. 2. This figure shows the average and variance of the measurement distance error from all the bins based on measurement angle, additionally a polynomial line of degree 2 is drawn to smooth the data.

above model, and the true groundtruth value (x, y, θ) provided by the dataset, which should give a good estimate for the actual process noise.

This can be achieved by iterating through the control data. Every control reading is applied to the groundtruth robot position at the moment[3] of the previous control. Subsequently, the difference is calculated between that state and the groundtruth robot state at the time of the new control. These differences serve as a mean to estimate the error between the system evolution derived using control readings, and the actual robot motion calculated using groundtruth data. The process noise estimate is then computed as the covariance matrix of these differences (used in Eq. (3)). Moreover, there are several scopes of data that one can use to compute the covariance. The estimate can be obtained using differences from data readings of a single robot or more broadly data readings from the whole experiment or even differences coming from the entire dataset (this is further discussed in Sect. 5).

5 Results

The dataset contains many robots that are purported to move randomly during their experiment. However after some analysis one can find that some robots got 'stuck' and stopped moving for a period of time.

There are several robots with similar movement in the dataset. For these robots the state estimate error remains constant for a long period, which does not produce realistic results when evaluating error statistics.

In order to gain meaningful results, we consider only the robots that kept moving randomly for the whole duration of their experiment. In addition the 9-th experiment that contained obstacles in the environment is discarded from the analysis, as it had different environmental conditions from the other 8 experiments.

[3] Linear interpolation on the groundtruth data is used, so there are estimates of the robot state at any moment.

The analysis of this paper is focused on a single robot trying to localize itself inside its environment, using measurements coming only from landmarks. A general algorithm is developed, which allows experimentation with different robots from the dataset. We then study several scenarios:

- For the process noise estimate (p.n.) one can use different scopes to estimate the noise:
  - using data from each robot run, to estimate the process noise in its run
  - using data averaged over the whole experiment, i.e. all 5 robots that operated concurrently in the environment
  - using data averaged over the whole dataset, i.e. all 8 experiments

  The variance of error of the needed scope of data is used in Eq. (3).
- The measurement noise estimate (m.n.) can also be calculated using different scopes for estimation. The variance of the needed scope of data is used in Eq. (9). Otherwise, the algorithm can also use the equal width bin method as explained in Subsect. 4.1.
- In this dataset robots perceive their environment by periodically taking pictures and then processing them to obtain relative range and bearing to recognized targets (each object in the environment has a bar-code that uniquely identifies it [12]). This means that at some distinct time a single robot potentially has measurements to several landmarks. For the case where a robot has concurrent landmarks measurements, the algorithm can choose to include all of them, or just use a single landmark measurement, in Eq. (5).

For each of these scenarios the algorithm provides an error calculated from the average difference between the estimated robot's state and the actual groundtruth robot state. Since the groundtruth and control data from the dataset are not synchronous, the state estimations occur at different moments than the groundtruth data. To obtain a valid error estimate, the algorithm uses linear interpolation to compute groundtruth data for the moments when the estimations are calculated. We then focus on the results coming from the whole dataset and results when including only the top 5 robots of the dataset (the robots which are best localized by the algorithm). For each error estimate the algorithm calculates the absolute average error, and the standard deviation of the error. The results are summarized in Tables 1 and 2.

The tables demonstrate a fairly big difference between the top 5 robots and the rest. Because of this a further direction of research might be into visualizing the robot motion and determining reasons why these robots are localized better.

Concerning the measurement noise, the equal width bin method performs good on the dataset, mainly because it takes into account both the changing variance based on the measurement angle, and the unsymmetrical measurement distance error. The method is worse when using smaller scopes of data for estimation. However it is unrealistic that one can obtain specific estimates when operating in a real environment. Moreover, the method actually performs best when focusing on the top robots of the dataset (Table 2). Further analysis could

Table 1. Error statistics (absolute average and standard deviation) for different parameters, described at the beginning of this section. This data comes from the **first 8 experiments** in the dataset.

Different scenarios	Avg.; sd. of position er.[m]	Avg.; sd. of angle er.[rad]
p.n. from whole dataset	0.1506; 0.3798	0.1177; 0.2599
p.n. from one experiment	0.1513; 0.3805	0.1179; 0.2602
p.n. from single robot	0.1512; 0.3799	0.1180; 0.2603
m.n. with equal width bins	0.1586; 0.4384	0.1455; 0.3471
m.n. from single robot	0.1506; 0.3798	0.1177; 0.2599
m.n. from one experiment	0.1521; 0.3752	0.1180; 0.2570
m.n. from whole dataset	0.1652; 0.3971	0.1416; 0.3246
Multiple landmarks	0.1506; 0.3798	0.1177; 0.2599
Single landmark	0.1598; 0.3947	0.1225; 0.2696

Table 2. Error statistics (absolute average and standard deviation) for different parameters, described at the beginning of this section. This data comes from the **5 most precisely localized robots** in the dataset.

Different scenarios	Avg.; sd. of position er.[m]	Avg.; sd. of angle er.[rad]
p.n. from whole dataset	0.0471; 0.0632	0.0540; 0.0833
p.n. from one experiment	0.0484; 0.0646	0.0561; 0.0855
p.n. from single robot	0.0490; 0.0658	0.0572; 0.0866
m.n. with equal width bins	0.0471; 0.0632	0.0540; 0.0833
m.n. from single robot	0.0558; 0.0752	0.0417; 0.0752
m.n. from one experiment	0.0607; 0.0801	0.0442; 0.0767
m.n. from whole dataset	0.0706; 0.0881	0.0603; 0.0876
Multiple landmarks	0.0471; 0.0632	0.0540; 0.0833
Single landmark	0.0477; 0.0635	0.0560; 0.0846

be directed into finding methods that use different segmentation techniques and better smooth the data in the different segments.

For the landmark option, as expected, the algorithm gets better results when using multiple landmarks. This is especially true when focusing on the whole dataset, however, for the top 5 robots this option does not make a big change in the error. More investigation is needed into the choice of landmark measurements used, perhaps only including the closest and most centred landmarks will give better results.

6 Conclusions and Future Work

This paper presents a study on localization of robots based on real data. As it can be expected with such data there are certain problems pertaining to synchronizing the input data and uncertain robot's movements. However the results demonstrate several findings.

The error is very much dependent on the quality of the robot's motion through the environment with the best 5 localizations of robots achieving around 3 times better results, as compared to all the other robots in the dataset (Tables 1 and 2). When the robots view multiple targets and keep perceiving landmarks for a longer time they perform better. To achieve even better results, aspects such as the unsymmetrical measurement distance and the changing measurement variance need to be included in the computation.

This paper provides a solid foundation for further analysis in cooperative multi-robot localization, which can be performed using the same dataset as it also contains robot-to-robot measurements. Cooperative multi-robot approaches have been described in [13,14] using distributed EKF. In such a multi-robot scenario robot-to-robot and robot-to-landmark measurements need to be combined, which have different characteristics as the former accumulates error on its multi-hop path, while the latter is prone only to single hop measurement noise. Therefore, the localization could be performed better using a modified version of the EKF that allows weights to be given to the different types of measurements.

References

1. Leonard, J.J., Durrant-Whyte, H.F.: Mobile robot localization by tracking geometric beacons. IEEE Trans. Robot. Autom. **7**(3), 376–382 (1991)
2. Thrun, S., Fox, D., Burgard, W., Dellaert, F.: Robust Monte Carlo localization for mobile robots. Artif. Intell. **128**(1–2), 99–141 (2001)
3. Niculescu, D.: Positioning in ad hoc sensor networks. IEEE Netw. **18**(4), 24–29 (2004)
4. Mao, G., Fidan, B., Anderson, B.D.O.: Wireless sensor network localization techniques. Comput. Netw. **51**(10), 2529–2553 (2007)
5. Li, H., Nashashibi, F.: Cooperative multi-vehicle localization using split covariance intersection filter. IEEE Intell. Transp. Syst. Mag. **5**(2), 33–44 (2013)
6. Juang, P., Oki, H., Wang, Y., Martonosi, M., Peh, L.S., Rubenstein, D.: Energy-efficient computing for wildlife tracking: design tradeoffs and early experiences with Zebranet. ACM Sigplan Not. **37**(10), 96–107 (2002)
7. Smith, G.L., Schmidt, S.F., McGee, L.A.: Application of statistical filter theory to the optimal estimation of position and velocity on board a circumlunar vehicle. National Aeronautics and Space Administration (1962)
8. Welch, G., Bishop, G.: An introduction to the Kalman filter. University of North Carolina, Department of Computer Science (2006)
9. Kalman, R.: A new approach to linear filtering and prediction problems. J. Fluids Eng. **82**(1), 35–45 (1960)
10. Fox, D., Hightower, J., Liao, L., Schulz, D., Borriello, G.: Bayesian filtering for location estimation. IEEE Pervasive Comput. **3**, 24–33 (2003)

11. Leung, K.Y.K.: Cooperative localization and mapping in sparsely-communicating robot networks. Ph.D. thesis, University of Toronto (2012)
12. Leung, K.Y., Halpern, Y., Barfoot, T.D., Liu, H.H.: The UTIAS multi-robot cooperative localization and mapping dataset. Int. J. Robot. Res. **30**(8), 969–974 (2011)
13. Roumeliotis, S.I., Bekey, G.A.: Distributed multirobot localization. IEEE Trans. Robot. Autom. **18**(5), 781–795 (2002)
14. Madhavan, R., Fregene, K., Parker, L.E.: Distributed cooperative outdoor multirobot localization and mapping. Auton. Robots **17**(1), 23–39 (2004)

Evaluation of Automatically Generated Conceptual Database Model Based on Business Process Model: Controlled Experiment

Danijela Banjac(✉), Drazen Brdjanin, Goran Banjac, and Slavko Maric

Faculty of Electrical Engineering, University of Banja Luka, Patre 5,
78000 Banja Luka, Bosnia and Herzegovina
{danijela.banjac,bdrazen,goran.banjac,ms}@etfbl.net

Abstract. This paper presents the results of the controlled experiment that we have conducted in order to evaluate an approach to automated design of the initial conceptual database model based on the collaborative business process model. The source business process model is represented by BPMN, while the target conceptual model is represented by UML class diagram. The results of the experiment imply that the approach enables generation of the target conceptual model with a high percentage of completeness (>85%) and precision (>85%), which confirms the results of the initial case-study based evaluation.

Keywords: BPMN · Collaborative business process model · Conceptual database model · Evaluation · Experiment · Model-driven · UML

1 Introduction

Data modeling is a very important part of information system design. Data models are used to define and analyze data representing the essence of any information system. The process of data modeling involves professional data modelers, as well as business experts, and it is not straightforward, meaning it often requires many iterations before designing the final model. Therefore, automatic generation of data models is of great interest and it has been the subject of research for many years. Although the idea of model-driven design of data models is more than 25 years old, the survey [1] shows that only a small number of papers present the implemented automatic model-driven generator of the data model and the corresponding evaluation results.

In this paper, we present the results of the controlled experiment that we have conducted in order to evaluate an approach to automated synthesis of the conceptual database model (CDM) based on the collaborative business process model (BPM). The source BPM is represented by BPMN [2], while the target CDM is represented by UML [3] class diagram. The initial case-study based evaluation of the proposed approach [4] implies that the approach and implemented generator enable generation of the target model with very high precision. In order to evaluate the approach more extensively, we have conducted four experiments with undergraduate students at the University of Banja Luka (UoBL).

G. Stojanov and A. Kulakov (eds.), *ICT Innovations 2016*,
Advances in Intelligent Systems and Computing 665,
https://doi.org/10.1007/978-3-319-68855-8_13

The paper is structured as follows. After the introduction, the second section presents the related work. The third section presents a short overview of the evaluated approach to automatic synthesis of the initial CDM based on the collaborative BPM. The fourth section describes the experiments. The results are analyzed in the fifth section. The final section concludes the paper.

2 Related Work

The survey [1] shows that the current approaches to model-driven synthesis of data models (MDSDM) can be classified as: *function-oriented*, *process-oriented*, *communication-oriented*, and *goal-oriented*. In most papers, a process-oriented model (POM) is used as the source model. The survey [1] shows that the semantic capacity of POMs has still not been sufficiently identified to enable automatic synthesis of the complete target data model.

The BPMN is used in [4–18] as the starting point for MDSDM. There are two QVT [19]-based proposals [8,11], but with modest achievements in the automated generation of analysis level class diagrams, and there are also several proposals [6,7,10,14,16] for semi-automated generation. A MDSDM based on BPMN is also considered in [12,13,16], but without implementation. The large majority of all proposals are based on an incomplete source model i.e. single diagram (a real model contains a finite set of diagrams). Only [18] considers a set of interrelated BPMs, but with no explicit rules and implementation. This overview does not contain approaches based on other POMs, although there is a paper [20] considering a finite set of interrelated BPMs. An overview of BPMN-based MDSDM approaches is given in Fig. 1.

The formal rules for automated CDM synthesis based on BPMN are presented in [4], and partially in [15,18]. Other papers consider only guidelines that do not enable automated CDM synthesis. In this paper, we evaluate an approach [4] that enables automated CDM synthesis.

There are no papers presenting experiments for evaluation of automatically generated CDMs based on POMs. There are two papers [4,20] presenting case-study based evaluation of POM-based approaches. There is also a paper [21] presenting a controlled experiment which compares two techniques for deriving conceptual models from requirements models, but none of them is a POM.

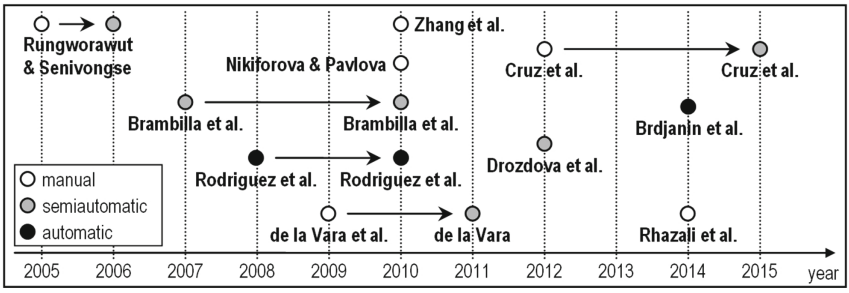

Fig. 1. Overview of BPMN-based MDSDM approaches

3 Overview of Evaluated Approach for Automatic CDM Synthesis Based on Collaborative BPM

The semantic capacity of the collaborative BPM represented by BPMN, and the corresponding rules for automatic CDM synthesis are presented in [2]. Due to the paper length limitation, in this section we give only a short illustration of these rules in Fig. 2.

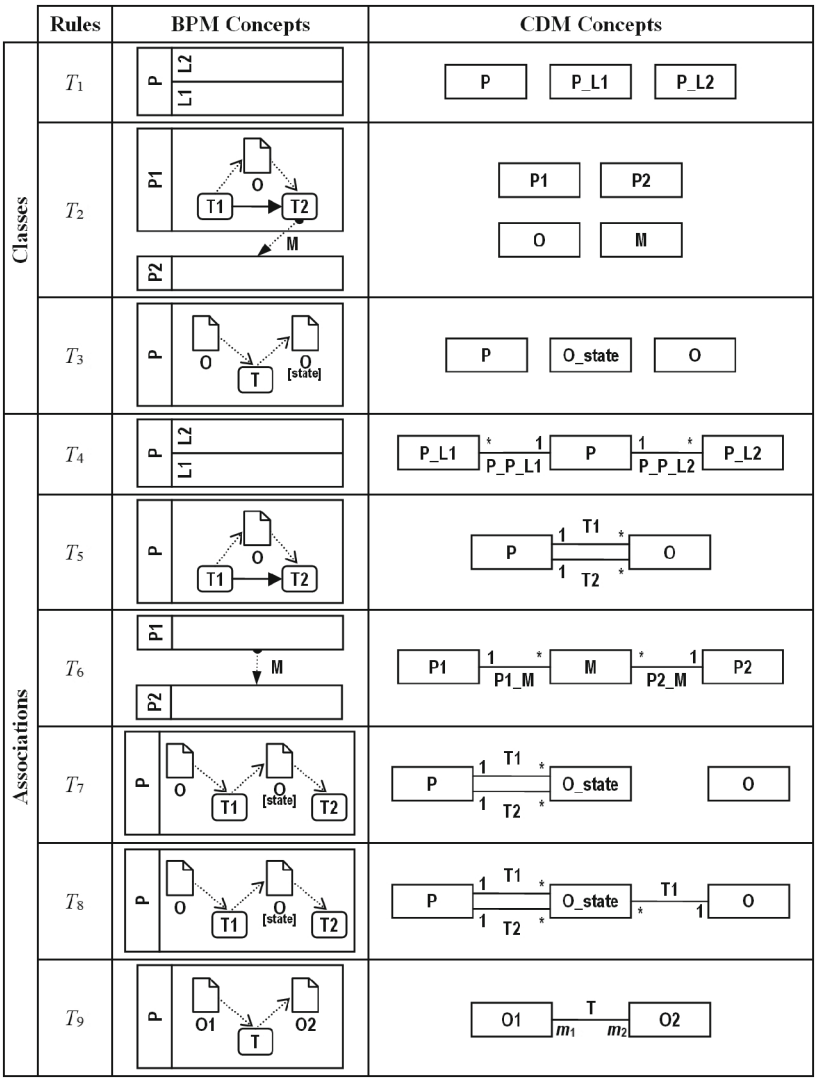

Fig. 2. Mapping of BPM concepts into CDM concepts

4 Experiment Design

This section describes the design of the experiments, including the experimental context, variables, as well as the subjects, settings and assignments for each experiment.

4.1 Experimental Context

The fourth-year (240 ECTS[1]) undergraduate study program *Computing and Informatics* at the UoBL Faculty of Electrical Engineering (FEE) offers a course entitled *Object-Oriented Design and Programming* (OODP) in the 8^{th} semester. Through this course, students acquire the necessary knowledge and practical skills in object-oriented analysis and design of software systems. The course is elective and 24 students (3^{rd} and 4^{th}-year students) took it in 2014/15 academic year. Prior to taking this course, the students took several courses on programming and database modeling, in which they studied data structures and algorithms, object-oriented programming, database design, software engineering, information systems, UML, etc.

Before taking these experiments, we had to train students in order to achieve approximately the same level of knowledge. The introductory lessons included a short reminder of database modeling by using UML class diagrams. Since the students had little prior knowledge of BPMN, they had to learn BPMN concepts and notation before the experimental tasks. They were also trained to use the Topcased platform for modeling. The training lasted four weeks and it included both theoretical and practical classes.

Given their prior knowledge about database modeling and object-oriented design and knowledge gained in the OODP course, the students were appropriate participants in the experiments. The students had four assignments during the semester and every assignment was done individually.

4.2 Variables

We identified the following types of variables, according to [22].

Response Variables. The quantitative outcome of an experiment is referred to as a response variable. The response variable of an experiment must reflect the data that is collected from experiments so it can be used in the analysis. Appropriate measures and metrics need to be used in order to acquire the values of the response variables. There are no metrics and measures for the quantitative evaluation of automatically generated CDMs based on POMs, but there are some metrics and measures for the evaluation of automatic CDM generators based on natural language processing (NLP). Some of NLP metrics and measures can be used to perform the quantitative evaluation of the implemented generator. We

[1] European Credit Transfer and Accumulation System.

have adopted some of them that were introduced in [23,24] and later adjusted in [25].

The most commonly used metrics for quantitative evaluation of automatically generated CDMs are: $N_{generated}$ (the total number of automatically generated concepts), $N_{correct}$ (the number of correctly generated concepts that can be kept in the target model), $N_{incorrect}$ (the number of incorrectly generated concepts that cannot be kept in the target model), $N_{excessive}$ (the number of excessively generated concepts that should not be kept in the target model), and $N_{missing}$ (the number of missing concepts that should be in the target model, but are not generated). In this experiment we use *recall* and *precision* as response variables used for evaluation of automatically generated CDMs.

Recall represents the percentage of the target CDM that is automatically generated (the estimated percentage of automatically generated concepts in the total number of concepts in the target model). It may be defined as

$$Recall = \frac{N_{correct}}{N_{correct} + N_{missing}} \cdot 100\%. \tag{1}$$

Precision represents the percentage of correctly generated concepts in an automatically generated model (the percentage of correctly generated classes and the percentage of correctly generated associations). It may be defined as

$$Precision = \frac{N_{correct}}{N_{correct} + N_{incorrect}} \cdot 100\%. \tag{2}$$

Parameters. Qualitative or quantitative characteristics that are invariable in the experimentation process are called parameters. Such characteristics are to be fixed so they do not influence the results of the experiment. We established the following:

- *Modeling language* used for modeling BPMs was BPMN.
- *Modeling language* used for modeling CDMs was UML class diagram.
- *Modeling tool. Topcased* with *BPMN Modeler* plugin is used as a tool for modeling BPMs (BPMN) and CDMs (UML class diagram).
- *Business processes modeling training.* All students participated in the same BPMN training, because they had very little prior knowledge of BPMN.
- *Conceptual database modeling training.* Although the students had experience in database modeling using Information Engineering (IE) notation and tools, all students participated in the same UML database modeling training.

4.3 Subjects, Settings and Assignments

Experiment #1. The goal of Experiment #1 was to compare an automatically generated CDM with a manually designed CDM for the same business system. In this experiment, students had to create manually a DM based on a given collaborative BPM. The source model used in this experiment was a BPM

representing *Order processing*. Due to the space limitations, we are not able to provide figures representing source models nor automatically generated CDMs (models can be obtained from the authors).

Eight students participated in this experiment, but only six models were considered for evaluation because two models were incomplete. The time for modeling was limited to 90 min. The students were in the same laboratory during the experiment and there was also a teacher present in order to preserve the validity of the experiment and, if necessary, to help the students to understand the source model.

The students' individual work resulted in different CDMs for the same BPM, making the comparison of automatically generated and manually designed CDMs very challenging. We tried to find an equal or equivalent concept in manually designed CDMs for each concept in the automatically generated model. If an equal or equivalent concept was found in a manually designed CDM, it was considered as suitable and it was retained in the target CDM without any change. If an equal or equivalent concept was not found in a manually designed CDM, it was necessary to decide whether the given concept is excessive or it could be retained in the target CDM. Although some concepts may be considered as redundant, designers sometimes introduce redundant associations to achieve better performance in data retrieval. It is easier for the designer to remove some excessive concept from an automatically generated CDM that is correctly generated, than to add some new concept. Missing concepts are the relevant concepts that were introduced in the manually designed CDMs but are missing from the automatically generated CDM.

Experiment #2. Setup of Experiment #2 was similar to Experiment #1. The purpose of Experiment #2 was also to compare an automatically generated CDM and manually created CDMs. In the experiment, the students had to create CDMs based on the given collaborative BPM representing *E-mail voting*. The source model is taken from the BPMN specification [26] and it illustrates resolving issues through e-mail votes. The source model is very complex and it provides examples for many of BPMN features. Like in Experiment #1, all students had the same source model.

Fourteen students participated and six manually created CDMs were considered for evaluation. Other models were evaluated as incorrect. The main difference between Experiments #1 and #2, in addition to the source model complexity, is that Experiment #2 was done as homework (students had more time to do it). The automatically generated and manually designed models were compared in the same way as in Experiment #1.

Experiment #3. Experiment #3 was different compared to the first two. In this experiment, the students analyzed the CDM which was automatically generated based on the *E-mail voting* BPM. The goal of the experiment was to compare the results of the initial evaluation [4,27] and the results of the students' evaluation. The students evaluated the CDM from the database designer's point

of view. For each concept (class or association) in the generated CDM, they had to determine whether the concept should be retained unchanged, or it should be retained with corrections (if it was generated incorrectly) or it should not be contained in the model (if it is redundant).

The students evaluated the same generated model within a 60-min time frame. They were in the same laboratory during the experiment and the teachers were also present in order to preserve the validity of the experiment and to help the students to understand the model. During the experiment, the students also had the source BPM (*E-mail voting*) at their disposal. We did not accept all evaluations, because some of them were incorrect. Thirteen students participated in the experiment, but only six models were considered for evaluation, since the source BPM was too complicated for some students.

Experiment #4. Experiment #4 was completely different from previously described experiments. The goal of this experiment was to test the generator [4,27] on a set of different real BPMs. Each student had to create his/her own collaborative BPM representing a real business process and use that model as the source model to create manually a target CDM. The students had to choose and model different processes. Fifteen students participated in the experiment and seven models were considered for evaluation. The experiment was also done as homework. We used the generator to create target CDMs based on the students' collaborative BPMs, which we compared with the manually designed CDMs in the same way as in Experiments #1 and #2.

5 Results Analysis and Discussion

Table 1 shows the results of the initial quantitative analysis of the automatically generated CDM [4,27], as well as the results of comparing the automatically generated and manually designed CDMs obtained in Experiment #1. The initial case-study based results show that the generated CDM has very high recall and precision (both over 90%). All generated classes could be retained in the target CDM. There are only several generated associations that could not be retained in the target CDM because of partially incorrect cardinalities. The main reason for this are some control patterns that are presently not covered by the rules. The results of comparing the automatically generated and manually designed CDMs show that the objectified evaluation does not significantly differ from the initial evaluation, i.e. the initial results were confirmed in Experiment #1.

Table 2 shows the results of the initial quantitative analysis of the automatically generated CDM [4,27], as well as the result of comparing the automatically generated and manually designed CDMs obtained in Experiment #2. The obtained values in Experiment #2 are lower than in Experiment #1 – especially precision for associations, but it is still very high (>75%). The main reason for lower precision in Experiment #2 is the source model complexity. Taking into account the high complexity of the source model (four complex loops, two sub-processes, etc.), recall and precision are still very high.

The results of the students' analysis of the automatically generated model in Experiment #3 are shown in Table 3 (left part). The students' results confirmed the initial case-study based results shown in Table 2. Precision is almost the same as the initial precision, but recall is slightly lower. Recall is lower because the students evaluated that there were some classes and associations missing from the generated CDM. There are some classes (and corresponding associations) that could not be generated based on just one collaborative BPM, because the corresponding objects do not exist in the source model, but we presume that some of the missing classes could be generated based on a set of source BPMs.

Table 1. Results obtained in Experiment #1

Concepts	Case-study based [4,27]		Experiment #1	
	Recall [%]	Precision [%]	Recall [%]	Precision [%]
Classes	100	100	96.43	100.00
Associations	97	97	88.35	92.78

Table 2. Results obtained in Experiment #2

Concepts	Case-study based [4,27]		Experiment #2	
	Recall [%]	Precision [%]	Recall [%]	Precision [%]
Classes	100	100	95.56	100.00
Associations	97	86	83.54	77.76

Table 3. Results obtained in Experiments #3 and #4

Concepts	Experiment #3		Experiment #4	
	Recall [%]	Precision [%]	Recall [%]	Precision [%]
Classes	94.45	100.00	98.09	100.00
Associations	87.47	89.98	91.86	85.79

The results obtained in Experiment #4 are shown in Table 3 (right part). Recall and precision for classes are almost 100%. There are a few classes missing, as previously explained. The analysis of models shows that there are more classes manually designed than those automatically generated, mostly because the students used generalizations/specializations.

Table 3 also shows the results of Experiment #4 for associations. We observed that there were more automatically generated associations than those manually designed. Some of these associations are excessive, but it is easier for designers to remove excessive associations than to add new associations. In particular, we especially analyzed the source models with lower results for automatically generated CDMs. We concluded that lower results were obtained when the source

collaborative BPMs had many decisions/merges, because those control patterns are presently not covered by the transformation rules. We also found out more about the process flow influence on the end multiplicities of the generated associations. These findings will also be used in the future to improve the rules and generator.

Table 4 presents the summary results for all experiments. The results imply that: (i) generated classes are completely suitable and they could be retained in the target CDM without any change, (ii) there are some associations that could not be retained in the target CDM (because of partially incorrect cardinality), and (iii) there are some classes and associations missing in the generated CDM.

Table 4. Summary results for experiments

Experiments	Classes		Associations	
	Recall [%]	Precision [%]	Recall [%]	Precision [%]
#1	96.43	100.00	88.35	92.78
#2	95.56	100.00	83.54	77.76
#3	94.45	100.00	87.47	89.98
#4	98.09	100.00	91.86	85.79
Mean:	96.13	100.00	87.81	86.58

5.1 Threats to Validity

This section describes potential threats to the validity of the experiments.

Measuring Quality. According to Conway's Law [28], independent work of several database designers will result in the creation of several different CDMs for the same system. According to Date [29], the problem of finding the logical design that is incontestably the right one is still a rather intractable problem. Therefore, the objectivity of comparing an automatically generated CDM with some manually designed CDM for the same system is questionable since the degree of compliance will differ from one case to another. With respect to that, and in order to obtain some reliable evaluation of automatically generated CDMs, qualitative evaluation was carried out from the database designer's point of view. Each generated concept was analyzed and it was determined whether it was suitable and correctly generated to be retained in the design of the target CDM. All models were reviewed by (at least) three teachers from FEE.

Conclusion Validity. Although all students started the training with the same level of competence in BPM design, it turned out that they acquired different levels of modeling competence during the training. Thus, we considered only those models that were evaluated as valid and complete.

We also held a training for database modeling using UML class diagrams, since the students had different levels of knowledge and skills in modeling using IE. Therefore, only valid and complete models were used in the experiments.

Since the two experiments were designed as homework, the students had to present their homework in front of the class. It turned out that some of them were copying assignments from each other, so their models were excluded.

We started the experiment assuming that students were not familiar with the transformation rules. It turned out that two students had come across some papers describing the transformation rules, and consequently their models were not considered.

6 Conclusions and Future Work

Previously we analyzed the semantic potential of the collaborative BPMN for automated CDM generation, and, based on that analysis, we defined the formal rules for automated CDM design [4]. An ATL [30]-based generator [4,27] was implemented based on these formal rules. The initial case-study based evaluation of the automatically generated CDMs implied that the generator is able to generate very high percentage of the target CDM with very high precision.

Controlled experiments within FEE were conducted in order to evaluate the approach more extensively. The results of the experiments were analyzed and used for evaluation of the automatically generated CDMs. This paper has presented the experiments conducted, as well as the results of the evaluation of the approach.

These experiments with students confirmed the results of the initial case-study based evaluation. The results of the experiments imply that the specified transformation rules cover the automated generation of the majority of concepts of the target CDM. Recall and precision for classes are very high (>95%) and they are slightly lower for associations (>85%). Therefore, considering the initial results [4] and the results of the experiments presented in this paper, we conclude that the proposed approach can be used in practice.

Based on these experiments, we have further identified how the process flow affects the association end multiplicities, and that knowledge will be used to further improve the generator. Of course, further identification of the semantic capacity of BPMs for automated CDM design will be part of the future work, as well as the evaluation of automatically generated CDMs based on more source models and with participants more experienced in database design.

References

1. Brdjanin, D., Maric, S.: Model-driven techniques for data model synthesis. Electronics **17**(2), 130–136 (2013)
2. OMG: Business Process Model and Notation (BPMN), v2.0. OMG (2011)
3. OMG: Unified Modeling Language (OMG UML), v2.5. OMG (2015)

4. Brdjanin, D., Banjac, G., Maric, S.: Automated synthesis of initial conceptual database model based on collaborative business process model. In: Bogdanova, M.A., Gjorgjevikj, D. (eds.) ICT Innovations 2014: World of Data. AISC, vol. 311, pp. 145–156. Springer International Publishing, Cham (2015)
5. Rungworawut, W., Senivongse, T.: From business world to software world: deriving class diagrams from business process models. In: Proceedings of the 5th WSEAS International Conference on Aplied Informatics and Communications, WSEAS, pp. 233–238 (2005)
6. Rungworawut, W., Senivongse, T.: Using ontology search in the design of class diagram from business process model. PWASET **12**, 165–170 (2006)
7. Brambilla, M., Cabot, J., Comai, S.: Automatic generation of workflow-extended domain models. In: Engels, G., et al. (eds.) MoDELS 2007. LNCS, vol. 4735, pp. 375–389. Springer, Heidelberg (2007)
8. Rodriguez, A., Fernandez-Medina, E., Piattini, M.: Towards obtaining analysis-level class and use case diagrams from business process models. In: Song, I.Y., et al. (eds.) ER Workshops 2008. LNCS, vol. 5232, pp. 103–112. Springer, Heidelberg (2008)
9. de la Vara, J.L., Fortuna, M.H., Sanchez, J., Werner, C.M.L., Borges, M.R.S.: A requirements enegineering approach for data modelling of process-aware information systems. In: Abramowicz, W. (ed.) BIS 2009. LNBIP, vol. 21, pp. 133–144. Springer, Heidelberg (2009)
10. Brambilla, M., Cabot, J., Comai, S.: Extending conceptual schemas with business process information. Adv. Softw. Eng. **2010** (2010). Article ID 525121
11. Rodriguez, A., Garcia-Rodriguez de Guzman, I., Fernandez-Medina, E., Piattini, M.: Semi-formal transformation of secure business processes into analysis class and use case models: an MDA approach. Inf. Softw. Technol. **52**(9), 945–971 (2010)
12. Zhang, J., Feng, P., Wu, Z., Yu, D., Chen, K.: Activity based CIM modeling and transformation for business process systems. Int. J. Softw. Eng. Knowl. Eng. **20**(3), 289–309 (2010)
13. Nikiforova, O., Pavlova, N.: Application of BPMN instead of GRAPES for two-hemisphere model driven approach. In: Grundspenkis, J., et al. (eds.) ADBIS 2009 Workshops. LNCS, vol. 5968, pp. 185–192. Springer, Heidelberg (2010)
14. de la Vara, J.L.: Business process-based requirements specification and object-oriented conceptual modelling of information systems. Ph.D. thesis, Valencia Polytechnic University (2011)
15. Cruz, E.F., Machado, R.J., Santos, M.Y.: From business process modeling to data model: a systematic approach. In: Proceedings of QUATIC 2012, pp. 205–210. IEEE (2012)
16. Drozdová, M., Mokryš, M., Kardoš, M., Kurillová, Z., Papán, J.: Change of paradigm for development of software support for elearning. In: Proceedings of ICETA 2012, pp. 81–84. IEEE (2012)
17. Rhazali, Y., Hadi, Y., Mouloudi, A.: Transformation method CIM to PIM: from business processes models defined in BPMN to use case and class models defined in UML. Int. J. Comput. Inf. Syst. Control Eng. **8**(8), 1334–1338 (2014)
18. Cruz, E.F., Machado, R.J., Santos, M.Y.: Deriving a data model from a set of interrelated business process models. In: Proceedings of ICEIS 2015, pp. 49–59 (2015)
19. OMG: MOF 2.0 Query/View/Transformation Specification, v1.0. OMG (2008)
20. Brdjanin, D., Maric, S.: Towards the automated business model-driven conceptual database design. In: Morzy, T., Harder, T., Wrembel, R. (eds.) Advances in Data-

bases and Information Systems. AISC, vol. 186, pp. 31–43. Springer, Heidelberg (2012)
21. Espana, S., Ruiz, M., Gonzalez, A.: Systematic derivation of conceptual models from requirements models: a controlled experiment. In: Proceedings of RCIS 2012, pp. 1–12. IEEE (2012)
22. Juristo, N., Moreno, A.: Basics of Software Engineering Experimentation. Springer, Heidelberg (2001)
23. Harmain, H., Gaizauskas, R.: CM-Builder: a natural language-based CASE tool for object-oriented analysis. Autom. Softw. Eng. **10**(2), 157–181 (2003)
24. Omar, N., Hanna, P., McKevitt, P.: Heuristics-based entity-relationship modelling through natural language processing. In: Proceedings of AICS 2004, pp. 302–313 (2004)
25. Brdjanin, D., Maric, S.: An approach to automated conceptual database design based on the UML activity diagram. Comput. Sci. Inf. Syst. **9**(1), 249–283 (2012)
26. OMG: BPMN 2.0 by Example, v.1.0. OMG (2010)
27. Banjac, G.: Automated synthesis of conceptual database model based on collaborative business process model. Master thesis, University of Banja Luka (2014)
28. Conway, M.: How do committees invent? Datamation **14**(4), 28–31 (1968)
29. Date, C.: An Introduction to Database Systems, 8th edn. Addison-Wesley, Boston (2003)
30. Jouault, F., Allilaire, F., Bezivin, J., Kurtev, I.: ATL: a model transformation tool. Sci. Comput. Program. **72**(1–2), 31–39 (2008)

Analysis of Protein Interaction Network for Colorectal Cancer

Zlate Ristovski(✉), Kire Trivodaliev, and Slobodan Kalajdziski

Faculty of Computer Science and Engineering,
Ss. Cyril and Methodius University, Skopje, Macedonia
ristovskizlate@gmail.com,
{kire.trivodaliev,slobodan.kalajdziski}@finki.ukim.mk
http://www.finki.ukim.mk

Abstract. In this paper we create and analyze a protein-protein interaction network (PPIN) of colorectal cancer (CRC). First we identify proteins that are related to the CRC (set of seed proteins). Using this set we generate the CRC PPIN with the help of Cytoscape. We analyze this PPIN in a twofold manner. We first extract important topological features for proteins in the network which we use to determine CRC essential proteins. Next we perform a modular analysis by discovering CRC significant functional terms through the process of GO enrichment within densely connected subgroups (clusters) of the PPIN. The modular analysis results in a mapping from the CRC significant terms to CRC significant proteins. Finally, we combine the topological and modular evidence for the proteins in the CRC PPIN, exclude the initial seed proteins and obtain a list of proteins that could be taken as possible bio-markers for CRC.

Keywords: Colorectal cancer · Protein-protein interaction network · Network analysis · Gene Ontology · Clustering · Cytoscape

1 Introduction

Colorectal cancer is a very complex disease where many proteins, genes and molecular functions are involved. Usually proteins are performing common biological functions, but when some of the proteins change their biological function then a disease, such as cancer, will evolve in the organism [1].

In the past few decades, the research in the field of system and molecular biology induced a good knowledge about functions and molecular characteristics of the proteins. This knowledge is stored in, and later used from protein sequence databases, the most prominent one being UniProt [2]. Proteins hardly ever act in isolation from other proteins, i.e. proteins interact, forming protein complexes. Protein-protein interactions are commonly represented in the form of a network, where individual proteins and their interactions correspond to nodes and edges, accordingly [3]. The advent of high-throughput technologies

G. Stojanov and A. Kulakov (eds.), *ICT Innovations 2016*,
Advances in Intelligent Systems and Computing 665,
https://doi.org/10.1007/978-3-319-68855-8_14

has increased the volume of protein interaction data, thus enabling high-curated biological networks, and with the existing knowledge about networks and the tools and techniques for their analysis we are one step closer to fully understand the complex mechanisms behind protein interactions, and making valid hypothesis for biomarkers and/or pathways in cancer.

Computational approaches that use the protein-protein interaction network (PPIN) to identify important proteins involved in cancer and metastasis of cancer have been the focus of previous research. Wachi et al. have discovered high centrality in different genes of lung cancer [4]. Rhodes et al. conducted an integrated analysis of cancer by using a sequence of DNA segments using the high–throughput approach [5]. Another study has used concepts from system biology to improve the prognosis of lung cancer [6]. The authors of the later research analyze the molecular interactions that are unregulated for a given type of cancer using a large set of sequences of DNA segments. Other cancer research include topological analysis of PPINs [7], and PPIN based candidate gene prediction [8].

All these papers show the importance of computational methods for reaching conclusions and understanding cancer related PPINs. However, most of the papers have used very limited level of network analysis of the PPIN. To get a better picture of the protein interactions in colorectal cancer (CRC), a systematic and thorough analysis is needed of all the cancer network related features through the use of the available tools and algorithms for network analysis.

The aim of this paper is to create and analyze the PPIN of colorectal cancer (CRC). By applying different network analysis and GO enrichment analysis, we will identify the proteins that are "most important" for CRC. If we exclude the proteins that are proved to be CRC-related, we can define possible bio-marker CRC proteins. These proteins should be further analyzed to be confirmed as valid bio-markers. The rest of the paper is organized as follows: in the second section we provide the overview of the used methodology (generation of colorectal cancer PPIN and its network analysis); in the third section we provide the obtained results with a discussion, and finally the forth section concludes the paper.

2 Research Methods

The steps for creating and analyzing the CRC PPIN are shown on Fig. 1. As can be seen, the first step is the acquisition of the most important CRC proteins. This set of proteins is passed on the second step, where we generate the CRC PPIN. The creation of the CRC PPIN is done by merging data from different protein-protein interaction databases. The generated CRC PPIN is represented in the form of a graph, where a node correspond to a protein, while an edge depicts the corresponding interaction between the connected pair of nodes (proteins). The third step is the most important, and the most complex one. This includes the CRC PPIN analysis and the deduction of meaningful results i.e. proteins that should be used as possible bio-markers for CRC. The CRC PPIN analysis is done in a two-fold manner. First, by using *topological analysis* we extract some important features for all nodes of the graph and identify target nodes by

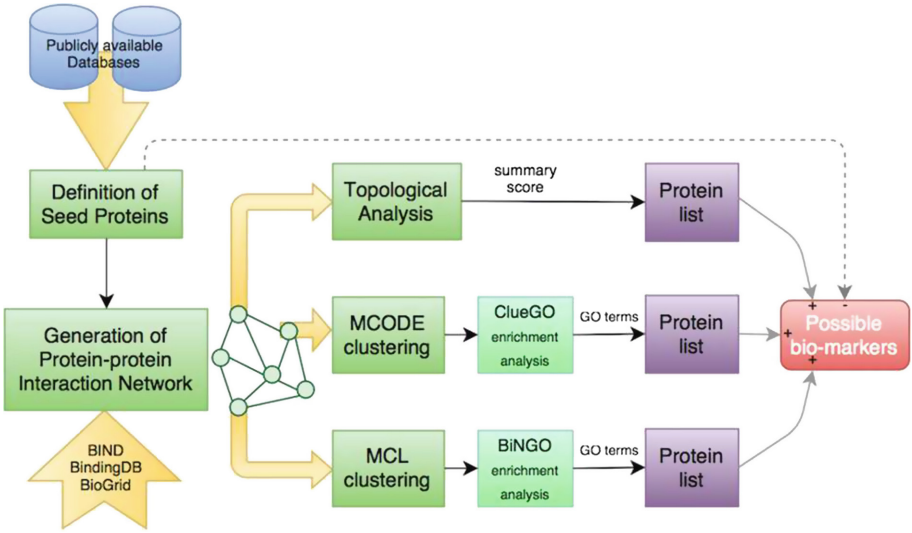

Fig. 1. Step-by-step methodology for creating and analyzing the CRC PPIN

calculating a summary score based on the topological features. Next we do a *modular analysis* that produces the graph organization (the partitioning of the CRC PPIN) in meaningful clusters. Gene Ontology (GO) enrichment is used to assign biological meaning to the clusters resulting from the modular analysis. The significant over-representation of some biological characteristics elicits the target nodes in a cluster. The list of identified target nodes (GO terms) is used to define the CRC-related proteins. By excluding the seed proteins we obtain the final result.

2.1 Identifying Seed Proteins

The seed proteins are the proteins with the highest level of interest in the PPIN. In the case of CRC, these proteins are chosen from COSMIC (Catalogue of somatic mutations in cancer), which is a database of somatically acquired mutations that are found in human cancer [9]. The data in COSMIC is curated from the scientific literature and from large-scale experiments. We have converted all protein symbols from the COSMIC database into NCBI's Entrez IDs [10], because this type of protein identification is supported by majority of tools. The obtained seed proteins for colorectal cancer (20 total) are given in Table 1.

2.2 Colorectal Cancer Protein-Protein Interaction Network

2.2.1 CRC PPIN Generation

For the CRC PPIN generation we used the PSICQUIC plugin for Cytoscape [11]. Cytoscape is a Java based visualization and analysis tool, one of the most

Table 1. CRC seed proteins (Entrez ID - Protein symbol)

7157-TP53	4089-SMAD4	8289-ARID1A	8085-KMT2D
324-APC	5290-PIK3CA	5727-PTCH1	999-CDH1
3845-KRAS	55294-FBXW7	673-BRAF	8295-TRRAP
472-ATM	4763-NF1	1387-CREBBP	58508-MLL3
5728-PTEN	5925-RB1	3875-KIT	4292-MLH1

commonly used with biological networks. The PSICQUIC plugin takes a list of seed proteins as input, and searches the available protein interaction databases for proteins that interact with the ones in the seed list. At the time we conducted the experiments, the tool was using the following interaction databases: BIND [12], BindingDB [13], and BioGrid [14].

The resulting network has a total of 1672 nodes and 6032 edges. However, in this network there are proteins from different species, which is due to the fact that the BIND database stores information about interactions, molecular complexes and pathways from different species (human, mouse, rat). Therefore, we need to filter the network nodes to exclude all non-human proteins. We used the NCBI taxonomy embedded in the Entrez IDs of the proteins to select only the human proteins (the taxonomy ID of human proteins is 9606), and we produced the final network of 1500 nodes and 5837 edges.

2.2.2 Topological Analysis

A network is said to be scale-free if the number of links originating from a given node exhibits a power law distribution, which in simple words means that several of the nodes in the network are highly connected (hubs or essential nodes) and most of the nodes are connected with one or several neighbors [15]. Scale-free networks are particularly resistant to random node removal but are extremely sensitive to the targeted removal of hubs. This information should be taken into account in the process of identifying target nodes for the CRC PPIN. There are different topological features that can encode a node's essentiality in the sense as defined here, of which we use degree, betweeness centrality and maximum neighborhood component of nodes.

We can define a PPIN graph with $G = (V, E)$, where V is the node set, and E is the undirected edges set. The degree $Deg(v)$ of the node $v \in V$ refers to the number of edges connected to the node. If we denote with $N(v)$ the set of nodes adjacent to node v i.e. its neighbors, we can define $Deg(v)$ as $Deg(v) = |N(v)|$.

The betweenness centrality $BC(v)$ is a metric which calculates average number of shortest paths that pass through the node v. It can be calculated by using the following expression:

$$BC(v) = \sum_{s \neq t \neq v \in C(v)} \frac{\sigma_{st}(v)}{\sigma_{st}} \tag{1}$$

where $s, t, v \in V$, C(v) is the connected component that contains node v, σ_{st} is the number of shortest paths from node s to node t that pass through node v, and σ_{st} is the total number of shortest paths from node s to node t.

Let $G_{NV} = (N(v), E_{NV})$ be the subgraph of G induced by the neighborhood set $N(v)$ of node v. The maximum neighborhood component score of node v, $MNC(v)$, is defined to be the size of the maximum (largest) connected component in G_{NV}. The MNC-score is computed by using the expression:

$$MNC(v) = |MC(G_{NV})||V(MC(v))| \tag{2}$$

where $MC(G_{NV})$ is the maximum connected component of G_{NV}.

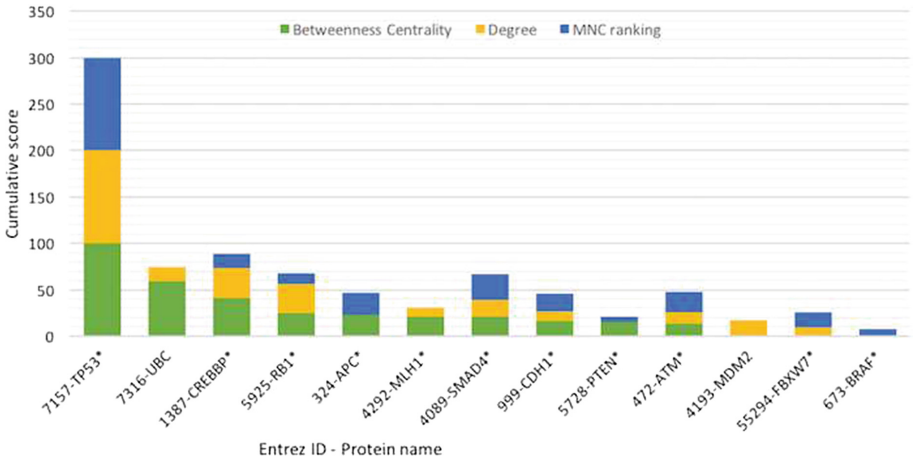

Fig. 2. Proteins with highest cumulative topological score

Figure 2 shows the proteins with the highest cumulative topological score, calculated as the sum of the normalized values of $Deg(v)$, $BC(v)$, and $MNC(v)$, for each $v \in V$. As can be seen, the topological features clearly distinguish the seed proteins (those proteins marked with the asterisk-sign), which is to be expected since the seed proteins are the ones that are known to be esential for CRC. Our focus is on the non-seed proteins in these "high scoring" nodes and these are our target proteins, i.e. the ones that might be esential to CRC.

2.2.3 Modular Analysis

The modular structure of cancer related PPINs is of great importance since it gives an insight of the molecular complexes and signaling pathways involved in the disease and thus offers the possibility of creating hypotheses about the causes. We use the Molecular complex detection (MCODE) [16] and Markov cluster algorithm (MCL) [17] as the most common and widely used clustering

algorithms, which are initially designed for detecting functional modules or protein complexes, i.e. groups of densely interconnected proteins that are loosely connected with other such groups. These modules are in line with a property that disease-related clusters (disease genes causing similar diseases) exhibit an increased tendency for their protein products to interact with each other.

Molecular Complex Detection (MCODE)

Molecular Complex Detection (MCODE) detects densely connected regions in PPINs as protein complexes. The algorithm is based on node weighting by local neighborhood density and outward traversal from a locally dense seed protein to isolate densely connected regions. To identify modules in our CRC PPIN we used the MCODE plugin for Cytoscape.

Applied to our CRC PPIN, MCODE found seven putative complexes, but only two of them are important. A network complex is said to be important if its score is greater than one and has a decent number of nodes and edges. Let $C = (V_c, E_c)$ be a complex (subgraph), then the score of C is calculated as the product of the density and the number of vertices in the complex ($D_c * |V_c|$) [16].

The first important complex in our CRC PPIN (Complex1) consists of 6 proteins (ATM, TRRAP, RB1, TP53 and CREBBP belong to the seed proteins set, while MDM2 is a non-seed protein). While, the second important complex (Complex2), consists of 4 proteins (NF1 and SMAD4 are the seed proteins, while SMAD2 and SMAD3 are non-seed proteins).

After obtaining the two complexes, we performed GO enrichment analysis in order to identify important biological functions and processes related to these clusters. The GO enrichment analysis is done by using the ClueGO plugin [18] in Cytoscape. ClueGO uses kappa statistics to link the terms present in a network. It generates a dynamical network structure for the terms (reflecting the relationships between the terms based on the similarity of their associated proteins), and takes into consideration the protein list of interest in its initial run.

Grouping of terms into functional groups in ClueGO is based on the similarity distances measure, as described in the paper for DAVID tool [19]. As DAVID tool suggests, the terms that share global functional annotation profiles are functionally very similar to each other. The analysis with ClueGO on the two complexes found with MCODE, Complex1 and Complex2, produced a networks of GO's terms (biological processes, functions and pathways) where terms that share similar functions are grouped together and the most important term in every group is the term with smallest p-value.

After calculating the most important terms in ClueGO, the most important terms for Complex1 are: "regulation and cellular response to heat" (associated proteins: ATM, CREBBP), "p53 Signaling Pathway" (ATM, MDM2, TP53) and "Cell Cycle: G1/S Check Point" (ATM, CREBBP, MDM2), while for the Complex2, the most important terms are: "I-SMAD binding" (SMAD2, SMAD4), "Transforming growth factor beta receptor, pathway-specific cytoplasmic mediator activity" (SMAD2, SMAD3), "Transforming growth factor beta receptor, cytoplasmic mediator activity" (SMAD2, SMAD3, SMAD4) and "Transforming growth factor beta2 production" (SMAD3, SMAD4).

Markov Cluster Algorithm (MCL)
The Markov cluster algorithm (MCL) simulates a flow on the graph by calculating successive powers of the associated adjacency matrix. It iteratively enhances the contrast between regions of strong or weak flow in the graph. The process converges towards a partition of the graph, with a set of high-flow regions (the clusters) separated by boundaries with no flow. By applying MCL on our CRC PPIN we got 17 clusters, as presented on the Fig. 3.

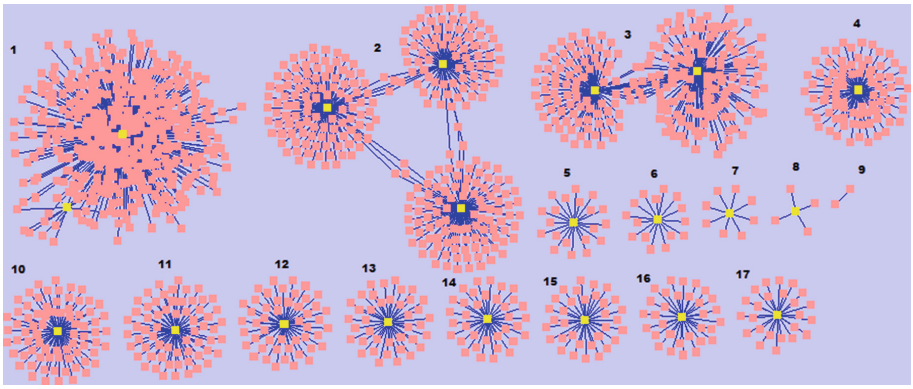

Fig. 3. MCL Clusters (yellow nodes are the seed proteins)

If we take a closer look at the clusters presented on the Fig. 3, the most interesting clusters for GO enrichment analysis will be the first three clusters (the only ones that have more than one seed protein). The GO enrichment analysis is done by using the BiNGO tool [20] in Cytoscape. This tool calculates the p-values for each GO term associated to the proteins in the cluster, and the term with the smallest p-value is the most important. For the Cluster1 the most important term is: "Negative regulation of neuroblast proliferation" (associated proteins: NF1, TP53), for the Cluster2: "Gamma-catenin binding" (APC, CDH1), while for the Cluster3: "TFC beta signaling pathway" (CREBBP, SMAD4).

3 Results and Discussion

The GO terms that we found via the modular analysis of the CRC PPIN can be used to identify proteins that are possible bio-markers. From the GO terms and pathways we can find all proteins that are associated with these GO terms. Table 2 lists the GO term and the associated proteins for each of the GO terms and pathways, together with associated p-value for every GO term.

But not all of these proteins are important for us. To filter this list, first we select only the proteins (shown on Table 3) that are part of more than two GO terms, or the proteins that have a high cumulative topological score (Fig. 2).

Table 2. Top 10 important GO terms and pathways

GO term	Associated proteins	p-value 10^{-6}
Regulation and cellular response to heat	YWHAE, BAG1, HSP90AB1, TPR, HSP90AA1, MAPK1, MTOR, SIRT1, POM121, EP300, HSPA8, ATM, DNAJB1, NUP54, DNAJB6, ATR, RPA2, NUP214, MAPK3, RPA1, NUPL2, NUPL1, NUP98, RANBP2, NUP153	52
p53 signaling pathway	ATM, CHEK2, ATR, MDM2, MDM4, TP53, CKK4, CCNE1	1.2
Cell cycle: G1/S check point	SMAD3, SMAD4, ATR, SKP2, CDKN1A, TP53, GSK3B, CDK4, CDK6, CDK2	12
I-SMAD binding	SMURF1, SMAD1, SMAD2, SMAD4, AXIN1, SMAD7, SMAD6, TGFBR1	2.2
Transforming growth factor beta receptor, pathway-specific cytoplasmic mediator activity	SMAD1, SMAD2, SMAD3, SMAD5, SMAD93	0.4
Transforming growth factor beta receptor, cytoplasmic mediator activity	SMAD1, SMAD2, SMAD3, SMAD4, SMAD5, SMAD7, SMAD6	0.0055
Transforming growth factor beta2 production	SMAD3, SMAD4	1.1
Negative regulation of neuroblast proliferation	NF1, TP53	0.41
Gamma-catenin binding	LEF1, CTNNA1, APC, CDH1, FZR1	1.8
TGF beta signaling pathway	TGFBRAP1, CDH1, SMAD2, SMAD3, SMAD4, APC	0.15

Table 3. List of proteins and number of times each protein appears in selected list of GO terms (proteins in bold are candidate bio-markers)

472-ATM	4	4087-SMAD2	4	4088-SMAD3	5	324-APC	3
545-ATR	3	**4092-SMAD7**	2	4089-SMAD4	6	999-CDH1	4
4193-MDM2	2	4091-SMAD6	2	7157-TP53	5	**4090-SMAD5**	2
4086-SMAD1	3						

Then, we excluded the seed proteins and the proteins with functions not related to cancer. This final list of proteins (proteins in boldface from Table 3) could be taken as possible list of bio-marker candidates.

From the public accessible databases we found that these proteins (ATR, MDM2, SMAD5 and SMAD7) and their mutations are involved in several biological and molecular processes, for example, cell communication, cell shape and apoptosis. Also they are involved in the pathways of carcinogenesis, transduction, and metastasis. These four proteins and their mutations may play important roles in CRC PPIN, and they may serve as possible CRC bio-markers. Also, these proteins may have the key impact in design of some new drugs for CRC cancer. However, further analysis, investigations and experiments are needed if we want these hypothesis to be confirmed or rejected, because all these findings came from experimental data gathered from different databases.

4 Conclusion

In this paper we have presented a methodology for creation and analysis of protein-protein interaction network (PPIN) of colorectal cancer (CRC). We start with the list of CRC seed proteins and with the help of Cytoscape we have generated a CRC PPIN. With the help of well-known topological network characteristics we have identified non-seed proteins that are characteristic to CRC. The modular network analysis, based on MCODE and MCL algorithms, generates PPIN complexes that are additionally analyzed with the help of GO enrichment analysis. The identified "most important" GO terms defined the list of "important" proteins. By excluding the seed proteins we have obtained a list of four proteins (ATR, MDM2, SMAD5 and SMAD7) that could be taken as possible bio-markers for CRC. These proteins and their mutations may play important roles in CRC PPIN, and may serve as possible CRC bio-markers. But, these computationally obtained results should be taken with care and must be explored more deeply to check if these proteins have influence to CRC and its metastasis.

Acknowledgement. The work in this paper was partially financed by the Faculty of Computer Science and Engineering, Ss. Cyril and Methodius University, Skopje, as part of the "Analysis of nutrigenomic data" project.

References

1. Kreeger, P.K., Lauffenburger, D.A.: Cancer systems biology: a network modeling perspective. Carcinogenesis **31**(1), 2–8 (2010)
2. Consortium, U., et al.: UniProt: a hub for protein information. Nucleic Acids Res. gku989 (2014)
3. Alberghina, L., Höfer, T., Vanoni, M.: Molecular networks and system-level properties. J. Biotechnol. **144**(3), 224–233 (2009)
4. Wachi, S., Yoneda, K., Wu, R.: Interactome-transcriptome analysis reveals the high centrality of genes differentially expressed in lung cancer tissues. Bioinformatics **21**(23), 4205–4208 (2005)
5. Rhodes, D.R., Chinnaiyan, A.M.: Integrative analysis of the cancer transcriptome. Nat. Genet. **37**, S31–S37 (2005)

6. Mani, K.M., Lefebvre, C., Wang, K., Lim, W.K., Basso, K., Dalla-Favera, R., Califano, A.: A systems biology approach to prediction of oncogenes and molecular perturbation targets in B-cell lymphomas. Mol. Syst. Biol. **4**(1), 169 (2008)
7. Jonsson, P.F., Bates, P.A.: Global topological features of cancer proteins in the human interactome. Bioinformatics **22**(18), 2291–2297 (2006)
8. Aragues, R., Sander, C., Oliva, B.: Predicting cancer involvement of genes from heterogeneous data. BMC Bioinform. **9**(1), 1 (2008)
9. Forbes, S.A., Bindal, N., Bamford, S., Cole, C., Kok, C.Y., Beare, D., Jia, M., Shepherd, R., Leung, K., Menzies, A., et al.: COSMIC: mining complete cancer genomes in the catalogue of somatic mutations in cancer. Nucleic Acids Res. gkq929 (2010)
10. Maglott, D., Ostell, J., Pruitt, K.D., Tatusova, T.: Entrez gene: gene-centered information at NCBI. Nucleic Acids Res. **33**(Suppl. 1), D54–D58 (2005)
11. Aranda, B., Blankenburg, H., Kerrien, S., Brinkman, F.S., Ceol, A., Chautard, E., Dana, J.M., De Las Rivas, J., Dumousseau, M., Galeota, E., et al.: PSICQUIC and PSISCORE: accessing and scoring molecular interactions. Nat. Methods **8**(7), 528–529 (2011)
12. Bader, G.D., Betel, D., Hogue, C.W.: BIND: the biomolecular interaction network database. Nucleic Acids Res. **31**(1), 248–250 (2003)
13. Liu, T., Lin, Y., Wen, X., Jorissen, R.N., Gilson, M.K.: BindingDB: a web-accessible database of experimentally determined protein-ligand binding affinities. Nucleic Acids Res. **35**(Suppl. 1), D198–D201 (2007)
14. Stark, C., Breitkreutz, B.J., Reguly, T., Boucher, L., Breitkreutz, A., Tyers, M.: BioGRID: a general repository for interaction datasets. Nucleic Acids Res. **34**(Suppl. 1), D535–D539 (2006)
15. Barabási, A.L., Albert, R.: Emergence of scaling in random networks. Science **286**(5439), 509–512 (1999)
16. Bader, G.D., Hogue, C.W.: An automated method for finding molecular complexes in large protein interaction networks. BMC Bioinform. **4**(1), 1 (2003)
17. Morris, J.H., Apeltsin, L., Newman, A.M., Baumbach, J., Wittkop, T., Su, G., Bader, G.D., Ferrin, T.E.: clusterMaker: a multi-algorithm clustering plugin for cytoscape. BMC Bioinform. **12**(1), 1 (2011)
18. Bindea, G., Mlecnik, B., Hackl, H., Charoentong, P., Tosolini, M., Kirilovsky, A., Fridman, W.H., Pagès, F., Trajanoski, Z., Galon, J.: ClueGO: a cytoscape plug-in to decipher functionally grouped gene ontology and pathway annotation networks. Bioinformatics **25**(8), 1091–1093 (2009)
19. Alvord, G., Roayaei, J., Stephens, R., Baseler, M.W., Lane, H.C., Lempicki, R.A.: The david gene functional classification tool: a novel biological module-centric algorithm to functionally analyze large gene lists. Genome Biol. **8**(9), 183 (2007)
20. Maere, S., Heymans, K., Kuiper, M.: BiNGO: a cytoscape plugin to assess over-representation of gene ontology categories in biological networks. Bioinformatics **21**(16), 3448–3449 (2005)

Using Sentiment Analysis of Twitter Data for Determining Popularity of City Locations

Nikola Dinkić[1(✉)], Nikola Džaković[1], Jugoslav Joković[1], Leonid Stoimenov[1], and Aleksandra Đukić[2]

[1] Faculty of Electronic Engineering, University of Niš, Niš, Serbia
{dinkicnikola, ndzakovic}@elfak.rs, {Jugoslav.Jokovic, Leonid.Stoimenov}@elfak.ni.ac.rs
[2] Faculty of Architecture, University of Belgrade, Belgrade, Serbia
adjukic@rcub.bg.ac.rs

Abstract. The paper considers mining and analyzing data generated by Twitter social network, regarding content classification, language determination and sentiment analysis of tweets. Analyzes are based on geospatial tweets collected in timespan of four months within region Vračar in Belgrade, Serbia. All of collected data is first being preprocessed, filtered and classified by given criteria, by using "Twitter search engine" (TSE) application, that has been upgraded in order to detect tweet language and execute sentiment analysis of the tweets written in English. This type of analysis can be used for determining popularity of city locations of interest and public spaces in general.

Keywords: Natural language processing · Sentiment analysis and opinion mining · Geospatial data · Twitter social network

1 Introduction

The synergy between technology and built environment generate urban culture with digital streams. On the other hand, cities and their open public spaces are reflections of users changing needs. Furthermore, the future of urban space depends on the role of information and communication technologies (ICT) and importance of their networks should be reconsidered since they have become indispensable ingredients of urban life [1]. ICT provides the overlapping of real and virtual spaces and allows creative participation of users.

With the explosive growth of social media (e.g., reviews, forum discussions, blogs, micro-blogs, Twitter, comments, and postings in social network sites) on the Web, individuals and organizations are increasingly using the content in these media for decision making. Many big corporations have also built their own in-house decision making solutions, e.g., Microsoft, Google, Hewlett-Packard, SAP, and SAS. Although linguistics and natural language processing have a long history, research about people opinions and sentiments in social media is actual in last ten years.

This paper will present and analyze the connections which are established and intensified between users and open public spaces via Twitter. Twitter is one the most popular data sources for research [2] because of its open network allowing access to

G. Stojanov and A. Kulakov (eds.), *ICT Innovations 2016*,
Advances in Intelligent Systems and Computing 665,
https://doi.org/10.1007/978-3-319-68855-8_15

information published through the platform. Twitter is a novel microblogging service launched in 2006 with more than 310 million monthly active users. On Twitter, every user can publish short messages with up to 140 characters, so-called "tweets", which are visible on a public message board of the website or through third-party applications. The public timeline conveying the tweets of all users worldwide is an extensive real-time information stream of more than one million messages per hour. The original idea behind microblogging was to provide personal status updates. However, these days, postings cover every imaginable topic, ranging from political news to product information in a variety of formats, e.g., short sentences, links to websites, and direct messages to other users.

The method that was used in analysis is the method of mapping users on the social maps (via social networks). It was based on a software application TSE [3]. The aim was tracking and measuring the intensity of users in the monitored territory, testing the latest behavioral patterns of them as well as tracing the "positive routes". The obtained results have enabled the determination of the image of the open public spaces perceived by the users, as well as the potential of the analyzed area for the formation of transverse and longitudinal pedestrian flows that could help improving networking of open public spaces.

2 Related Work

Natural language processing (NLP) is a field of computer science, artificial intelligence, and computational linguistics concerned with the interactions between computers and human (natural) languages. NLP is an area of research and application that explores how computers can be used to understand and manipulate natural language text or speech to do useful things. NLP researchers aim to gather knowledge on how human beings understand and use language so that appropriate tools and techniques can be developed to make computer systems understand and manipulate natural languages to perform desired tasks.

This paper is focused on sentiment analysis, also called opinion mining. It is the field of NLP that analyzes people opinions, sentiments, evaluations, appraisals, attitudes, and emotions towards entities such as products, services, organizations, individuals, issues, events, topics, and their attributes. It represents a large problem space. While in industry, the term sentiment analysis is more commonly used, but in academia, both sentiment analysis and opinion mining are frequently employed. They basically represent the same field of study.

Sentiment analysis and opinion mining mainly focuses on opinions, which express or imply positive or negative sentiments. In paper [4], Hu and Liu proposed a lexicon-based algorithm for aspect level sentiment classification, but the method can determine the sentiment orientation of a sentence as well. It was based on a sentiment lexicon generated using a bootstrapping strategy with some given positive and negative sentiment word seeds and the synonyms and antonyms relations in WordNet.

The sentiment orientation of a sentence was determined by summing up the orientation scores of all sentiment words in the sentence. A positive word was given the sentiment score of +1 and a negative word was given the sentiment score of −1. In [5]

the relationships between the NFL betting line and public opinions in blogs and Twitter were studied. In [6] Twitter sentiment was linked with public opinion polls. In [7] Twitter sentiment was also applied to predict election results. In [8] Twitter data, movie reviews and blogs were used to predict box-office revenues for movies. In [9] Twitter moods were used to predict the stock market. In [10] they tracked opinions about movies on Twitter and predicted box-office revenues with very accurate results. They simply used their opinion parser system to analyze positive and negative opinions about each movie with no additional algorithms.

In general, sentiment analysis has been investigated mainly at three levels:

- **Document level:** The task at this level is to classify whether a whole opinion document expresses a positive or negative sentiment [11]. For example, given a product review, the system determines whether the review expresses an overall positive or negative opinion about the product. This task is commonly known as document-level sentiment classification. This level of analysis assumes that each document expresses opinions on a single entity (e.g., a single product). Thus, it is not applicable to documents which evaluate or compare multiple entities.
- **Sentence level:** The task at this level goes to the sentences and determines whether each sentence expressed a positive, negative, or neutral opinion. Neutral usually means no opinion. This level of analysis is closely related to subjectivity classification, which distinguishes sentences (called objective sentences) that express factual information from sentences (called subjective sentences) that express subjective views and opinions.
- **Entity and Aspect level:** Both the document level and the sentence level analyzes do not discover what exactly people liked and did not like. Instead of looking at language constructs (documents, paragraphs, sentences, clauses or phrases), aspect level directly looks at the opinion itself. It is based on the idea that an opinion consists of a sentiment (positive or negative) and a target (of opinion). An opinion without its target being identified is of limited use. Realizing the importance of opinion targets also helps us understand the sentiment analysis problem better. The goal of this level of analysis is to discover sentiments on entities and/or their aspects.

3 Classification of Geospatial Data

Twitter search engine [3] application (TSE) allows gathering, mining and storing of geospatial data produced on Twitter social network. This paper describes new features of application TSE and its ability to process and analyze data from this social network. Also in order to illustrate functionality of this application, this paper shows results of analysis of data collected from tweets for Vračar region in Belgrade, Serbia.

In addition to the collection and storage of data, TSE offers visualization and analysis, but also it can execute complex queries over stored data. This queries use special geospatial functions that are built within MySQL database. These functions represent correlation between two objects that are defined by geospatial points. This application also offers users to draw polygons on Google map, in order to define boundaries of their

analysis. Note, that all polygons must be within regions for which data is collected. Polygon drawing is done by using Google Maps JavaScript API. Web application TSE also has the ability to detect the language and perform sentiment analysis.

The most important indicators of sentiments are sentiment words, also called opinion words. These words are commonly used to express positive or negative sentiments. For example, good, wonderful, and amazing are positive sentiment words, and bad, poor, and terrible are negative sentiment words. Sentiment words and phrases are instrumental to sentiment analysis for obvious reasons. A list of such words and phrases is called a sentiment lexicon (or opinion lexicon). Although sentiment words and phrases are important for sentiment analysis, only using them is far from sufficient. The problem is much more complex. In other words, we can say that sentiment lexicon is necessary but not sufficient for sentiment analysis of complex texts. Since, tweets are generally short and informal, and use many Internet slangs and emoticons, they are easier to analyze due to the length limit because the authors are usually straight forward, and immediately get right to the point. Thus, it is often easier to achieve high sentiment analysis accuracy. Reviews are also easier because they are highly focused with little irrelevant information. Because of that for sentiment analysis, this paper uses lexicon-based algorithm to determine the sentiment orientation of a sentence.

Researchers have proposed many approaches to compile sentiment words. Three main approaches are: manual approach, dictionary-based approach, and corpus-based approach. [4] used a dictionary to compile sentiment words. This is an obvious approach because most dictionaries (e.g., WordNet) list synonyms and antonyms for each word. Thus, a simple technique in this approach is to use a few seed sentiment words to bootstrap based on the synonym and antonym structure of a dictionary. Specifically, this method works as follows: A small set of sentiment words (seeds) with known positive or negative orientations is first collected manually, which is very easy. The algorithm then grows this set by searching in the WordNet or another online dictionary for their synonyms and antonyms. The newly found words are added to the seed list. The next iteration begins. The iterative process ends when no more new words can be found. Their dictionary was compiled over many years starting from their first paper. Original dictionary consists of 4783 negative and 2006 positive words, but to the original dictionary were added emoticons, which are now very popular, and can also show if it is a positive or negative opinion. Tweets can be classified as a positive or negative depending on which group of words they contain. This gives similar results as simply counting positive and negative words, since Twitter messages are so short (about 11 words). Since the area of Serbia belongs to the world top by multilingualism, it is necessary to detect only the tweets that are in English. TSE uses web service "Language detection API" [12] for language detection. Language detection API has the ability to detect 160 different languages and offers 5000 requests for free on daily basis.

4 Data Processing and Analysis

The analysis of geospatial data requires data to be in the specified format so that geospatial queries can be executed. However, since all information obtained from the Twitter REST API is in JSON format, before any analysis it is necessary to perform

transformation of geo-information to specific format. This process of transformation of the original data to geospatial data types represents the pre-processing, and this is the first step in this analysis.

In order to illustrate possibilities of TSE application, tweets collected over a period of four months (December 2015–March 2016) for region Vračar in Belgrade, were analyzed and results of this analysis are shown in this paper. This space is defined by the corresponding polygon on the map, as shown in Fig. 4. The execution of geospatial queries for the given polygon was obtained the cumulative data presented in Table 1.

Table 1. Cumulative figures for region Vračar

Type of analysis	Value
Number of tweets	3002
Number of users	603
Number of followers	1079721
Number of friends	421780
Number of retweets	35
Number of likes	490
Number of applications	8

In addition to the cumulative analysis, TSE allows filtering data based on the analysis in specified time intervals, in other words this means classification by months of the year, days of the week or otherwise defined time intervals. Figure 1 shows the distribution of tweets by month, which are shared in the studied area. It can be concluded that the Twitter users in the previous four-month period were the most active during the March 2016.

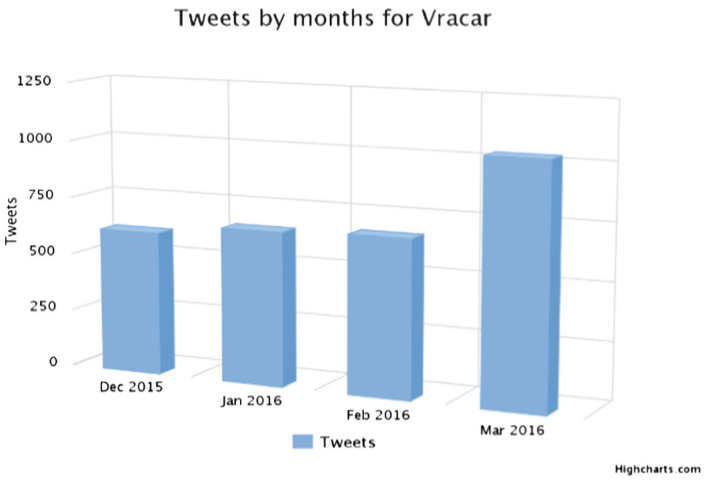

Fig. 1. Tweet count by months

The results of data classification by days of the week are shown in Fig. 2. Based on them, we can conclude that the users were most active on Saturdays.

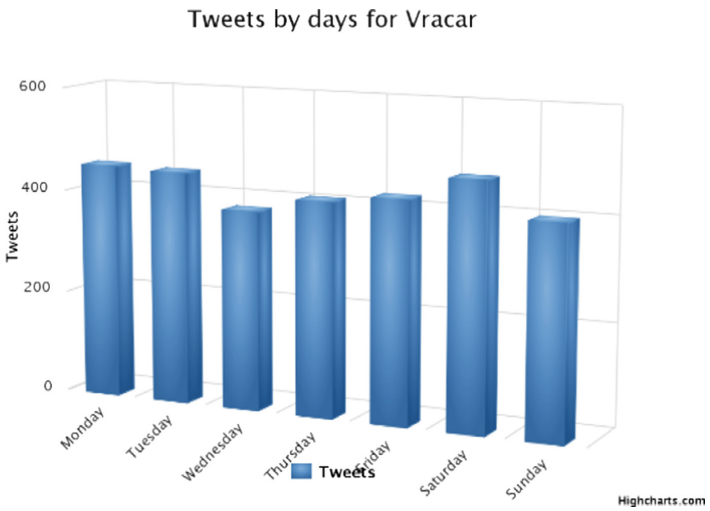

Fig. 2. Classification of tweets by days of the week

In addition to analysis of data for a given time, the type of content of tweet itself could classify the collected tweets. Figure 3 represents the percentage representation of content of analyzed tweets.

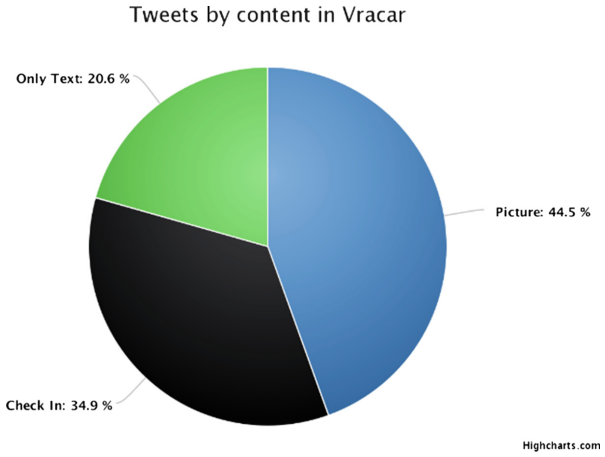

Fig. 3. Classification of tweets by content

Based on the distribution of tweets per application used to post it, it can be concluded, which content type has a tweet, without the need for a deeper analysis. For example, all tweets, which are sent by Instagram, must contain a picture. From the analysis results, it can be concluded that each Twitter user from community of Vračar on average posted 4.97 tweets, the users were most active during March, the largest number of tweets has been posted on Saturday and the most popular application is Instagram with 44.5%, following Foursquare with 34.9%, which indicates high attractiveness of the area.

The geospatial tweets classified by content are shown in Fig. 4. Tweets are displayed on the map with markers in different colors depending on the content of the tweet, picture (red), check in (green) and only text (blue).

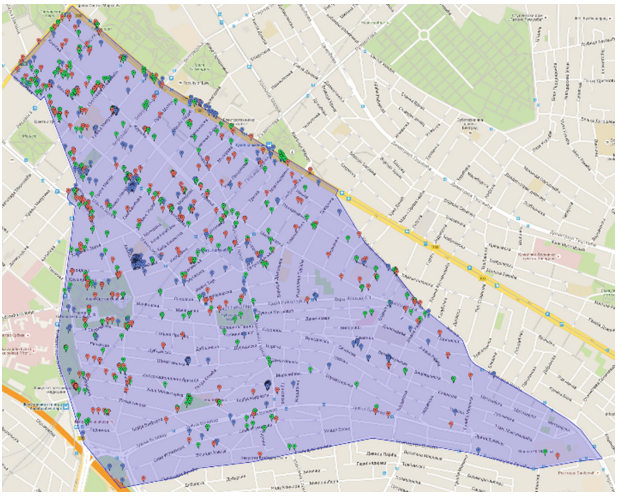

Fig. 4. Geospatial tweets for region Vračar classified by content

Analysis of all tweets detected 12 different languages: Serbian, English, German, French, Japanese, Thai, Russian, Turkish, Scottish, Bulgarian, Spanish and Portuguese, of which the most common are English with 67.4% and Serbian with 30.6%.

Based on sentiment analysis of content posted in region Vračar, tweets were divided into three groups, tweets which contain positive words, negative words and which contain both positive and negative. Since on Twitter it is a very popular to use hashtags (#), tweet content can be divided into two groups, text and hashtags. The results of sentiment analysis of tweets that contain either positive or negative words are shown in Table 2.

Table 2. Sentiment analysis of tweets

	Hashtag(#)	Text	Both
Positive	55	155	200
Negative	9	43	52
Complex	5	10	14
$\sum$	69	208	266

Sentiment analysis can be executed only on tweets that contain text (including hashtags). Application detected 266 text tweets to belong to one of three groups (positive, negative, and complex) and this distribution chart is shown in Fig. 5. From 266 classified text tweets, 75.2% of them carried a positive message. The map of the tweets, which are classified as positive is shown in the Fig. 6.

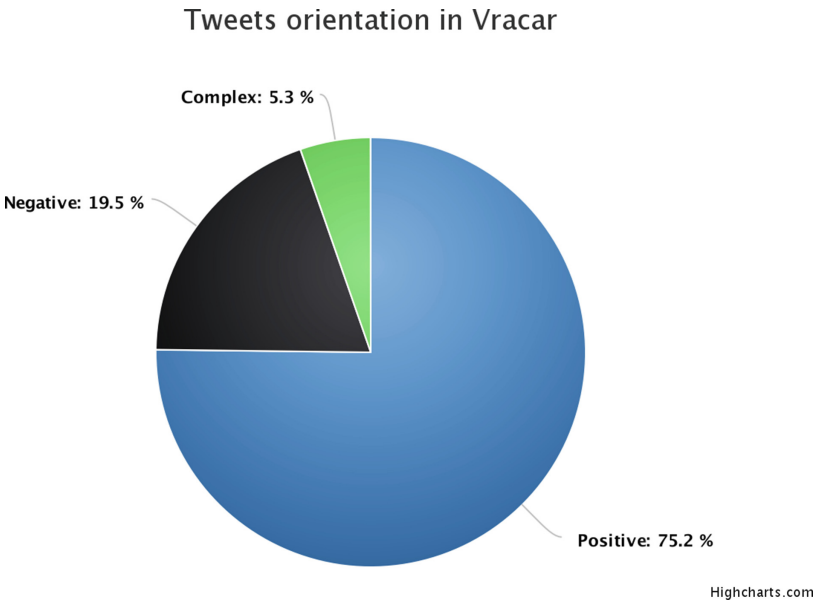

Fig. 5. Tweets orientation

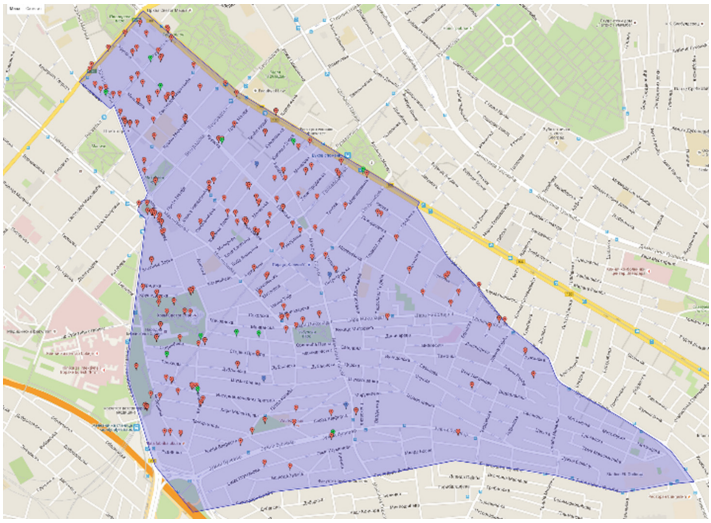

Fig. 6. Distribution of positive tweets

5 Conclusion

Generally, Twitter social network turned out to be a great basis for analysis of public space popularity. Its API provides a lot of publicly available information about tweets, but also about the users, which is the most important thing for every successful research. New feature of TSE application for language detection confirms the fact that Serbia belongs to the world top by multilingualism, which indicates that Vračar is very popular for foreign tourists. Sentiment analysis also shows that attraction sites of this region leave a positive impression on tourists who come to visit them. All analyses shown in this paper represent only a portion of possibilities that TSE application can offer and all of them can be used for creating better urban plans, in terms of (re)design of public spaces. These analyses can be used to quantify popularity of locations of interest and public spaces in general, as well as to determine correlations between locations.

References

1. Pigg, K.E., Crank, L.D.: Building community social capital the potential and promise of information and communications technologies. J. Commun. Inf. **1**(1), 58–73 (2004)
2. dos Santos, A.D.P., Wives, L.K., Alvares, L.O.: Location-Based Events Detection on Micro-Blogs (2012)
3. Nikola, D., Dinkić, N., Joković, J., Stoimenov, L.: Web application for mining, storing, processing and geo-analysis data from Twitter social network, YU INFO, Kopaonik, Srbija, March 2016
4. Hu, M., Liu, B.: Mining opinion features in customer reviews. In: American Association for Artificial Intelligence (2004)
5. Hong, Y., Skiena, S.: The wisdom of bookies? Sentiment analysis versus the NFL point spread. In: Proceedings of the Fourth International AAAI Conference on Weblogs and Social Media (2010)
6. O'Connor, B.: From tweets to polls: linking text sentiment to public opinion time series. In: Proceedings of the Fourth International AAAI Conference on Weblogs and Social Media (2010)
7. Tumasjan, A.: Predicting elections with Twitter: what 140 characters reveal about political sentiment. In: Proceedings of the Fourth International AAAI Conference on Weblogs and Social Media (2010)
8. Asur, S., Huberman, B.A.: Predicting the future with social media. In: 2010 IEEE/WIC/ACM International Conference on Web Intelligence and Intelligent Agent Technology (WI-IAT) (2010)
9. Bollena, J., Mao, H., Zeng, X.-J.: Twitter mood predicts the stock market. J. Comput. Sci. **2**, 1–8 (2011)
10. Liu, B.: Sentiment Analysis and Opinion Mining (2012)
11. Pang, B., Lee, L., Vaithyanathan, S.: Thumbs up?: Sentiment classification using machine learning techniques. In: Proceedings of the Conference on Empirical Methods in Natural Language Processing (EMNLP), Philadelphia (2002)
12. Language detection API. https://detectlanguage.com/. Accessed 15 Apr 2016

Internet Addiction: Evaluating the Psychometric Properties of the IAT in Macedonia

Martin Mihajlov[1(✉)] and Aleksandar Stojmenski[2]

[1] Faculty of Economics, Ss. Cyril and Methodius University, Skopje, Macedonia
martin@eccf.ukim.edu.mk
[2] Faculty of Computer Science and Engineering,
Ss. Cyril and Methodius University, Skopje, Macedonia
aleksandar.stojmenski@finki.ukim.mk

Abstract. In this digital age there is a growing importance in global research of Internet addiction. The purpose of this research study is to establish a valid instrument for measuring the addictive use of Internet. We investigated the psychometric properties of the established Young's Internet Addiction Test (IAT) on a Macedonian population. Since its development, there has been a number of culture-specific validation studies of the IAT, but never in cultures from south-east Europe. In a sample of 322 undergraduate participants, exploratory factor analysis (EFA) determined the presence of a three factor structure of the IAT with 17 items. The three factors, "Withdrawal and social problems", "Time management" and "Failure and neglect" explained 38.43% of the total variance with good internal consistency for the IAT (Cronbach's a = .89) and good reliability for the factors (.65–.84). Hence, this version of the IAT is a valid instrument with sound psychometric properties for measuring Internet addiction in a sample of participants from south-east Europe and may be used for further research.

Keywords: Internet addiction · Internet Addiction Test (IAT) · Macedonia

1 Introduction

The terminology, definition and theoretical basis of addictive Internet use has been and still is the subject of scientific debates. The term most widely used in the literature, "Internet addiction" was defined by Young [1] as "an impulse-control disorder without intoxication that has symptoms such as preoccupation with the Internet, problem with control over Internet use, lower mood, excessive amount of time spent online, lower performance at school or work, deteriorating physical health, jeopardized relationships with family or friends, and lying about the Internet use". Besides "Internet addiction" there are other terms in the literature including problematic Internet use [2], Internet abuse [3], pathological Internet use [4], and compulsive Internet use [5].

With over 46.4% of the population online [6] the Internet has become an essential tool in all aspects of everyday life. The increasing number of Internet users is followed by an increase in the number of hours spent online, mostly due to the anytime-anywhere access enabled by mobile devices with an almost constant Internet

G. Stojanov and A. Kulakov (eds.), *ICT Innovations 2016*,
Advances in Intelligent Systems and Computing 665,
https://doi.org/10.1007/978-3-319-68855-8_16

connection. The increased accessibility of the Internet also increases the potential for addictive use, especially among young people who generally find life without the Internet almost impossible. With a few notable exceptions [7], the research on Internet addiction has mostly been restricted to selected developed countries. Hence, for the purpose of advancing the understanding of this phenomenon it is necessary to evaluate its properties in less-developed countries, like Macedonia. With only provisional access in the beginning of this century when Internet connectivity was available to only 2.5% of the population, the number of Internet users in Macedonia has grown rapidly to almost 70% in 2016 [8]. According to the latest report by the State Statistical Office, in 2015 approximately 89.3% of the population aged 15–24 used the Internet daily, whereas 65.8% of these users accessed the Internet via a mobile device (SSO, 2015).

When it comes to measuring Internet addiction, according to Laconi et al. [9], there are 45 tools, which measure and assess addictive Internet use through scales, interviews or diagnostic criteria. According to the same research, only 17 tools have had their psychometric properties evaluated more than once. The development of these tools includes different approaches such as adaptation of DSM-IV criteria regarding substance abuse and dependence or pathological gambling [10, 11], cognitive-behavioral modeling [2, 12], or behavioral addiction modeling [13].

From these tools, the Internet Addiction Test [13] is one of the earliest constructs for evaluating addictive online behavior. With widely studied psychometric properties, this test has been translated into many languages and is the most popular evaluation tool. Regarding the properties of the test, its internal consistency is reported as high, ranging from Cronbach's $\alpha = .85$ to $\alpha = .93$ [14, 15] while the temporal reliability of the test is reported as good, ranging from $r = .73$ to $r = .85$ [16, 17]. However, the factorial structure of the test has significantly varied across studies and samples ranging from one-dimensional [18, 19, 20], two-dimensional [21], three [15], four [16], five [22], and six-dimensional solutions [16]. A sample overview of factors is presented in Table 1. Considering the high variance of the factor structure between studies it is necessary to validate the test before it can be applied to a new culture. Instead of using Internet addiction as an overall concept, examining the factor structure and dimensionality of the IAT will provide us with a greater detail of the culture-specific nature of addictive use.

Table 1. Factor extraction overview in analysis of other cultures

No	Factors	Language	Reference
1	/	French	[19]
2	Dependent use and excessive use	English	[26]
3	Psychological/emotional conflict, time-management problems, and mood modification	English	[25]
3	Withdrawal & social problems, time management & performance, and reality substitute	Chinese	[10]
5	Lack of control, neglect of duty, problematic use, social relationship disruption, and email privacy	Malay	[23]

(*continued*)

Table 1. (*continued*)

No	Factors	Language	Reference
6	Salience, excessive use, neglect work, anticipation, lack of control, and neglect social life	English	[17]
6	Compromised social quality of life, compromised individual quality of life, compensatory usage of the Internet, compromised academic/working careers, compromised time control, and excitatory usage of the Internet	Italian	[24]

Addictive Internet use can greatly influence the everyday life of the individual. Nevertheless, due to a significant lack of research the impact of addictive Internet to the personal life of individuals in South-East Europe is unknown. Hence, as a first step towards developing this field of research in this paper we examine and validate the IAT within the cultural context of Macedonia.

2 Method

2.1 Participants

A total of 322 undergraduate students from three different departments participated in this study. As we excluded 5 responses as unengaged entries (SD < 0.3), the final dataset consisted of responses from 317 participants. The age of the participants varied between 19 and 25 (M = 20.79, SD = 1.269) and the gender distribution was rather even with 49.21% female (n = 156, M = 20.71, SD = 1.042), and 50.79% male (n = 161, M = 20.85, SD = 1.435) participants. Based on their field of study 37.2% (n = 118) of the participants were in economics, 49.2% (n = 156) in computer science and 13.6% (n = 43) in civil engineering.

2.2 Instrument/Measures

The Internet Addiction Test is a questionnaire designed for self-evaluation of Internet addiction. As an expanded version of the Internet Addiction Diagnostic Questionnaire (IADQ) [22] it acts as a self-report instrument used to measure an individual's Internet use from the perspective of psychological symptoms and behaviors. The questionnaire consists of 20 items rated on a 5-point Likert scale, ranging from 1 (rarely) to 5 (always). The minimum obtainable score is set at 20 and the maximum at 100, with a higher score indicating a greater level of Internet addiction. Based on the severity score participants can be classified as:

- **minimal users** (20–39), the average online users with complete control over their Internet use;
- **moderate users** (40–69), the users who experience occasional or frequent problems due to their Internet use;
- **excessive users** (70–100), the users with significant problems caused by Internet use.

2.3 Procedure/Analysis

A web link to an online questionnaire was provided to all participants. Following a declaration of informed consent, the volunteering participants completed the IAT questionnaire, along with basic demographic data (age, gender, field of study) at a time of their leisure.

After the preliminary evaluation of the collected data we proceeded with the statistical analysis in three phases using SPSS. First we examined the response distributions of all IAT items to estimate their internal consistency through inter-item correlations. We then proceeded with the exploratory factor analysis (EFA) using principal axis factoring as an extraction method since the Likert-scale data had an expected non-normal distribution.

3 Results

3.1 Preliminary Analysis

The distribution of responses were not excessively skewed or kuriotic implying sufficient variance on all items. The correlation matrix contained no negative values indicating that all of the items measured the same characteristic, and had 182 (95.79%) significant inter-item coefficients with an average r = 0.254. The items of the IAT also had a good internal consistency with a Cronbach's alpha value of 0.87.

The suitability of data for factor analysis was examined with measures of sampling adequacy. A substantial number of coefficients (35.79%) had a value of 0.3 or above with the determinant of the R-matrix at .004 indicating no multicolinearity or singularity problems. The Kaiser–Meyer–Olkin measure (KMO) indicated a value of .890, exceeding the minimum value of .600, while all KMO values for individual items were greater than .78, well above the acceptable limit of .5. Additionally, the Bartlett's Test of Sphericity was statistically significant ($\chi 2 = 1735.021$, df = 190, $p < .0001$), supporting the factorability of the correlation matrix.

3.2 Factor Analysis

The initial exploratory factor analysis was run to obtain factors with eigenvalues greater than Kaiser's criterion of 1.00. The results of the factor extraction returned five factors explaining 40.41% of the variance. Considering that the individual communalities after extraction were less than .7, and the average communality was 0.404, the retention of all the extracted factors was highly unlikely. The ambiguous scree plot showed inflexions that would justify the retention of 2 to 4 factors. Additionally, the factor structure after rotation revealed several items with initial loadings below 0.3 for all factors. Hence, we iterated the SPSS analysis by removing different items in each iteration and evaluating the state of the resulting factors. The optimal factor extraction occurred when we removed items q4, q7 and q10 either due to low communalities or low factor loadings (< 0.3). The reduced 17-item rotated solution returned three factors explaining 38.43% of the variance (Table 2). We identified a cross-loading on item 14 between Factor 1 and Factor 2, whereas the item was grouped on Factor 2 because of

Table 2. Reduced IAT pattern matrix

	F1	F2	F3
Item 03	0.42		
Item 05	0.32		
Item 09	0.47		
Item 11	0.47		
Item 12	0.61		
Item 13	0.64		
Item 15	0.67		
Item 18	0.46		
Item 19	0.57		
Item 20	0.80		
Item 1		0.62	
Item 2		0.37	
Item 14	(.31)	0.36	
Item 16		0.45	
Item 6			0.61
Item 8			0.60
Item 17			0.32
Eigenvalue	4.52	2.09	2.74
Variance explained	28.67	6.03	3.74
Cronbach's α	0.84	0.66	0.65

its larger loading and conceptual fit. Hence, Factor 1 comprises of items 3, 5, 9, 11, 12, 13, 15, 18, 19 and 20, Factor 2 comprises of items 1, 2, 14 and 16 and Factor 3 comprises of items 6, 8 and 17. Factor 1 can be classified as "Withdrawal and social problems", factor 2 as Time management and factor 3 as "Failure and neglect".

The convergent validity of the IAT results were examined by evaluation inter-factor correlations (Table 3). The strongest correlation was between the "Withdrawal and social problems" factor and the "Failure and neglect" factor (r = 0.477). While the correlations between "Withdrawal and social problems" and "Time management" and "Failure and neglect" and "Time management" were similar with r = 0.323 and r = 0.325 respectively.

Table 3. Reducet factor correlation matrix

	F1 - Withdrawal and social problems	F2 - Time management	F3 - Failure and neglect
F1 - Withdrawal and social problems	1.000	.323	.477
F2 - Time management	.323	1.000	.325
F3 - Failure and neglect	.477	.325	1.000

Regarding reliability, we calculated the Cronbach's α for all factors. The "Withdrawal and social problems" subscale of the IAT had a good reliability with Cronbach's $\alpha = 0.84$. Conversely, the "Time management" subscale had an acceptable reliability with Cronbach's $\alpha = 0.71$, while the "Failure and neglect" subscale had a questionable reliability with for Cronbach's $\alpha = 0.65$.

4 IAT Analysis

Using the IAT cutoff score system, a total of 82 participants (25.87%) were classified as minimal users, the majority, 215 participants (67.82%), were classified as moderate users, and only 20 participants (6.31%) were classified as excessive users. Based on gender the distribution of participants was similar for minimal users (45.1% male, 54.9% female) and moderate users (51.2% male, 48.8% female), while there was a difference in excessive users (70% male, 30% female). Nevertheless, a one-way ANOVA revealed no significant effect of gender on the level of Internet addiction, $F(1, 315) = 3.22$, $p = 0.74 > 0.5$. Additionally, we tested for differences in Internet addiction based on field of study and the one-way ANOVA also revealed no significant effect, $F(1, 315) = 2.477$, $p = 0.86 > 0.5$.

The mean score of the IAT score for all participants was 48.55 (SD = 12.71). Disregarding the participants gender, the mean score for minimal users was 33.65 (SD = 40.08), for moderate users was 61.67 (SD = 7.979), and for excessive users was76.15 (SD = 5.153). A one-way ANOVA revealed no significant difference between participants of different genders for the three factors defined in the EFA.

5 Discussion

The results presented in the previous section present the psychometric properties of the IAT for a Macedonian population. The factor analysis suggested the existence of three factors to explain this phenomenon: the first relates to withdrawal from offline activities that may or may not include other people, the second relates to the inability to manage time spent online the third relates neglect of academic and professional activities as well as the failure to avoid the use of Internet in general.

Although initially designed as a single-dimension construct, IAT has repeatedly shown a multidimensional structure in most studies. Our three factor solution is partially in accordance with previous investigations, most notably [10, 15] with whom it shares two of the extracted factors, "Withdrawal and social problems" and "Time management". The same two factors are also present in [27] 5-factor solution, while time management is also a part of [24] 6-factor construct.

The lower factor loadings of IAT items and the exclusion of items in general suggests that the IAT should be refined in accordance with technological advancement and changes in social life [7], which have made significant differences in how people interact with online environments. Specifically, item 7 related to the frequency of checking email has been surpassed by the use of a myriad of messaging and communication apps.

The limitations of this study follow several directions which suggest avenues for future studies. The results from the sample might not be generalized on a wider population without a larger longitudinal study. Additionally, by not including another instrument for comparison we couldn't determine the convergent and discriminant validity of the IAT. The IAT itself is limited as it doesn't consider the use of mobile devices nor the context of Internet. Furthermore, the IAT generally lacks temporal stability as it ignores the transient nature of Internet use. Nevertheless, despite these limitations, the fitting factor structure along with the internal consistency and reliability confirm the IAT is a valid instrument for measuring Internet addiction in different cultures.

References

1. Young, K.S.: Internet addiction: symptoms, evaluation and treatment. Innovations Clin. Pract.: Source B. **17**, 19–31 (1999)
2. Davis, R.A., Flett, G.L., Besser, A.: Validation of a new scale for measuring problematic internet use: implications for pre-employment screening. CyberPsychol. Behav. **5**, 331–345 (2002)
3. Morahan-Martin, J.: Internet abuse addiction? disorder? symptom? alternative explanations? Soc. Sci. Comput. Rev. **23**, 39–48 (2005)
4. Niemz, K., Griffiths, M., Banyard, P.: Prevalence of pathological internet use among university students and correlations with self-esteem, the General Health Questionnaire (GHQ), and disinhibition. CyberPsychol. Behav. **8**, 562–570 (2005)
5. Meerkerk, G.-J., Eijnden, R.J.V.D., Garretsen, H.F.: Predicting compulsive internet use: it's all about sex! CyberPsychol. Behav. **9**, 95–103 (2006)
6. Internet World Stats. World Internet Users and 2015 Population Stats (Accessed 2015). http://www.internetworldstats.com/stats.htm
7. Karim, A.R., Nigar, N.: The Internet addiction test: assessing its psychometric properties in Bangladeshi culture. Asian J. Psychiatry **10**, 75–83 (2014)
8. Internet Live Stats, Republic of Macedonia Internet Users. (Accessed 2016). http://www.internetlivestats.com/internet-users/macedonia/
9. Laconi, S., Rodgers, R.F., Chabrol, H.: The measurement of internet addiction: a critical review of existing scales and their psychometric properties. Comput. Hum. Behav. **41**, 190–202 (2014)
10. Chang, M.K., Law, S.P.M.: Factor structure for young's Internet Addiction Test: a confirmatory study. Comput. Hum. Behav. **24**, 2597–2619 (2008)
11. Chen, S., Weng, L., Su, Y., Wu, H., Yang, P.: Development of a Chinese internet addiction scale and its psychometric study. Chin. J. Psychol. **45**, 279 (2003)
12. Meerkerk, G.-J., Van Den Eijnden, R.J., Vermulst, A.A., Garretsen, H.F.: The compulsive internet use scale (CIUS): some psychometric properties. Cyberpsychol. behav. **12**, 1–6 (2009)
13. Young, K.S.: Internet addiction: the emergence of a new clinical disorder. CyberPsychol. Behav. **1**, 237–244 (1998)
14. Conti, M.A., Jardim, A.P., Hearst, N., Cordás, T.A., Tavares, H., de Abreu, C.N.: Evaluation of semantic equivalence and internal consistency of a Portuguese version of the Internet Addiction Test (IAT). Arch. Clin. Psychiatry **39**, 106–110 (2012). (São Paulo)

15. Lai, C.-M., Mak, K.-K., Watanabe, H., Ang, R.P., Pang, J.S., Ho, R.C.: Psychometric properties of the Internet Addiction Test in Chinese adolescents. J. Pediatr. Psychol. **38**, 794–807 (2013)
16. Lee, K., Lee, H.-K., Gyeong, H., Yu, B., Song, Y.-M., Kim, D.: Reliability and validity of the Korean version of the internet addiction test among college students. J. Korean Med. Sci. **28**, 763–768 (2013)
17. Widyanto, L., McMurran, M.: The psychometric properties of the Internet Addiction Test. CyberPsychol. Behav. **7**, 443–450 (2004)
18. Hawi, N.S.: Arabic validation of the internet addiction test. Cyberpsychol. Behav. Soc. Networking **16**, 200–204 (2013)
19. Khazaal, Y., Billieux, J., Thorens, G., Khan, R., Louati, Y., Scarlatti, E., Theintz, F., Lederrey, J., Van Der Linden, M., Zullino, D.: French validation of the internet addiction test. CyberPsychol. Behav. **11**, 703–706 (2008)
20. Panayides, P., Walker, M.J.: Evaluation of the psychometric properties of the internet Addiction Test (IAT) in a sample of Cypriot high school students: the Rasch measurement perspective. Eur. J. Psychol. **8**, 327–351 (2012)
21. Pawlikowski, M., Altstötter-Gleich, C., Brand, M.: Validation and psychometric properties of a short version of Young's Internet Addiction Test. Comput. Hum. Behav. **29**, 1212–1223 (2013)
22. Young, K.S.: Psychology of computer use: XL. Addictive use of the internet: a case that breaks the stereotype. Psychol. R. **79**, 899–902 (1996)
23. Guan, N.C., Isa, S.M., Hashim, A.H., Pillai, S.K., Singh, M.K.H.: Validity of the malay version of the Internet Addiction Test a study on a group of medical students in Malaysia. Asia Pac. J. Public Health **27**, NP2210–NP2219 (2015)
24. Ferraro, G., Caci, B., D'amico, A., Blasi, M.D.: Internet addiction disorder: an Italian study. CyberPsychol. Behav. **10**, 170–175 (2006)
25. Widyanto, L., Griffiths, M.D., Brunsden, V.: A psychometric comparison of the Internet Addiction Test, the Internet-Related Problem Scale, and self-diagnosis. Cyberpsychol. Behav. Soc. Networking **14**, 141–149 (2011)
26. Jelenchick, L.A., Becker, T., Moreno, M.A.: Assessing the psychometric properties of the Internet Addiction Test (IAT) in US college students. Psychiatry Res. **196**, 296–301 (2012)
27. Kesici, S., Sahin, I.: Turkish adaptation study of Internet Addiction Scale. Cyberpsychol. Behav. Soc. Networking. **13**, 185–189 (2010)

Health Care Domain Mobile Reminder for Taking Prescribed Medications

Eleonora Milić(✉), Dragan Janković, and Aleksandar Milenković

Faculty of Electronic Engineering, University of Niš, Niš, Serbia
eleonora.milic@elfak.rs, {dragan.jankovic, aleksandar.milenkovic}@elfak.ni.ac.rs

Abstract. Nowadays, majority of people as a main problem for their poor health and bad psycho-physical condition states the lack of time. Commitments, dynamic and stressful way of life lead to people being negligent of themselves. Thus, their health condition is damaged. The big problem are acute patients, but also the patients who have a chronic disease and who should take prescribed medications regularly, and who, for some reason, are prevented or have forgotten to take the prescribed dosage of the medicaments. Due to the inadequate taking of the therapy, the time for patient's recovery is significantly prolonged or the existing problem is not relieved (with chronic patients). *PersonalMedicationReminder* is an Android application that downloads the prescriptions from the server of a health care institution or allows the user to insert the over-the-counter drugs (without prescription therapy). The application allows patients to create reminders and receive notifications which would inform them about the time for the next receiving of the therapy. The application downloads the prescriptions from the electronic medical record of the patient from the medical information system MEDIS.NET which is used in health institutions for primary health care in Republic of Serbia [1, 2]. The problems that occurred during the application development are also shown in the paper. In the conclusion are stated the directions of the further research and improvement of the mobile application.

Keywords: mHealth · Personal medical reminder · Health care · Medicine reminder

1 Introduction

Today in the domain of the health care of patients the biggest mistakes happen because the obligations and the everyday life lead people to the lack of care for themselves and they do not follow the doctors' orders. Patients are people of a different profile. No matter if they are students, businessmen, programmers, housewives, retirees or children, they all can be equally careless about their health. Life, as is lead today, is full of responsibilities and stress, which makes people prone to a variety of diseases. In desire to maintain health using modern technologies we are getting a chance to, by relying on our smartphones, stay healthy and in good shape.

In health care the important problem is that the patients often forget to take the right amount of medicines in the right time. It is important to mention that, for example, taking

G. Stojanov and A. Kulakov (eds.), *ICT Innovations 2016*,
Advances in Intelligent Systems and Computing 665,
https://doi.org/10.1007/978-3-319-68855-8_17

antibiotics is time dependent since if the medicine is not taken in the right time, its effect is annulled. The situation is similar with some other medications. In order not to depend on other people to remind them about taking the medicines, patients need to adopt taking the medicines as a part of their routine, while not allowing anything to distract them or to make them forget about the medicines. A certain percentage of people thus use technologies like the reminder, most frequently the alarm on their smartphones.

As a solution of the mentioned problem is imposed the idea of the Android application which goal would be to remind the patient to take the right medicine and the right amount, as well as to warn them that the pills or capsules are running out and that the patient should visit the chosen doctor and get the new prescription. The prescriptions must be valid and taken from the medical information system of the health institution where the user is being treated. MEDIS.NET is a medical information system developed for the needs of the institutions of primary health care. It is used in more than 25 institutions of that type in the Republic of Serbia [1, 2]. *PersonalMedicationReminder* application downloads prescriptions for the certain patient from the electronic medical record from MEDIS.NET medical information system. Patients should be enabled to, besides getting the predefined values, customize on their own the number of tablets per box, the period of taking the medicine, recommended dose (for certain medications that are taken as needed or tablets such as vitamins or diet supplements is already made possible to independently change the default dose or period recommended by the doctor), as well as to set the alarm for the next medicine for all the prescriptions that the application gets from the server. Also, for over-the-counter medicines, patient should be enabled to input all the important data for the medicine bought at the drugstore and to set the alarm for it. It is also necessary to make possible the permanent deletion of the prescription at any moment if the user wants that, or to temporarily turn the reminder off for a medicine taken as needed. In this way, the possibility of taking the wrong dose of a certain medicine or not taking it can be brought to a minimum.

In this paper is presented the Android application in which, by incorporating the electronic reminder with an alarm, the solution to the described problem was implemented. While some applications are developed in such a way that for their use they need to be connected to an additional hardware, for using the *PersonalPillsReminder* application it is enough for the user to stick to the prescriptions and medicines with a simple interaction with the application and minimal time spent. Patients do not have to remember the time and the amount of the medicine that they are to consume. Instead of them, the smart mobile application, in which the alarms are set for the time when the right dosage of the right prescribed medicine should be taken, is taking care of that. Authentication for the access to the application and the server where the medical record of the patient is stored is done through the personal identification number of the insured (LBO) and the PIN which are stored in the database on the server. All the communication with the server is protected by using the *HTTPS* protocol. When the alarm starts, the notifications are shown to the user on the display of the smartphone until the he confirms taking the prescribed dose of the medicine. The number of the remaining tablets for each medicine is stored separately. The system is developed to provide the simple navigation and user interface.

Throughout this work will be presented the earlier researches and conceptual description of the solutions. The architecture and the design of the Android application

PersonalMedicationReminder and its components were implemented using *Eclipse* development environment and *Restful* web service [2, 3]. After the evaluation of the proposed solution, the directions of the further researches are shown and the conclusion was made.

2 Earlier Research

Applications that represent a kind of medical reminders, according to the functionality they offer, are sorted into three main categories:

- *SMR (Simple Medication Reminders)*: applications that offer basic functionality of remembering prescriptions, notifying the user, setting the alarm, choosing the type of notifications and accompanying sound effects, postponing the alarm, etc.
- *AMR (Advance medication reminders)*: provides additional options like the time zone change support, overdose protection, different description, instructions, etc.
- *MMA (Medication management apps)*: basically AMR applications that support multiple user accounts. They enable users to store important information, contacts of the chosen doctors, reminders for the future checkups, etc. [4].

The usage of the applications in the field of health care and protection is increasing every day. Some of them need additional hardware as sensors, RFID tags or motion detectors [5]. Many attempts to reduce the administrative mistakes in treating patients were focused on the development of the medical dispensers. Below are given the examples of the applications which are results of the earlier researches.

MyMediHealth application is the reminder for children. It is performed on the smartphones and it enables configuring reminders for notifying the user about the medicine that is scheduled at that time [6, 7].

Wedjat represented an attempt of the integration of the support in the health care and wireless computing. The application was conceptualized so that is prevents patients from making mistakes caused by administration. Main functionalities are: reminder of the necessary daily intake of the medicines, instructions related to the allowed intake of the medicaments and storing the data about the consumed medicines [8].

Med Minder application is a simple and free solution envisioned as a planer application which main flaw was that it took to much manual settings thus too much time [9].

Medical Reminder and Healthcare. Android application's goal is to remind the patients with the ringing of the alarm to take their dose of the medicine. Through this application they could see the contacts of the doctors and hospitals, in order to schedule an appointment. It is possible to set the date, the time of the alarm and the instructions for multiple medicines at the same time. Besides the alarm, the user would get the notification via SMS or e-mail [10].

Medication Reminder System is also an Android application for patients. It automatically sets the time when the patient should take the next dose of the medicine. Those data the application takes from the prescription of the patient and in that way makes the possibility for mistakes that the patient can make by setting the time by himself smaller [11].

Majority of the applications on the market offer reminders that are based on timers. Some of these applications allow only one notification for a certain medicine a day, and do not support time intervals such as reminders every few hours or every few days. Small number of applications has the option of postponing the alarm for certain medications, which is bad if the user does not react immediately, because he can forget to take the medicine. The weak point of the current systems is that the user must input all the medications he uses alone, which takes a lot of time. There is no service that stores the original prescriptions by medical institutions. There are no notifications for the patient that his medicines will run out in a certain number of days and that he should visit the doctor for the new prescription. Because of the manual input of the prescriptions there is a big possibility for mistakes which could result in big problems in patient's treatment. Bigger problem present the reminders that were notifying the user to take the medicine at a certain time, but without the doctor prescribed dose and periods, which again can cause a significant damage for the patient.

3 Proposed Solution

Studying the previous solutions and the needs of the users, a set of functionalities that would in the most adequate way be made into an Android application was listed. Application would on its own download the prescriptions from the server of the medical institution or let the user input the medications that are bought over-the-counter. It would make possible for the user to get the prescribed therapy (one medicine per prescription) and to create the events through which it would notify the user that it's time to take the therapy.

For starting the application, it would be necessary to authenticate the patient by inputting the LBO (personal identification number of the insured) and a PIN (which is provided by the doctor). It should be made possible (configurable) to memorize the credentials in the memory of the telephone so that the users would not have to input them every time, if they want to.

From the system of the health institution, it is needed to deliver to the mobile application the exact date, as well as the prescriptions for the authenticated user. Each prescription should have the diagnosis, medicine (code, name, strength, unit of measure) and the frequency of taking the medicine. Each medicine has a certain amount of tablets/capsules per package (e.g. 20 capsules of a certain antibiotic in the package).

That number is different between different producers, so, the patient should input the number of tablets in the package taken from the pharmacy each time they get the new prescription. The user should be reminded that he had consumed the whole package a few days earlier so that he would have enough time to visit the doctor for further treatment (this option should be configurable, e.g. notify 1 day earlier, 7 days earlier). The user would be able to change the number of the remaining tablets/capsules in the package (lost one tablet, the package in gotten in the pharmacy contained 20 instead of 30 tablets, etc.)

The problem would be if the user does not take the medicine in the scheduled time (e.g. the user does not have the medicine with him, does not see the notification in time, sees but forgets to take the medicine). Depending on the medicine, it can be taken

immediately, or taken as scheduled. If the medicine should be taken as soon as possible, than it is necessary to change the time for the next taking of the medicine (if the medicine is taken every 8 h, than it is necessary to take the medicine from that moment on every 8 h). There are some medicines (e.g. vitamins) that can be taken at any time of the day, but it is important to take them that day. Then, there are medicines that are taken according to a scheme (e.g. 2 tablets in the morning, 1 tablet in the afternoon, 0.5 mg in the evening, and a different scheme for each day). The doctor can tell the patient to take the medicine every six hours, but after two days to take it every 8 h if he feels better. For that reason, the user should be given the option to change the frequency of taking the medicine (the default frequency should be suggested which the user would be able to change as needed).

The important request is that the notification about the therapy must be delivered always to the patient, even if there is the power or the internet connection outage. The time of the next taking of the therapy shouldn't be dependent on the time zone.

When the application is started for the first time, the service for downloading the active prescriptions would be summoned if the user chooses to turn on the reminders. It is necessary to define the time after which the application would download the prescriptions from the server by itself. For example, the application would once a day download the status from the database of the medical information system. That option would be configurable (e.g. every 8 h, or every 24 h, etc.). It would be good to enable the option for the user to reload the prescriptions on request.

There should also be the option to delete the prescription from the application. The user would be able to change at any time: the frequency of taking the medicine, number of tablets in the package, in how many hours should he take the medicine, the total number of tablets per package, how many days earlier should he be notified that he needs the new prescription and to download new prescriptions not older than the configured number of days.

The background service would take care about the time when the alarm should be activated and for which prescription, as well as when the alarm should remind the user when to get the new prescription. It would start automatically when starting the phone. The data about the prescriptions that are downloaded via the service, time for taking the next medicine, and everything else relevant for the prescription would be stored in the phone's memory and reached from there, as long as the application reloads the list searching for the new prescriptions from the server.

Frequency in taking therapy can be: once a day every other day, once a week, once a month, once a year, as needed and according to a scheme. When the prescriptions are downloaded for the first time, the user is immediately notified to input the number of tablets/capsules for the new prescriptions and to activate the alarms. The user should decide whether he would take the therapy according to the defined scheme (the determined number of hours) or he would adjust the time (input the time in hours or minutes). The same is applicable to the amount of the medicine used.

When the alarm starts when it is time for taking the medicine on an Android telephone a notification would appear (sound, vibration and light). If the user ignores the notification it would repeat every 15 min. When the patient opens the notification and clicks on it, a prescription would open and the user would have two options: to confirm taking the medicine or to postpone the alarm for some time. After a certain

time of taking the therapy when the number of tablets would be smaller than the configured number of days, the user would be notified to schedule a new doctor's appointment. In each moment the user would be able to delete each prescription individually, to turn off the notifications for it or to delete all the prescriptions from the list. When the prescription is marked for deletion, it will remain on the list for another 48 h if the user wants to undo the deletion, and after that it will be deleted from the application. No matter if the prescription was downloaded from the database of the medical information system of the health institution or the user input the data by himself, the alarms and the notifications will function just the same.

4 Implementation and Solution Architecture

The client application was developed for Android API 3.0 and higher. The development environment used for this purpose was *Eclipse Juno 4.2* and *Java* programming language.

A client application *PersonalMedicationReminder*, which communicates with the server of the medical information system via *Restfull* web service for downloading prescriptions, was developed for Android devices. Basic functionalities illustrated in the example of the demo application from *mHealth* (abbreviation for the term used to describe the usage of mobile devices and services for the practice of medicine and public health) field are:

- The service starts upon starting the phone.
- LBO and PIN can be but do not have to be stored in the phone's memory, depending on whether the user wants to input them every time he checks or updates the prescriptions in the application.
- Once the LBO is input and the prescriptions are downloaded, the user cannot input a different LBO before the previous reminders are deleted.
- All the prescriptions are remembered in the phone's memory.
- The service performs checks for new prescriptions not older than the date set by the user.
- Frequency of updating the prescriptions and notifications about the lack of medicines the user configures in the application.
- The alarm and the notifications for the medicines function independently from the Internet connection.
- The user gets a predefined period for taking the medicine which can be customized. It is necessary to input the number of tablets in the package to start the reminder for the medicine.
- If the battery on the phone is drained, and the telephone is turned off in the moment when the notification about the therapy should appear, the user will be notified about it as soon as the phone is turned back on.
- When the user clicks on the notification the application is started, and the user can postpone the alarm or confirm that he took the medicine and set the alarm for the next taking of the therapy.

- The prescription can be marked for deletion and will be permanently deleted from the list after 48 h. During that period, the user can restore the marked prescription.
- When the user is left with less than, for example, 7 days of medication supply (the predefined number of days in the application), he is notified that he needs a new prescription. The user also gets a similar notification when the whole package is consumed (Fig. 1).

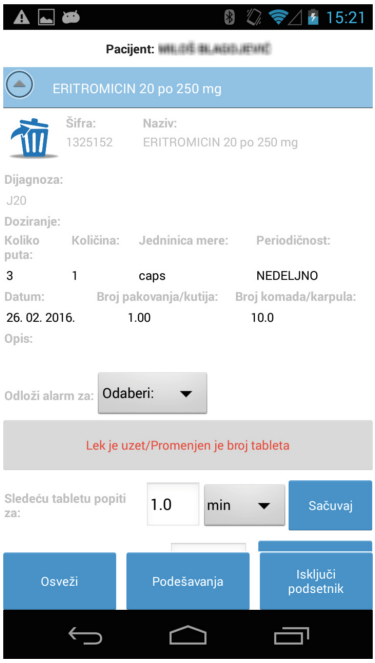

Fig. 1. *PersonalMedicalReminder*-screen with prescription data

The Fig. 2 shows the organization and the architecture of the system. In the architecture there is: a service that works in the background, a layer which deserializes the data from the server, processes them and stores them in the application and a *U/I* component for setting the changeable parameters of the service and for the interaction of the user with the application.

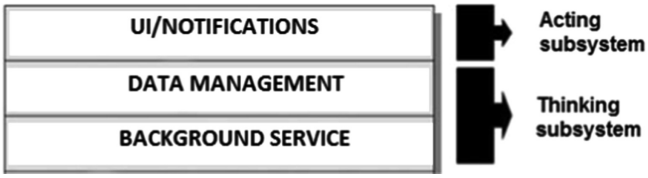

Fig. 2. The system architecture.

The background service starts automatically after turning the Android device on and for the customizable parameters in the stated cases, it sets a predefined value that is stored in the telephone memory. If there is a need for the change of those parameters, it was made possible for the user to input the wanted values, and the changes would be stored in the memory of the device. All the values in the application are stored in the. *xml* file, in the application folder. It takes care of the reminders related to each separate prescription, activates the alarms and the reminders and sends them further to the user's interface.

The advanced level, i.e. the level for gathering, deserialization and storing of the data from the prescriptions accepts the given data and classifies them into predefined objects for storing the values used in the application.

The user interface helps in signing in the user for the server of the medical institution, shows the prescriptions and the notification, but it also makes it possible for the user to set the parameters used in the application.

Pictures of the display of the application are shown below.

One of the shortcomings which can be seen in the very beginning is that the reminder must be manually set for each medicine. Since there is no data about the number of tablets/capsules per package on the server of the medical institution, the user must input that number by himself and then start the reminder and the alarm.

One more shortcoming is that the database permanently stores all the prescriptions and does not delete them when the patient finishes the therapy. Due to this, the application must take care about it by itself which prescriptions it would show and which prescriptions it would consider expired. After each taking of the therapy, the number of tablets in the prescription is automatically decreased. The moment when that number is zero, the reminder for the medication is turned off. The prescription stays visible until the user deletes it or until it is older than three months. After three months the service automatically removes the prescription from the list.

5 Conclusion

Methods that are currently used for reminding patients to follow the therapy can be demanding in terms of time and resources, and are based on either the help of the family and friends or on paying the person who would periodically check the patient and take care of him. The automatic planner would enable lowering the amount of mistakes that can happen for previously stated reasons and at the same time it would lead to the quality improvement of the care since it would decrease the amount of time that the patient or the medical stuff would have to spend.

For the development of the application that will be used by majority of people, Android platform is seen as the best solution. Android makes the development of the application easy since Java gives a whole set of libraries. Of course, it is possible to use Java on the other embedded Linux platforms, but there such a wide variety of user APIs does not exist.

In this paper is presented a developed Android mobile application which is simple for use and that helps patients to follow the prescribed therapies. The service is done as a background service and it contacts the sever as often and the user wants it (parameter

is possible to set in the mobile application). The prescriptions are stored in the telephone's memory, while taking very little memory space due to the fact that the data are texts.

Further steps in improving the application would be adding the option for scheduling the appointments with the chosen doctor through the mobile application which will save a lot of time to the user. The default value of the tablets per package could be configurable on the level of application, so that the reminder could be started automatically without waiting for the patient to input the number of tablets for a newly downloaded prescription. For the mobile application to be available to all the patients for the three major smartphone operation systems versions for the iOS and Windows Phone mobile platforms will be developed.

References

1. Medis.NET-Health Care Information System (2016). http://www.elfak.ni.ac.rs/downloads/projekti/tehnicka-resenja/katalog/medis-net.pdf
2. Janković, D., Milenković, A., Rajković, P., Stanković, T., Marković, I., Cvetković, S., Vučković, D., Pešić, S.: Medicinski informacioni sistem MEDIS.NET. Laboratorija za medicinsku informatiku, Elektronski fakultet Niš (2010). http://www.elfak.ni.ac.rs/phptest/new/html/nauka/tehnicka_resenja/resenja/0259.html
3. Eclipse (2016). https://eclipse.org/
4. Representatial State Transfer (2016). https://en.wikipedia.org/wiki/Representational_state_transfer
5. Stawarz, K., Cox, A.L., Blandford, A.: Don't forget your pill! designing effective medicationreminder apps that support users' daily routines. In: CHI 2014 Proceedings of the SIGCHI Conference on Human Factors in Computing Systems (2014). ISBN 978-1-4503-2473-1
6. Motion Sensors (2016). http://developer.android.com/guide/topics/sensors/sensors_motion.html
7. Harris, C.E., Davison, C.L., Culpepper, D.K., Scott, P., Johnson, K.B.: MyMediHealth – designing a next generation system for child-centered medication management. J. Biomed. Inf. **43**(5), 27–31 (2011)
8. Wang, M.Y., Tsai, P.H., Liu, J.W. S., Zao, J.K.: Wedjat: a mobile phone based medication reminder and monitor. In: 2009 Bioinformatics and BioEngineering, BIBE 2009 (2009). ISBN 978-0-7695-3656-9
9. Med Minder (2016). https://play.google.com/store/apps/details?id=com.garland.medminderfree&feature
10. Ameta, D., Mudaliar, K., Patel, P.: Medication reminder and healthcare – an android application. Int. J. Managing Public Sect. Inf. Commun. Technol. (IJMPICT) **6**(2) (2015)
11. Bhadane, A., Sapna, K., Ishwari, B., Pallavi, P., Achaliya, P.N.: An android based medication reminder system based on OCR using ANN. In: IJCA Proceedings on International Conference on Recent Trends in Engineering and Technology 2013 (2013)

Enhancing Text-Based Relatedness Measures with Semantic Web Data

Ana Gjorgjevikj(✉), Riste Stojanov, and Dimitar Trajanov

Faculty of Computer Science and Engineering,
Ss. Cyril and Methodius in Skopje, Skopje, Macedonia
ana.gorgevic@gmail.com, {riste.stojanov,dimitar.trajanov}@finki.ukim.mk

Abstract. Entity relatedness measures quantify the amount of association between two entities, such as people, places or events, and are fundamental part of many Natural Language Processing and Information Retrieval applications. Calculating entity relatedness requires access to entity specific information, so a very common practice is to use Wikipedia or its Semantic Web representations as source of knowledge. This paper explores which of the different semantic relationships that associate two entities in DBpedia are good indicators of their relatedness and could be used to enhance some of the standard text-based relatedness measures. The ultimate goal is learning a well performing relatedness calculation method that does not require vast amount of preprocessing, but is applicable in cases when entities lack either textual context or semantic relationships. The KORE entity relatedness dataset was used for learning a convenient and well performing method for measuring relatedness and its evaluation.

Keywords: Entity relatedness · Semantic relatedness · Entity ranking · DBpedia

1 Introduction

The rapidly growing amount of textual data, encoding knowledge in an unstructured manner, imposes an urgent need for techniques that enable its efficient analysis and exploration. Much of the research in the areas of Natural Language Processing (NLP), Information Extraction (IE) and Information Retrieval (IR) is focused on extracting some structure from the textual data that can lead to easier information access. With the expansion of the structured knowledge available as part of the Semantic Web, this knowledge is frequently used for addressing the aforementioned issues and making the textual data more machine understandable. Research areas such as Entity Disambiguation and Linking, semantic search and ranking are particularly focused on leveraging the semantic knowledge in solving NLP and IR tasks.

One of the core components of the algorithms exploiting semantic data in NLP and IR tasks is the calculation of semantic relatedness between entities.

G. Stojanov and A. Kulakov (eds.), *ICT Innovations 2016*,
Advances in Intelligent Systems and Computing 665,
https://doi.org/10.1007/978-3-319-68855-8_18

Semantic relatedness can be defined as a measure of the amount of association between two entities, considering any kind of relationships between them. The terms semantic relatedness and semantic similarity frequently appear together in literature and in some cases are even used interchangeably [1]. However, they represent different concepts, i.e. semantic similarity is a quantification of how much two concepts are alike [2] and a special case of relatedness [3]. It is usually limited to hyponymy/hyperonymy relations in a taxonomy [4], whereas two concepts can be related in other ways than similarity, for example through meronymy or functional relations. Reasoning about semantic relatedness usually requires understanding of the entities context and larger amount of common-sense and domain-specific knowledge, so a simple hyponymy/hyperonymy hierarchy is insufficient.

The Semantic Web [5] provides standardized representation of the human knowledge in a computer understandable format, particularly useful for reasoning about semantic relatedness of two entities. In the past decade large amounts of digital corpora have been transformed into semantic representations, increasing the amount of well structured and interconnected data available. The DBpedia dataset[1] is one of the oldest and most widely used, extracting knowledge from Wikipedia[2] and making it available following the Semantic Web and Linked Data principles [6]. Many research works have already shown the usefulness of Wikipedia in NLP and IR tasks due to its common properties with the lexical resources, as well as the unique features coming from the world and domain specific knowledge it encodes [7]. DBpedia exhibits those properties in a more structured manner, making them even more useful.

Even though the semantic datasets seem as a promising source of relatedness information, only a small number of recent works [8,9] exploit them, while most of the state-of-the-art methods are based on entities textual descriptions solely or the Wikipedia hyperlink structure. In this paper we propose a relatedness calculation method that is based on the data available in DBpedia and machine learning techniques. A set of features that are based on DBpedia taxonomical and ontological structure are defined, some of which novel and not evaluated in the previous works and some already proven as effective when applied to the Wikipedia data. Considering the fact that not all entities have well linked representations in DBpedia, the feature set is further extended with features purely based on the entities textual context. The relatedness function was evaluated on the entity ranking task where set of entities is ranked based on their relatedness to one main entity. This work focuses on Named Entities only.

2 Related Work

The early research related to measuring semantic relatedness and similarity has been focused on general terms or concepts, and therefore most of the approaches have exploited statistical techniques or lexical resources like WordNet [3,10,11]. The extension of the task to more specific concepts and entities that do not

[1] http://wiki.dbpedia.org/.
[2] https://www.wikipedia.org/.

exist in lexical resources has imposed a need for domain-specific knowledge and popularized the use of datasets like Wikipedia. Strube and Ponzetto [4] were one of the first to use Wikipedia as source of information for term relatedness through adjustment of the known WordNet based measures to the Wikipedia hierarchical category structure. Gabrilovich and Markovitch [12] proposed the Explicit Semantic Analysis (ESA) approach in which terms are represented as vectors of concepts (articles) from Wikipedia. The relevance of a concept for a term is based on the TF-IDF measure and the term occurrence frequency across the Wikipedia articles. Terms are compared using measures specific to the vector-space model. Milne and Witten [13] define a relatedness measure that adjusts the Normalized Google Distance formula to the Wikipedia hyperlink structure, which has become one of the most frequently used relatedness measures in entity extraction systems.

Hoffart et al. [14] define a set of relatedness measures based on the entities textual context (single-word keywords and multi-word keyphrases mined from text describing the entities). The keywords and keyphrases are weighted with regard to the entity using a variation of the TF-IDF weighting and compared through a set of different measures. Aggarwal and Buitelaar [15] base their work on the ESA approach and improve its accuracy. While ESA takes into consideration all mentions of a word in a Wikipedia article when calculating the TF-IDF score, this new approach considers only the links created by humans. Ceccarelli et al. [16] present a method for learning to rank entities based on their relatedness to another entity. Through definition of a set of 27 features, mainly based on the Wikipedia link structure, they model the relatedness calculation problem as a ranking problem. Schuhmacher and Ponzetto [8] calculate entity relatedness using the semantic relations from DBpedia in two ways, first by calculating the cheapest paths between the two entities in a sub-graph derived from DBpedia, with previously learned link weights, and through comparison of the weighted semantic graph representations of the entities abstracts using the Graph Edit Distance formula. Hulpuş et al. [9] present a graph-based relatedness measure as well, where graph edges are assigned a weight called exclusivity and the relatedness is calculated as a sum of the paths with highest weights between the entities.

The approach presented in this paper measures the relatedness between Named Entities through a combination of text-based and structure-based features, i.e. takes into consideration both the entities textual descriptions and their semantic relations. The approach is similar to the one presented in [16] and adjusts few of its best performing features to DBpedia, while adding new ones specific to the DBpedia semantics. The entity relatedness model is different than the one in [16], where the authors try to directly learn an entity ranking model through learning to rank algorithms, while we try to learn a model that predicts a continuous-valued relatedness. None of the other related approaches uses machine learning to model the entity relatedness and only few make use of semantically structured data [8,9].

3 Entity Relatedness Calculation

This section describes the methodology used to learn a non-linear function for calculation of relatedness between two Named Entities from a set of features. It starts with a general overview of the data and feature sets, while ending with description of the machine learning algorithm used to learn the function.

3.1 Data Preparation

From the few cross-domain knowledge bases available as part of the Semantic Web (e.g. DBpedia, Yago,[3] Freebase[4]) DBpedia was selected for the purpose of this work. From the English version of DBpedia 2014[5] the extended abstracts of the DBpedia resources, corresponding to the first paragraph of the Wikipedia article, were used as source of entities textual context. The article categories dataset, associating the DBpedia resources to the categories they belong to through the dct:subject[6] relation, and the SKOS categories dataset, which contains information about the hierarchical and associative relations between the Wikipedia categories represented using the SKOS vocabulary,[7] were used as sources of relatedness information, together with the properties of the DBpedia resources and the DBpedia ontology. The datasets were preprocessed for removal of the unneeded data that may lead to wrong results (e.g. administrative categories) and the preprocessed datasets were imported in a local instance of the Openlink Virtuoso server, making them available for use by the application modules.

3.2 Feature Selection

For the purpose of relatedness calculation between two entities, the entity pairs were described through a set of features that quantify the amount of their association from different aspects. We started with a set of 16 features, summarized in Table 1, out of which 9 most informative ones were selected. An attempt was made to make distinction between features that are more likely to indicate semantic similarity and those more likely to indicate semantic relatedness, considering the similarity as a special case of relatedness. In the rest of this section the features are described into more details.

There are only two features that use the entities textual descriptions, represented through their extended abstracts in DBpedia, while all the other are structure-based. The text-based features (1 and 2 in Table 1) rely on well-known string comparison measures, the Jaccard similarity coefficient and the TF-IDF based cosine similarity. The Jaccard similarity coefficient is used for measuring

[3] http://www.mpi-inf.mpg.de/yago/.
[4] https://www.freebase.com/.
[5] http://wiki.dbpedia.org/services-resources/datasets/dbpedia-data-set-2014.
[6] http://purl.org/dc/terms/subject.
[7] http://www.w3.org/2004/02/skos/.

Table 1. Summary of the features considered for entity relatedness calculation

	Feature	Description
1	$J_{abstr}(e_1, e_2)$	$J_{abstr}(e_1, e_2) = \frac{\lvert tokens(e_1) \bigcap tokens(e_2) \rvert}{\lvert tokens(e_1) \bigcup tokens(e_2) \rvert}$
2	$cos_{abstr}(e_1, e_2)$	Cosine similarity between entities extended abstracts
3	$\lvert cat_{l=1}(e_1) \bigcap cat_{l=1}(e_2) \rvert$	Number of common categories on level one
4	$\lvert cat_{l=2}(e_1) \bigcap cat_{l=2}(e_2) \rvert$	Number of common categories on level two
5	$\lvert cls(e_1) \bigcap cls(e_2) \rvert$	Number of common ontology classes
6	$\lvert p(c_i, c_j) \rvert, c_i \in cat(e_1), c_j \in cat(e_2), len(p) = 1$	Number of skos:related links between the entities categories
7	$\lvert p(t_i, t_j) \rvert, t_i \in cls(e_1), t_j \in cls(e_2), len(p) = 1$	Number of object properties defined between the DBpedia ontology classes which the entities belong to
8	$\lvert p(e_1, e_2) \rvert, len(p) = 1$	Number of paths with length one between the entities
9	$\lvert p(e_1, e_2) \rvert, len(p) = 2$	Number of paths with length two between the entities ($e_1 \rightarrow x \rightarrow e_2$ and $e_1 \leftarrow x \leftarrow e_2$)
10	$\lvert inlinks(e_1) \bigcap inlinks(e_2) \rvert$	Number of entities to which both e_1 and e_2 point ($e_1 \leftarrow x \rightarrow e_2$)
11	$\lvert outlinks(e_1) \bigcap outlinks(e_2) \rvert$	Number of entities pointing to both e_1 and e_2 ($e_1 \rightarrow x \leftarrow e_2$)
12	$P(e)$	Probability of link to entity e equal to the number of entities linking to e divided by total number of entities in DBpedia (4,584,616 in the English DBpedia 2014). Calculated for each of the two entities
13	$P(e_1 \lvert e_2)$	$P(e_1 \lvert e_2) = \frac{\lvert inlinks(e_1) \bigcap inlinks(e_2) \rvert}{\lvert inlinks(e_2) \rvert}$
14	$J_{inlinks}(e_1, e_2)$	Jaccard similarity coefficient based on the number of entities linking to e_1 and e_2 $J_{inlinks}(e_1, e_2) = \frac{\lvert inlinks(e_1) \bigcap inlinks(e_2) \rvert}{\lvert inlinks(e_1) \bigcup inlinks(e_2) \rvert}$
15	$friend(e_1, e_2)$	Equals to 1 if e_1 has link to e_2, or $friend(e_1, e_2) = \frac{\lvert outlinks(e_1) \bigcap inlinks(e_2) \rvert}{\lvert outlinks(e_1) \rvert}$ otherwise
16	$avgFrnd(e_1, e_2)$	$avgFrnd(e_1, e_2) = \frac{friend(e_1, e_2) + friend(e_2, e_1)}{2}$

similarity between two sets by dividing the size of their intersection by the size of their union. The abstracts similarity was calculated on a token level, i.e. the two texts are represented as sets of tokens. For calculation of the cosine similarity, the abstracts were represented as vectors of tokens in an n-dimensional vector space, where n is the total number of tokens in the texts. The value of each dimension is the TF-IDF score of the token for the specific text. Since it is a corpus-based measure, when calculating it we took into consideration all the

entities that we wanted to rank with regard to the main entity. Although called similarity measures, these two measures are actually based on the shared words between the texts which can indicate relatedness as well.

Features 3–5 can be considered as similarity indicators since they are based on taxonomical structures. The first two are defined with regard to the DBpedia category taxonomy, considering the membership of the entities in categories through dct:subject relation and the skos:broader relation between the categories. The third one considers the membership of the entities in ontology classes through the rdf:type[8] relation. Only the membership into the most specific classes of the ontology was considered, since the classes at the higher levels can be too generic. Two additional features (6 and 7) capture the number of skos:related links between the categories which the two entities belong to and the object properties defined between the DBpedia ontology classes of the entities (object properties that have them as rdfs:domain[9] or rdfs:range[10]). Although all the properties defined between two ontology classes might not be applicable to all their instances, this feature can still contain some relatedness information useful in cases when relations between the instances are deficient. Features 8–11 are based on the paths (object properties) between the two entities. The first one counts the paths with length equal to one between the two entities, while the second one counts the paths with length two, starting from one of the entities and ending into the other. Two features that consider cases in which the two entities point to a common entity or a common entity points to them both were defined as well. Five additional features (12–16) were taken from [16] and adjusted to work with the object properties in DBpedia. In the original work, the authors calculate their values using the Wikipedia hyperlink structure, i.e. the hyperlinks between the appropriate articles. In this work the object properties between the DBpedia entities were used.

The initial set of features was subjected to a feature selection process that eliminated those that have little value for relatedness calculation. The usefulness of each feature was evaluated on a subset of an existing dataset designed specifically for evaluation of entity relatedness and ranking functions, i.e. the KORE dataset [14]. The dataset, consisting of 420 Named Entity pairs, was divided into two subsets, one used as a training set for learning the relatedness function and one as a test set. The KORE dataset consists of 21 seed entities for which an additional 20 candidate entities linked from the seeds' Wikipedia articles have been selected and ranked manually. Since the candidate entity ranking with respect to the seed entity is a key aspect of the evaluation process, during the creation of the training and test subsets the 420 entity pairs were not divided randomly, but the separation was done on the seed entity level. Out of the 21 seed entities, 6 entities were randomly chosen for the training subset and the other 15 were left as a test subset. All 20 candidate entities for the chosen 6 seed entities were included in the training subset, resulting with 120 entity pairs, and the candidate

[8] http://www.w3.org/1999/02/22-rdf-syntax-ns#type.
[9] http://www.w3.org/2000/01/rdf-schema#domain.
[10] http://www.w3.org/2000/01/rdf-schema#range.

entities of the remaining 15 seed entities were included in the test subset. The training subset contains around 30% of the whole KORE dataset, whereas the test subset around 70%. For better validation, the same process was repeated ten times, resulting into ten different combinations of training and test entities. The nine features that were selected through the feature selection process are the abstracts Jaccard similarity (feature 1 from Table 1), the abstracts cosine similarity (feature 2), the number of paths with length one (feature 8), the probabilities $P(e_1)$ and $P(e_2)$ (feature 12), the conditional probabilities $P(e_1|e_2)$ and $P(e_2|e_1)$ (feature 13), Jaccard coefficient based on inlinks (feature 14) and the average friendship (feature 16). Further details are presented in Sect. 4.2.

3.3 Learning a Relatedness Function

After the feature selection process, the next phase was learning a relatedness function that outputs a continuous relatedness value for an entity pair. Since our training subset is relatively limited in size, more complex prediction models such as neural networks were considered to achieve better results. Through experiments with different configurations of feedforward neural networks, a neural network consisting of four layers, i.e. one input layer with one input neuron for each feature, two hidden layers, each with four neurons and an output layer with one neuron was designed. The sigmoid function is used as activation function of the neurons in the hidden layers, whereas the output node is linear. The training of the neural networks was done using the machine learning software Weka [17]. The trained networks were evaluated the on the appropriate test subsets and the achieved performance is presented into details in the next section.

4 Evaluation

This section describes the evaluation of the learned relatedness calculation model and provides analysis of the results achieved in the different phases.

4.1 Evaluation Dataset and Methodology

For the purpose of learning and evaluating the relatedness calculation model, few available datasets were considered, out of which the KORE entity relatedness dataset was selected as the most appropriate. The other considered datasets either do not make clear distinction between the concepts of similarity and relatedness or deal with general terms and not with Named Entities. The KORE entity relatedness dataset is specifically designed for evaluation of Named Entity relatedness metrics. It consists of entities belonging to four domains - IT companies, Hollywood celebrities, video games and television series and in contrast to the other available datasets that specify numeric scores to the term pairs, the KORE dataset assigns the entity pairs relative ranking judgments [14]. Since the KORE dataset provides only the names of the entities and not an URI, these names were mapped to the appropriate DBpedia entities. As described

in Sect. 3, 30% of the data or 6 randomly chosen seed entities and their candidate entities were used to learn a function for relatedness calculation, and the remaining 15 seed entities were used for evaluation. For each of the 15 seed entities and their candidates, a relatedness score was calculated using the learned relatedness function and these scores were used to produce a relative ranking of the 20 candidates. This ranking was compared with the gold standard using the Spearman's rank correlation coefficient ρ. This coefficient is used to test the association between two ranked variables and has a value between -1 and 1, indicating negative, no or positive correlation. This coefficient was calculated separately for each seed entity and then averaged for the whole test dataset. As described in Sect. 3, ten random training/test datasets were created and used to determine if there is any significant deviation between the achieved ρ coefficient with the learned relatedness functions.

4.2 Evaluation Results

In the feature selection phase highest correlation coefficient ρ was achieved by the abstracts cosine similarity feature (0.573), the Jaccard similarity (0.568) and the number of paths with length one (0.554). Based on these scores, nine features were selected as input for the neural network. The maximum Spearman's rank correlation coefficient achieved in the 10 repetitions of the relatedness function learning and evaluation process was 0.725, with a low standard deviation between the repetitions equal to 0.014.

For the purpose of further evaluation, an additional set of 40 named entities from different domains in Wikipedia (companies, places, scientists, actors, novels, television series and etc.) was created. The entities (Wikipedia articles) that were linked from the Wikipedia articles of the main entities were extracted as candidate entities and ranked with regard to the main entity using the learned relatedness functions. The produced relatedness scores and rankings were then manually evaluated and few examples are shown in Table 2. It contains three main entities - Oracle Corporation,[11] Tim Berners-Lee[12] and Mont Blanc,[13] together with 15 candidate entities ranked in descending order by their relatedness to the main entity. The presented rankings were produced with the best performing relatedness function.

Below we summarize the results achieved by the related work on the KORE dataset, mentioning only the best results reported in the referenced papers. The best performing methods on the KORE dataset are the KPCS method presented in [14] which is a variation of the base KORE method and performs comparison of the entities textual context ($\rho = 0.698$), as well as the methods presented in [15], which compare entities representations in a vector space derived from Wikipedia ($\rho = 0.781$). The methods based on structured data contained in semantic knowledge bases have slightly worse results than the previous methods, with ρ equal to 0.624 [8] and 0.63 [9]. The relatedness calculation method

[11] https://en.wikipedia.org/wiki/Oracle_Corporation.
[12] https://en.wikipedia.org/wiki/Tim_Berners-Lee.
[13] https://en.wikipedia.org/wiki/Mont_Blanc.

Table 2. Example entities from the extended evaluation dataset

	Oracle Corporation	Tim Berners-Lee	Mont Blanc
1	Oracle Applications	W3C	Mont Blanc massif
2	Safra A. Catz	World Wide Web	Haute-Savoie
3	Oracle Enterprise Manager	Web Foundation	Italy
4	Jeffrey O. Henley	Robert Cailliau	Graian Alps
5	Oracle Fusion Middleware	Semantic Web	France
6	Ed Oates	Royal Academy of Engineering	Aosta Valley
7	Mark Hurd	Douglas Engelbart	Jacques Balmat
8	Bob Miner	Nigel Shadbolt	Courmayeur
9	Oracle Database	Royal Society	Aiguille du Midi
10	Larry Ellison	Order of the British Empire	Chamonix
11	Sun Microsystems	Order of Merit	Michel-Gabriel Paccard
12	Redwood Shores, California	MIT	Mount Everest
13	Java(programming language)	Plessey	Mont Blanc Tunnel
14	MySQL	University of Southampton	Switzerland
15	Oracle Application Express	England	Mont Blanc du Tacul

presented in this paper achieves satisfactory results, while being relatively simple and only requiring access to the DBpedia data for the entities of interest. There is no need for considering a broader set of data nor extensive preprocessing of the whole Wikipedia/DBpedia dataset. The approach can be easily extended with entities textual data from outside DBpedia or relations from other datasets. The main contribution of this paper is the demonstration that through use of more complex machine learning algorithms good entity ranking results can be achieved even with simple features. It proves the usefulness of structural data available in DBpedia for enhancement of the relatedness measures based on text comparison.

5 Conclusion

This paper presents a method for measuring relatedness of Named Entities existing in a semantic knowledge base, learned from a set of simple features. The semantic relatedness measures are crucial part of more complex tasks like Named Entity linking or document retrieval, together with other computationally-intensive algorithms, which was the reason why simplicity was one of the main goals of this work. The presented approach uses the data available in DBpedia to enhance the well-known text-based relatedness measures. Through combination of simple text and structure-based features, satisfactory results were achieved, proving the usefulness of the semantic data for relatedness calculation, while addressing the potential problem with lack of semantic relations for certain entities. The approach does not require any significant preprocessing of the data coming from DBpedia nor the entities textual context. Considering the limited

size and domain coverage of the KORE dataset, further evaluations on more extensive datasets are planned, as well as utilization of more complex machine learning techniques, which makes this work a base for a more extensive future research on effective ways to exploit Semantic Web data for relatedness calculation.

References

1. Budanitsky, A., Hirst, G.: Evaluating wordnet-based measures of lexical semantic relatedness. Comput. Linguist. **32**(1), 13–47 (2006)
2. Pedersen, T., Patwardhan, S., Michelizzi, J.: Wordnet:: Similarity: measuring the relatedness of concepts. In: Demonstration papers at HLT-NAACL 2004, pp. 38–41. Association for Computational Linguistics (2004)
3. Resnik, P.: Using information content to evaluate semantic similarity in a taxonomy. arXiv preprint cmp-lg/9511007 (1995)
4. Strube, M., Ponzetto, S.P.: WikiRelate! computing semantic relatedness using Wikipedia. In: AAAI, vol. 6, pp. 1419–1424 (2006)
5. Berners-Lee, T., Hendler, J., Lassila, O., et al.: The semantic web. Sci. Am. **284**(5), 28–37 (2001)
6. Lehmann, J., Isele, R., Jakob, M., Jentzsch, A., Kontokostas, D., Mendes, P.N., Hellmann, S., Morsey, M., van Kleef, P., Auer, S., et al.: DBpedia-a large-scale, multilingual knowledge base extracted from Wikipedia. Semant. Web J. **5**, 1–29 (2014)
7. Medelyan, O., Milne, D., Legg, C., Witten, I.H.: Mining meaning from Wikipedia. Int. J. Hum.-Comput. Stud. **67**(9), 716–754 (2009)
8. Schuhmacher, M., Ponzetto, S.P.: Knowledge-based graph document modeling. In: Proceedings of the 7th ACM International Conference on Web Search and Data Mining, pp. 543–552. ACM (2014)
9. Hulpuş, I., Prangnawarat, N., Hayes, C.: Path-based semantic relatedness on linked data and its use to word and entity disambiguation. In: The Semantic Web–ISWC 2015, pp. 442–457. Springer (2015)
10. Wu, Z., Palmer, M.: Verbs semantics and lexical selection. In: Proceedings of the 32nd Annual Meeting on Association for Computational Linguistics, pp. 133–138. Association for Computational Linguistics (1994)
11. Leacock, C., Chodorow, M.: Combining local context and Wordnet similarity for word sense identification. In: WordNet: An Electronic Lexical Database, vol. 49, no. 2, pp. 265–283 (1998)
12. Gabrilovich, E., Markovitch, S.: Computing semantic relatedness using Wikipedia-based explicit semantic analysis. IJCAI, vol. 7, pp. 1606–1611 (2007)
13. Witten, I., Milne, D.: An effective, low-cost measure of semantic relatedness obtained from Wikipedia links. In: Proceeding of AAAI Workshop on Wikipedia and Artificial Intelligence: An Evolving Synergy, Chicago, USA, pp. 25–30. AAAI Press (2008)
14. Hoffart, J., Seufert, S., Nguyen, D.B., Theobald, M., Weikum, G.: KORE: keyphrase overlap relatedness for entity disambiguation. In: Proceedings of the 21st ACM International Conference on Information and Knowledge Management, pp. 545–554. ACM (2012)
15. Aggarwal, N., Buitelaar, P.: Wikipedia-based distributional semantics for entity relatedness. In: 2014 AAAI Fall Symposium Series (2014)

16. Ceccarelli, D., Lucchese, C., Orlando, S., Perego, R., Trani, S.: Learning relatedness measures for entity linking. In: Proceedings of the 22nd ACM International Conference on Conference on Information & Knowledge Management, pp. 139–148. ACM (2013)
17. Hall, M., Frank, E., Holmes, G., Pfahringer, B., Reutemann, P., Witten, I.H.: The WEKA data mining software: an update. ACM SIGKDD Explor. Newsl. **11**(1), 10–18 (2009)

Power Consumption Analysis of Application Layer Protocols for the Internet of Things

Aleksandar Velinov(✉) and Aleksandra Mileva

Faculty of Computer Sciences, Shtip, Republic of Macedonia
aleksandar.2101106@student.ugd.edu.mk,
aleksandra.mileva@ugd.edu.mk

Abstract. In this paper, we present power consumption analysis of application layer protocols CoAP, MQTT and XMPP for the Internet of Things. With this modern concept of the future will be connected all devices which can be connected. Sensors, home appliances, vehicles, mobile devices are just some of the physical objects that will be affected. Here especially may be mentioned the sensory devices. These are devices used to detect events and changes in the environment by generating appropriate output. Many of them are with limited performances, memory and battery. They are often placed in inaccessible areas. Therefore, the power consumption is very important, and which of the protocols used for the Internet of Things provide greater energy savings. According to the test results, MQTT and CoAP provide major energy savings, unlike XMPP which consumes more power. For all protocols, the most energy is spent in a state RX, while the least is spent in a state LPM.

Keywords: Internet of Things · CoAP · MQTT · XMPP

1 Introduction

The term Internet of Things (IoT) was first introduced by British entrepreneur Kevin Ashton back in 1999. With the discovery, industrial IoT passed a long way into the past, but it did not have the form and momentum currently present in the IoT space [1].

Internet of Things is a computer concept that represent the connection of various types of devices. Using the Internet and modern communication networks they can identify and exchange data with each other. IoT predicts that thousands of end devices with sensing, actuating, processing and communication capabilities will be able to connect to the Internet. Unlike the past, when mostly mobile technologies were globally connected via the internet, now most types of electronic equipment can be connected. This trend is expected to accelerate in the coming years due to the reduction in hardware costs as well as the maturity of Internet technology [2]. These devices can be connected directly using mobile technologies such as 2G, 3G, LTE (4G), and the latest 5G. The connection can be established by using different types of wireless technologies such as: Zigbee (based on IEEE 802.15.4 standard), Wi-Fi (based on IEEE 802.11 standard), 6LowPAN over Zigbee (IPv6 over Low Power Personal Area Networks), or Bluetooth (based on IEEE 802.15.1) [3].

G. Stojanov and A. Kulakov (eds.), *ICT Innovations 2016*,
Advances in Intelligent Systems and Computing 665,
https://doi.org/10.1007/978-3-319-68855-8_19

According to analysts there will be nearly 26 billion devices on the IoT by 2020. Cisco estimates that 50 billion devices and objects will be connected to the internet by 2020. Other vendors have slightly different predictions. Irrespective of these differences, it is very clear that the number of devices/things connected would be in the range of billions, not millions [1].

IoT has standardized suite of protocols at every layer of the protocol stack (Fig. 1). IEEE 802.15.4 protocol operates at the network/link layer. IPv6/6LoWPAN operates at the Internet layer. The transport layer uses UDP. At this level can also be used TCP (Table 1). The top layer is application layer. This is the layer at which take place all communications between devices to access other networks, the public Internet, and final applications. This way allows online servers to update to the latest values of end devices but also enables the transfer of commands from applications to end devices. Here, we use multiple protocols such as: CoAP, MQTT and XMPP. These protocols will be the topic of our research.

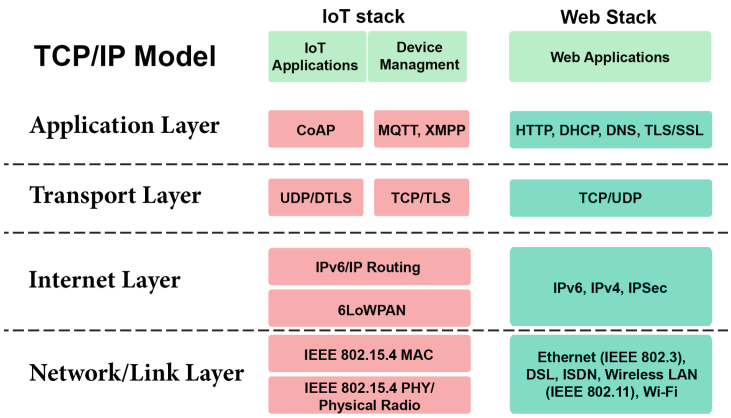

Fig. 1. Standardized protocols for the Internet of Things

Table 1. Differences between the application layer protocols for the Internet of Things

Protocol	Transport	QoS options	Architecture	Security
CoAP	UDP	Yes	Request/response	DTLS
MQTT	TCP	Yes	Publish/subscribe	TLS/SSL
XMPP	TCP	No	Request/response, publish/subscribe	TLS/SSL

After Introduction Section, in Sect. 2 we will present the scenario for measuring the power consumption of application layer protocols for the Internet of Things. Here, we will provide an overview of the protocols and their architecture. We will introduce the operating system for IoT, and the tools that come with it. The main results are placed in the Sect. 3, where a brief overview of the analysis on various protocols is given, followed by discussions and final conclusions.

1.1 Previous Work

To our knowledge, there are no many papers and researches relating to power consumption of application layer protocols for the IoT. Son Han used the Contiki operating system for IoT, and tools Powertrace and Energest to assess power consumption [4]. He also gives an overview of analyzes carried out using the CM5000 wireless sensor module and a simplified version of Powertrace [5]. Dunkels et al. gave a solution for implementation of energy efficient CoAP protocol [6]. They used more sensor modules in their research, but they did not elaborate the energy consumptions in different time intervals at different stages on module.

2 Scenario

We will perform measurements for three IoT application layer protocols: CoAP, MQTT and XMPP. These protocols have different architecture, and if we use in practice, we have to know it.

The Constrained Application Protocol (CoAP) is a specialized web transfer protocol for use with constrained nodes and constrained networks. The nodes often have 8-bit microcontrollers with small amounts of RAM and ROM, while constrained networks such as IPv6 over Low-Power Wireless Personal Area Networks often have high packet error rates and a typical throughput of 10 s of kbit/s. CoAP provides a request/response interaction model between application endpoints, supports built-in discovery of services and resources, and includes key concepts of the Web such as URIs and Internet media types. CoAP is designed to easily interface with HTTP for integration with the Web while meeting specialized requirements such as multicast support, very low overhead, and simplicity for constrained environments [7].

Message Queue Telemetry Transport (MQTT) protocol was discovered by IBM and targets lightweight Machine to Machine (M2M) communications. It is an asynchronous publish/subscribe protocol that runs on top of the TCP stack. This type of protocol meet better the IoT requirements then request/response since clients do not have to request updates thus, the network bandwidth is decreasing and the need for using computational resources is dropping. In MQTT there is a Broker (server) that contains topics. A client can be a publisher that sends information to the broker at a specific topic or subscriber that receives automatic messages every time there is a new update of the topic [3].

Extensible Messaging and Presence Protocol (XMPP) is a protocol that is based on XML (Extensible Markup Language) and intended for instant messaging and online presence detection. It functions between or among servers, and facilitates near-real-time operation. The protocol may allow Internet users to send instant messages to anyone else on the Internet, regardless of differences in operating systems and browsers. In our examples we will use Contiki OS [8]. It is operating system for IoT. The distribution of Contiki known as Instant Contiki is Ubuntu Linux virtual machine that runs in the VMWare Player and contains all the tools, compilers and simulators needed to develop applications for IoT. We will use the latest version of Instant Contiki 3.0 which offers

improvements over its older versions. One of the improvements in the latest version is implementation of the MQTT protocol.

In our research for power consumption we will use network simulator Cooja [12]. It allows simulation on small and large networks of Contiki sensor modules. The modules can be emulated at the hardware level. It is slower but always true examination of the properties of the system, or the less detailed level, which is faster and allows simulation of large networks.

For our scenario, in our Cooja simulation we will use the Z1 Zolertia wireless sensor module (WSN) [9]. Z1 is equipped with the second generation of MSP430F 2617 low power microcontroller which owns 16-bit RISC CPU with 16 MHz clock speed, 8 KB RAM, 92 KB flash memory. In our Cooja simulation, sensor nodes have 8 MHz clock speed, and we will take that into account in the calculations of energy consumption. This module includes the CC2420 transceiver, which is suitable for 802.15.4, and operates at 2.4 GHz with an effective data rate of 250 Kbps. For CoAP protocol, we will use Z1 mote on the client and on the server side. We will measure power consumption on the client and on the server side, and in cases where we have 1–5 clients that access the server sensor module or without clients. Doing so will determine the changes in power consumption in this case. For the other two protocols MQTT and XMPP, we will use Z1 only on client side since the implementation of MQTT broker and XMPP server is a web oriented. We will use RPL border router to establish a communication. The main goal of a router is to connect one network to another.

In the analysis of the CoAP protocol, the connection is established between client and server. First the client creates a connection to the server and then periodically sends data to any of the predefined URL for service discovery. The selection is made randomly using random function.

For the MQTT protocol, Mosquitto broker is installed on the local machine, which we will use to connect Z1 module from Cooja. On one side we have client with installed client program on Z1 module. To connect Z1 to the broker we have used a RPL border router which is also installed on another Z1 module [10]. The router opens a port to establish a connection with the broker using tunslip6. This tool is activated through the terminal in Instant Contiki directory:/home/user/contiki-3.0/tools. Communication is done by running this command (while we are still in the same directory):

```
sudo./tunslip6 aaaa::1/64 -L -a localhost -p 60002
```

60002 is a port that is open by RPL border router module in the Cooja simulation. The program that will be used is written in the C programming language as all others Contiki OS programs. With the execution of the program multiple messages will be published on the topic (topic_name) of mosquitto broker. This is done using the following function:

```
mqtt_publish(“topic_name”, “message”, 0, 1);
```

On the local machine we have client that is subscribed to all topics of the broker.

For XMPP, we will use Prosody XMPP server that is installed on the local machine, and Pidgin client. XMPP client accessing the chat room in Pidgin and it prints

predefined text that was previously adjusted in the program which is installed as firmware of the wireless sensor module in Cooja:

```
xmpp_send_muc_msg("contiki rocks",
"'room@conference.localhost'");
```

Klauck developed XMPP client for Contiki OS that is optimized and supports chat for multiple users (Multi user chat) [11].

3 Analysis of Power Consumption

By executing the application in Cooja, in the mote output we can see module power consumption in several stages of the module as: ALL_CPU, ALL_LPM, ALL_TX and ALL_RX. ALL_CPU is the total (high) CPU (CPU in active mode), in the form of number of ticks. ALL_LPM is the total number of ticks in state LPM (CPU in Low Power Mode). ALL_TX and ALL_RX are the total number of clock ticks in state TX (Transmit) and RX (Receive), respectively. These outputs are enabled by using the tool called Powertrace which is part of Instant Contiki. To use it we have to add this in the program Makefile:

```
APP += powertrace
```

While in the code of the program we have to add this:

```
#include "powertrace.h"
powertrace_start(CLOCK_SECOND * 10);
```

The last expression shows that Powertrace will print the results every 10 s. We can change it depending on the needs. In our research we use 10 s as time interval.

3.1 Power Consumption Calculations

We calculated the power consumption by using the following formula:

$$Power\_consumption = \frac{Energest\_Value * Current * Voltage}{RTIMER\_SECOND * Runtime} \quad (1)$$

Energest_Value represents the difference between number of ticks of the clock (spent in a particular state as CPU, LPM, TX or RX) between the two time intervals. These are values obtained from Powertrace marked with the prefix ALL. We got a value of Current for CPU, LPM, TX and RX from the Z1 Datasheet. The Voltage for Z1 module is 3 V. RTIMER_SECOND is 32768. Runtime is the time interval in which we perform measurements. In our case it is 10 s. The total time interval is 110 s, i.e. 00:00.000 to 01:50.000 in Cooja simulation.

3.2 Results and Discussions

The results obtained are presented in tables and graphs. In the graphs, time intervals are represented on the x-coordinate, while power consumptions (in mW) are represented on the y-coordinate.

Figure 2 shows the power consumption of CoAP client (Z1 module) at all time intervals. Based on the average capacity of AA battery that is 2500 mAh, and the nominal voltage of 1.5 V, we can estimate the battery life of wireless sensor module (Z1 module). As we can see from the graph on Fig. 2, the highest consumption of energy is approximately 1.523 mW (60 s.). The lowest power consumption is approximately 0.8299 mW (30 s.). In other time intervals the power consumption is similar, and it is approximately 0.8 mW. For CoAP client the average power consumption of the test interval is 0.90796957 mW (Fig. 2).

Energy Consumption(Power - mW)				
CPU	LPM	TX	RX	Total
0.29191589	0.00029414	0.07949158	0.46506592	0.83676752
0.26719666	0.00029463	0.09175781	0.47195068	0.83119978
0.27488708	0.00029447	0.07678345	0.47797485	0.82993986
0.27301025	0.00029451	0.08920898	0.47160645	0.8341202
0.28056335	0.00029436	0.099245	0.4640332	0.84413592
0.49108887	0.00029015	0.51167725	0.5197998	1.52285607
0.28340149	0.00029431	0.07981018	0.48279419	0.84630016
0.27932739	0.00029439	0.08920898	0.4729834	0.84181416
0.27209473	0.00029453	0.08920898	0.48210571	0.84370395
0.28683472	0.00029424	0.099245	0.46248413	0.84885808
				0.90796957

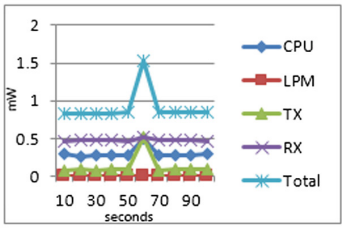

Fig. 2. Power consumption for CoAP client

The battery life of the Z1 module using CoAP protocol would be [4]:

$$(2500\text{mAh} * 1.5\text{V} * 2)/(0.90796957\text{mW} * 24\text{h} * 365\text{days}) = 0.942943917\,\text{years} \quad (2)$$

Figures 3, 4, 5, 6, 7 and 8 show the consumption in cases when CoAP server has 1–5 clients, or without clients. In Table 2 we can see the battery life of the module which is used as CoAP server, in cases where we have from 1 to 5 clients, or if we do not have clients. According to our analysis the battery life is reduced if multiple clients accessing the server. The average power consumption of CoAP server with 1 client is approximately 0.843 mW. As we can see from the graphs, the average power consumption increases by approximately 0.3 mW, with each added client.

Figure 9 shows the power consumption of MQTT client (Z1 module) at all time intervals. As we can see in the graph on Fig. 9, the highest power consumption of MQTT protocol is approximately 1.25 mW (10 s). The lowest power consumption is approximately 0.45 mW (90 s), The average power consumption derived from our research for MQTT protocol is 0.779582753 mW, therefore the battery life of the module using this protocol would be approximately 1.098234126 years.

Energy Consumption (Power - mW)				
CPU	LPM	TX	RX	Total
0.23117065	0.00029535	0.09828918	0.48985107	0.81960627
0.21025085	0.00029577	0.09127991	0.46300049	0.76482702
0.20722961	0.00029583	0.10067871	0.4531897	0.76139385
0.21432495	0.00029569	0.1086438	0.44458374	0.76784818
0.21881104	0.0002956	0.08299622	0.48658081	0.78868366
0.42718506	0.00029143	0.53063416	0.50224365	1.4603543
0.20787048	0.00029582	0.08347412	0.46971313	0.76135356
0.21620178	0.00029565	0.1084845	0.44372314	0.76870508
0.19747925	0.00029602	0.09414734	0.42943726	0.72135987
0.22009277	0.00029558	0.09112061	0.50413696	0.81564592
				0.84297777

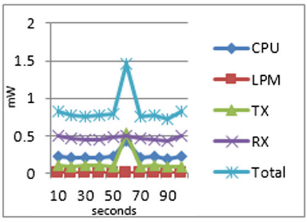

Fig. 3. Power consumption for CoAP server that has 1 client

Energy Consumption (Power - mW)				
CPU	LPM	TX	RX	Total
0.3968811	0.00029202	0.23911194	0.68176392	1.31804898
0.30775452	0.00029381	0.16678894	0.58950806	1.06434532
0.34025574	0.00029316	0.21585388	0.58520508	1.14160785
0.33879089	0.00029319	0.20263184	0.58227905	1.12399497
0.33370972	0.00029329	0.18287842	0.63339844	1.15027986
0.5365448	0.00028923	0.62478149	0.65697876	1.81859429
0.32510376	0.00029346	0.1814447	0.59966309	1.10650501
0.32881165	0.00029339	0.20438416	0.56455078	1.09803997
0.3182373	0.00029359	0.20326904	0.56231323	1.08411317
0.33197021	0.00029332	0.17459473	0.64131592	1.14817418
				1.20537036

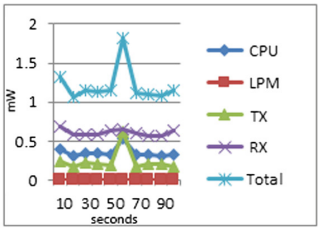

Fig. 4. Power consumption for CoAP server that has 2 clients

Energy Consumption (Power - mW)				
CPU	LPM	TX	RX	Total
0.54547119	0.00028906	0.50052612	0.67246948	1.71875586
0.46815491	0.00029061	0.17156799	0.92823853	1.56825204
0.43936157	0.00029119	0.26714905	0.71601563	1.42281743
0.45002747	0.00029098	0.31063843	0.77866699	1.53962386
0.43496704	0.00029127	0.27830017	0.68916504	1.40272352
0.65716553	0.00028683	0.70475098	0.84940796	2.21161129
0.46440125	0.00029068	0.29263733	0.69587769	1.45320694
0.45812988	0.00029081	0.27065369	0.73271118	1.46178556
0.45172119	0.00029094	0.3085675	0.73804688	1.49862651
0.42599487	0.00029146	0.26810486	0.72720337	1.42159456
				1.56989976

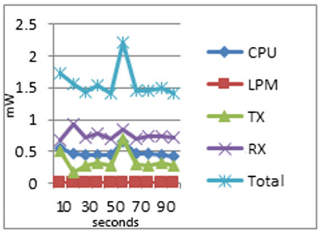

Fig. 5. Power consumption for CoAP server that has 3 clients

Energy Consumption (Power - mW)				
CPU	LPM	TX	RX	Total
0.6002655	0.00028788	0.35062317	0.92686157	1.87803813
0.62644958	0.00028743	0.4530542	0.86541504	1.94520625
0.57971191	0.00028836	0.39650208	0.89192139	1.86842374
0.55279541	0.0002889	0.34839294	0.86042358	1.76190084
0.55773926	0.0002888	0.40717529	0.89002808	1.85523143
0.77554321	0.00028445	0.80479248	0.94613892	2.52675906
0.56707764	0.00028862	0.37611145	0.86489868	1.80837639
0.58277893	0.0002883	0.39968811	0.85164551	1.83440085
0.54977417	0.00028896	0.36527893	0.88159424	1.7969363
0.57165527	0.00028853	0.40637878	0.82169678	1.80001936
				1.90752924

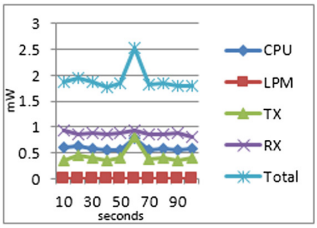

Fig. 6. Power consumption for CoAP server that has 4 clients

Energy Consumption (Power - mW)				
CPU	LPM	TX	RX	Total
0.70628357	0.00028584	0.44763794	1.01240479	2.16661213
0.74789429	0.00028501	0.54624573	1.0943335	2.38875852
0.66508484	0.00028667	0.44620422	0.98211182	2.09368755
0.67991638	0.00028638	0.48889709	0.9810791	2.15017895
0.68453979	0.00028628	0.48873779	0.98882446	2.16238833
0.94633484	0.00028104	0.91678162	1.1168811	2.9802786
0.6787262	0.0002864	0.45130188	0.98125122	2.11156569
0.68692017	0.00028623	0.50084473	0.98125122	2.16930235
0.68330383	0.0002863	0.45687744	0.99192261	2.13239018
0.67025757	0.00028655	0.46850647	0.95870361	2.09775421
				2.24529165

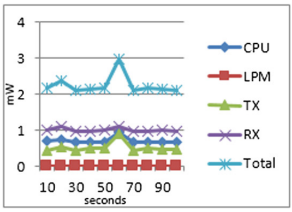

Fig. 7. Power consumption for CoAP server that has 5 clients

Energy Consumption (Power - mW)				
CPU	LPM	TX	RX	Total
0.09960938	0.00029796	0	0.33046875	0.43037609
0.0978241	0.000298	0	0.33046875	0.42859085
0.09786987	0.000298	0	0.33046875	0.42863662
0.09915161	0.00029797	0	0.33046875	0.42991833
0.09887695	0.00029798	0	0.33046875	0.42964368
0.30665588	0.00029382	0.42214966	0.33873047	1.06782983
0.10107422	0.00029793	0	0.33046875	0.4318409
0.09928894	0.00029797	0	0.33046875	0.43005566
0.0987854	0.00029798	0	0.33046875	0.42955213
0.0995636	0.00029796	0	0.33046875	0.43033031
				0.49367744

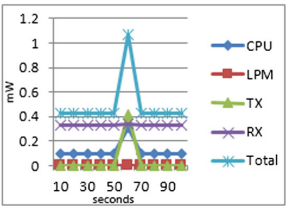

Fig. 8. Power consumption for CoAP server without clients

Table 2. Power consumption and battery life for CoAP server

	Power consumption (mW)	Lifetime (year)
1 client	0.84297777	1.015642896
2 clients	1.205370361	0.710291551
3 clients	1.569899757	0.545362454
4 clients	1.907529235	0.448834213
5 clients	2.245291651	0.381315444
Without clients	0.493677441	1.734258674

Energy Consumption (Power - mW)				
CPU	LPM	TX	RX	Total
0.35453796	0.00029279	0.50419006	0.39329224	1.25231305
0.33192444	0.00029324	0.49080872	0.37745728	1.20048367
0.13961792	0.00029709	0.01274414	0.35353271	0.50619186
0.12432861	0.0002974	0	0.37108887	0.49571488
0.34780884	0.00029292	0.50387146	0.36179443	1.21376765
0.16470337	0.00029658	0.02867432	0.42651123	0.62018549
0.1197052	0.00029748	0	0.33046875	0.45047143
0.11920166	0.00029749	0	0.33046875	0.4499679
0.1187439	0.0002975	0	0.33046875	0.44951015
0.32675171	0.00029334	0.49144592	0.33873047	1.15722144
				0.77958275

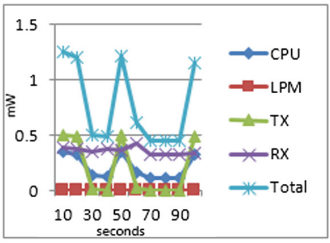

Fig. 9. Power consumption for MQTT client

Figure 10 shows the power consumption of XMPP client. As we can see in the graph on Fig. 10, the highest power consumption of XMPP protocol is approximately 56.9765 mW (40 s), while the lowest power consumption is approximately 56.5576 mW (90 s). According to our research, average power consumption is approximately 56.73892177 mW. The battery life according to these data would be 0.015089543 years. XMPP is the largest consumer of energy in comparison with the other two protocols on application layer for the IoT.

Energy Consumption (Power-mW)				
CPU	LPM	TX	RX	Total
0.53329468	0.00028925	0.08936829	56.3024084	56.9253607
0.54382324	0.00028903	0.20167603	56.1810645	56.9268528
0.5625	0.00028866	0.38821838	55.9777917	56.9287988
0.60978699	0.0002877	0.3807312	55.9857092	56.9765151
0.43107605	0.00029129	0.08650085	56.3058508	56.823719
0.16914368	0.00029652	0.01274414	56.3857141	56.5678984
0.15760803	0.00029675	0	56.4	56.5579048
0.15779114	0.00029674	0	56.4	56.5580879
0.1572876	0.00029675	0	56.4	56.5575844
0.16767883	0.00029655	0.01624878	56.3822717	56.5664959
				56.7389218

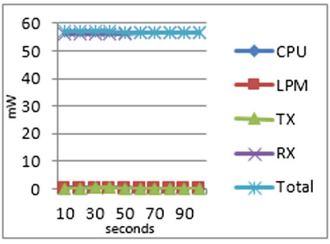

Fig. 10. Power consumption for XMPP client

For all protocols, the most energy is spent in a state RX, while the least is spent in a state LPM.

4 Conclusion

From the analysis of the application layer protocols for the IoT, we can conclude that the average power consumption varies between CoAP, MQTT and XMPP protocol. The average power consumption depends on several states: CPU, LPM, TX and RX. According to the test results, we can conclude that CoAP and MQTT protocols provide major power savings, which is not the case with the XMPP protocol.

References

1. Emerging open and standard protocol stack for internet of things. http://www.slideshare.net/aniruddha.chakrabarti/mphasis-digital-pov-emerging-open-standard-protocol-stack-for-iot
2. Gehrmann, C., Selander, G., Seitz, L.: Authorization framework for the internet-of-things. In: 2013 IEEE 14th International Symposium and Workshops, pp. 1–6, Madrid (2013)
3. Gallego, F.V., Zarate, J.A., Chatzimisios, P., Karagiannis, V.: A survey on application layer protocols for the internet of things. Trans. IoT Cloud Comput. **3**(1), 11–17 (2015)
4. Contiki, O.S.: Using powertrace and energest power profile to estimate power consumption. http://thingschat.blogspot.mk/2015/04/contiki-os-using-powertrace-and.html
5. Sample data for powertrace using CM5000 motes. https://github.com/sonhan/contiki-sonhan/
6. Dunkels, A., Kovatsch, M., Duquennoy, S.: A low-power CoAP for Contiki. In: MASS 2011 Proceedings of 2011 IEEE 8th International Conference on Mobile Ad-Hoc and Sensor Systems, pp. 855–860. IEEE Computer Society, Washington, DC, USA (2011)
7. Bormann, C., Hartke, K., Shelby, Z.: The constrained application protocol (CoAP), internet engineering task force (IETF), Universitaet Bremen TZI, Germany (2014)
8. Contiki: The open source OS for the internet of things. http://www.contiki-os.org/
9. Z1 Datasheet. http://zolertia.sourceforge.net/wiki/images/e/e8/Z1_RevC_Datasheet.pdf
10. RPL border router. http://anrg.usc.edu/contiki/index.php/RPL_Border_Router
11. Kirsche, M., Klauck, R.: Chatty things - making the internet of things readily usable for the masses with XMPP. In: Proceedings of 8th International Conference on Collaborative Computing: Networking, Applications and Worksharing, Pittsburgh, Pennsylvania, USA, pp. 60–69, (2012)
12. Get started with Contiki, http://www.contiki-os.org/start.html

Improving Medical Cases Retrieval Using an Online Fact Database

Ivan Kitanovski(✉), Katarina Trojacanec, Ivica Dimitrovski, and Suzana Loshkovska

Faculty of Computer Science and Engineering,
University "Ss. Cyril and Methodius", Skopje, Macedonia
{ivan.kitanovski,katarina.trojacanec,ivica.dimitrovski,
suzana.loshkovska}@finki.ukim.mk
http://www.finki.ukim.mk

Abstract. This paper presents an approach for retrieval of medical cases using a novel query expansion method. The approach relies purely on the text data in the medical cases. The cases are indexed with Terrier IR search engine based on their text content including the caption of the figure contained within them. Furthermore, in the retrieval phase there is an input consisted of a long text query in a narrative form. The input query is expanded by using on-line fact databases, such as Freebase, with the aim that this will add more terms relevant to the concepts mentioned in the text. The goal is to provide a way of query expansion, so that the query is more defined, which should provide more narrowed and precise results in the retrieval. The retrieval is done with the BM25 weighting model. Our approach shows that expanding the input text query in this fashion can provide a boost in the retrieval performance.

Keywords: Medical articles retrieval · Query expansion · Pubmed articles · Terrier IR · Freebase

1 Introduction

The rapid advances in technology are in-part resulting in tools which we use everyday and help make our lives easier. These tools depend on the data collections, which are growing constantly. Thorough research on such data is needed, since these tools can range from simple applications to complex decision making systems. The data that these tools use can appear in multiple forms like text, image, web pages, video clips etc. The value that it brings depends on the context of the situation where it is used.

Our main focus of interest in this paper is how to use the data in the medical context. Finding the right data related to a medical question is a very complex task, but an important one as it can help the physician with the current case he is working on or provide valuable insight for a researcher or student. In this sense we focus on a information retrieval system, which is a vital tool in the

G. Stojanov and A. Kulakov (eds.), *ICT Innovations 2016*,
Advances in Intelligent Systems and Computing 665,
https://doi.org/10.1007/978-3-319-68855-8_20

medical context, if we take into consideration that there are 12400 different categories of medical conditions [1]. More precisely, we focus on retrieval of medical articles (cases), since they contain a lot of biomedical information and empower healthcare experts by allowing them to find related data or explore cases with similar symptoms or conditions [2] in medical information repositories. Already, there are many systems which allow such retrieval services: Pubget [3], Pubmed [4], eTBLAST [5], etc. PubMed, for instance, is a search engine created for easier access to the Medline database [6], which contains over 22 million articles. Currently, Pubmed (as well the other systems) work based on keyword search on different fields such as the main text, author, and date. But, according to [7] a more real-life scenario would be where the queries are narrative and where the user can explain his current condition in more details.

In this paper we propose a query expansion method for text-based retrieval of medical articles. The method uses a medical knowledge tool to detect medical terms in a given query and uses a generic on-line fact database to provide a broader explanation of the detected terms. Then, the expanded terms are added to the original query. The idea behind this approach is that on-line fact databases maintained by a large community of users with diverse backgrounds should help provide better retrieval results.

The rest of the paper is organized as follows: Sect. 2 holds the related work. The prosed method for query expansion is presented in Sect. 3. The experimental setup and evaluation measures are detailed in Sect. 4. Section 5 contains the experimental results and discussion. The concluding remarks and planned future work is presented in Sect. 6.

2 Related Work

Medical case retrieval is an ongoing challenge in the medical information systems domain. There have been many attempts at tackling the issue, usually based on proven and existing search engine platforms.

Herrera et al. [8] based their platform on the Lucene search engine. The proposed approach took into consideration the entire article content for indexing. The approach concatenated the title, abstract and the text content of the article and built and index based on that. This is a standard retrieval approach and it is important to note that this performed well only on the 2012 version of the ImageCLEF dataset.

Vahid et al. [9] use the Terrier IR search engine as a platform on top which they built their retrieval system. In this system, the entire text content of the article is taken into consideration and it is preprocessed in the following manner: special signs and stop words are removed, the stemming is applied. In the retrieval stage they apply TF-IDF weighting model, which is one of the most frequently used models in IR systems. The approach is stable and provides consistent results across different versions of the dataset.

Simpson et al. [10] use the Essie search engine as a retrieval platform. Their approach is based on UMLS concept expansion, which is a built-in feature in

Essie. The approach provided good results for text-based image retrieval tests, but poor on the case-based retrieval ones.

There are many more approaches [11,12] based on existing search engines, but Lucene and Terrier IR are the ones which are most frequently used, since they are generic and easily accessible. One of the best results were reported with the Terrier IR, also, it has efficient search methods for large-scale document collections. Hence, based on that and our previous work [13] in the field, we decided to use it in our experiments.

The other aspect of our research is related to query expansion. Query expansion has proven useful in generic information retrieval systems by making queries match to more relevant documents that might not contain the exact terms. The effect of this is more visible in short queries [14]. Typical query expansion techniques [15] take into consideration statistical correlation, synonyms, the knowledge of morphology of words and the use of dictionaries to improve the retrieval results.

Voorhees [16] found that automatic query expansion using WordNet can lead to degradation in performance, while hand picking the concepts improves ambiguous queries.

Hersh et al. [17] found that adding MeSH terms to the query is a simple yet effective approach that leads to better retrieval performance.

An interesting text-based retrieval framework is presented in [18]. The authors use the Indri search engine as a retrieval platform for their framework. The retrieval phase is consisted of using unigram language model with Dirichlet prior smoothing. The novel part of this approach in the way they apply query expansion. The framework uses an external bibliographic source i.e. Medline. Each query is first executed against the Medline database and the top n documents are retrieved. Then, the MeSG terms of the retrieved documents are added to the query and the expanded query is executed against the ImageCLEF database. This approach is, to our knowledge, the best reported on the dataset, but not for all versions, so we believe there is room for improvement.

The work done in query expansion is diverse and with varying results. Hence, most of the approaches focus on expansion by adding medical terms to the query. Hence, we focus on providing a automated way of query expansion for medical contact, but with publicly available generic and domain-specific knowledge databases.

3 Query Expansion with On-Line Fact Database

The diagram of the proposed approach is presented on Fig. 1. The approach is separated in two stages i.e. an on-line and off-line stage.

The off-line stage deals with the indexing structure of the data. It is consisted of preprocessing and indexing of the medical cases. Preprocessing is a procedure where the cases have to be processed so that they are cleaned up for creating a more efficient index. First, the special signs are removed from the cases. Afterwards, all the stop words are removed. These are words which have no semantic

meaning, but appear frequently in the text and add unnecessary noise. Token normalization is the next step. At this step all words are converted to lower case. The final step of the preprocessing is called stemming. At this stage, the words are reduced to their root form. After the preprocessing is done a inverted index is created using single-pass indexing.

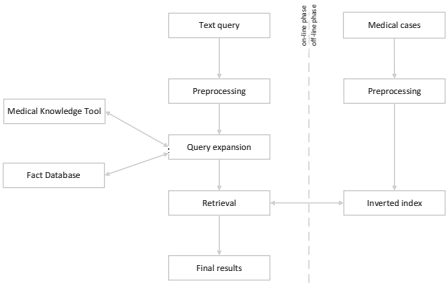

Fig. 1. Diagram of retrieval of medical cases with the proposed query expansion method

In the on-line stage the user provides the input in the form of a narrative text query. First, the query is preprocessed in the same manner as the medical cases. The next phase in the on-line stage is the query expansion. In this phase, we use a medical knowledge tool to detect the medical terms in the query. Afterwards, we query the detected medical terms on the fact database and use the synonyms to expand the query. In the end, we use the expanded query to search against the inverted index using a weighting model and provide the results. The weighting model is a mathematical model which computes a numeric score, which gives an estimate of how similar a given query is to a given article. The more similar the items, the higher the number of the computed score. The score is calculated for each query against each article and the articles are sorted in a descending manner grouped by the query and the final result is provided.

4 Experimental Setup and Evaluation

4.1 Dataset

To evaluate our proposed approach, we referred to the ImageCLEF 2013 [12] data collection. It contains text and visual data. There is a specific subset in it which is designed with the purpose to evaluate medical case-based retrieval algorithms. It is consisted of 74 654 medical articles (cases), which are predominantly journal articles from PubMed/Medline database. The articles are stored in a XML format presented on Fig. 2. Each article is consisted of several parts: title, abstract, text content of the articles (referred as full-text) and text captions for the images depicted in the article. We have expanded the articles by incorporating their MeSH heading terms from the PubMed description of the articles.

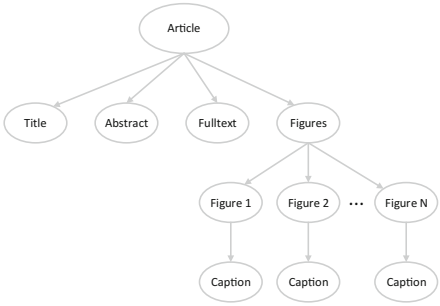

Fig. 2. Diagram of the XML structure of a medical article

The data collection also provides 35 queries which should be used to case-based retrieval approaches. All queries are short narrative case descriptions, each containing 2–3 image for allowing multimodal or content-based retrieval experiments. Our primary focus is on text-based retrieval, so in our experiments we only used the text part of the queries. A small subset of the provided queries is presented below:

- **Query 1**. A 56-year-old woman with Hepatitis C, now with abdominal pain and jaundice. Abdominal MRI shows T1 and T2 hyperintense mass in the left lobe of the liver which is enhanced in the arterial phase.
- **Query 2**. A 50-year-old man with severe right flank pain and hematuria. Renal ultrasound shows a markedly echogenic lesion with a posterior acoustic shadow measuring about 8x10mm in the right kidney.
- **Query 3**. A 49-year-old woman with a prolapsed mass in the opening of her urethra. Pelvic CT shows a heterogeneously enhanced mass on the female urethra. Pathology shows ramifying papillae, high nuclear/cytoplasmic ratio, and brisk mitotic activity.

4.2 Retrieval Details

For the experimental part of approach we used a open source search engine platform. We referred to Terrier IR [19] as a comprehensive, flexible and transparent platform for research and experimentation in text retrieval. We used Terrier IR to preprocess, index the articles and retrieve them in the later stage. In the preprocessing stage, we use Terrier's built-in tokenizer for English and the standardized list of stop-words for stop-words removal. Whereas, for stemming we used Porter stemmer [20], which is the most frequently used stemmer for English. In the retrieval stage we needed a weighting model to perform the retrieval and here we referred to BM25 [21] as it is reported as of the most appropriate models for this type of retrieval problems [22]. The query expansion method consisted of two stages: 1. medical term detection, 2. expansion using a fact database. For medical term detection we used the Medical Text Index (MTI) which is a part of MetaMap developed and maintained by the National Library of Medicine [23].

MTI accepts large pieces of text (up to 10000 words) and returns descriptions for each term (or phrase) detected in the text. Each detect term/phrase is assigned a score, which represents it's *importance* in the text. We treated all terms/phrases above the term "Homo sapiens" which we treated as noise, since it appears in all queries. After the medical term detection stage, we query the detected terms against an on-line fact database. In our experiments we used Freebase [24], which is a collaboratively created database for structuring human knowledge. For each query, we used it's medical terms to query Freebase and add the Freebase synonyms for the provided term to the query.

4.3 Evaluation Measures

For evaluation metrics, we used the standardized ImageCLEF evaluation metrics:

- Mean Average Precision (MAP) - the mean of the average precision scores for each query
- Precision at first 10 (P10) - precision of the first (top) 10 returned articles (cases)
- Precision at first 30 (P30) - precision of the first (top) 30 returned articles (cases).

According to ImageCLEF [12] practices MAP is processed over the 1000 top returned cases per query.

5 Results and Discussion

The goal of our research was to answer the question: *Can query expansion using on-line fact database increase the retrieval over standard retrieval?*

For that purpose we created two types of experiments. The first experiment is the standard (baseline) retrieval, where we perform the retrieval using the original query, without any additional modification. The second experiment is the retrieval using the query expansion method we proposed. The results from our experiments are presented in Table 1.

Table 1. Results from the two experiments performed.

	MAP	P10	P30
Baseline	0.2004	0.2029	0.1476
Freebase expansion	0.2179	0.2086	0.1695

The presented results show that using query expansion from on-line fact databases can increase the retrieval performance. There is even an increase in P10 and P30 metrics. These are key metrics as they measure the top returned

results, which is what users interact with mostly. Overall, the reason for the increase in performance is due to the fact that the terms used for the expansion i.e. the freebase synonyms for the medical terms are more descriptive than the original medical terms in the query in the sense that they are more widely described.

6 Conclusion

In this paper we presented a novel method for query expansion in text-based retrieval of medical articles. Our experiment showed that the presented method provided a boost in retrieval performance. The proposed method relies on a medical term detection tool and an on-line fact database. The key feature is expanding with queries with terms extracted from a generic database of knowledge. The logic behind this is that it brings more descriptive and non-medical terms into the queries, which broadens the queries and allows for better performance.

In the future we plan on integrating on-line medical retrieval systems, combine their datasets and retrieval features into our retrieval platform. The goal is to use standardized techniques for medical articles retrieval and boost them by applying them with our expansion methods.

Acknowledgments. This work is partially supported by the Faculty of Computer Science and Engineering, Skopje, Macedonia as a part of the project "Scalable Photo Annotation".

References

1. Dye, C., Reeder, J.C., Terry, R.F.: Research for universal health coverage. World Health Organization (2013)
2. Mourão, A., Martins, F., Magalhães, J.: Multimodal medical information retrieval with unsupervised rank fusion. Comput. Med. Imaging Graph. **39**, 35–45 (2015)
3. Pubget. http://www.nlm.nih.gov/pubs/factsheets/medline.html. Accessed 9 June 2016
4. Bodenreider, O.: The unified medical language system (umls): integrating biomedical terminology. Nucleic Acids Res. **32**(suppl 1), D267–D270 (2004)
5. Errami, M., Wren, J.D., Hicks, J.M., Garner, H.R.: eTBLAST: a web server to identify expert reviewers, appropriate journals and similar publications. Nucleic Acids Res. **35**(suppl 2), W12–W15 (2007)
6. Pubget. http://pubget.com. Accessed 9 May 2015
7. Peters, C.: Cross language evaluation forum. D-Lib (2000)
8. de Herrera, A.G.S., Markonis, D., Eggel, I., Müller, H.: The medgift group in imageclefmed 2012. In: CLEF (Online Working Notes/Labs/Workshop) (2012)
9. Vahid, A.H., Alpkocak, A., Hamed, R.G., Caylan, N., Ozturkmenoglu, O.: Demir at imageclefmed 2012: inter–modality and intra–modality integrated combination retrieval. Working Notes CLEF vol. 2012 (2012)

10. Simpson, M.S., You, D., Rahman, M.M., Demner-Fushman, D., Antani, S.K., Thoma, G.R.: ITI's participation in the 2013 medical track of imageclef. In: CLEF (Online Working Notes/Labs/Workshop) (2013)
11. Vanegas, J.A., Caicedo, J.C., Camargo, J.E., Ramos-Pollán, R., González, F.A.: Bioingenium at imageclef 2012: textual and visual indexing for medical images. In: CLEF (Online Working Notes/Labs/Workshop) (2012)
12. de Herrera, A.G.S., Kalpathy-Cramer, J., Demner-Fushman, D., Antani, S., Müller, H.: Overview of the imageclef 2013 medical tasks. Working Notes of CLEF (2013)
13. Kitanovski, I., Dimitrovski, I., Loskovska, S.: FCSE at imageclef 2012: evaluating techniques for medical image retrieval. In: CLEF (Online Working Notes/Labs/Workshop) (2012)
14. Navigli, R., Velardi, P.: An analysis of ontology-based query expansion strategies. In: Proceedings of the 14th European Conference on Machine Learning, Workshop on Adaptive Text Extraction and Mining, Cavtat-Dubrovnik, Croatia, pp. 42–49. Citeseer (2003)
15. Carpineto, C., Romano, G.: A survey of automatic query expansion in information retrieval. ACM Comput. Surv. (CSUR) **44**(1), 1 (2012)
16. Voorhees, E.M.: Query expansion using lexical-semantic relations. In: SIGIR94, pp. 61–69. Springer (1994)
17. Hersh, W., Price, S., Donohoe, L.: Assessing thesaurus-based query expansion using the umls metathesaurus. In: Proceedings of the AMIA Symposium, p. 344. American Medical Informatics Association (2000)
18. Choi, S., Lee, J., Choi, J.: Snumedinfo at imageclef 2013: medical retrieval task. In: CLEF 2013 Evaluation Labs and Workshop, Online Working Notes (2013)
19. Ounis, I., Amati, G., Plachouras, V., He, B., Macdonald, C., Lioma, C.: Terrier: a high performance and scalable information retrieval platform. In: Proceedings of the OSIR Workshop, pp. 18–25. Citeseer (2006)
20. Macdonald, C., Plachouras, V., He, B., Lioma, C., Ounis, I.: University of glasgow at webclef 2005: experiments in per-field normalisation and language specific stemming. In: Accessing Multilingual Information Repositories, pp. 898–907. Springer (2006)
21. Amati, G., Van Rijsbergen, C.J.: Probabilistic models of information retrieval based on measuring the divergence from randomness. ACM Trans. Inf. Syst. (TOIS) **20**(4), 357–389 (2002)
22. Kitanovski, I., Dimitrovski, I., Loskovska, S.: FCSE at medical tasks of imageclef 2013. In: CLEF (Working Notes) (2013)
23. Aronson, A.R.: Effective mapping of biomedical text to the UMLS metathesaurus: the metamap program. In: Proceedings of the AMIA Symposium, p. 17. American Medical Informatics Association (2001)
24. Bollacker, K., Evans, C., Paritosh, P., Sturge, T., Taylor, J.: Freebase: a collaboratively created graph database for structuring human knowledge. In: Proceedings of the 2008 ACM SIGMOD International Conference on Management of Data, pp. 1247–1250. ACM (2008)

Improving Scalability of Web Applications by Utilizing Asynchronous I/O

Gjorgji Rankovski(✉) and Ivan Chorbev

Faculty of Computer Science and Engineering,
University of Ss. Cyril and Methodius,
Rugjer Boskovikj 16, P.O. Box 393, 1000 Skopje, Republic of Macedonia
gorgi.rankovski@gmail.com, ivan.chorbev@finki.ukim.mk

Abstract. The focus of the paper is the use of asynchronous I/O calls in web applications to improve their scalability, by increasing the number of requests per second that it can process and decreasing the average response time of the system. Popular development frameworks have always included only blocking I/O APIs in their base, making asynchronous I/O methods hard to implement and maintain. Significant effort has been made in recent years to enrich these frameworks with better syntax for asynchronous API to improve developers' experience and encourage its use. Such improvement in .NET's syntax is put to the test in this paper and the results are presented and evaluated.

Keywords: Distributed system · Web application · Web service · Asynchronous programming · I/O · Load test

1 Introduction

Web applications that are publically available to wide audiences have a requirement to handle growing amount of traffic, or have the potential to be enlarged in order to adapt to that growth. This scalability property of web applications is one of the most important issues in modern web development. Today's users are unpredictable in the means of accessing web applications; from the classic approach using a web browser on a desktop computer, through a variety of smart devices available on the market in many shapes. Real-time communication and push notifications are another important characteristic of this modern era where users expect to receive messages without their action.

To adapt to these users' needs, web developers have been in constant search for new frameworks and paradigms that will enable development of highly-scalable systems in a safe and easy way. As a result, Node.js has emerged as a new technology for developing web applications and was quickly accepted by developer communities and companies. Embracing JavaScript's event system, Node.js has made asynchronous I/O a first class citizen in its framework, which makes programming of highly scalable servers both easy and safe [6].

The approach in traditional web development frameworks is based on threads. Namely, when an incoming request reaches the web server, the main process that handles the request spans a new thread and allocates the request to it. That thread is busy

G. Stojanov and A. Kulakov (eds.), *ICT Innovations 2016*,
Advances in Intelligent Systems and Computing 665,
https://doi.org/10.1007/978-3-319-68855-8_21

with processing the request for its entire life cycle, and it is unable to handle a different request in the meantime. To make things worse, traditional frameworks have synchronous API for I/O operations, which means that the thread processing a HTTP request will be blocked when an I/O access is required to process it. This inherently makes the web application's scalability limited to the number of threads that the web server can create both time and resource wise. Event-based approach in Node.js is thread agnostic and uses the natural asynchronous API of operating systems for I/O access, making it suitable for web applications composed of distributed components [7].

Even though event systems are solving the performance problem in high concurrency systems very well, they do not make the thread-based servers obsolete [1]. The focus of this paper is analysis of the transforming of a legacy web application, developed in ASP.NET, which uses blocking I/O, into an architecture that uses asynchronous I/O to access components it is dependent on. Results from tests made against endpoints of the application before and after the transformations are being presented in this paper as well. The results have shown that with threads, similar or higher performance can be achieved. Related issues with threads are not in the paradigm itself, but a simpler programming model was missing in the traditional frameworks. Developers of these frameworks have been trying to come up with a simpler model and have achieved that by close integration between the compiler and the thread system. Specifically of interest in this paper is the async/await pair of keywords introduced in .NET version 4.5.

2 Previous Research

The event-based approach has been utilized for asynchronous approach in I/O access in many papers for developing complex distributed systems [1–5]. Mostly, their work is focused on combining the thread approach and events together into a hybrid solution, resulting in a library for an existing platform like Java or .NET. Some of the topics covered in these papers are:

- Missing callback syntax for asynchronous events in the underlying platform [2, 4].
- New mental model needed for programmers to write chains of callbacks [2, 3].
- In [3] the authors point out that high allocation of memory and CPU time during thread's context switching is the main reason event-based solutions perform better.
- Library solution for improving the syntax for writing asynchronous code [4].
- A proposed mechanism for dynamic stack growth is available in [5] to avoid large stacks for managing thread state.

A library-based solution can help improve the development with an asynchronous I/O. However, a true effort is needed by the stakeholders of existing frameworks to make a widely accepted solution. As mentioned in these papers, solutions to scalability issues of thread-based servers lie in the tight integration between the compiler and the thread system. Such tight integration is introduced in .NET 4.5 with the new pair of keywords (async/await). Their utilization for improving scalability of a legacy system is presented in this paper.

3 Proof of Concept

Before starting with the transformation process, a proof of concept was needed in order to demonstrate the power of the improved syntax for asynchronous programming in .NET, and its underlying mechanism. One of the biggest gains is in the server-side programming frameworks, like ASP.NET, which represents a thread-based server. When a request comes in the system, a thread from the thread pool is assigned to that request and is responsible for generating a response to the requesting client. Before version 4.5, all of the I/O libraries in .NET consisted of synchronous APIs, such as reading from a file, accessing a database or other services over the network. An asynchronous approach was used in rare cases, mostly because support was missing from the framework and writing a wrapper around the synchronous API requires experience, as it is considered unsafe and hard to maintain. Therefore, when access to an I/O system is needed, a blocking approach is used, which makes the thread processing the request to be in a blocking state, basically not doing anything, but unable to accept different requests in the meantime. A busy web application can easily end up without available threads in the thread pool, making incoming requests wait longer period in the queue before processing them. This effectively increases the average response time of the system, and the approach in this case is to scale the system horizontally, by creating new instances of the web application on a separate server. Operating costs are rising, even though the full potential of the system is not used.

By introducing the async/await pair of keywords, developers are encouraged to use asynchronous code when making I/O calls. By using the asynchronous API, the thread is not blocked when I/O call is in progress, but it is being released in the thread pool, available to accept new requests. When the I/O call finishes, a new thread from the pool is assigned to continue executing the request, therefore using the full potential of the system. To confirm these claims, the following web application has been put to load tests:

In Fig. 1 two methods are presented. The "Sync" function calls the Sleep method on the current thread, which blocks the executing thread for 2 s and then returns a result to the client. This way, synchronous API is emulated for an I/O call that lasts 2 s. The "Async" method on the other hand, implements the new async/awaits pair of keywords and emulates an asynchronous I/O call that lasts 2 s. It is using the Task. Delay

```
public string Sync()
{
Thread.Sleep(2000);
return "Hello, Sync!";
}
public async Task<string> Async()
{
await Task.Delay(2000);
return "Hello, Async!";
}
```

Fig. 1. Emulation of an I/O call for both synchronous and asynchronous approach

method, which registers a timer with the operating system and releases the current thread. The thread is free to go back to the thread pool and accept more requests, while the operating system doesn't use any thread for timer implementation. When the timer ticks, a new thread from the thread pool continues the execution of the program and returns a result to the client. The code after the Task. Delay method call is effectively an event handler that executes on the timer tick, but the syntax is quite simplified, because there's no extra function or variables declared to handle the callback.

These two tests have been put to load tests in a controlled environment. The web application hosting these methods is published on an IIS server configured to have only 10 threads available in the pool. Each method has been tested with 1 min of constant user load with three setups – 10, 11 and 20 users making constant request to the method.

As it can be seen in Table 1, performances degrade when using blocking I/O methods as number of users increases. The number of requests that can be executed remains the same (4.41–4.37) after increasing requests over the thread pool limit, but the average response time decreases significantly. When 11 users are making simultaneous requests, the 11^{th} user will have to wait for 2 s for a thread to be available to accept their request, which means that their request will last 4 s. That effectively increases the average response time to 2.51 s. As expected, when the number of requests doubles the number of threads in the pool, the average response time doubles as well, from 2.06 s to 4.58. The system doesn't scale well in this situation.

Table 1. Load test results against synchronous method

Indicator	10 constant users	11 constant users	20 constant users
Total tests	249	225	223
Requests/second	4.88	4.41	4.37
Average request time (seconds)	2.06	2.51	4.58

In Table 2, results from the asynchronous methods are presented. The number of requests that can be accepted always meets the number of requests that are going in the application (total tests and requests/second indicators). The average response time is always constants, no matter how many users are simultaneously accessing the system. This means that the system scales very well with the growing number of users. Scalability is not limited by the number of threads that can be created inside the thread pool, and horizontal scale is avoided.

Table 2. Load test results against asynchronous method

Indicator	10 constant users	11 constant users	20 constant users
Total tests	240	264	480
Requests/second	5	5.5	10
Average request time (seconds)	2.01	2.01	2.01

4 Transforming a Legacy Application into a Hybrid Approach

Results from proof of concept tests are encouraging to apply asynchronous I/O calls to an existing web application that is built with the traditional approach of blocking I/O methods. The web application in question is a Video on Demand solution, hosted on Microsoft Azure cloud platform, and is already in production stage, used by real users.

The video on demand service's overall architecture is presented on Fig. 2. The web application is hosted on a web server and represents an entry point into the system. This system represents a distributed system, composed from 4 independent components. Beside the web server, an SQL Server is used for persisting relational data, a cache server is used for storing customer's authentication sessions and elastic search server is used for textual search of available contents. All these components can be scaled and tested independently of each other, and each of them has its own function in the system. To generate a response to requests that come in the system, the web application needs to make at least two I/O calls: one against the Redis cache, to validate user's authentication claims, and one against the Database, to compose data for the response.

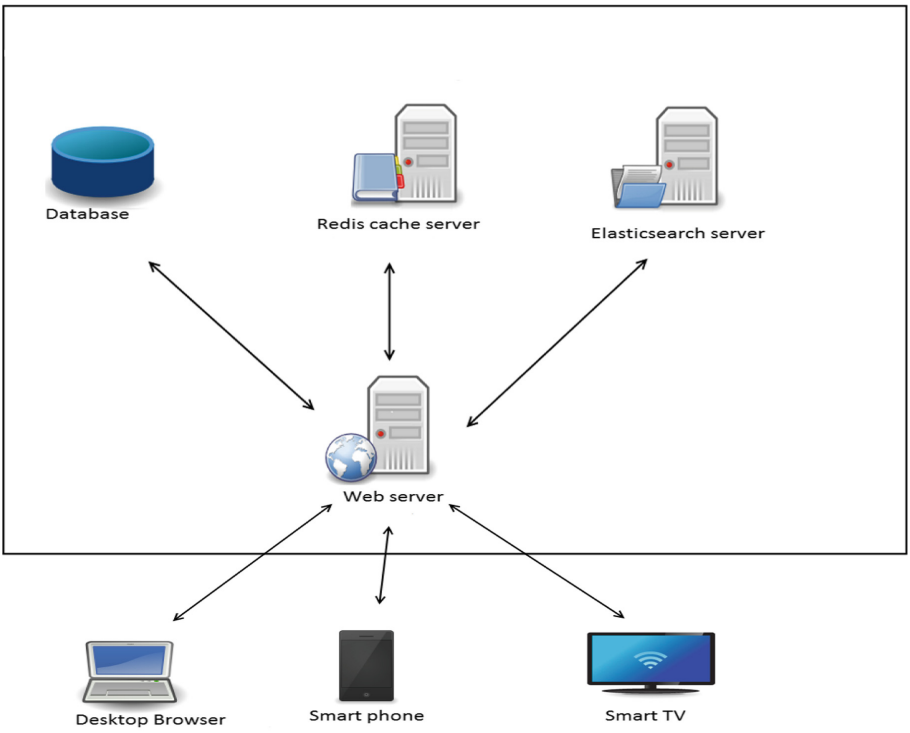

Fig. 2. Logical overview of the system

The biggest challenge during the transformation of the system was the fact that an asynchronous code uses or it is being used by another asynchronous code. With other words, the asynchronous code spans across the whole architecture of the web application, from the entry point to the exit point of the system. In a way, the asynchronous code has infectious effect, because it insists the code that's in its immediate surrounding be asynchronous as well. Transformation of the system has been done in steps, for each web endpoint separately. The asynchronous and synchronous code can live together in the same space, as long as they are not mixed in the same HTTP call.

5 Test Results

5.1 Tests Configuration

To test the performances of a system, it needs to be simulated in an environment that mirrors the environment where the system is running. The two architectures of the system have been published to a similar environment as the live system in the Microsoft Azure cloud infrastructure, but with scaled down performances. The point is to test differences between the two approaches, so both of them are set up in the same hardware environments. The tests are created to target 7 system endpoints, which actually are 7 web services that are available publically. They have been chosen with criteria to include multiple I/O calls and that they are one of the most used web services.

Tests are developed using the Visual Studio Load Testing environment and they are executed by agents in the cloud, located near the physical location of the servers. This removes the unpredictability of the internet connection and the delay that can show up because of long distance between the environment that executes the tests and the environment of the simulated system. Two test scenarios are developed with the following configuration:

1. Test scenario with a constant load of the system. This test simulates 25 users making constant requests for a period of 1 min.
2. Test scenario with increasing number of requests by using steps. The test starts with 10 users and every 10 s, it adds 20 more users to the execution. This test also lasts for 1 min, where the maximum number of users (100) reaches at the 50^{th} second of the test.

Both tests are configured to run for one minute. Beside the regular run time, there are warm-up and cool-down periods of 3 s. During the warm-up period, results are not included in the test results and this period is used for the application to warm up, by establishing connections to the I/O systems. The cool-down period is used to include results of requests initiated during the regular run time, but that have not received response during that time. No requests are initiated during cool-down, but requests that end in this period are included in the final results.

Since there are 7 endpoints under tests, to avoid any randomness, tests are configured such that each virtual user makes requests to the endpoints in the same order, without think time between the requests.

5.2 Evaluation

Both tests are run against each architecture for 5 times and the results presented here are the best results from each testing.

From the summary results under constant load (Table 3), significant improvements can be noticed when using asynchronous I/O calls. One of the important indicators is the number of requests that can be executed per seconds, and with this hardware setup, the synchronous architecture can perform 8.5 requests per second, where the asynchronous architecture gives 13.5. Also, the average response time is much better, giving 1.42 s with the asynchronous approach, and 2.35 s for the synchronous approach. We can conclude that asynchronous I/O calls make the following improvements:

- Increase of ***60%*** in number of requests per second
- Decrease of ***40%*** in average response time

Table 3. Summary results from constant load test

Indicator	Synchronous Approach	Asynchronous approach
Total tests	72	110
Tests/second	1.2	1.83
Average test cycle (seconds)	14.3	9.68
Average requests/second	8.5	13.4
Average response time (seconds)	2.35	1.42

In Table 4, summary results from the step increasing load test show that in this scenario, asynchronous approach for I/O calls is again giving significant improvements, with ***46%*** increase in number of requests per seconds and ***44%*** decrease in average response time.

Table 4. Summary results from step increasing load test

Indicator	Synchronous Approach	Asynchronous approach
Total tests	47	108
Tests/second	0.78	1.80
Average test cycle (seconds)	14.8	13.8
Average requests/second	9.2	13.5
Average response time (seconds)	4.09	2.31

6 Conclusion

If we compare results from Tables 3 and 4 for the same architecture, we can notice that performances degrade significantly for the synchronous approach. The system can accept fewer requests per second, which effectively decreases the average response time for the whole system. For the asynchronous approach, a constant performance is showing up for number of requests that can be accepted per second. An increase in average response time is showing up, which means that one of the components is degrading in performance due to the increasing number of requests. But, the scalability limit of the web application is removed thanks to the transformation of the legacy code with asynchronous I/O calls.

References

1. von Behren, R., Condit, J., Brewer, E.: Why events are a bad idea (for high-concurrency servers). Computer Science Division, University of California at Berkeley (2003)
2. Cugola, G., Di Nitto, E., Fuggetta, A.: Exploiting an event-based infrastructure to develop complex distributed systems. CEFRIEL – Politecnico di Milano (1998)
3. Haller, P., Odersky, M.: Scala actors: unifying thread-based and event- based programming. EPFL, Switzerland (2009)
4. Cunningham, R., Kohler, E.: Making events less slippery with eel. University of California, Los Angeles (2005)
5. Haller, P., Odersky, M.: Event-based programming without inversion of control. EPFL, Switzerland (2006)
6. Hughes-Croucher, T., Wilson, M.: Node: Up and Running. O'Reilly, Sebastopol (2014)
7. Wilson, J.R.: Node.js the Right Way. The Pragmatic Programmers (2013)
8. Henderson, C.: Building Scalable Web Sites. O'Reilly, Sebastopol (2006)
9. Chrysanthakopoulos, G., Singh, S.: An asynchronous messaging library for c#. In: Proceedings of Workshop on Synchronization and Concurrency in Object-Oriented Languages (SCOOL), OOPSLA (2005)
10. von Behren, R., Condit, J., Zhou, F., Necula, G.C., Brewer, E.: Capriccio: scalable threads for internet services. In: 19th ACM Symposium on Operating Systems Principles, Bolton Landing, Lake George, New York, October 2003
11. Ousterhout, J.K.: Why threads are a bad idea (for most purposes). Presentation at the 1996 USENIX Annual Technical Conference, January 1996
12. Cleary, S.: Async programming – introduction to async/await on ASP.NET. MSDN Magazine (2014)
13. Ammann, P., Offutt, J.: Introduction to Software Testing. Cambridge University Press, Cambridge (2008)
14. Henderson, C.: Building Scalable Web Sites: Building, Scaling and Optimizing the Next Generation of Web Applications. O'Reilly, Sebastopol (2006)
15. Redkar, T., Guidici, T.: Windows Azure Platform. Apress, New York City (2011)

Relevance Re-ranking Through Proximity Based Term Frequency Model

S. Sathya Bama[1(✉)], M.S. Irfan Ahmed[2], and A. Saravanan[1]

[1] Sri Krishna College of Technology, Coimbatore 641042, Tamil Nadu, India
ssathya2l@gmail.com, a.saravanan2l@gmail.com
[2] Nehru Institute of Engineering and Technology,
Coimbatore, Tamil Nadu, India
msirfan@gmail.com

Abstract. In this internet era, people rely on the most significant tool called search engine for retrieving attractive information from the web. Also, the rapid growth in the usage of the web increases the volume of data on the web, due to which most of the documents retrieved by the search engine is overwhelmed with inappropriate and redundant information called outliers. This not only increases the result space, but also roots in wasting the user's time and effort that makes them to surf uninteresting data. Consequently, a method is essential for the web user community to remove uninteresting information and to present the interesting data in an organized manner based on their request. Web content outlier mining is promising research area that serves these features to the web users. In this research work, proximity based term frequency model has been developed for retrieving the appropriate information and for refining the quality of the results offered by the search engine. Experimental results indicate that proximity based term frequency model improves the performance in terms of relevancy re-ranking of the retrieved documents.

Keywords: Relevance ranking · Search engine · Term frequency · Proximity · Web content outlier

1 Introduction

Due to digital evolution, the web is offering a massive amount of information for the people to perform their transaction over the web. As a result, a growing number of people are currently using the Internet to ascertain the exact information, to communicate or to share their knowledge and their views through social networking. Among all these activities, web search is the leading application on the internet. It is a type of information retrieval where the web users demand fast and appropriate response. Thus, search engine came into existence. Search engines are the most familiar and popular tool among people that allows them to search interesting information from the web. The search engine uses a variety of algorithms to make the search effective and to help the users in accessing desired information. Conversely, web search is effective only if people aware of the information what they are seeking for. But in many cases, people are unaware of the information; however, they need interesting and relevant content in

G. Stojanov and A. Kulakov (eds.), *ICT Innovations 2016*,
Advances in Intelligent Systems and Computing 665,
https://doi.org/10.1007/978-3-319-68855-8_22

a faithful manner. Thus, the key problem in information retrieval is providing the user with interesting and relevant information when they do not have any awareness about information need [1].

Search engine employs methods and techniques of web content mining which is the process of extracting useful information from the contents of web documents. Even though, the result produced by the search engine is not considered as effective since it contains irrelevant and redundant information called as outliers. Conventional outlier mining algorithms have been devised to find rare patterns that well suit numeric data sets. These algorithms cannot be used directly for web data since it contains different types of data like text, number, image etc. There are three types of web outliers; web content outliers, web structure outliers, and web usage outliers [2]. This paper primarily focuses on the problem of identifying outliers from web contents called web content outlier mining. A web content outlier is described as a web document with different contents compared to similar documents taken from the same category.

2 Outlier Mining

According to Hawkins, Outlier is defined as an observation that deviates too much from other observations that it arouses uncertainties that it was generated by a different mechanism from other observations [3]. The exact definition of an outlier depends on the context. Definitions fall roughly into following categories [4, 5]: (i) Distribution based, (ii) Depth based (iii) Distance based (iv) Deviation based (v) Density based.

Distribution-based methods originate from statistics. Here normal data objects follow a known given distribution and occur in a high probability region of this model where as an outlier deviates strongly from underlying distribution. The outliers deviate more than 3 times the standard deviation from the mean [5–7]. One of the statistical approach drawbacks is it requires knowledge about parameters of the data set, such as the data distribution. However, in many cases, the data distribution may not be known [8]. General idea of depth based method is that the search for outliers is made at the border of the data space but independent of the statistical distributions. The Basic assumption here is Outliers are located at the border of the data space and Normal objects are in the center of the data space [5].

Distance based methods was originally proposed by Knorr [9]. He defines outlier as an observation that is d_{min} distance away from p percentage of observations in the dataset. The problem is then finding appropriate and such that outliers would be correctly detected with a small number of false detections. This process usually needs domain knowledge [10].

Deviation based method identifies outliers by examining the main characteristics of objects in a group. Objects that "deviate" from this description are considered outliers. Hence, in this approach the term deviations are typically used to refer to outliers [8, 11]. Density based was proposed by Breunig [12]. The density around a point is compared with the density around its local neighbors. The density around a normal data object is similar to the density around its neighbors where as it differs for outliers.

3 Measuring Proximity for Outlier Mining

A proximity measure explores the actual closeness of terms in a given segment of text. In IR proximity can be defined as the similarity of query-terms within a sample of text. The underlying hypothesis of this research paper is that documents in which query terms appear closer together are more useful to the user since it improves the degree of relevance. A complete proximity function should include the relationships between all query-terms. Thus, increase in the closeness of two query terms increases the document score. This score is subject to the distance between the terms in a document.

This paper provides a framework for re-ranking the retrieved documents based on the relevancy score that includes proximity based term frequency of all the words in the given query called keywords and term frequency of other words. A pair-wise proximity measure is used in which a pair of terms is given as an input for the proximity function. To calculate the proximity based term frequency, position vectors for each keyword in the retrieved documents have to be defined which includes the relative position of the terms in that document.

4 Related Work

Finding outliers in web is difficult than finding outliers in numeric data due to the dynamic and diverse structure of the web. While searching information from the web, since user expects the accurate data in less time, implementing the model that present the accurate data quickly by removing irrelevant and redundant data is a very big challenge to the research community. Most of the existing algorithms concentrate on numeric data and for structured data.

Agyemang [13] developed the method of finding outliers on the web using full word matching assuming the existence of domain dictionary. The above authors developed the work with n-gram techniques for partial matching of strings with domain dictionary [2, 13]. Agyemang et al. enhanced the same work without domain dictionary. Based on the above ideas, they prolonged the work by presenting HyCOQ which a hybrid algorithm that draws from the power of n-gram based and word based system [14, 15]. Poonkuzhali et al. presented a mathematical approach based on signed and rectangular representation [16] and a mathematical approach based on correlation analysis [17] have been developed to detect and remove the redundancy between unstructured web documents. Another statistical approach has been proposed by Poonkuzhali et al., in which the keywords and other words are given with equal weights [18]. Sathya Bama et al., introduced a weighted approach [19]. For many of the above methods the dictionary has to be compiled for every domain as a pre-processing step which consumes lot of time and effort.

There have been many recent attempts to incorporate proximity into IR models [20–24]. The relatedness of terms in a semantic sense can be mapped to a proximity measure [23]. Ronan has presented 12 measures related to proximity either implicitly or explicitly. Work has been presented [25] that makes use of a fuzzy set theoretic measure of proximity in a Boolean model of retrieval. This framework is elegant and presents results for a number of different system parameter settings. Previous research

[26] has used a window or passage method to determine proximity within a certain threshold. The work shows that proximity can increase performance on small collections. Proximity information is incorporated into an existing ad hoc retrieval function to improve the performance of short queries [27]. They create a proximity function at the sentence level, whereby if two query terms appear within the same sentence the document score will be increased. More recently some approaches have been successful in employing proximity into a number of keyword based retrieval functions [23].

Introduction and analysis of a novel approach for determining the "goodness" of a span of terms in a document [28]. The integration of term proximity in to probabilistic model BM25 using pseudo-term frequency instead of term frequency has been introduced in [29]. When considering only top retrieved documents, term proximity information can lead to improved retrieval effectiveness [30]. The structured nature of web documents may also contribute to the significant improvements that can be obtained through the use of phrases and term proximity information in web retrieval [31]. Recent work by Song et al. indicates that using flexible proximity terms within an information retrieval model such as BM25 results in improved retrieval effectiveness [32]. This paper aims to create a proximity function which deals with pair of adjacent query-terms.

5 PTF – A Framework for Web Content Outlier

The architecture of the proposed model is given in Fig. 1.

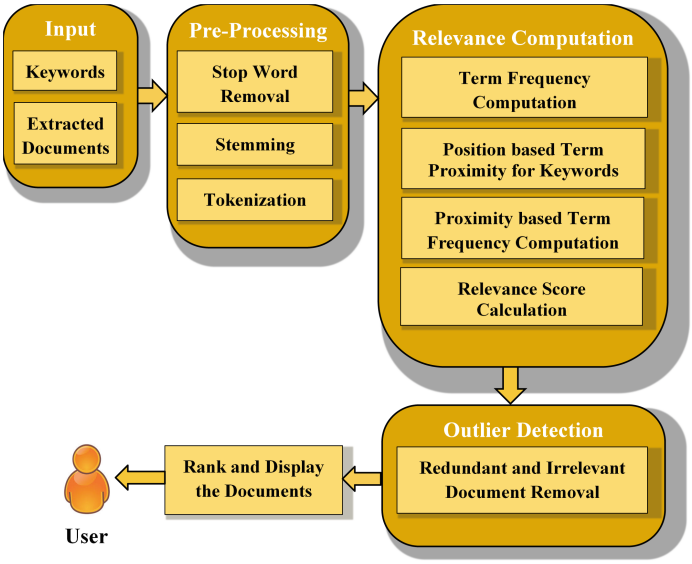

Fig. 1. Architecture of proximity based term frequency model

Consider a sample document D. The set of terms in the document D is assumed as TD = {a b c d a b a c a b d e} and the set of integer position for each term in the document D can be given as PD = {1 2 3 4 5 6 7 8 9 10 11 12}. Let the Query Term Q = {a b c}. Thus to calculate the proximity based term frequency for the keywords in the document, non-query terms can be discarded since most of document holds minimum number of query terms, maximum number of non-query terms and computing proximity score for non-query terms incorporate the generation of large number of term pairs in which an enormous amount time has been involved. Thus the content of the document D can be represented as TD = {a b c x a b a c a b x x} where 'x' denotes the non-query terms.

The position vector for each query term a, b, c in the document D can be given as $P_D(a) = \{1, 5, 7, 9\}$, $P_D(b) = \{2, 6, 10\}$, $P_D(c) = \{3, 8\}$ respectively. Thus the frequency of all the query terms a, b, c in the document D is $f_D(a) = 4$, $f_D(b) = 3$ and $f_D(c) = 2$. Also for Relevance Score the frequency of other terms will also be calculated to normalize the relevance score. $f_D(rt) = 3$ where $f_D(rt)$ is the frequency of remaining terms in the document D. Intuitively, two factors affect the proximity score is the distance between terms in term-pair and the order of occurrence of the terms in term-pairs.

The term-pairs involving adjacent terms for the given query Q can be generated. Then the distance between all the adjacent term pair t_i and t_j can calculated based on the position vectors of the terms in keywords in the document. Thus for the above query the adjacent term pairs can be generated as ab, bc. Therefore, the distance between a term-pair can be computed as in Eq. (1).

$$dis(t_i, t_j) = \left(P_D(t_j) - P_D(t_i)\right) \tag{1}$$

Here $dis(t_i, t_j)$ is the distance between two terms and $PD(t_i)$ is the position of term t_i in document D. The term proximity measure can be used in the calculation of relevance score by satisfying the unique constraint as in Condition 1.

Condition 1: The relevance/proximity score should decrease as the distance between the query terms increases.

The Proximity based Term Frequency can be computed using Eq. (2).

$$PTF(t_i) = f(t_i) + \sum_{j=1, j\neq i}^{n} TP(t_i, t_j) \tag{2}$$

where PTF(t) is the proximity based frequency measure, f(t) is the frequency of the term t in the document and n is the number of term-pairs for the given query. The proximity function TP() (Term Proximity) has been defined as a function that takes the input as the term-pair and this ensures the unique constraint given in Condition 1 and it is given in Eq. (3).

$$TP(t_i, t_j) = \frac{1}{\min\{dis(t_i, t_j)\}} \tag{3}$$

When more than one t_j occurs near t_i, the one with the smallest distance can be used to calculate proximity function.

Thus PTF(t) will be calculated for each term in the keyword. Then this new proximity based term frequency of a keyword is combined with the term frequency of other words in the document to calculate the relevance score. The relevance score can be calculated with the below formula in Eq. (4).

$$RS(D)_r = \frac{\left[f_D(t_i) + \sum_{j=1, j\neq i}^{n} TP_D(t_i, t_j)\right] + (\beta * f_D(rt))}{N_D} \tag{4}$$

RS(D) is the relevance score of a document D, for all the document in the retrieved set of documents. ND is the total number of terms in the document D. β is the scaling factor and it is set as 0.5, since non-query terms has less weightage when compared to keywords. Then the documents are arranged in the descending order of the relevance score. If more than one document contains the same relevance score, then it can be compared to find out the redundant documents.

6 Experimental Results

An experimental analysis has been made for the proposed model. The experiment is conducted for the user query "Recent Research in Web Content Mining" against a Google search engine. The top 10 documents which are listed in Table 1 are retrieved and it becomes the input for the proposed approach which is then pre-processed by removing stop words. The Keywords are extracted from the user query.

Table 1. List of input documents

Did	Retrieved documents
D1	www.cs.uic.edu/∼liub/publications/editorial.pdf
D2	dmr.cs.umn.edu/Papers/P2004_4.pdf
D3	www.ijarcsse.com/docs/papers/Volume_3/11_November2013/V3I11-0352.pdf
D4	www.ijcsit.com/docs/Volume%205/vol5issue03/ijcsit20140503316.pdf
D5	ebiquity.umbc.edu/_file_directory_/papers/214.pdf
D6	esatjournals.org/Volumes/IJRET/2014V03/I03/IJRET20140303009.pdf
D7	www.kdd.org/sites/default/files/issues/2-1-2000-06/kosala.pdf
D8	citeseerx.ist.psu.edu/viewdoc/download?doi10.1.1.258.8941&rep=rep1&type=pdf
D9	www.upet.ro/annals/economics/pdf/2012/part1/Dinuca-Ciobanu.pdf
D10	arxiv.org/pdf/cs/0011033.pdf

Initially the term frequency and position vectors for all the keywords are generated for all the retrieved documents. Then based on the position vector proximity measure for all the keywords are calculated. Finally term frequencies for non-query terms are also calculated. Then the relevance score can be calculated as in Table 2 with the above formula. Finally the documents are arranged in descending order of their relevance

score. Since the relevance score for the documents D7 and D10 are same, the common terms for the two documents can be counted. If the number of common words is same as the number of words in the documents, then one of the documents is redundant which can be removed.

Table 2. Document score for the given query

Did	Frequency of keywords	Term proximity of keywords	Frequency of remaining terms	Total frequency	Relevance score
D1	163	1116.90	2176	2339	0.5472
D2	99	249.59	485	584	0.5969
D3	187	572.75	1052	1239	0.6132
D4	129	448.31	848	977	0.5909
D5	210	699.95	1375	1585	0.5741
D6	128	306.09	565	693	0.6264
D7	347	1126.82	2181	2528	0.583
D8	187	333.04	584	771	0.6745
D9	55	296.26	584	639	0.5497
D10	347	1126.82	2181	2528	0.583

The precision value is calculated at each position and the values always result between 0 and 1. The precision for the proposed method is compared with the Google rank and existing method given in [19]. The graph is shown in Fig. 2. Thus, the proposed method gives better performance in terms of relevancy and it always lies between 0 and 1.

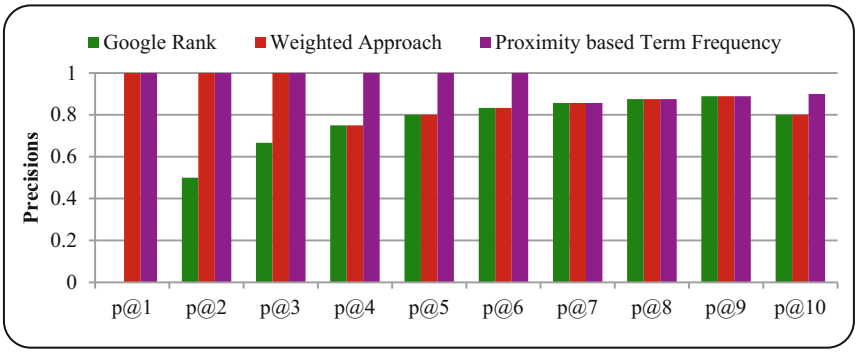

Fig. 2. Precision comparison at each position

The proposed method is compared with existing methods against the labelled dataset having 125 relevant documents and 25 outlier documents. The experiment is performed by varying the number of relevant documents and outliers and the results are shown in Table 3. The number of outliers detected, percentage of Precision rate,

percentage of false rate and execution time for the proposed method is compared along with the existing correlation analysis [17], Weighted Approach [19] and N-Gram approach [14] are shown in the table. The graph for the above results are shown in the Figs. 3 and 4.

Table 3. Comparative study for proposed methods

Query #		1	2	3	4	5
Relevant documents		25	50	75	100	125
Actual outliers		5	10	15	20	25
Proximity based approach	Outliers detected	5	9	14	18	22
	Precision (%)	100	90	93.33	90	88
	False rate (%)	0	10	6.67	10	12
	Execution time (Secs)	5	8	12	17	21
Correlation analysis	Outliers detected	3	7	12	16	21
	Precision (%)	60	70	80	80	84
	False rate (%)	40	30	20	20	16
	Execution time (Secs)	10	16	23	31	39
Weighted approach	Outliers detected	4	8	13	17	22
	Precision (%)	80	80	86.67	85	88
	False rate (%)	20	20	13.33	15	12
	Execution time (Secs)	4	7	12	15	19
N-gram approach	Outliers detected	2	7	11	15	19
	Precision (%)	40	70	73.33	75	76
	False rate (%)	60	30	26.67	25	24
	Execution time (Secs)	12	17	25	32	41

From the results shown in Fig. 3, the accuracy for weighted term frequency approach is better than weighted correlation and N-gram methods. However, proximity based approach provides even better precision rate. Also, as in Fig. 4, the false rate is very for proximity based approach when compared with other approaches.

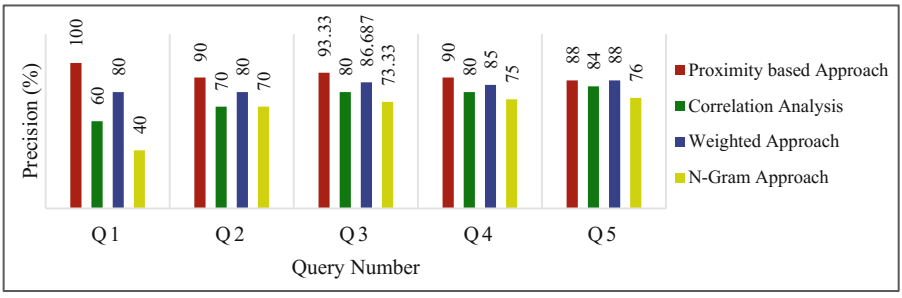

Fig. 3. Comparison of accuracy for proposed methods

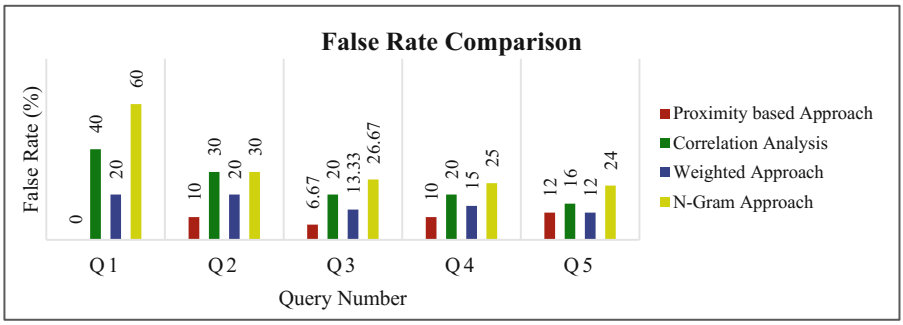

Fig. 4. Comparison of false rate for proposed methods

The comparison on execution time is given in Fig. 5. However, the execution time is less for weighted approach, but the drawback in this method of is that it has to compile and maintain domain dictionary. Thus the proposed method provides better result when compared to others.

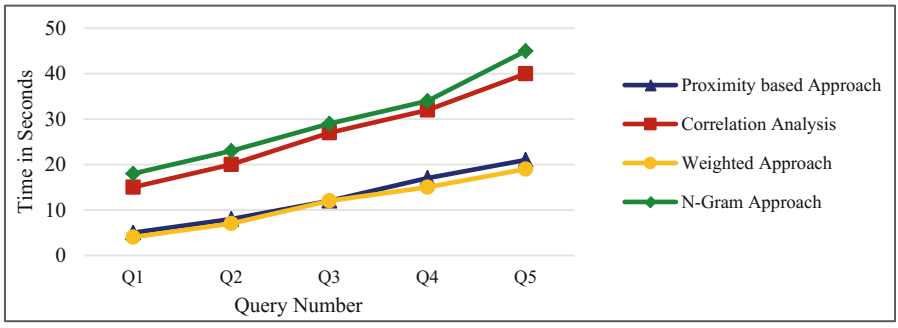

Fig. 5. Comparison of execution time

7 Conclusion and Future Work

The enormous growth of information sources available on the World Wide Web has forced the web mining researchers to develop new and effective algorithms and tools to identify relevant information without duplicates. In this paper proximity based term frequency model (PTF) has been proposed that computes the position based relevance score. This method reduces the time and space since the compilation of domain dictionary has been eliminated. However, this work focuses on outlier mining in web documents especially for text. Experimental results show that the proposed model outperforms well than the exiting methods. Future work aims at mining outliers in web documents that not only includes text but also images and either multimedia data. Also, other mathematical tools can be used to improve the results further.

References

1. Mele, I.: Web usage mining for enhancing search-result delivery and helping users to find interesting web content. In: Proceedings of the Sixth ACM International Conference on Web Search and Data Mining. ACM (2013)
2. Agyemang, M., Barker, K., Alhajj, S.R.: Framework for mining web content outliers. In: Proceedings of 19th ACM Symposium on Applied Computing, Nicosia, Cyprus, pp. 590–594 (2004a)
3. Hawkins, D.M.: Identification of Outliers, vol. 11. Chapman and Hall, London (1980)
4. Jin, W., Tung, A.K., Han, J.: Mining top-n local outliers in large databases. In: Proceedings of the Seventh ACM SIGKDD International Conference on Knowledge Discovery and Data Mining, pp. 293–298. ACM (2001)
5. Kriegel, H.P., Kröger, P., Zimek, A.: Outlier detection techniques. In: Tutorial at the 13th Pacific-Asia Conference on Knowledge Discovery and Data Mining (2009)
6. Freedman, D., Pisani, R., Purves, R.: Statistics. W.W. Norton & Company, Inc., New York (1978)
7. Hautamäki, V., Kärkkäinen, I., Fränti, P.: Outlier detection using k-nearest neighbour graph. In: ICPR, vol. 3, pp. 430–433 (2004)
8. Han, J., Kamber, M.: Data Mining Concepts and Techniques. Morgan Kaufmann, Burlington (2001)
9. Knorr, E.M., Ng, R.T.: Algorithms for mining distance based outliers in large datasets. In: Proceedings of the International Conference on Very Large Data Bases, pp. 392–403 (1998)
10. Knorr, E.M., Ng, R.T., Tucakov, V.: Distance-based outliers: algorithms and applications. Int. J. Very Large Data Bases **8**(3–4), 237–253 (2000)
11. Bakar, Z.A., Mohemad, R., Ahmad, A., Deris, M.M.: A comparative study for outlier detection techniques in data mining. In: 2006 IEEE Conference on Cybernetics and Intelligent Systems, pp. 1–6. IEEE (2006)
12. Breunig, M.M., Kriegel, H.P., Ng, R.T., Sander, J.: LOF: identifying density-based local outliers. ACM Sigmod Rec. **29**(2), 93–104 (2000)
13. Agyemang, M., Barker, K., Alhajj, R.: Framework for mining web content outliers. In: Proceedings of the 2004 ACM Symposium on Applied Computing, pp. 590–594. ACM (2004b)
14. Agyemang, M., Barker, K., Alhajj, R.S.: Mining web content outliers using structure oriented weighting techniques and N-grams. In: Proceedings of the 2005 ACM Symposium on Applied Computing, pp. 482–487. ACM (2005a)
15. Agyemang, M., Barker, K., Alhajj, R.: Hybrid approach to web content outlier mining without query vector. In: Data Warehousing and Knowledge Discovery, pp. 285–294. Springer, Heidelberg (2005b)
16. Poonkuzhali, G., Uma, G.V., Sarukesi, K.: Detection and removal of redundant web content through rectangular and signed approach. Int. J. Eng. Sci. Technol. **2**(9), 4026–4032 (2010)
17. Poonkuzhali, G., Kishore Kumar, R., Kripa Keshav, R., Sudhakar, P., Sarukesi, K.: Correlation based method to detect and remove redundant web document. In: Advanced Materials Research, vol. 171, pp. 543–546 (2011a)
18. Poonkuzhali, G., Kumar, R.K., Keshav, R.K., Thiagarajan, K., Sarukesi, K.: Statistical approach for improving the quality of search results. In: Proceedings of the 10th WSEAS International Conference on Applied Computer and Applied Computational Science, pp. 89–93. World Scientific and Engineering Academy and Society (WSEAS) (2011b)
19. Sathya Bama, S., Irfan Ahmed, M.S., Saravanan, A.: Enhancing the search engine results through web content ranking. Int. J. Appl. Eng. Res. **10**(5), 13625–13635 (2015)

20. Bhatia, M.P.S, Kumar Khalid, A.: Contextual proximity based term-weighting for improved web information retrieval. In: KSEM, pp. 267–278 (2007)
21. Bai, J., Chang, Y., Cui, H., Zheng, Z., Sun, G., Li, X.: Investigation of partial query proximity in web search. In: Proceeding of the 17th International Conference on World Wide Web, WWW 2008, pp. 1183–1184. ACM (2008)
22. Na, S.-H., Kim, J., Kang, I.-S., Lee, J.-H.: Exploiting proximity feature in bigram language model for information retrieval. In: Proceedings of the 31st Annual International ACM SIGIR Conference on Research and Development in Information Retrieval, SIGIR 2008, pp. 821–822. ACM (2008)
23. Tao, T., Zhai, C.X.: An exploration of proximity measures in information retrieval. In: Proceedings of the 30th Annual International ACM SIGIR Conference on Research and Development in Information Retrieval, SIGIR 2007, pp. 295–302. ACM (2007)
24. Cummins, R., O'Riordan, C.: Learning in a pair-wise term-term proximity framework for information retrieval. In: Proceedings of the 32nd International ACM SIGIR Conference on Research and Development in Information Retrieval, pp. 251–258. ACM (2009)
25. Beigbeder, M., Mercier, A.: An information retrieval model using the fuzzy proximity degree of term occurrences. In: Proceedings of the 2005 ACM Symposium on Applied Computing, pp. 1018–1022. ACM (2005)
26. Possas, B., Ziviani, N., Meira, Jr., W.: Enhancing the set-based model using proximity information. In: String Processing and Information Retrieval, pp. 104–116. Springer, Heidelberg (2002)
27. Rasolofo, Y., Savoy, J.: Term proximity scoring for keyword-based retrieval systems, pp. 207–218. Springer, Heidelberg (2003a)
28. Svore, K.M., Kanani, P.H., Khan, N.: How good is a span of terms?: exploiting proximity to improve web retrieval. In: Proceedings of the 33rd International ACM SIGIR Conference on Research and Development in Information Retrieval, pp. 154–161. ACM (2010)
29. Song, R., Taylor, M.J., Wen, J.R., Hon, H.W., Yu, Y.: Viewing term proximity from a different perspective. In: Advances in Information Retrieval, pp. 346–357. Springer, Heidelberg (2008)
30. Rasolofo, Y., Savoy, J.: Term proximity scoring for keyword-based retrieval systems. In: ECIR, p. 207 (2003b)
31. Mishne, G., de Rijke, M.: Boosting web retrieval through query operations. In: ECIR, pp. 502–516 (2005)
32. Song, R., Yu, L., Wen, J., Hon, H.: A proximity probabilistic model for information retrieval. Technical report, Microsoft Research (2011)

Information System for Biosensors Data Exchange in Healthcare

Monika Simjanoska, Bojana Koteska(✉), Magdalena Kostoska, Ana Madevska Bogdanova, Nevena Ackovska, and Vladimir Trajkovikj

Faculty of Computer Science and Engineering, University Ss. Cyril and Methodius, Rugjer Boskovikj 16, 1000 Skopje, Macedonia
{monika.simjanoska,bojana.koteska,magdalena.kostoska, ana.madevska.bogdanova,nevena.ackovska,vladimir.trajkovik}@finki.ukim.mk

Abstract. This paper presents a novel cloud information system (BIOHIS - Biosensors Healthcare Information System) whose main goal is to enable vital data exchange obtained from biosensors. BIOHIS corresponds to the requirements of the existing protocols for MRMI (medical response to major incidents). This system aims to ease and improve the data exchange between the different institutions involved in the MRMI protocols. BIOHIS is one step closer to the interoperable data flow among the various medical system interfaces, ensuring structured data capture. The system is intended to use cloud leverages as infinite storage, computing capacities and full time authorized access.

Keywords: Biosensors · Information system · Medical protocols

1 Introduction

The purpose of biosensors inclusion in people's everyday life is to increase the overall quality of life, but also to improve the quality of response to life-threatening situations. The biosensors technology has potential to aid the medical protocols that deal with both civilian and military disasters.

The benefits of introducing biosensors in the existing medical protocols is multi-fold, especially during the triage process where the manual measurements are substituted with automatic vital data gathering [1]. Biosensors provide multiple triage processes to run in parallel which speeds up process of prioritization in case of multiple injuries. It enables the reduction of the number of medical persons needed for performing the measurements at the location of the incident and the inclusion of volunteers with no medical experience.

Our information system, as a centralized cloud solution, provides continuous monitoring and transfer of patients' data. In order to enable the continuous data flow among the different entities involved in the medical protocols, we must ensure structured data environment. Having combined the vital data together with the rest of patient data as demographic records, lab analysis, clinicians notes, etc., we can ease the transfer of the vitals to whoever involved in

G. Stojanov and A. Kulakov (eds.), *ICT Innovations 2016*,
Advances in Intelligent Systems and Computing 665,
https://doi.org/10.1007/978-3-319-68855-8_23

the MRMI. Bringing the right information in the right hands at the right time requires cautious design of an information system that will meet the medical protocol requirements. In this paper we describe our BIOHIS architecture and data structure in details and the benefits from the implementation of such a system. Our system enables efficient resource allocation of medical facility capacities and ambulance vehicles, depending on triage decision. The biosensor digital transfer of vital parameters improves the coordination and communication between hospitals in a case of losing any patients' information. The early and fast detection of patient state with the biosensors also reduces the number of possible deaths.

The paper is organized as follows: in the next Sect. 2, we give an overview of the existing solutions such as electronic health records. In Sect. 3, we describe the BIOHIS architecture. Section 4 provides the data structure model of our system. Different possible scenarios are provided in Sect. 5. The system constraints are experimentally explained in Sect. 6 and conclusive remarks are given in the last Sect. 7.

2 Related Work

Data can be useful only if gathered in a meaningful, digital form. The necessity of evidence is enormous due to the fact of the exponential data increase - the predictions say up to 25,000PB of data by 2020 [2]. Data should be constantly gathered and analyzed upon which actions will be triggered. This problem still remains a challenge in the real-life context [3].

Electronic Health Record (EHR) is an initiative to collect all kind of patients data, whether it is demographics data, clinicians notes, medications, laboratory data, vital signs reports, etc. A complete documentation is expected to provide easy access by different medical institutions, deliver more reliable health-care and support evidence-based practice. Each clinical system has unique and dynamic work flow and a customized EHR system adapted to the local user requirements. A standardized EHR format is very hard to achieve, thus interoperable standards are developed for data exchange between different EHR formats. The goal is to access a structured data template, automatically populate the template from existing EHR data, store and transmit the completed template to the appropriate organizations or researchers [4].

There are several distinguished EHR standards. Virtual Data Warehouse (VDW) is a virtual setting of parallel databases that have been constructed by extracting data directly from the local EHR systems. It is a method for standardizing and pooling EHR data for multi-site research [5].

Health Level Seven (HL7) makes possible the exchange of demographics and other textual information. It is not a type of software, instead it provides a specification for making systems interoperable. In HL7's strategies description the interoperability is defined in three different contexts that affect how the software is designed, the data is stored and used [6].

Developing a standard that maintains the semantic meaning is really hard to achieve. Systematized Nomenclature of Medicine Clinical Terms - SNOMED

CT in a period of 40 years has developed from a pathology-specific nomenclature into a logic-based health care terminology [7].

As previously discussed, there are several recently developed healthcare systems that implement EHR standards.

A customized healthcare service by means of wellness clothing which includes digital yarns and biosensors is presented in [8]. It's goal is to acquire, analyze, and present bio-engineering data including ECG, respiration, acceleration, and body temperature.

In [9], the authors propose a framework to collect patients' data in real time, perform monitoring, and propose medical and/or life style engagements. The framework integrates mobile technologies to collect and communicate vital data from a patient's wearable biosensors. The data are stored in the Cloud and are available to physicians, paramedics, etc.

An intelligent home-based platform is implemented in [10]. The platform involves an open-platform-based intelligent medicine box, intelligent pharmaceutical packaging with communication capability enabled by passive radio-frequency identification and a flexible and wearable bio-medical sensor device.

3 BIOHIS Architecture

In this section we present a novel cloud information system, BIOHIS, whose main goal is to enable vital data exchange obtained from biosensors.

BIOHIS consists of several component: biosensors, local electronic devices for communication with the biosensors, cloud server, connectivity to the cloud server (different links) and real-time monitoring of the stored data by medical personnel. Figure 1 presents the BIOHIS system overview.

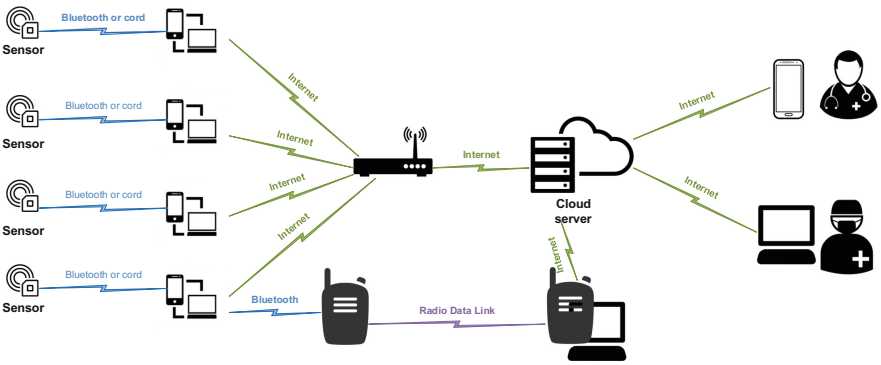

Fig. 1. BIOHIS system overview

We consider two possible cases for data transmission presented in Fig. 1:

- Data can be transmitted to the cloud by Internet, or
- Data can be transmitted to the cloud via High Frequency (HF) radios.

In general case, where Internet is available, the data is transmitted to the cloud and then distributed to whoever needs them. In cases where Internet is not available, HF radios can also be used for data transfer.

4 BIOHIS Data Model

The data model of BIOHIS system is shown in Fig. 2. Each system user has an opportunity to access data for multiple hospitals that he/she is authorized for. Some users have a permission to manage data for different hospitals. The data for the patients are stored in the database by using the centralized cloud solution for our system on the battlefield or at the location of a major incident. The measured vital parameters from the biosensors are stored in the table "Vital Parameters" (ECG, respiratory rate, oxygen rate, temperature and blood pressure). These data are measured periodically and an authorized user can see the history of vital parameters value for a patient.

Before the triage process begins, a new ID is generated for each injured person. Software automatically proposes a new "personId" which is also attached to the injured person. At the place of the incident, the medical person who does the triage inserts only the information about injured body parts and medication, and later, in the hospital, the rest of the information is fulfilled on the basis on the person's ID. The triage process also includes identification and marking of the injured body parts which are stored in the table "InjuredBodyParts". The level of injury is calculated by using the Glasgow Coma Score (GCS), and Triage Sort Score and data are inserted in the table "LevelofInjury". Concerning the medications that can be given to a injured person at the place of the incident or later at the hospital, one can use the table "Medication" - a history of medication records are stored at this table. After the triage process, if needed, the patient is sent to a hospital with free capacity to accommodate.

5 Implementation Scenarios

The protocols for medical response to major incidents is comprised of: triage, medical response before hospital treatment, transport to hospital, hospital response, communication, command and coordination. The effective medical response to major incidents does not depend only on these components, but also on the way how they function together.

5.1 Civil Disasters

In a case of a civil mass disaster, the main hospital communicates with the dispatch center for sending ambulance vehicles at the location of the incident. The dispatch center is responsible for coordination with other hospitals and inspection of the capacity to accommodate patients. The data obtained from the patients triage are sent to the main hospital by HF radios. This practice

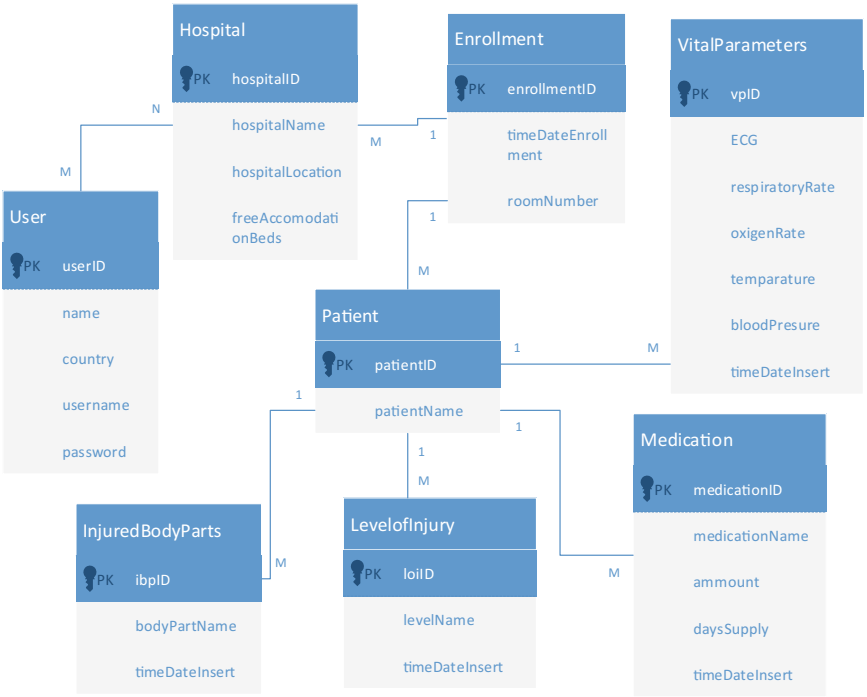

Fig. 2. BIOHIS data model

usually results in errors and misunderstandings in the coordination, communication and issued commands, which is actually the weakest link of the saving protocol implementation. Failure of sending data is the main reason for inclusion of the biosensors in the triage process which includes monitoring of the patient vital data signs and determining the severity of injuries. The advantage of using biosensors is the data transfer to local electronic devices via Bluetooth technology. The measured data are stored to local devices and this is especially useful when Internet connection is temporary lost or not existing. Figure 3 shows an architecture of a general protocol for medical response with biosensors incorporated. Additionally, depending on the available data communications, the data from the local electronic devices can be transmitted to the centralized cloud application in real time and then distributed to main hospital, communication center and other hospitals which are authorized to view these data.

5.2 Military Environment

Figure 4 presents the biosensors usage in military environments. The place of incident is the battlefield where specially trained first aid responders come to the wounded soldiers and perform the triage procedure. Since the Internet is not available on the battlefield, the data are transmitted via Bluetooth to the

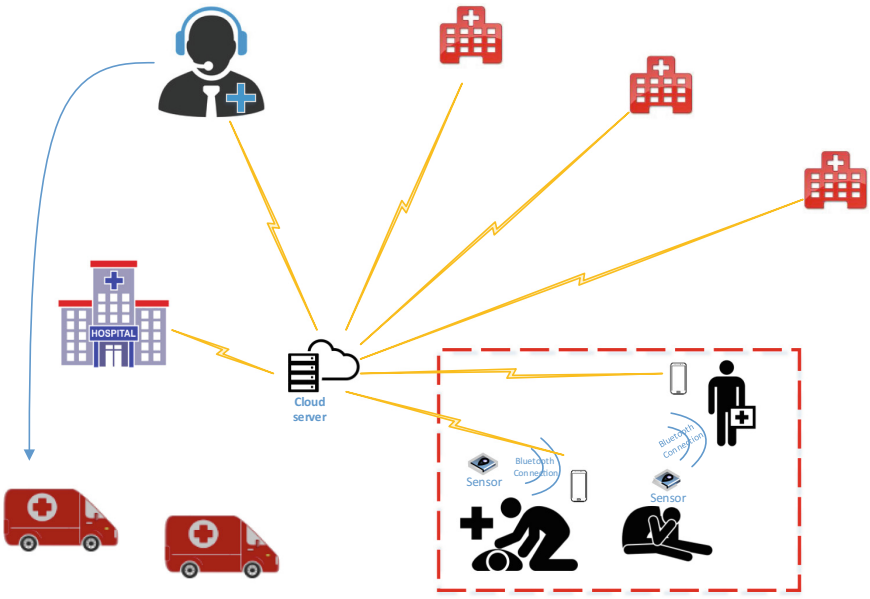

Fig. 3. Biosensors incorporation in civil environment

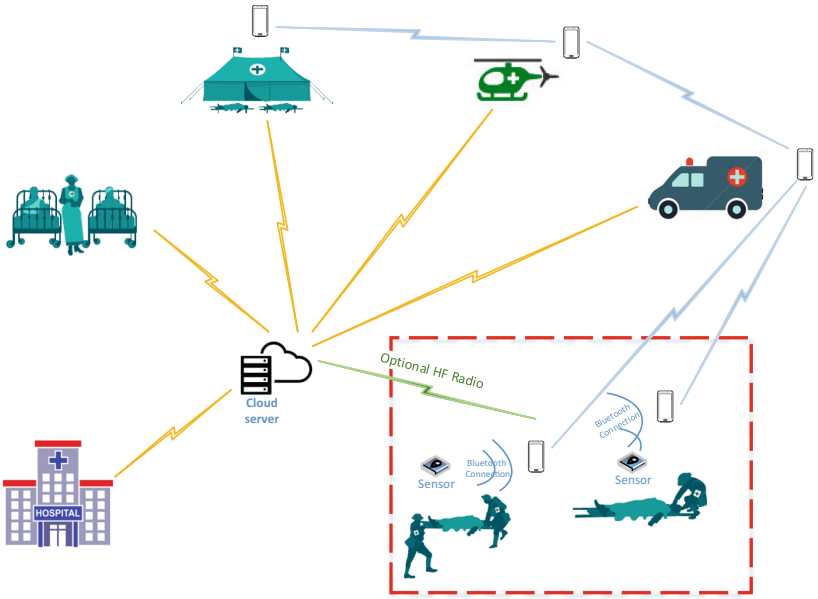

Fig. 4. Biosensors incorporation in military environment

mobile terminals. The temporary stored data are synced to the cloud as soon as there is Internet connection established. On the battefield, only the data for the injured body parts and medications are inserted. The entities involved in the saving protocol are the military transport ambulance/helicopter, the improvised hospital tent, and the remote hospital. All of them can access the central database, retrieve the patients' data collected from the battlefield, during the transport and from the hospital tent. The advantages of the digital capture of patients' vitals are the early preparation for appropriate intervention, and the history availability for future treatment.

6 Experiments and System Constraint Results

The system constraints are imposed due to different use cases and communication technologies. One of the most important constraint is the size of data and the ability to transfer the data to the target environment using the available communication.

In order to predict and model the data size created by the sensors we have created laboratory environment where we have conducted numerous experiments using different sensors [11] and observed the data size per minute:

1. 50 SPO2 sensor readings at 2 and 1000 Hz rate each;
2. 50 Airflow sensor readings at 1000 Hz rate;
3. 100 ECG sensor readings at 125, 200, 500 and 1000 Hz rate each.

Table 1 shows the obtained results. During the experiment we have established that wearing the standard airflow sensor won't be practical, but these data can be extracted from ECG measurements. Given Table 1, we can conclude that total size of the data used for vital signals (per person) is 40 KB/min at 125 Hz reading rate and 310 KB/min at 1000 Hz reading rate. From these measurements, we can conclude that for an hour of observation and sensor readings for 10 persons, the total size of generated data will be 24 MB at 125 Hz reading rate and 186 MB at 1000 Hz reading rate. This gives us the initial data storage capacity we need to provide in order to ensure that our system is efficient.

Another important constraint is the data transfer rate which depends on the communication technologies. Depending on the scenario used, the HF radio and Bluetooth communication define the tightest constraints. Table 2 gives data rate transfer of these technologies. Given the slowest data rate in this table (HF radios), the 125 Hz sample rate will be satisfactory to transfer sensor data for 10 persons.

We have also created model of data size given the vital data parameters used in standard triage protocols as well as their ranges. The result for each parameter, as well as the total data size are shown in Table 3. Given each reading is 6B and 125 Hz sample rate is used, the total size is 750 B/s and the total size per minute is 45 KB. Assuming usage of data delimitation doubles the value, we obtain 90 KB per minute. With all parameters included in every reading we are still within the calculated 192 KB/min bandwidth per person (obtained by the

Table 1. Laboratory measured sensor data size

Sensors included	Data size per minute
SPO2 sensor readings at 2 Hz rate	2 KB/min
SPO2 sensor readings at 1000 Hz rate	130 KB/min
Airflow sensor readings at 1000 Hz rate	40 KB/min
ECG sensor readings at 125 Hz rate	30 KB/min
ECG sensor readings at 200 Hz rate	50 KB/min
ECG sensor readings at 500 Hz rate	110 KB/min
ECG sensor readings at 1000 Hz rate	180 KB/min

Table 2. Communication technologies data rate

Technology	Data rate
Bandwidth of HF military radios currently in use in Macedonian army	256 KB/s = 1920 KB/min
Bandwidth of HF military radios currently in process of acquisition in Macedonian army	1 MB/s
Bluetooth 2.0	3 MB/s
Bluetooth 3.0	24 MB/s
Bluetooth 4.0	24 MB/s

Table 3. Triage vital data parameters size

Vital data parameter	Data range	Data size
Pulse rate	60 to 100 beats	1B per reading
Respiratory rate	12–20 breaths per minute	Less than 1B per reading
Blood pressure	2 values normally in range between 80 and 180	2B per reading
Temperature	Small integer	Less than 1B per reading
Total		6B

lowest communication rate HF radio scenario where 10 persons wear sensors). We measured ECG, SO2 and airflow in order to determine data size per minute and the data rate given the technology that will be used. The experiment has shown that if we use 125 Hz sample rate, we can transfer biosensor data for 10 persons.

7 Conclusion

In this paper we propose a biosensors healthcare information system (BIOHIS) as centralized cloud solution which provides continuous monitoring and transfer

of patients' data. The incorporation of biosensors technology replaces the manual measurements with automatic vital data gathering, enables parallel triage process and reduces the number of medical persons needed for performing the measurements. The digital transfer of patients vital parameters also improves the coordination and communication between hospitals in a case of losing any patients' information, provides early and fast detection of patient state and early preparation for appropriate future intervention.

We also describe the BIOHIS architecture and data structure. The data model replaces the current EHR system practices to store the clinical and administrative data in unstructured fields. It enables the interchange of vital data to gather combined with the rest of patient data as lab analysis, clinicians notes, etc. among the different entities involved in the medical protocols.

Our biosensors healthcare information system can be applied both to civil disasters and medical environment scenarios. When Internet is available, the data are transmitted to the cloud and then distributed to whoever needs them. If Internet is not available, HF radios can be used for data transfer. In both cases, the measured vital data are transferred and stored to the local electronic devices using the Bluetooth technology. This is especially useful when Internet connection is temporary lost or not existing.

We identified the data size and transfer technologies availability as biggest system constraints. We have conducted laboratory experiments in order to predict and model the data size created by the biosensors. We performed numerous measuring activities using different biosensors and observed the data size per minute which gives us the initial data storage capacity we need to provide. Taking into consideration the data transfer rate which depends on the communication technologies, we concluded that the 125 Hz sample rate will be satisfactory to transfer sensor data for 10 persons. We have also created a model of data size given the vital data parameters used in standard triage protocols.

Acknowledgment. This paper is supported by SIARS, NATO multi-year project NATO.EAP.SFPP 984753.

References

1. Madevska Bogdanova, A., Simjanoska, M., Ackovska, N., Kostoska, M., Koteska, B., Tashkoski, M.: Biosensors technology in massive civil disasters. In: 23th International Symposium on Emergency Medicine, Slovenian Society for Emergency Medicine, pp. 355–359 (2016)
2. Healthcare IT Connect (HITC): Big Data Infographic (2012)
3. Caulfield, B.M., Donnelly, S.C.: What is connected health and why will it change your practice? QJM **106**(8), 703–707 (2013)
4. S&I Framework: Structured Data Capture
5. Ross, T.R., Ng, D., Brown, J.S., Pardee, R., Hornbrook, M.C., Hart, G., Steiner, J.F.: The HMO research network virtual data warehouse: a public data model to support collaboration. EGEMS **2**(1) (2014)
6. HL7: Health Level Seven International (2016)

7. Cornet, R., de Keizer, N.: Forty years of SNOMED: a literature review. BMC Med. Inf. Decis. Making **8**(Suppl. 1), S2 (2008)
8. Lee, T.G., Lee, S.H.: Dynamic bio-sensing process design in mobile wellness information system for smart healthcare. Wirel. Pers. Commun. **86**(1), 201–215 (2016)
9. Benharref, A., Serhani, M.A.: Novel cloud and SOA-based framework for E-health monitoring using wireless biosensors. IEEE J. Biomed. Health Inf. **18**(1), 46–55 (2014)
10. Yang, G., Xie, L., Mäntysalo, M., Zhou, X., Pang, Z., Da Xu, L., Kao-Walter, S., Chen, Q., Zheng, L.R.: A health-iot platform based on the integration of intelligent packaging, unobtrusive bio-sensor, and intelligent medicine box. IEEE Trans. Ind. Inf. **10**(4), 2180–2191 (2014)
11. Kostoska, M., Koteska, B., Simjanoska, M., Tashkoski, M., Ackovska, N., Madevska Bogdanova, A., Golubovski, R.: eHealth platform prototype for real-time biosensor data transfer. In: 13th International Conference on Informatics and Information Technologies (2016, in print)

An Automatic Tracking System for Natural Hazard Events with Satellite Remote Sensing

Assen Tchorbadjieff(✉)

Institute of Mathematics and Informatics, Bulgarian Academy of Science,
Acad. Georgi Bonchev Str., Block 8, 1113 Sofia, Bulgaria
atchorbadjieff@math.bas.bg

Abstract. The atmosphere satellite data for atmosphere parameters are the most important source of information for monitoring of areas without or with very rare environment research facilities. With growing dynamic of Climate change, the detailed observation, research and risk management is with a vital importance for nations in regions as the South-East Europe. Due to insufficient ground based research infrastructure and qualified personal, the satellites are main source of reliable data of atmosphere process. The presented paper describes the basic available functionalities of a system for automatic atmosphere events location and transport prediction based on available open data form NASA satellites.

Keywords: Satellites · Computational physics · Natural events · Spatial-temporal data

1 Introduction

The different developments due to climate change cause very strong impact on mankind living behavior. Most of them are connected to atmosphere processes, which are the most imminent and dynamic in impact. The range of their influence is from brief to long term climate changes and from short haze through causing serious damage floods to long term drought and desert spread. The first big serious event that was observed in contemporary history is The Year Without a Summer in 1816 when massive eruption of Mount Tambora a year earlier caused global cooling. Since then the interest in study of atmosphere and its impact have been growing. As a part of this efforts, with technical revolution many new scientific instruments was involved in the ground and space observations of atmosphere.

The most perspective and very important sources of scientific data in last decades came from space satellites. Moreover, with their fast technical improvements the possibilities for monitoring are expanded. In addition to classical meteorology observations, the monitoring of air quality, aerosols particles and volcano eruptions, wildlife fires and Dust storms are enabled. With acquired data and its appropriately proceeding with computer programs it is possible to detect and

G. Stojanov and A. Kulakov (eds.), *ICT Innovations 2016*,
Advances in Intelligent Systems and Computing 665,
https://doi.org/10.1007/978-3-319-68855-8_24

distinguish different sources of pollution. A very good demonstration of effectiveness and usefulness of such type of analysis is the latest advanced research of regional SO2 and NO2 pollution changes from 2005 to 2015 with data from AURA OMI satellite [1].

The importance and usefulness of data from satellites are even more extended in areas and territories where ground based observatories are very rare and not well equipped. The similar region is Balkan peninsula, where only one permanent observation facility is available. It is Basic Environmental observatory at Moussala, the highest place in the Balkans [2]. However, the region is an area that is very strongly exposed to environmental changes, caused either from anthropogenic and natural factors. The region is exposed on the path of Sahara dust air masses transport [3,4], there are many local pollutants, the devastating wildfires are usual events during the late summer. Despite the fact that satellites data are not enough detailed mainly because of lack of permanent measurements [4], the available satellite data are important for region monitoring.

2 Automatic Detection System

2.1 Software Configuration

The specially dedicated software for observation of pollutants and extreme events detection and location is under development. For development are selected the fully functional tools for statistical computing based on R [5]. The R environment enables the usage of all possible resources of contemporary computational science and meteorology multiprocess and cluster computations, automatic data acquisition, parsing and segmentation, air transport simulation and finally- the machine learning based on all possible available statistical tools. For current version, the system is only used for training based on historical data observations. However, the development of R and technical infrastructure allows further functionality expansion of current system to real time analytical tool.

The model is designed to run on distributed computing infrastructure due to design requirements of large memory and computational power. The current results are computed on high-performance grid computing infrastructure at Institute of Information and Communication Technologies BAS in Sofia [6]. The raw satellite data, available in HDF format, are acquired by standard wget procedure. Then, the specially developed script in R processes and extracts the required data subsets from HDF format to more convenient for processing in R data formats. For advanced computing the High-Performance and Parallel Computing functionalities in R are used [7]. With them the access to every different satellite parameter is autonomous and could be processed next to parametric dependent analytic tools. The general view of the infrastructure is shown in (Fig. 1).

The data analysis system relies mainly on quality of NASA published data. The first step in data processing is data extraction based on available metadata for validity and measurement errors. This process is run by different multiprocessing data drivers, each one of them enables autonomy of different

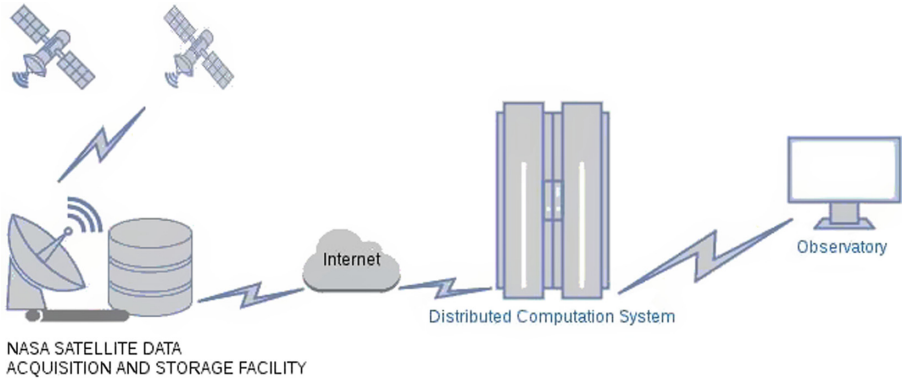

Fig. 1. The system relies mainly on NASA satellite open data system. The required data is downloaded via Internet to high-performance grid computing system for computation. The computations are observable and produced results are accessible through direct link.

parameters observation. The R computational environment enhances the customization of quick and reliable statistical analysis with acquired data. The most possible outcomes from these analyses are air pollutant detection and large scientific information for research. Then, for the further data analysis of air mass transport, the most important information could be acquired from air mass backward and forward in time trajectories. For modeling air mass transport the system relies on NOAA HYSPLIT model dedicated for atmospheric trajectory and dispersion calculations [8]. For automatic computations of required trajectories and their plot in R are selected the functionalities of Openair R library [9]. The software library is distributed with a number of R scripts, which allows complete automatic raw meteo data acquisition from NOAA and proceeding of obtained data to trajectory computations with custom selected parameters in both directions, backward and forward in time. The acquired results are preprocessed and stored in shared system directory and could be accessed by different systems analytical drivers (Fig. 2).

2.2 Spatio-Temporal Design

The preprocessed trajectory records enable discovering of number of possible sources or predict the destination of air pollution immediately after its detection from satellite based on HYSPLIT trajectories. For this purpose, the statistical analysis of merged information of satellite data and computed particle transport trajectories is assumed to locate the most probable source and/or destination of pollutant. This combination of remote sensing data with trajectory creates 4-dimensional spatial-temporal space. The 2-dimensional spatial domain S (latitudes and longitudes) and temporal domain T (time of measurements) define 3-dimensional spatio-temporal sample $z = (z(s_1, t_1), ..., z(s_n, t_n))$, with locations

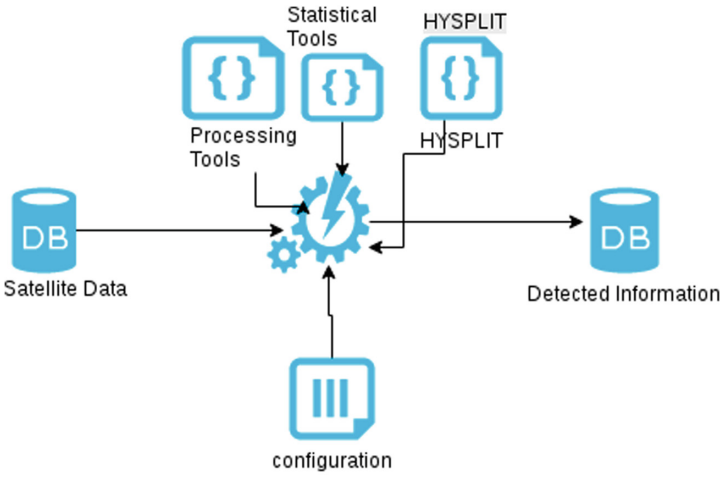

Fig. 2. The automatic system consists of assembly of preprocessing, statistical and trajectory computation software scripts and tools. The system management and synchronization between different parts are relied on configuration file.

$(s_1, t_1), ..., (s_n, t_n) \subseteq R^2 \times R$ [10,11]. For statistical analysis of spatial and temporal dispersion of pollutant particles are used spatial-temporal covariance for spatial distance h and temporal distance u: [10,11]:

$$C_{st}(h, u) = cov(Z(s, t), Z(\bar{s}, \bar{t})) \tag{1}$$

for $(s, t), (\bar{s}, \bar{t}) \in SxT$ and $||s - \bar{s}|| < h; ||t - \bar{t}|| < u$. Respectively, spatial-temporal variograms are equal to [11]:

$$\gamma_{st}(h, u) = C_{s,t}(0, 0) - C_{s,t}(h, u) \tag{2}$$

Having computed in parallel of multiple different in initial altitude trajectories from the same spatial-temporal location, the vertical 3-rd spatial dimension is yielded in comparison between them.

The implemented solution is based on output results from particle transport trajectories. They are with time resolution of 1 h. However, the satellites could not scan observed place from same stationarity less than once a day. Due to this constrains the different implementations are assumed for approximation of distances between trajectories and coordinates of remotely scanned cites. The coincident between trajectory and satellite data is assumed to occur when the region where both, the coordinates of the latitude and longitude of trajectory $W_t(\Delta_i)$ and these of the remote scan $W_s(\Delta_i)$, are in the same location window during equal time interval Δ_i:

$$\sqrt{|W_t(\Delta_i) - W_s(\Delta_i)|} <= \epsilon \tag{3}$$

With ϵ is denoted the maximum allowed distance. For practical analysis three different equal values for location with $\epsilon = (0.5, 1, 1.5)$ and time with $\Delta_i = 3; 6; 12$ h are assumed.

3 Results and Demonstrations

For numerical demonstration the explanatory information from Sahara dust events (SDE) over Balkan region during the Spring 2013 is used. The data are acquired from NASA Aqua/AIRS satellite as dust score index, which is computed from several different infrared channels on board of satellite [12]. The score values above 360 indicate presence of mineral dust in atmosphere. However, this score should not be assumed as being a quantitative measure since this satellite is not trained on the Balkan Peninsula territory. Thus, the dust scores with flag for land uncertainties equal to 1 over observed territories may be considered only as a qualitative confirmation of SDE detection, rather than a quantitative measure. The wrongness due to clouds were excluded because of very high error [12].

3.1 Quantitative Results

The selected SDEs are three mineral outbursts which are detected above Balkans on May 28th, May 19–20th and on May 16–17th [4]. The observed coordinates are for the area above the territory of Republic of Macedonia. The dust scores confirm mineral dust arrival with relatively low values in between 360 and 370 during the midnight on May 18th. The next available observations for SDE are from midnight of May 20th, where the score range is between 438 and 502. The last SDE on May 29th and May 30th are confirmed with day and night observations with values between 406 and 511. The visual maps available on NASA Worldview [14], as well as raw data directly extracted from processing software, show that the main area for the first event is mainly on South-East direction and detected particles most probably are dispersed from the main front. However, the two bigger events which occurred later completely covers the territory of Republic of Macedonia.

For simplicity, the computed trajectories begin from place with averaged coordinates for multiple observations during the same hour above territory of Republic of Macedonia. But the software originally is designed to obtain coordinates directly from satellite data output. The number of selected levels about ground levels are also optional. Due to atmosphere models, the higher altitude yields the longer directories and investigated travel distances are longer. The demonstrative trajectories with starting point from Skopje with 4000 and 100 m above ground level (m AGL) with time of beginning during the SDE of May 19–20th are generated and shown in Fig. 3.

The results from comparison between the events show correlation between intensity and number of coincidences in the trajectories and satellite data over all different distance intervals. Because the detected particles at 18 May 2013 are from SDE which is not directly associated with the territory of Republic of Macedonia, the number of coincidences are very lower than the direct SDE events from May 19–20th and May 29. The magnitude of differences for these numbers could be more than 7 times for 36 h backward trajectories. This may be explained with the nature of particle transport. Because the event from May 18th

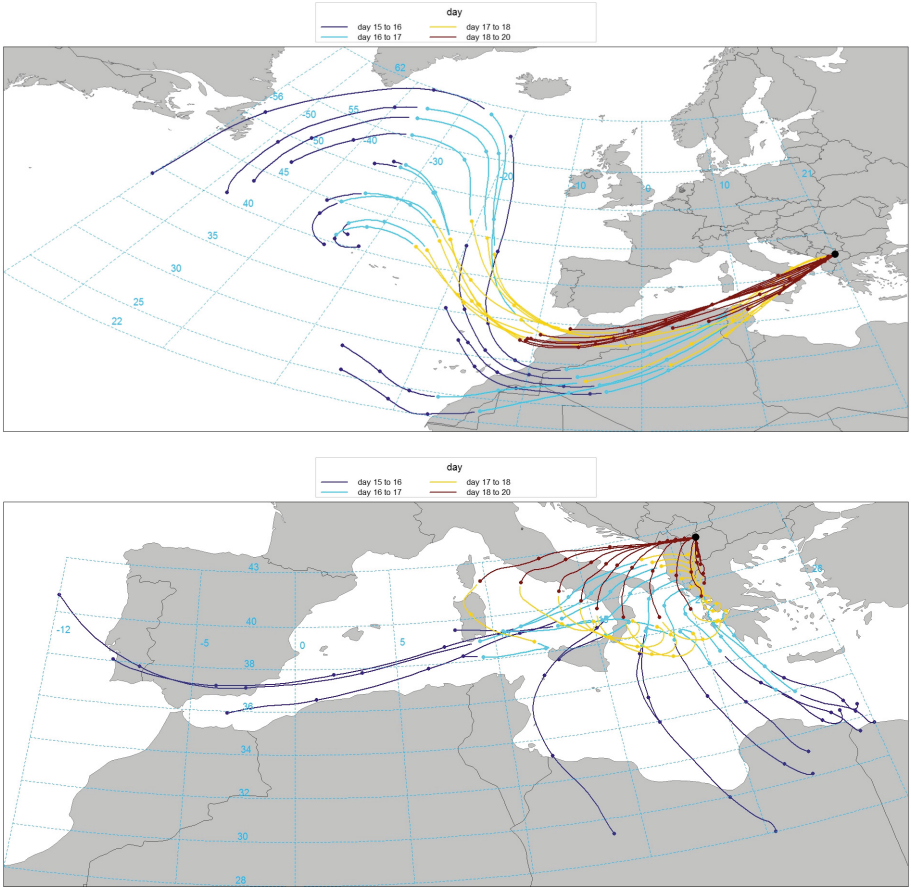

Fig. 3. The graphics show automatically generated backward trajectories with OpenAir library [9] in R for HYSPLIT model. The starting point is the region of Skopje in between 0000UTC at May 19th to 0000UTC at May 21st. The starting altitude for upper graphic is 4000 m agl and 100 m agl for lower. The backward paths are 96 h long.

is mainly associated with dispersed local transport from different source of mineral plume, the coincidences are missed during backward trajectories of air-masses. The only detected reliable coincidences except those above mainly observed territory are at nearby region above Albania and their Mediterranean coasts, which is more likely to show availability of similar dispersed particles. However, the coincidences during the next two events are available over the backward part of air-masses, which confirm hypothesis of direct transport.

Besides, the comparison between number of coincidences in trajectories and satellite data confirms the expectations of tradeoffs between lower precision in spatial-temporal domains and the area of covered territory. The data from tests show that when the model is run with larger window for coincidences the

observed area is also larger, conversely to the case with more narrow observations sample space (Fig. 4). Moreover, as data from both figures show that lack of results during backward transport is possible outcome in case of small spatial-temporal window of coincidences. The most acceptable explanation for this are uncertainties in trajectory models and time synchronization between them and satellite measurements.

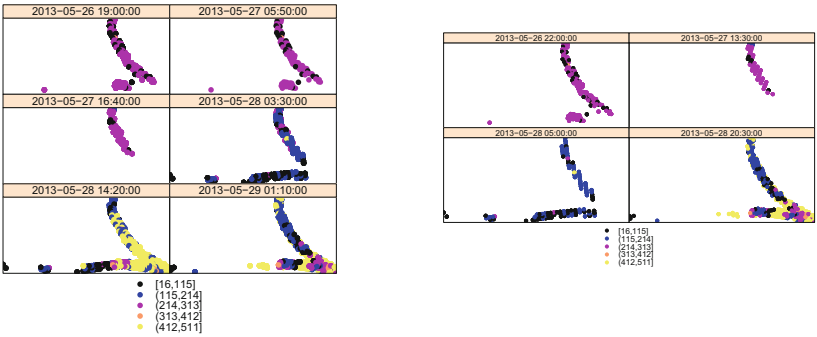

Fig. 4. The graphics show the number of registered satellite data and their Dust score with time window $\Delta = 6$ (left) and $\Delta = 3$ (right) hours for 72 h long trajectory with starting time at 29 May 2013 1200 UTC at 1000 m. AGL

The data from Table 1 show the different pattern of computational output as a result of the initial trajectory altitude. When the altitude is higher the longer distance range is covered but the counts of coincidence are smaller. This could be noticed at the Fig. 3 where long time backward trajectory paths reach the Atlantic Ocean, the place where mineral dust is not observed. Conversely, when the initial altitude is lower, the covered area for the same observed time window is smaller. This allow to investigate smaller area. Following this dependency the initial trajectory altitude is parameter dependent. In case of Sahara dust transport the higher altitudes yields better results. But when satellite data is used for local pollutants, as forest fires for example, the very small values of altitude, like 10 or 100 m agl for example, should be considered.

3.2 Spatial-Temporal Statistics

The geostatistical analysis confirms the intuitive expectations and quantitative results. As the variograms show, that computations with higher initial altitudes are more suitable for long range rural transport in comparison to these with lower ones. As the data from Table 1 show, the lower altitude trajectory missed the source and only intercept the plume transport above Greece and Mediterranean. These results yield random spatial-temporal distribution in diurnal basis (Fig. 5). Conversely, the variogram produced from data form transport in higher altitudes (2000m AGL starting point) shows clear trend in both domains - time and

Table 1. The most distant area of registered Sahara dust plume during the SDE event from May 29th 2013 with computed coincidences for 36 h long backward trajectories for altitudes of 1000 and 2000 m above ground level.

Trajectory start time dd-mm-yyyy hh	ϵ	Lat/Long	Initial altitude of 2000 m agl	Initial altitude of 1000 m agl
29-05 2013 0900	0.5	Lat	21.16087	21.37168
		Long	29.50668	36.076
29-05 2013 1200	0.5	Lat	20.86322	21.13143
		Long	31.58606	36.4857
29-05 2013 1500	0.5	Lat	20.2287	20.86723
		Long	31.558	36.68876
29-05 2013 1800	0.5	Lat	16.07134	20.4431
		Long	38.3999	37.0137

location (Fig. 6). This trend follows intensity decrease and dispersion of dust plume from event source place, measured with lower number and values of index score.

However, the variograms show very strong Nugget Effect - very high initial values of $\gamma_{st}(h = 0, u = 0)$ [13]. This result is due to noise from measurement error and microscale variation in used dust score data. They are produced mainly because dust score index records are used without any filtering procedure and their values are in the range between 1 to 511. Thus, for model improvements, the functionalities must be expanded further with methods for filtering, robust estimation of particle dispersion and spatial prediction (kriging) [13].

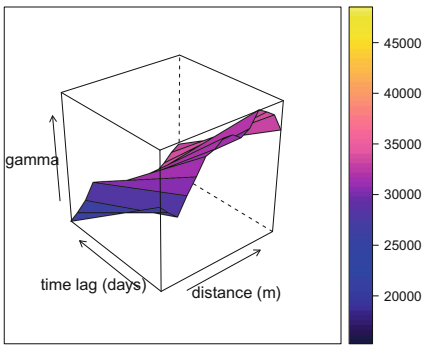

Fig. 5. 3D diurnal spatial-temporal variograms for a model with resolutions $\epsilon = 0.5$ and $\Delta_i = 6$ h for SDE registered on May 29th 2013 1200 UTC. The initial trajectory resolution is 1000 m AGL (left). Backward trajectories are computed for 48 h.

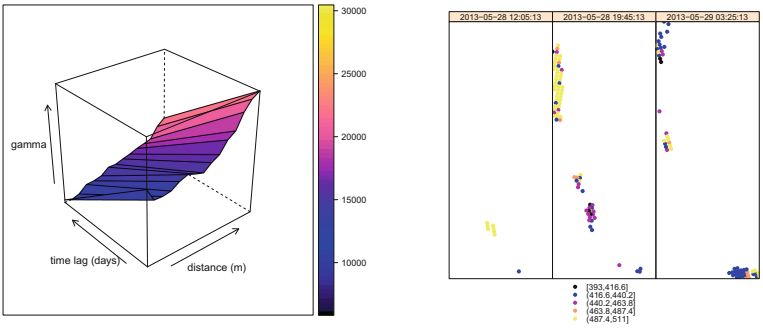

Fig. 6. 3D diurnal spatial-temporal variogram (left) and spatial-temporal distribution of Dust Index (right) for a model with resolutions $\epsilon = 0.5$ and $\Delta_i = 6\,\mathrm{h}$ for SDE registered on May 29th 2013 1200 UTC. The initial trajectory resolution is 2000 m. AGL. Backward trajectories are computed for 48 h.

4 Conclusions

The results in this paper show the basic available functionalities of working model of satellite observations of atmospheric processes. The very simple tests are shown and its validity is confirmed with very well registered Sahara Dust Events ground measurements from BEO observatory in Moussala. However, firstly the model requires more detailed calibration for its complete functionality with all possible other parameters. For this purpose the detailed statistical verification and training with large data, obtained from satellites and ground measured quality data from different transnational sources are needed. Secondly, the model requires additional development for almost real-time functionality and possible prediction features. Having prediction enabled, the system could fix data gaps of irregular satellite scans and enable possible event expectation in area even before its detection.

References

1. Krotkov, N., et al.: Aura OMI observations of regional SO2 and NO2 pollution changes from 2005 to 2015. Atmos. Chem. Phys. **16**, 4605–4629 (2016)
2. Angelov, C., et al.: BEO Moussala a new facility for complex environment studies. In: Sustainable Development in Mountain Regions, pp. 123–139 (2011)
3. Pey, J., et al.: African dust outbreaks over the Mediterranean Basin during 2001–2011: PM10 concentrations, phenomenology and trends, and its relation with synoptic and mesoscale meteorology. Atmos. Chem. Phys. **13**, 1395–1410 (2013)
4. Tchorbadjieff, A., et al.: Sahara dust events over south-western Bulgaria during the late spring of 2013. Comptes rendus de lAcadmie bulgare des Sciences **68**(10), 1229–1234 (2013)
5. R-Project. https://www.r-project.org/
6. Atanassov, E., Gurov, T., Karaivanova, A., Ivanovska, S., Durchova, M., Georgiev, D., Dimitrov, D.: Tuning for scalability on hybrid HPC cluster. In: Mathematics in Industry, pp. 64–77. Cambridge Scholar Publishing (2014)

7. Ostrouchov, G., Chen, W.-C., Schmidt, D., Patel, P.: Programming with Big Data in R (2012). http://r-pbd.org/
8. Stein, A., Draxler, R., Rolph, G., Stunder, J., Cohen, M., Ngan, F.: NOAAs HYSPLIT atmospheric transport and dispersion modeling system. Bull. Am. Meteorol. Soc. **96**(12), 2059–2077 (2015)
9. Carslaw, D.C., Ropkins, K.: Openair-an R package for air quality data analysis. Environ. Model Softw. **27–28**, 52–61 (2012)
10. De Iaco, S., Myers, D.E., Posa, D.: Space-time analysis using a general product-sum model. Stat. Probab. Lett. **52**(1), 21–28 (2001)
11. Graler, B., Pebesma, E., Heuvelink, G.: Spatio-temporal interpolation using gstat. R J. **8**(1), 204–218 (2016)
12. DeSouza-Machado, S.G., et al.: Infrared retrievals of dust using AIRS: comparisons of optical depths and heights derived for a North African dust storm to other collocated EOS A-Train and surface observations. J. Geophys. Res. **115**(D15), CiteID D15201 (2010)
13. Cressie, N.: Statistics for Spatial Data. Wiley, New York (1993)
14. NASA Earth Data. https://earthdata.nasa.gov

Author Index

G. Stojanov and A. Kulakov (eds.), *ICT Innovations 2016*,
Advances in Intelligent Systems and Computing 665,
https://doi.org/10.1007/978-3-319-68855-8